Carnegie Mellon University

CARNEGIE INSTITUTE OF TECHNOLOGY

THESIS

SUBMITTED IN PARTIAL FULFILLMENT OF THE REQUIREMENTS

FOR THE DEGREE OF Doctor of Philosophy

TITLE **Exploring Spectrum Aggregation Technology: A Study of the Technical Techno-economic, Policy Implications and the Potential Impact on Economics**

PRESENTED BY **Mohammed Awaidh Alotaibi**

ACCEPTED BY THE DEPARTMENTS OF

Engineering and Public Policy

Marvin Sirbu	May 4, 2016
ADVISOR, MAJOR PROFESSOR	DATE
Douglas Sicker	May 4 2016
DEPARTMENT HEAD	DATE

APPROVED BY THE COLLEGE COUNCIL

Vijayakumar Bhagavatula	May 5, 2016
DEAN	DATE

Exploring Spectrum Aggregation Technology:
A Study of the Technical, Techno-economic, Policy Implications and the Potential Impact on Spectrum Economics

Submitted in partial fulfillment of the requirements for

the degree of

Doctor of Philosophy

in

Engineering and Public Policy

Mohammed Awaidh Alotaibi

B.S., Electrical Engineering, King Fahd University of Petroleum and Minerals
M.S., Electrical Engineering, University of Pennsylvania
M.S., Engineering and Public Policy, Carnegie Mellon University

Carnegie Mellon University
Pittsburgh, PA

May, 2016

This thesis is dedicated to the memory of my father. I miss him every day. I am glad he saw this process through and supported me in this journey till I returned home.

ACKNOWLEDGMENT

I am using this opportunity to express my gratitude to my advisors Professor Marvin Sirbu and Professor Jon Peha who supported me throughout the course of my study at CMU. I am thankful for their aspiring guidance, invaluably constructive criticism and friendly advice on my research on a weekly basis for more than four years. I am sincerely grateful to them for sharing their knowledge and expertise all this time. I have been lucky to be advised by them and I hope my work in this thesis met their standards.

I thank Dr. Joe Butler and Professor Ozan Tonguz for all their useful feedback and discussion about my research. In addition, I am thankful to all faculty, researchers, programmers and EPP staff who helped me while doing my research. Special gratitude is extended to Victoria Finney who made every obstacle disappears while studying in EPP.

I would like to thank the Saudi Communication and IT Commission for their support and funding of my scholarship. I, specifically, thank my superiors Habeeb Alshankiti, Abdullah Almehaimeed and Majed Alkahtani for helping me overcome any complications I faced during my stay in the United States. I convey special gratitude to my mentors Dr. Ahmed Adil and Dr. Mazin Aquil for the support and encouragement to pursue my PhD as well as all my colleagues in the Spectrum Affairs sector of CITC.

Most importantly, none of this would have been possible without the love and patience of my family. I can’t thank my parents, my siblings and my wife Jawaher enough. Without their support during difficult times of my life, I couldn’t imagine being able to finish my PhD. Thank you!

ABSTRACT

Spectrum Aggregation (SA) technology has been introduced in cellular standards. Long Term Evolution (LTE)-Advanced is expected to allow aggregation of multiple Component Carriers (CC) to fulfill the high data rate requirement. This thesis, presents an exploratory study of spectrum aggregation technology. First, it analyzes the technology's technical impact on wireless networks. Second, it estimates the costs and benefits of the SA technology when building out a wireless network. Then, it presents a study case to compare the feasibility of SA technology versus spectrum refarming. Furthermore, the thesis studies SA's impact on valuation of spectrum by operators. Finally, it discusses the implications of SA on spectrum policies.

Results show that LTE systems that use spectrum aggregation over fragmented blocks of spectrum can have better performance compared to Independent Carrier (IC) systems. In addition, aggregating carriers from multiple bands could permit the system to have a better performance in certain circumstances. Moreover, SA technology could have a positive impact on the benefits and costs of nationwide LTE networks. In a case study for using SA over fragmented spectrum in the TV band, the advantages and disadvantages of the use of the technology versus repacking the spectrum physically to create contiguous band are observed and discussed. After empirically studying operators' willingness to pay for contiguous and low-frequency spectrum, simulation is used to measure the impact of SA on the operators' valuation for spectrum blocks. Results show that the technology could lead to more linear valuation of spectrum units. Finally, SA impact on spectrum policies is studied and specific recommendations are given to regulators to help exploit fragmentation of spectrum through the technology and encourage fairer access to spectrum by competitors.

TABLE OF CONTENTS

Acknowledgment iii
Abstract iv
Table of Contents v
List of Tables x
List of Figures xi
List of Abbreviations and Glossary of Terms xiv
I. Introduction 1
1. Research Motivation 1
2. Thesis Question 4
3. Thesis Contribution 4
4. Literature Review 4
5. Definitions 7
6. Organization of the Thesis 9
7. Overview of the Analysis 10
II. Impact of spectrum aggregation on mobile network performance 13
1. Research Questions 13
2. Background 14
2.1. Carrier Aggregation in LTE 14
2.2. Simulation Platforms 18
2.3. Vienna LTE Simulator 20
3. Modeling Overview 24
3.1. Investigated Scenarios 24
3.2. Analysis Formulation 25
3.3. Analytical Overview 26
4. LTE Simulation Model 35
4.1. Setting up Parameters 36
4.2. Network Layout 37
4.3. Link Measurement (Channel Quality) 39

4.4. Link Performance 48
4.5. Initialization and Feedback 52
4.6. Traffic 53
4.7. Scheduling and Carrier Selections 54
4.8. Simulation Loop 57
4.9. Measuring Performance 58
5. Inputs and Assumptions 60
5.1. Main Inputs 60
5.2. Variable Inputs 60
5.3. Fixed Assumptions 61
6. Results and Discussion 61
6.1. Throughput 62
6.2. Fairness 69
6.3. Conclusion 70
III. Quantifying the Impact of Spectrum Aggregation on Radio Equipment 71
1. Research Question 71
2. Background 71
2.1. Technical Impact of SA on Radio Equipment 72
2.2. SA Implemented Chipsets 74
3. Modeling the Analysis 78
4. Input Data 80
5. Results and Discussion 82
IV. Impact of Frequency and Spectrum Aggregation on Capacity and Build-Out Cost of Cellular Networks 87
1. Research Questions 87
2. Background 88
2.1. Review of Wide Network Modeling 88
2.2. Multiband and Cell Coverage 91
3. Modeling the Analysis 91
3.1. Investigated Scenarios 91
3.2. Analysis Formulation 92

3.3. Large Network Modeling ... 93
4. Other Inputs and Assumptions ... 99
4.1. Population, Area and Environment ... 99
4.2. Market Share and Spectrum Holdings ... 101
4.3. Technical Assumptions ... 102
4.4. LTE Simulation Result ... 102
5. Results and Discussions ... 102
5.1. SA Costs ... 102
5.2. SA Capacity ... 106
5.3. SA Impact on Broadband Access ... 108
5.4. Conclusion ... 109
V. Case study: Converting TV channels to cellular use ... 111
1. Research Questions ... 111
2. Background ... 112
2.1. Review on TV Bands ... 112
2.2. Analytical Overview ... 113
3. Modeling the Analysis ... 114
3.1. Scenarios Investigated ... 114
3.2. Analysis Formulation ... 115
3.3. Analysis Models ... 116
4. Inputs and Assumptions ... 117
5. Results and Discussions ... 119
6. Conclusion ... 121
VI. Empirical Study regarding Spectrum Auctions ... 123
1. Research Questions ... 123
2. Background ... 124
3. Input Data ... 125
4. Modeling the Analysis ... 128
4.1. Independent Variables ... 128
4.2. General Analysis of the Data ... 130
4.3. Hypothesis ... 131

4.4. Regression Models 131
5. Results and Discussion 133
5.1. Australia 133
5.2. Germany 135
5.3. United States 136
5.4. Canada 137
5.5. United Kingdom 138
5.6. Brazil 138
5.7. Conclusion 138
VII. Implications of spectrum aggregation on spectrum economics 141
1. Research Questions 141
2. Background 142
2.1. Literature Review 142
2.2. Overview of the Impact of SA on Spectrum Valuation 143
3. Modeling the Analysis 144
3.1. Investigated Scenarios 144
3.2. Analysis Formulation 144
3.3. Costs Savings and Spectrum Value Estimation 145
4. Inputs and Assumptions 146
5. Results and Discussions 147
VIII. Policy Implications of spectrum aggregation 153
1. Band Planning 153
1.1. Block Size 153
1.2. Frequency Separation 154
2. Spectrum Allocation and Assignment 155
2.1. Spectrum Auction 155
2.2. Spectrum Cap limit 156
3. Flexible spectrum management 156
4. Illustrative Example on Spectrum Allocation 157
4.1. Market Variables 157
4.2. Assumptions on Operators 158

4.3. Policy Variables 159
4.4. Analysis Results 161
IX. Conclusion 165
References 167
Appendices 185
Appendix A: Source code for LTE Simulator 185
Appendix B: Result for inter-band cases with additional guardband 206
Appendix C: Results for rural environment 208
Appendix D: Plotted Curves from Simulation Runs 211
Appendix E: Data for LTE Radio Equipment 212
Appendix F: Data for Spectrum Auctions 214

LIST OF TABLES

Table 1: Data rates required for different traffic of mobile video streaming ... 2
Table 2: CA Impact on LTE Layer 1 (Physical Layer), Layer 2 (MAC, RLC and PDCP) and Layer 3 (RRC) ... 15
Table 3: Main Components of the Simulator [56] ... 19
Table 4: Pseudo-code of the simulator [57] ... 20
Table 5: Pseudo-code of the simulator [58] ... 24
Table 6: CA bandwidth classes and corresponding nominal guard bands (Table from [74]) ... 33
Table 7: LTE Guardbands and Assumed degradation of service due to ACI ... 34
Table 8: Traffic models ... 53
Table 9: Main inputs related to frequency bands ... 60
Table 10: Constant input assumptions and system configuration ... 61
Table 11: Qulacomm RF Transceivers ... 76
Table 12: Qualcomm Baseband and Modem Chips ... 76
Table 13: Regression results for increase in equipment costs ... 84
Table 14: Summary of results ... 85
Table 15: Inter-site distances for the existing network ... 98
Table 16: Data sets from auction database ... 127
Table 17: Statistics from Australian auction in 2001 ... 133
Table 18: Regression results for Australian auction ... 134
Table 19: Statistics from German auction in 2010 ... 135
Table 20: Statistics from the AWS-1 Auction ... 136
Table 21: Results for regressions on AWS-1 auctions ... 136
Table 22: Average prices paid in two Canadian auctions ... 137
Table 23: Specifications for different scenarios ... 147
Table 24: assigning values to the market variables ... 158
Table 25: Different spectrum allocations to operators, as regulator policy varies ... 160
Table 26:Collected costs data for LTE equipment ... 213

LIST OF FIGURES

Figure 1: Global mobile data traffic forecast. Y axis is Exabyte per Month 2
Figure 2: Spectrum designated to mobile service 3
Figure 3: Spectrum allocation within a band. A trade-off between number of licensees (a regulator wants to increase) and the contiguous bandwidth (an operator want to increase) 3
Figure 4: CA deployment scenarios (F2>F1) (Figure from [9]) 5
Figure 5: An example to demonstrate integral concepts that will be mentioned in the rest of the report 9
Figure 6: Overview of the proposed analysis pieces, and the interactions between them 11
Figure 7: Simulation Methodology [54], and Component Layers and Simulation Model [55] 19
Figure 8: LTE Link Level Simulator Structure [59] 21
Figure 9: Transmitter Structure [60] 21
Figure 10: Schematic block diagram of System Level simulator [58] 23
Figure 11: Flow diagram of the simulator [59] 23
Figure 12: Main blocks providing an overview of the analysis 26
Figure 13: Path loss for two frequency bands in urban environment 29
Figure 14: Illustration of the increase in coordination required as fragmentation increases (adapted from [4]) 31
Figure 15: Impact of fragmentation on a 20 MHz system capacity based on worst case scenario with regard to ACI (1) one 20 MHz, (2) two 10 MHz, (3) two 5 MHz, one 10 MHz (4) four 5 MHz, (5) two 5MHz, three 3 MHz (normalized) (6) five 3 MHz, one 5 MHz 35
Figure 16: High-level description of modification done to the simulator to handle SA 36
Figure 17: Scatter plot of hexagonal set of eNodeBs 38
Figure 18: Scatter plot for UEs 39
Figure 19: Cell pathloss maps for 700 MHz and 2600 MHZ carriers, respectively, in urban environment 41
Figure 20: Cell shadow fading maps for 700 MHz and 2600 MHZ carriers, respectively, in urban environment 43
Figure 21: SINR distributions as inter-site distances change in urban environment 45
Figure 22: Cell ranges based on Okumura-Hata and COST 231-Hata propagation models in urban environment 46
Figure 23: Coverage probability for a user at the cell-edge as frequency band and inter-site distance change in urban environment 47
Figure 24: SINR throughout the cell in urban environment 48
Figure 25: Sector Capacity based on Theoretical Calculation for SISO system in urban environment 49
Figure 26: BLER as function of SINR and spectral efficiency 50
Figure 27: SNR-CQI mapping function 51
Figure 28: CQI mapping across the cell for two frequency carriers 51
Figure 29: Stacking all subcarriers to create virtual contiguity for the joint scheduling 55
Figure 30: Simulation loop (on left) 58
Figure 31: Average system throughput (Mbps) as inter-site distance changes 63
Figure 32: Average UE throughput (Mbps) as inter-site distance changes 63
Figure 33: Throughput (Mbps) for UE at the cell edge 65
Figure 34: Average UE throughput (Mbps) as user density changes 66

Figure 35: Re-plot of two inter-band scenarios from the previous figure 67
Figure 36: Average UE throughput for finite buffer traffic 67
Figure 37: Peak UE throughput (Mbps) and impact of fragmentation 68
Figure 38: Measuring fairness for different cell sizes 69
Figure 39: Simplified block diagram of UE components [87] and eNB hardware architecture [88] 72
Figure 40: Two basic transceiver concepts to handle SA 73
Figure 41: Diagram for Qualcomm Chipsets introduced to accommodate CA 75
Figure 42: Components that might be affected by SA 78
Figure 43: Teardown of LTE devices components costs (based on data from teardown.com and technology.ihs.com) 81
Figure 44: Teardown of recent Releases LTE-A devices components costs (based on data from teardown.com and technology.ihs.com) 81
Figure 45: Projected increase in radio equipment cost due to CA 83
Figure 46: Predicted increase in radio equipment cost based on simple regressions 84
Figure 47: Flow diagram for dimensioning process used in [103] 90
Figure 48: An example showing the design complexity when multiple bands are aggregated. 91
Figure 49: Main blocks showing overview of the analysis 93
Figure 50: Algorithm for cost analysis 96
Figure 51: Algorithm for capacity analysis 98
Figure 52: US population density by county. Figure from census.gov 99
Figure 53: Breakdown of US area into five types of regions 100
Figure 54: Averaged population density across each region type (plot is approximated) 101
Figure 55: NPV of costs for the different scenarios (relative to the 700 MHz contiguous scenario) 104
Figure 56: Impact of increasing SA equipment cost 105
Figure 57: Impact of changing requirement to meet edge UE minimum throughput 106
Figure 58: Total capacity delivered by each scenario 107
Figure 59: Comparing scenarios with respect to cost effectiveness (measured in bps/$) 107
Figure 60: Peak Throughput for a single SA and IC user per sector 109
Figure 61: Option A: use of SA, Option B: spectrum repacking 115
Figure 62: Simplified flow diagram of the proposed analysis 116
Figure 63: The two options with guardbands 117
Figure 64: NPV of costs of the two scenarios 119
Figure 65: Costs when assuming SA has no equipment cost and repacking at maximum cost 120
Figure 66: Simplified flow diagram of the proposed analysis 145
Figure 67: Interpreting reduction in build-out cost due to additional block as value projected for block by operator 149
Figure 68: Projected value for spectrum by different scenarios 150
Figure 69: Projected value for additional spectrum added to two 10 MHz blocks of spectrum 151
Figure 70: the build-out cost for each of the four operators in each of the five cases. We assume all operators use SA 163
Figure 71: Fairness index as allocated spectrum blocks increase 163
Figure 72: The build-out cost for each of the four operators in each of the five cases (IC operation) 164
Figure 73: Changes when extra guard band applied 207

Figure 74: Cell ranges based on Okumura-Hata and COST 231-Hata propagation models in rural environment 208
Figure 75: Coverage probability for a user at the cell-edge as frequency band and inter-site distance change in rural environment 209
Figure 76: Average system throughput as inter-site distance changes........ 209
Figure 77: Throughput for UE at the cell edge 210
Figure 78: inter-site distances and users densities for five types of regions 211
Figure 79: Tear-down of all components (source: teardown.com) 212
Figure 80: Cost of each component in the device (source: teardown.com) 213

LIST OF ABBREVIATIONS AND GLOSSARY OF TERMS

3GPP	3rd Generation Partnership Project
ACI	Adjacent Channel Interference
ACS	Adjacent Channel Selectivity
ACLR	Adjacent Channel Leakage Ratio
AMC	Adaptive Modulation and Coding
BB	Baseband
CA	Carrier Aggregation
CC	Component Carriers
C-C	Contiguous Carriers
CQI	Channel quality indicator
CSI	Channel State Information
eNB	Evolved node B
HSPA	High Speed Packet Access
IC	Independent Carriers
IMT	International Mobile Telecommunication
IMT-A	International Mobile Telecommunication – Advanced
LTE	Long Term Evolution
LTE-A	Long Term Evolution - Advanced
MCS	Modulation and coding scheme
MIMO	Multiple Input Multiple Output
MU-MIMO	Multi-User Multiple Input Multiple Output
NCC	Noncontiguous Carriers
OOB	Out of band emission
PA	Power Amplifier
PF	Proportional Fair
PUSCH	Uplink shared channel
PUCCH	Uplink shared control channel
RB	Resource block
SA	Spectrum Aggregation

SINR	Signal-to-interference-and-noise ratio
TVWS	TV white space
UE	User equipment
WTP	Willingness to pay

I. INTRODUCTION

Spectrum Aggregation (SA) technology, also referred to as Carrier Aggregation, combines contiguous or non-contiguous spectrum fragments to create a virtual wideband channel. It allows multiple small fragments of spectrum to be exploited to provide high transmission rate broadband services, which cannot be achieved without this technology. Spectrum aggregation capability is incorporated in future mobile wireless standards, such as LTE-A and IEEE 802.16m, which require wideband channels to meet the high data rate requirements set by the ITU for IMT-A standards.

This thesis presents an exploratory study of spectrum aggregation technology. First, it analyzes the technology's technical impact on wireless networks. Second, it estimates the costs and benefits of the SA technology when building out a wireless network. Then, it presents a study case to compare the feasibility of SA technology versus spectrum refarming. Furthermore, the thesis studies SA's impact on valuation of spectrum by operators. Finally, it discusses SA's implications for spectrum policies.

In this section, we start by explaining the research motivation combined with some background on spectrum aggregation. Then, we list the thesis's main question and its contribution. After we clarify some definitions for the main terms to be used in this report, we review the literature on spectrum aggregation. Finally, we provide an overview of the thesis and the main analyses.

1. Research Motivation

Traffic on wireless mobile networks is forecast to increase [1] in two ways as shown in the following figure [2]:

- Total traffic will increase more than 10-fold over the next 5 years

– Traffic of mobile video, which requires high bit rate transmission for a user, will generate most of this growth

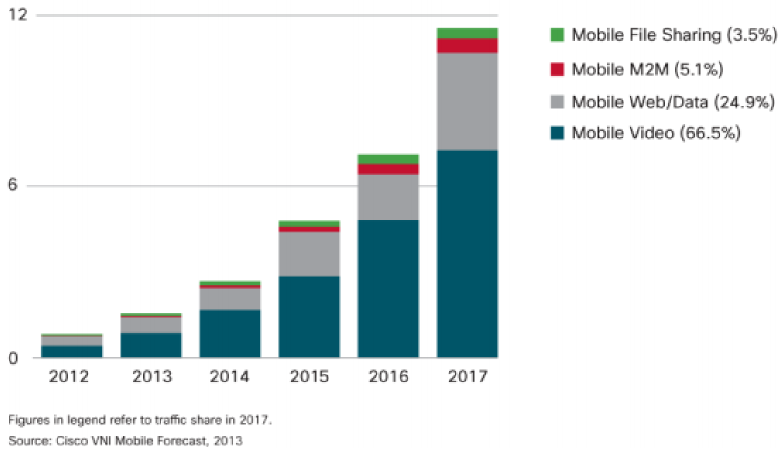

Figure 1: Global mobile data traffic forecast. Y axis is Exabyte per Month

Data rates required for different traffic of mobile video streaming [3] is shown in the table below. Interactive applications like video gaming might even require larger bandwidth.

Table 1: Data rates required for different traffic of mobile video streaming

Video Conferencing	3-4 Mbps
SD TV Streaming	3.5 Mbps
DVD movie quality steaming	9.8 Mbps
HD Video TV Streaming	10-15 Mbps

On the other hand, current spectrum policies and outcomes of spectrum markets lead to more fragmentation of spectrum bands. As shown in the first figure below, bands designated for mobile services are spread across 4 GHz of spectrum, and each band is subdivided further into blocks for different licensees. Although these fragments could be exploitable by narrow band applications, spectrum fragmentation might result in an inefficient use of the spectrum [4]. This fragmentation in spectrum available for mobile services might delay rolling out and expanding mobile broadband services like LTE [5]. However, a regulator might not be able to avoid fragmentation of a spectrum band if he plans to allow multiple licensees to access the band [6]. This problem is demonstrated in the second figure for better understanding.

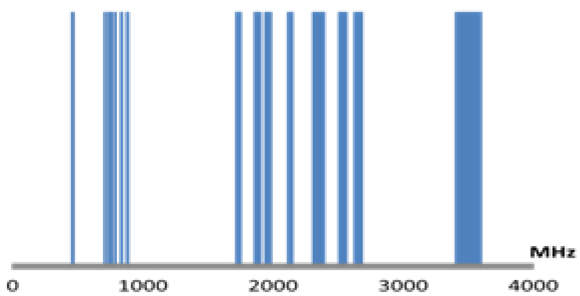

Figure 2: Spectrum designated to mobile service

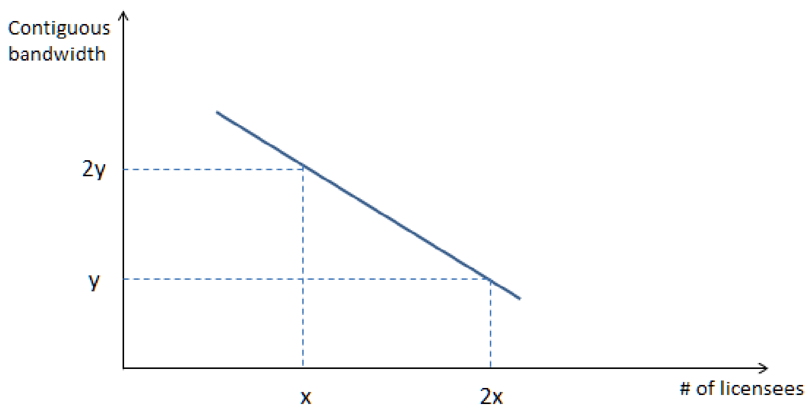

Figure 3: Spectrum allocation within a band. A trade-off between number of licensees (a regulator wants to increase) and the contiguous bandwidth (an operator want to increase)

The problem can be summarized as: "the increasing *demand* for higher bandwidth is challenged by the rare *supply* of wide spectrum blocks that can support high bit rates". One possible solution is the use of spectrum aggregation technology [7] and across multiple bands might increase the effective supply of spectrum that can meet the total mobile traffic and mobile video traffic demands.

2. Thesis Question

The primary objective of this research is to explore the impact of the use of spectrum aggregation technology on spectrum policy. In order to achieve this goal, we will answer the following high-level questions:

- What is the impact of spectrum aggregation on the performance of mobile networks?
- What is its impact on mobile operators' costs of building out a network that meets users demand and what is the benefit?
- What is its potential implication on spectrum economics?

Answering these three questions will provide technical and economic insights on spectrum aggregation impact which will help answering our main policy question.

3. Thesis Contribution

We conduct a broad technical analysis of wireless networks, as we consider multiple scenarios and vary many inputs to produce a comprehensive assessment of the technology's impact on wireless network performance. Moreover, we use this technical analysis to understand the benefits and the costs of the technology when building a nationwide network. Furthermore, these two types of analyses are used to study the implications of the technology on spectrum policies and economics.

4. Literature Review

Spectrum aggregation technology was discussed for first time in 2006 in a report prepared for Ofcom [4]. Demo of carrier aggregation started in early 2012 [8] and implementation of the technology in LTE networks started in the second half of 2013 [9] [10]. Many papers reviewed and analyzed the technology as we will present in this section.

In [11] and [12], survey and tutorial overview for radio resource management of SA in LTE-A is presented. Radio Resource Management (RRM) involves scheduler structure, CC selection and RB selection. In the three types of carrier aggregations, intra-band contiguous, intra-band non-contiguous and inter-band non-contiguous carrier aggregations, different deployment scenarios as shown in figure below.

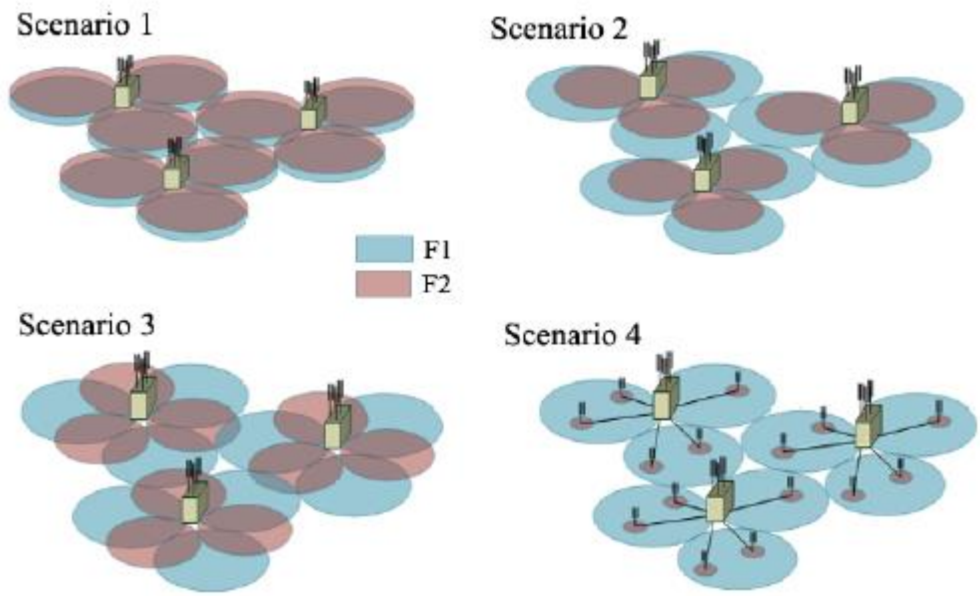

Figure 4: CA deployment scenarios (F2>F1) (Figure from [9])

By the end of 2012, 152 LTE networks were operating in 68 countries worldwide. However, LTE (Release 8) doesn’t meet the ITU IMT-A requirement which is considered the true 4G standard. 3GPP addressed this requirement by releasing the LTE-A standard (Release 10 and beyond) with a carrier aggregation (CA) feature that enables the standard to meet the IMT-A requirements [13]. The benefits of spectrum aggregation have been discussed qualitatively in a number of articles. First, CA can combine low-frequency FDD bands with high-frequency TDD bands to provide high-speed mobile broadband across large areas [14]. If an operator targets 5 Mbps for HD video streaming, the operator can offer this service over a broader portion of the network with carrier aggregation than without. Also, CA allows better utilization of spectrum assets as a whole.

By means of CA, users can have access to a total bandwidth of up to 100 MHz in order to meet the IMT-Advanced requirements [15]. This will allow target peak data rates in excess of 1 Gbps in the downlink and 500 Mbps in the uplink to be achieved [16]. Also, Multi-Carrier HSPA is considered an attractive means for operators to provide higher data rates [17]. In addition to 3GPP standards, the IEEE 802.22 standard discusses channel bonding and aggregation [18]. CA is considered the most distinctive feature for 4G systems and its impact on LTE Release 8,9 and 10 layers has been discussed thoroughly [19]. The combination of CA and MU-MIMO is discussed in many papers [20]. The European project called “Spectrum aggregation and multi-user MIMO: Real-World Impact (SAMURAI)” was initiated to study this technology [21]. It runs different analyses with different scenarios to test this technology in practice and it discusses CA at link level with implementation challenges and the system aspect of CA [22], [23]. Similarly, Wireless World Initiative New Radio (WINNER+) discusses this technology in their recent reports [24].

The available frequency bands are usually non-contiguous, which may cause impact on the spectrum utilization efficiency (SUE). [25] quantifies the impact of spectrum non-contiguity on the channel capacity. There are studies that investigate the spectrum fragmentation and determine the acceptable level of fragmentation for different systems [26]. One popular implementation for SA systems can be done with cognitive radios for systems with dynamic spectrum access to fragmented spectrum [27]. New interleaving schemes for downlink OFDMA of LTE-Advanced systems are proposed to capture CA-specific enhanced frequency diversity with simple implementation [28].

Furthermore, discussion in [29] includes the concept of primary cell (PCell) and secondary cell (SCell), mechanisms for activation and deactivation of CCs in cross-CC scheduling. Handover over the two carriers is discussed in [30]. Sometimes, they are called primary carrier and secondary carrier. It depends on the scheduling algorithm, but mainly users are assigned RBs in the primary carrier and when needed more capacity, RBs in the secondary carriers are aggregated.

Finally, many papers discussed the performance of SA system and analyzed it through network simulations [31]. Some of the papers apply aggregation in the uplink channel [32]. In both downlink and uplink, SA can show performance improvement over operating carriers independently. These papers analyze different scenarios of spectrum aggregation networks that use HSPA or LTE-A, inter-band and intra-band SA scenarios, many scheduling methods. Results in general show improvement in performance due to SA over IC operation. However, all these studies don't analyze impact of changing frequency band on inter-band SA performance, the aggregation of more than two carriers and how is the performance compared to other scenarios like contiguous spectrum. This big picture analysis would be the main contribution in first investigation of this thesis.

5. Definitions

Here we try to define important terms and concepts that are necessary to understand the rest of this report.

- Frequency band: a range of frequency spectrum that is designated to a specific use, for example the band 2.1 GHz (2110-2170 MHz) which designated mainly to IMT.
- Multiband: the use of frequency carriers over multiple frequency bands, for example band 700 MHz and 2600 MHz.
- Allocated block: the range of frequency that is allocated for a specific user, the bandwidth of the block determines its size in MHz.
- Contiguous carriers: the frequency carriers that are adjacent to each other with a single band
- Non-contiguous carriers: number of frequency carriers that are not adjacent with a single or across multiple bands which are allocated to a certain user
- Fragmented allocations: (similar to above) number of small blocks that are not adjacent with a single or across multiple bands which are allocated to a certain user
- Spectrum aggregation (or carrier aggregation): the capability of wireless system to bond two or more frequency carriers and form a virtual wider carrier
- Independent carriers: the opposite of carrier aggregation; operating carriers independently without aggregating them
- Inter-band spectrum aggregation: when carriers across multiple bands are aggregated
- Intra-band spectrum aggregation: when carriers within a single band are aggregated
- Inter-site distance: the distance between base stations in wireless cellular network

While some of these terms could be defined or used differently in the literature, the following figure provides a visual demonstration for these terms and concepts in this report.

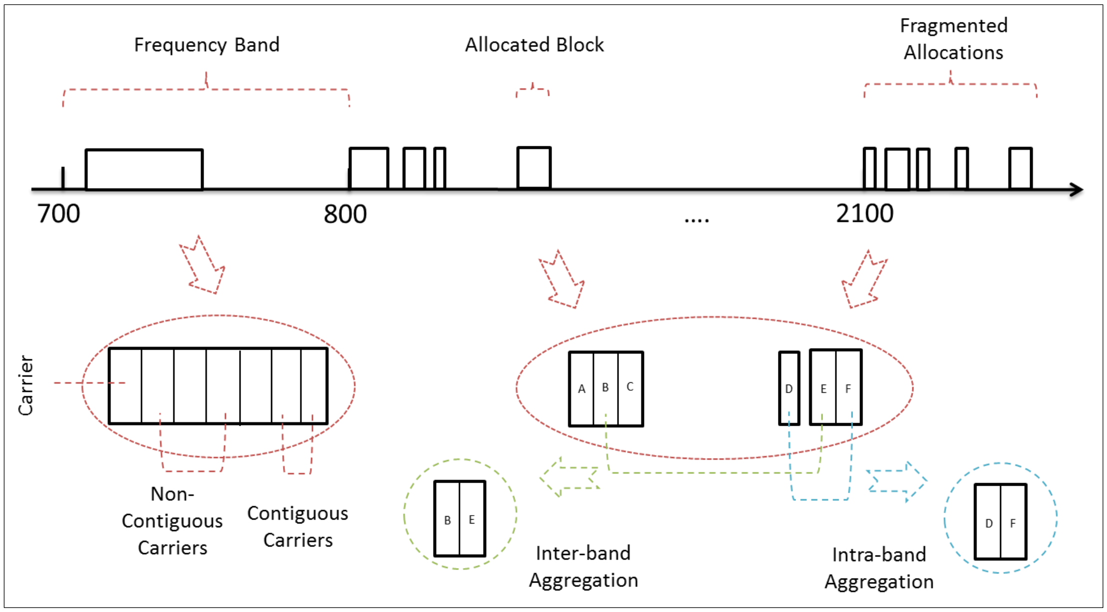

Figure 5: An example to demonstrate integral concepts that will be mentioned in the rest of the report

6. Organization of the Thesis

The dissertation is designed to have four main investigations as follows:

- Chapter II: Impact of spectrum aggregation on mobile network performance
- Chapter IV: Impact of spectrum aggregation on the costs of building out mobile networks to meet a given level of demand and the benefits
- Chapter V: Case study: Converting TV channels to cellular use
- Chapter VII: Implications of spectrum aggregation on spectrum economics
- Chapter VIII: Conclusion on policy impacts

The first investigation will shed light on the first high-level question posed in Section 2, while the next two investigations will deal with the second one. The answers for third question will be analyzed in the fourth investigation while the fifth section will be used to draw a conclusion for the main question about the policy impacts.

Each investigation's body text will be composed of the following main sections:

– Research questions: this section states the questions we try to answer in the investigation
– Analytical overview: it provides theoretical analysis and background to explain expected differences between the systems we analyze.
– Investigated scenarios: this section defines the main network scenarios we plan to analyze
– Analysis formulation: this section shows overview of the analysis proposed in this chapter, by displaying flow diagram that shows input, models and output
– Analysis modeling: it gives a brief description of the proposed model and its main elements
– Inputs: it highlights the main assumptions and inputs used in the model
– Results: it shows the expected results and how they can help answering the questions posed earlier

7. Overview of the Analysis

This thesis starts by investigating the impact of spectrum aggregation on the performance of mobile wireless networks. We quantify the difference in performance achievable with SA, the perforkance achievable with independent carriers, and the performance with contiguous blocks of spectrum.

The second investigation is a techno-economic analysis of rolling out a Greenfield mobile network that uses spectrum aggregation, using analysis that builds on the first investigation. This analysis will allows us to compare the costs with and without spectrum aggregation.

In the third investigation, spectrum aggregation is used in a case study in which cellular infrastructure is deployed in what used to be the TV band. This cost of using spectrum aggregation to operate within fragmented spectrum is compared to the cost of repacking to eliminate fragmented spectrum.

In the fourth investigation, multiple network scenarios are considered to quantify the impact of frequency and bandwidth of spectrum blocks on network cost, and how these change with and without spectrum aggregation technology. This will be followed by empirical analysis of spectrum auction results to see how frequency and bandwidth have affected spectrum bids in auctions.

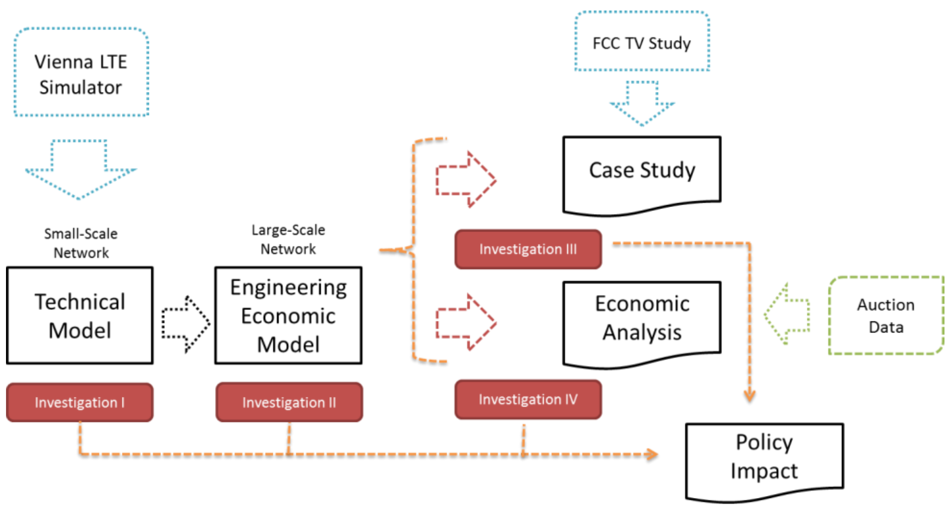

Figure 6: Overview of the proposed analysis pieces, and the interactions between them

II. IMPACT OF SPECTRUM AGGREGATION ON MOBILE NETWORK PERFORMANCE

In this chapter, we simulate wireless networks that use LTE technology to investigate the impact of spectrum aggregation on mobile network performance. We start the chapter by providing background information on wireless network simulation. Then, we state the questions to be answered in the chapter. This is followed by an overview describing our modeling approach. Next, we present a detailed view of the simulation model used. After that, we list the main inputs and the assumptions we made to run the network simulation. Finally, we plot and discuss the results of the SA impact.

1. Research Questions

The first task of this research is to answer the following three questions, each of which contains more detailed subquestions:

- What is the comparative system performance for each of the following mobile networks:
    - *a network that uses contiguous carriers within a single band*
    - *a network that uses non-contiguous carriers independently, i.e. is an Independent Carriers operation in which carriers are fragmented either across multiple bands or within a single band*
    - *a network that uses non-contiguous carriers by aggregating them, i.e. is a Spectrum Aggregation operation in which aggregation is either across multiple bands or within a single band*
  - What is the system throughput in these systems as the input varies?
  - What is the fairness of these systems?

- What is the average throughput received by users in each of these networks?
  - *users with different demand traffic types*
  - *users located different distances from the cell center*
- Based on responses to the above questions, what can we conclude about the SA impact on network performance?

2. Background

For wireless systems, mathematical analysis is not always achievable or sufficient to evaluate and compare the performance of different systems. Consequently, wireless system performance is often evaluated by using network simulation. Many simulation methodologies have been proposed and used for different wireless technologies. In this section, we provide a quick review of the literature on simulation for LTE networks and then explain details of the model we used. The first subsection below will provide an overview of different simulation platforms, and the second one will focus on the specific platform that we use in our modeling. Before that, we will provide very brief review on SA and LTE.

2.1. Carrier Aggregation in LTE

Since LTE is the most promising IMT-A technology and the most adopted one across the world, the focus in this thesis will be on LTE-based systems. LTE-Advanced extends LTE Rel.-8 with support for Carrier Aggregation, where two or more component carriers (CCs) are aggregated in order to support wider transmission bandwidths up to 100MHz and for spectrum aggregation [33]. Before this introduction, carrier aggregation was possible for only two contiguous carriers in the Dual Carrier HSPA systems [34].

CA is introduced gradually starting from LTE Release 10 which requires multiple changes on LTE protocols for the radio interface as we describe in table below briefly [7], [35], [11] and [36]

Table 2: CA Impact on LTE Layer 1 (Physical Layer), Layer 2 (MAC, RLC and PDCP) and Layer 3 (RRC)

Layer	CA Impact
Physical Layer	In addition to the need for multiple physical downlink shared channel (PDSCH) that carry downlink data, the following multiple physical control channels are required, one per CC: - Physical downlink control channel (PDCCH) which carries the downlink control information about scheduling - Physical uplink control channel (PUCCH) which carries Hybrid ARQ acknowledgments and channel state information (CSI)
Medium Access Control (MAC)	Multiple transport downlink shared channels (DL-SCH), one per CC, which carry downlink data and signaling. MAC must be able to handle scheduling and HARQ on multiple CCs. There are two main alternatives for CA scheduling, either resources are scheduled on the same carrier, or a cross-carrier scheduling may be used
Radio Link Control (RLC)	Larger buffer
Packet Data Convergence Protocol (PDCP)	None
Radio Resource Control (RRC)	Addition, removal and reconfiguration of multiple CCs. The base station might use this measurement report to trigger a change of secondary cell [37]. [7]. During a handover, the new base station tells the mobile about the new secondary cells using its RRC Connection Reconfiguration command

To meet the high data rate requirement, spectrum aggregation is used to allow access to multiple carriers. Cross-carrier scheduling Proportional Fair scheduler has been shown to maximize the log-measure utility in LTE systems [38]. An efficient scheduling strategy to reduce spectrum resource assignment delay in systems that make use of CA is developed, which is based on an a-priory organization of available RBs in sets [39]

The SA scheduling is obtained with an optimized General Multi-Band Scheduling algorithm with the aim of cell throughput maximization [40]. Other papers, like [41], [42] and [43] design efficient packet scheduling algorithm based on PF.

Resource allocation is easier to implement with contiguous spectrum [11]. Non-contiguous carriers face different path losses which might affect system performance due to Doppler frequency shift [44]. In general overview, in downlink communication using CA, each user equipment device (UE) will be allocated CC which will be called Primary (PCC). Depending on the traffic load, scheduling strategy and quality of service requirements, an additional CC might be allocated to a UE; it is called the secondary (SCC) [11]. This shows that the main difference in radio resource management with CA is the ability to allocate UEs on multiple CCs simultaneously.

Multiple resource scheduling schemes for SA have been proposed. Here are some of them:

- Joint Queue Scheduler (JQS) [45], [46] and [47]: this is one step scheduler with a single queue which should lead to the optimum performance
- Disjoint Queue Scheduler (JQS) [45], [46] and [47]: This is a two-step scheduler where first the carrier is selected then the resource block is assigned. Its performance is lower than JQS but the algorithm is less complex.
- CC Switching [45]: this allows switching of the of CC assigned for the user in order to improve resource utilization, but it increases signaling overhead.

Assigning CCs to a UE requires the use of feedback information about channel quality in addition to information like traffic level and requirement, QoS requirement and UE capability [11]. The use of such information would determine how many CCs is assigned to a UE.

Different CC selection and management algorithms and methods have been proposed in different papers. Here are some of them:

- G-factor based selection [48]: it identifies users near the cell edge and assigns them the CC with the best quality. It was introduced to deal with inter-band SA when some CCs can't serve users at cell-edge
- Least Load [49], [46] and [45]: this assigns users to the CC with lowest load or shortest queue, in an attempt to balance load across CCs.
- Modified Least Load [45]: modified version of LL that predicts users transmission rate in future
- Random Selection [49]: selects CCs randomly for users. This algorithm might balance load over the long term, but it might not work well for inter-band SA with large frequency gaps between CCs.
    - Inter-band carrier-switch [50]: it selects the lower frequency CC first, then moves the UE with the best CQI to higher frequency carriers. It doesn't select CCs simultaneously.

The last step in resource allocation is the assignment of resource blocks to UE. Different scheduling algorithms for SA have been proposed. Here are some of them:

- Round Robin (RR) [46], [47]: The conventional RR algorithm doesn't consider SA and difference between CCs frequency bands.
- Proportional Fairness (PF) [46], [49]: The conventional PF algorithm doesn't consider SA and difference between CCs frequency bands.
- Cross-CC PF [49]: This algorithm collects user previous throughput information and select CCs based on whether the user is capable of aggregating carriers. It increases fairness and exploits SA advantage.

- User grouping PF [51]: divide users according to how many CCs they can be served by, and then start carrier assignment to users in each group. It increases fairness and work well for inter-band SA

2.2. Simulation Platforms

Multiple simulation platforms have been implemented for LTE systems, such as those in [52] and [53]. In [54], a unified simulation of mobile broadband systems is proposed to evaluate different broadband technologies. As shown in Figure 7, below, the proposed methodology combines link-level simulation and system-level simulation, in which the latter is used to measure system performance based on the curves produced by the link-level simulation. The link-level simulation does the required link budget and capacity calculations whereas the system-level simulation focuses on managing the available radio resources based on channel measurements and traffic assumptions. Similar system-level methodology is presented [55], showing the different network layers in the two main components, as this figure illustrates. System-level simulation includes all layers higher than the physical layer which is represented in the link level simulation.

These simulator concepts are described broadly in order to analyze the generic structure of wireless systems without applying specific wireless standards. LTE technology-specific simulators are also proposed and implemented. This is because LTE has multiple layers with sets of specifications that must be implemented to simulate the performance of this technology as per 3GPP guidelines, the standard body of LTE technology. In [56], the main components of the simulation model are summarized in Table 3 below. The system is divided into four main components that respectively: plot network topology, create users mobility, predict coverage area, and finally represent traffic simulation.

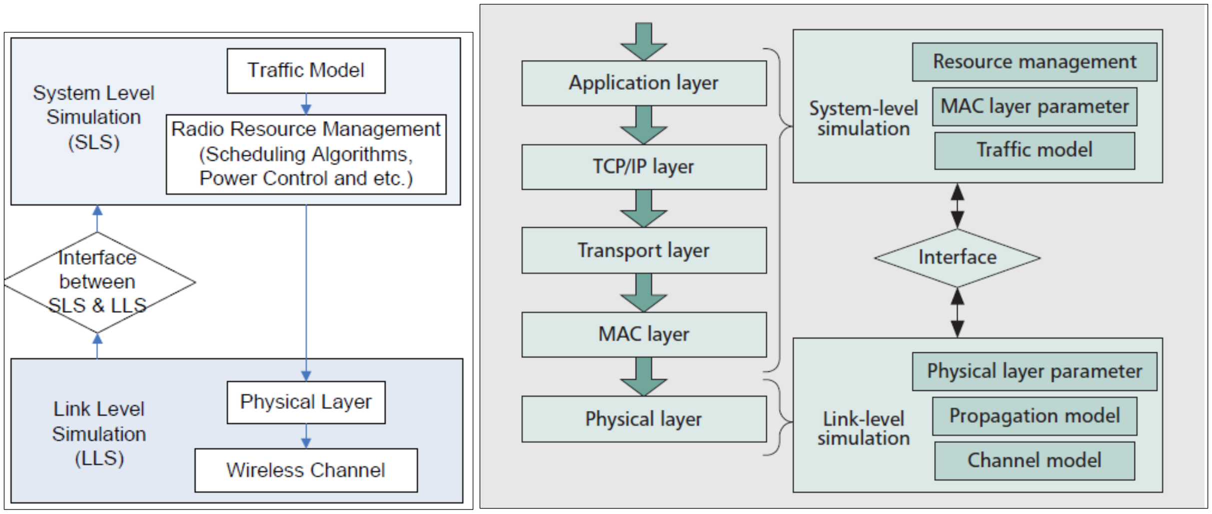

Figure 7: Simulation Methodology [54], and Component Layers and Simulation Model [55]

Table 3: Main Components of the Simulator [56]

Component	Function
Simulator	Start and end the simulation, create and execute events
Frame Manager	Handle the start and the end of LTE frame and sub-frame
Flows Manager	Create an application
Network Manager	Create UE device and LTE cell, update UE position and implement frequency reuse and handover

An example of pseudo code for the system-level simulator is shown in the box below [57]. It starts by initializing parameters of the physical part of the LTE network, including users' positions, eNodeB's and channels. Then, for each TTI cycle, the link transmission is executed to finish the transmission process of each user in this cycle. This includes the adaptive modulation, HARQ and scheduling for every user.

Other LTE simulators developed at the Technical University of Vienna [58], [59], [60] will be discussed in the next subsection in more detail since analysis within this chapter is based on the use of this simulator.

Table 4: Pseudo-code of the simulator [57]

```
Initialize (channel, users, BSs…)
for each frame
      Move UEs
  for each timeslot (TTI)
      for each BS do
          scheduling, HARQ
          for each user in BS do
              1.   Calc SINR
              2.   AMC
              3.   SL to LL mapping
              4.   Send feedback
```

2.3. Vienna LTE Simulator

Different LTE simulation platforms exist, and some of the most comprehensive ones are those developed at the Technical University of Vienna (TU Wien). They are implemented on the MATLAB platform and the university made the source code available to researchers in order to offer them more flexibility and ease when adding new functionalities and algorithms. There are two main simulators that have been developed to date, a link-level simulator and a system-level simulator.

2.3.1. Link-Level Simulator

This simulator focuses on the LTE physical layer. It allows investigation of: channel estimation, tracking, prediction algorithms, synchronization algorithms, Multiple-Input Multiple-Output (MIMO) gains, Adaptive Modulation and Coding (AMC) and feedback [60], [59]. The simulator is composed of three main parts: transmitter, channel model, and receiver, as shown in Figure 8 below.

.

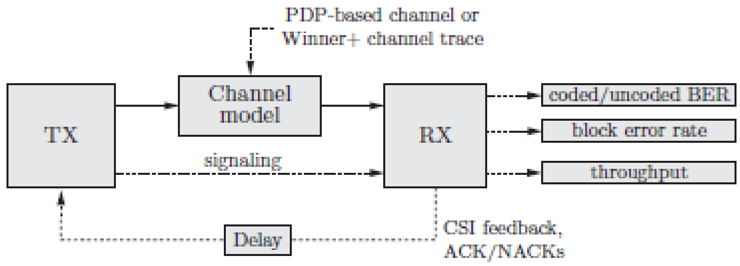

Figure 8: LTE Link Level Simulator Structure [59]

Since this simulator is intended for direct implementation of the LTE physical layer, the implementation complexity is high. As the Figure 9, below, shows, it simulates many physical layer functions, such as FFT and symbol mapping. Though this is kind of simulation could help in developing coding schemes or decreasing the error bit rate, for example, but it doesn't simulate the impact of system-level issues such as cell planning or scheduling. For this reason, we instead adopt the system-level simulator which is described next.

.

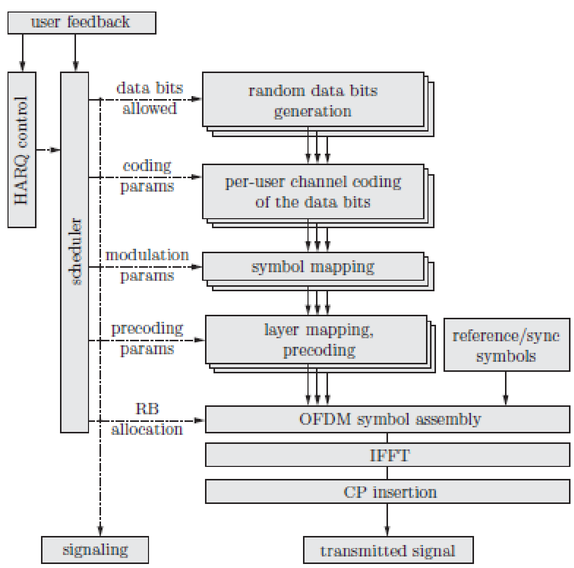

Figure 9: Transmitter Structure [60]

2.3.2. System-Level Simulator

This type of simulation focuses on network-related issues such as scheduling, resource allocation and interference management. The physical layer is implemented based on simplified link-layer models to reduce complexity. This type of simplified link layer model provides abstracted results from the link-level simulator we earlier said would be used in this system-level simulation.

As shown in Figure 10, below, the LTE simulator was structured to consist of two main models: the link-measurement module and the performance module [58]:

i. Link-Measurement Model: The main purpose of this model is to estimate the signal-to-noise ratio in order to assess the link quality per subcarrier for each user. After the network was generated by deploying base stations and users in the regions of interest, the state of the downlink channels was then estimated by combining results from three different parts of the model: macroscopic pathloss, shadow fading, and small-scale fading. After SINR is estimated, each UE sends feedback to the eNB to help the scheduler assign the resource blocks to users based on the traffic model implemented.

ii. Link Performance Model: This model takes SINR as an input along with the modulation and coding schemes in order to measure the performance of the system as a whole. MCS values are defined based on CQI values abstracted from estimated SINR, and then measurements of performance such as throughput can be estimated provided that the traffic model for each user is known.

Figure 10 below shows both the link between these two models and the main components of each model.

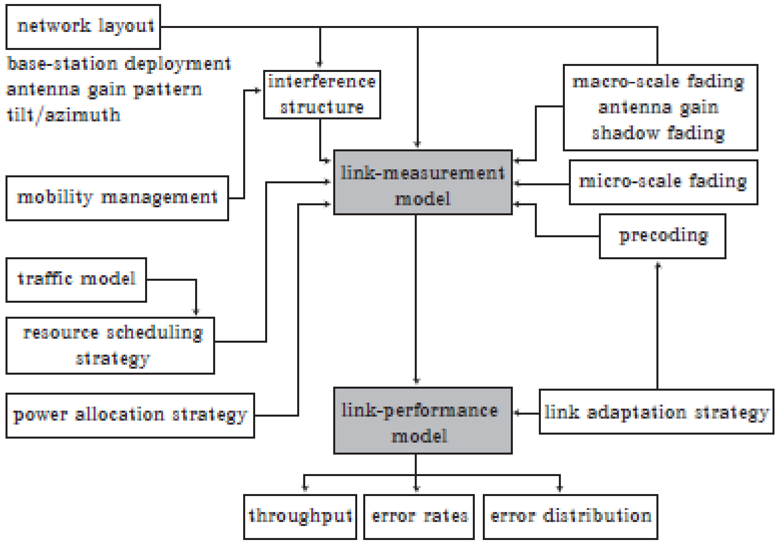

Figure 10: Schematic block diagram of System Level simulator [58]

The simulator maintains separate structures for many functions, sequentially, creating the network, estimating channel and signal quality, sending feedback from UE to eNB, allocating resources and finally measuring the performance. These tasks can be rearranged to represent a flow diagram consisting of the three basic blocks of the link level simulator we showed earlier: transmitter, channel and receiver as the Figure 11, below, shows.

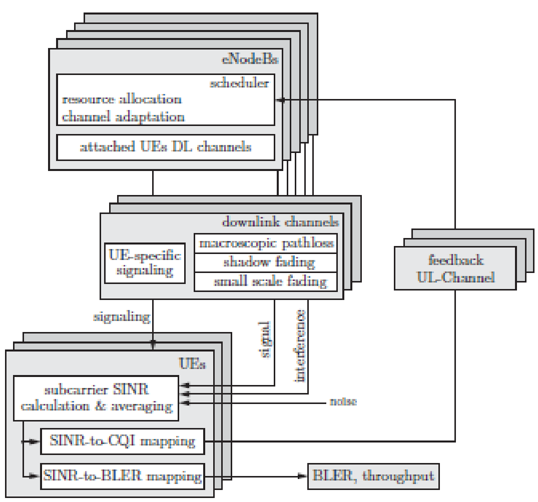

Figure 11: Flow diagram of the simulator [59]

Finally, pseudo code in the box below summarizes the process for the system level simulator and indicates how the inputs and outputs of each model are used. The simulator is composed of many files and functions that can be run through the LTE SL Simulator main file. In the next Section, a very detailed description that lists functions will be provided.

Table 5: Pseudo-code of the simulator [58]

```
for each simulated TTI do
  move UEs
  if UE outisde ROI then
    reallocate UE randomly in ROI
  for each eNodeB do
    receive UE feedback after a given feedback delay
    schedule users
  for each UE do
    1- channel state → link quality model → SINR
    2- SINR, MCS → link perf. model → BLER
    3- send UE feedback
```

3. Modeling Overview

Wireless system performance can be measured using different metrics, such as fairness and latency, and throughput. Throughput is the actual rate that information is transferred. Throughput depends on multiple factors, including spectrum bandwidth, signal-to-noise ratio, cell size, user locations, spectral efficiency and scheduling algorithm. These factors are inter-independent, making it hard to derive throughput analytically. Instead, network simulation is performed to help predicting throughput more precisely.

3.1. Investigated Scenarios

In the simulator we adopted, the network being simulated has a conventional macro-cell layout. In the center of each cell, a single Evolved Node B (eNodeB) serves UEs within the cell. In our system model, we assume an LTE-A technology based network that has been allocated a total bandwidth of B MHz with a frequency-reuse factor of 1. This allocated spectrum could be either a contiguous B MHz block or composed of N non-contiguous fragments, each of which has a bandwidth of B_i MHz, such that $\sum_{i=1}^{N} B_i = B$ MHz. It could be allocated in any of several frequency bands designated for IMT, spanning frequency bands between 450 MHz and 3.6 GHz. Based on this, we analyze the following five different network scenarios:

A. a network that uses contiguous carriers within a single band of either 700 MHz or 2600 MHz.

B. a network that uses non-contiguous carriers independently within a single band--either two or four carriers in either the 700 MHz band or 2600 MHz band.

C. a network that uses non-contiguous carriers independently across multiple bands (multiband)--either one or two carriers in the 700 MHz band and one or two carriers in the 2600 MHz band.

D. a network that aggregates non-contiguous carriers within a single band (intra-band aggregation)--either two or four carriers in either the 700 MHz or 2600 MHz band.

E. a network that aggregates non-contiguous carriers across multiple bands (inter-band aggregation), one or two in the 700 MHz band and one or two in the 2600 MHz band.

3.2. Analysis Formulation

The performance of wireless mobile networks can be evaluated through network simulation. We run a network simulation for the five network scenarios above. Following 3GPP guidelines [35] for analyzing an LTE system, a small-scale 19 hexagonal-cell network is adequate to test system performance. This deployment is a trade-off between low complexity and accurate interference analysis since the site being analyzed is surrounded by two rings (6+12=18) of interfering sites.

Based on the simulation of traffic and user distribution, the received signal power can be estimated and, consequently, the LTE cell coverage and capacity can be predicted. Figure 12, below, shows a flow diagram of the analysis. In the next three sections, we will explain each block in detail.

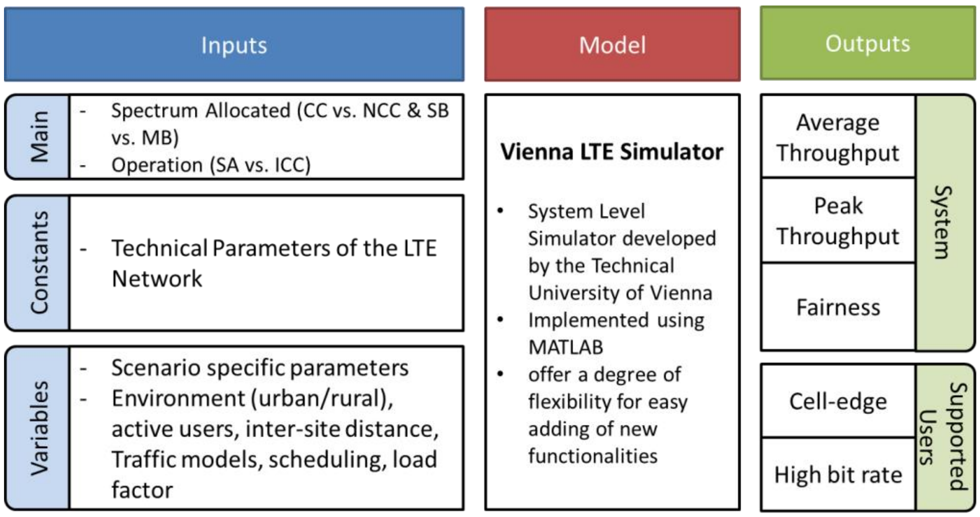

Figure 12: Main blocks providing an overview of the analysis

3.3. Analytical Overview

The systems to be investigated are distinct from each other in at least one of the following ways:

– Spectrum allocated: across one or multiple bands and allocated to contiguous or non-contiguous carriers.

– Spectrum operations: component carriers can either be aggregated or operate independently

These differences will affect certain characteristics of a wireless system that will impact the system performance as a whole. This section will discuss the affected characteristics: path loss, bandwidth, trunking efficiency and diversity.

3.3.1. Path loss

Path loss is the reduction in transmitted signal power as the signal propagates in space. It is used in link-budget calculations to determine the effective coverage area of a transmitter. The path loss depends on frequency band, environment and distance, and it can be predicted using different propagation models.

In LTE technology, The Okumura-Hata model is suitable for spectrum between 150 to 1500 MHz, while the Cost231-Hata model is appropriate for frequency bands above that [61]. The Okumura-Hata Model for path loss in urban areas is calculated with the following formula [62], [63]:

Equation 1

$$L_v = 69.55 + 26.16 \log_{10} f - 13.82 \log_{10} h_B - C_H + [44.9 + 6.55 \log_{10} h_B] \log_{10} d$$

Where:

- L_v is path loss in (dB)
- h_B is height of base station antenna in [m]
- h_M is height of mobile station antenna in [m]
- f is frequency of transmission in MHz
- C_H is antenna height correction factor $= 0.8 + (1.1 \log_{10} f + 0.7)h_M - 1.56 \log_{10} f$ for medium cities in urban environment.
- d is distance between the base and mobile stations in [km]

For open rural areas, the model is formulated as:

Equation 2

$$L_R = L_v - 4.78(\log_{10} f)^2 + 18.33 \log_{10} f - 40.94$$

The COST-Hata Model for path loss in urban areas is estimated using the following formula [62], [63]:

Equation 3

$$L = 46.3 + 33.9\log_{10} f - 13.82\log_{10} h_B - a(h_R) + [44.9 - 6.55\log_{10} h_B]\log_{10} d + C$$

Where:

- L is path loss in decibel (dB)
- h_B is height of base station Antenna in meter (m)
- h_R is height of mobile station Antenna in meters (m)
- f is frequency of Transmission in MHz
- $a(h_R)$ is antenna height correction factor = $(1.1\log_{10} f + 0.7)h_R - 1.56\log_{10} f + 0.8$
- C is 0 dB for medium cities in urban environment, for open rural areas, it is: $-4.78\,(\log_{10} f)^2 + 18.33\log_{10} f - 40.94$
- d is distance between the base and mobile stations in kilometers

As the first figure below shows, path loss is different for different frequency bands. This will affect performance of systems that use carriers from different frequency bands with or without aggregation; this will be explained in detail when we discuss the simulation model.

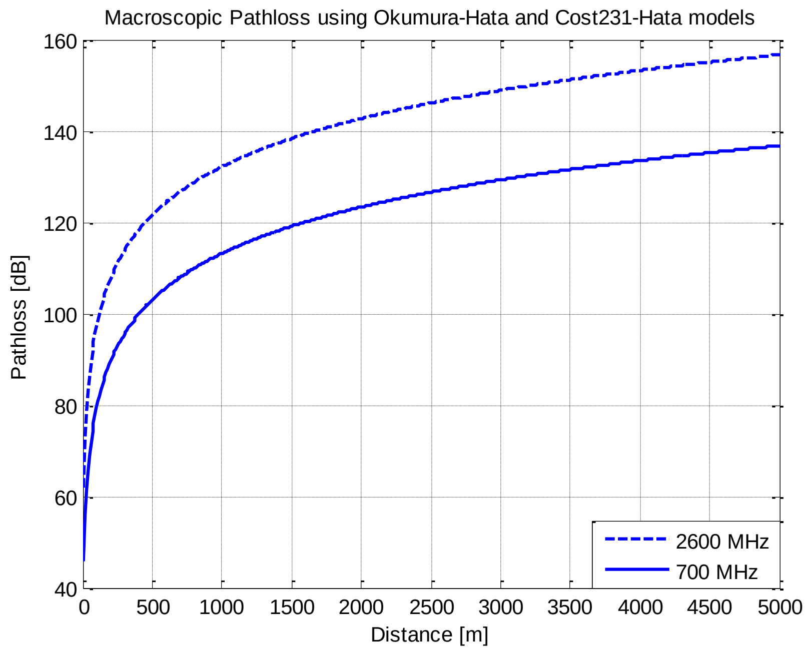

Figure 13: Path loss for two frequency bands in urban environment

3.3.2. Trunking Efficiency

When a set of devices all use a shared capacity, they can do so more efficiently than when that capacity is divided, and each device can only access some of the available capacity [64]. This is known as trunking efficiency. Therefore, when multiple non-contiguous multiple blocks of spectrum are allocated, the aggregation can result in a greater capacity than when they operate independently. This gain coming from trunking efficiency can be explained with this simple example. Assume a bursty transmission system with M equal bandwidth carriers and N users over each carrier can be represented as simple $M/M/1$ queuing system with λ arrival rate and μ departure rate. Little's law defines the average system delay as:

Equation 4

$$T = 1/(\mu - \lambda)$$

This is the delay experienced by users in each of the M carriers, when the carriers are operated independently with M different queues [46]. When the carriers are aggregated, it creates a one queue system with $M\lambda$ arrival rate and $M\mu$ departure rate. This makes the average system delay:

Equation 5

$$T_{SA} = 1/M(\mu - \lambda)$$

This shows a clear improvement in system performance.

3.3.3. Diversity

The concept of multi-user diversity states that in a large system--with users fading independently--at any time, there is likely to be a user with a very good channel. Opportunistic scheduling for best users of each carrier would result in throughput gain. With spectrum aggregation, there are more users for the scheduler to choose from, but with independent carriers, there are multiple schedulers, each with a fewer users. In addition, aggregation gives the scheduler more carriers to choose from, and these carriers might be in multiple bands, which result in a frequency selective scheduling gain.

3.3.4. Usable Bandwidth and Carriers Fragmentation

3.3.4.1. Carrier Fragmentation

Let’s assume the total bandwidth for a system is fixed at F MHz, while the number of spectrum fragments F is variable. As F increases, the “management overhead associated with frequency planning” increases [4]. As shown Figure 14, below, the two edges of each fragment or block require some form of coordination or management.

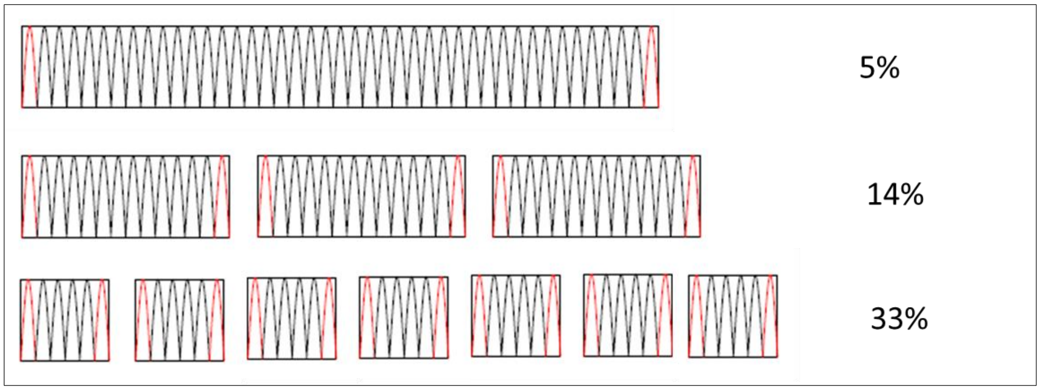

Figure 14: Illustration of the increase in coordination required as fragmentation increases (adapted from [4])

This coordination overhead could be one of the following types:

– Guardband: at the two edges of the spectrum block in order to avoid causing, or being affected by, interference to or from adjacent systems from the use the adjacent channels. Guardband setting depends on the characteristics of both systems, mainly their technology, power spectrum masks and bandwidth.

– Synchronization: coordination between the two systems in order to avoid the need to set a guardband in-between them.

– Degradation in performance: if power at the edges are minimized to avoid interference, the transmission rate will be at lower spectral efficiency levels

3.3.4.2. Guardband in LTE

Many papers (e.g. [64], [65], [66], [67], [68] and [69]) have analyzed adjacent channel interference (ACI) between LTE systems that use adjacent channels. In general, these studies show that the larger the edge guardband is set, the better the protection from causing or receiving interference. Multiple 3GPP technical reports, [70]- [71], derive the nominal guardband in an LTE system based on the bandwidth of the channel to be 5% of the channel bandwidth at each edge of the channel. As per the 3GPP minimum requirement for the limit on the adjacent channel leakage ratio (ACLR), this will produce enough edge guardband provided that the adjacent systems have the same bandwidth [70], use an FDD-based LTE system, and both networks utilize the adjacent spectrum for downlink transmission (i.e. are synchronized). If the adjacent system is LTE TDD, an additional guard band of 5 MHz between the two systems is required. If the adjacent system is GSM, UMTS or WiMAX, additional guard bands of up to 1 MHz are recommended [72] [73]. Non-mobile technologies like broadcasting services impose different requirements as well.

3.3.4.3. CA and Guardband in LTE

3GPP defines "carrier aggregation configuration" as a set of one or more operating bands across which the BS aggregates carriers [70]. Release 10 states that only two carriers can be aggregated. Aggregation can be within one of two defined bands for intra-band CA and it can be across two defined bands for inter-band CA. With the introduction of CA [74], use of a single nominal guardband can be considered, depending on the bandwidths of each aggregated carrier, the total bandwidth, and the number of carriers aggregated. However, setting guardbands for up to 5 aggregated carriers is more complicated. In addition to that, LTE future releases could allow contiguous carriers to utilize guardbands between them for data which would increase their efficiency compared to non-contiguous ones [75] [76]. As this work is still going on, many of these guardbands are still under FFS (for further study) status as more CA bandwidth configurations are being introduced (see Table 6, below).

Table 6: CA bandwidth classes and corresponding nominal guard bands (Table from [74])

CA Bandwidth Class	Aggregated Transmission Bandwidth Configuration	Maximum number of CC	Nominal Guard Band BW_{GB}
A	$N_{RB,agg} \leq 100$	1	$0.05BW_{Channel(1)}$
B	$N_{RB,agg} \leq 100$	2	FFS
C	$100 < N_{RB,agg} \leq 200$	2	$0.05\ max(BW_{Channel(1)}, BW_{Channel(2)})$
D	$200 < N_{RB,agg} \leq [300]$	FFS	FFS
E	$[300] < N_{RB,agg} \leq [400]$	FFS	FFS
F	$[400] < N_{RB,agg} \leq [500]$	FFS	FFS
NOTE: $BW_{Channel(1)}$ and $BW_{Channel(2)}$ are channel bandwidths of two E-UTRA component carriers according to Table 5.6-1.			

3.3.4.4. Assumptions about Usable bandwidth

Taking into consideration:

- the uncertainty about technology and bandwidth of adjacent systems for each block,
- the fact that guardband settings for CA systems are still under study by 3GPP,
- the advantage the contiguous 20 MHz spectrum system has because it can utilize in-between guardbands, and
- the expected additional coordination overhead for spectrum fragmentation,

we will assume two scenarios with regard to the guard bands in the LTE systems we analyze:

a) the first scenario: each spectrum block will need only the LTE built-in guardband of 10% of bandwidth, as shown in the first two columns of the table below, or

b) the second scenario: spectrum blocks, which, regardless of their bandwidth, are subject to ACI on subcarriers located within 1 MHz (the largest guardband in the LTE standard) from the channel edge, which will degrade the spectral efficiency at these subcarriers, as explained in the last two columns of Table 7, below. We will show results for this secondary scenario in Appendix B as a sort of sensitivity analysis for the first scenario results.

Table 7: LTE Guardbands and Assumed degradation of service due to ACI

Channel bandwidth	Edge guard band	Channel bandwidth	Assumed bandwidth at edge affected by ACI
20 MHz	1 MHz	20 MHz	0 MHz
10 MHz	0.5 MHz	10 MHz	0.5 MHz
5 MHz	0.25 MHz	5 MHz	0.75 MHz
3 MHz	0.15 MHz	3 MHz	0.85 MHz

To perform a simple test to understand the impact of the assumption we made in the second scenario, we now look at a system with a different number of spectrum blocks that comprise a total of 20 MHz of spectrum. This will make more fragmented-spectrum system, which since it is exposed to more adjacent channel interference as per our assumption, would have a lower total system capacity, as the example in the Figure 15, below, shows. In this example, we defined the system's theoretical capacity, which can be measured in bits/second, as the maximum rate that information can be transferred. Therefore, if the spectrum allocated has K subcarriers, the system capacity can be estimated as:

Equation 6

$$C = \sum_{i}^{K} SE_i \times B_i$$

Where SE_i and B_i are the spectral efficiency (in bps/Hz) for transmission over the subcarrier i with a bandwidth B (in MHz).

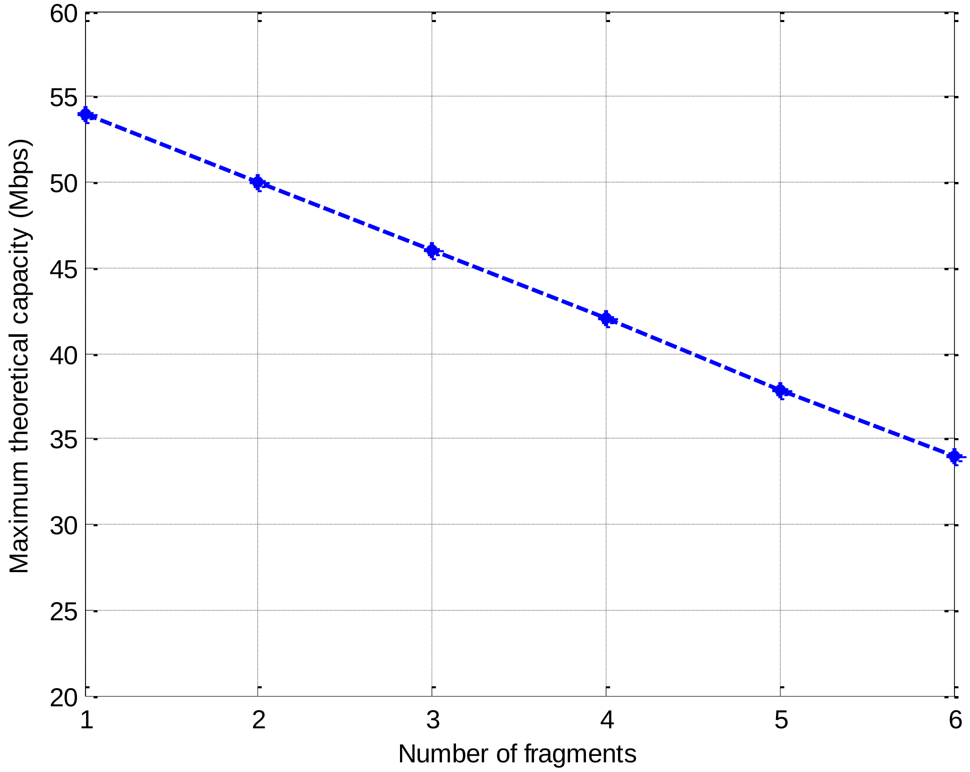

Figure 15: Impact of fragmentation on a 20 MHz system capacity based on worst case scenario with regard to ACI (1) one 20 MHz, (2) two 10 MHz, (3) two 5 MHz, one 10 MHz (4) four 5 MHz, (5) two 5MHz, three 3 MHz (normalized) (6) five 3 MHz, one 5 MHz

4. LTE Simulation Model

Vienna LTE system level simulator model was implemented using MATLAB and consists of many files and functions. We established some modifications in order to be able to run the spectrum aggregation scenarios, as summarized in the figure below. The first column shows the basic function executed by the simulator. The second columns shows the default value in the original simulator and the third column explain the changes in high-level description. In the following subsection, we explain these modifications in more details.

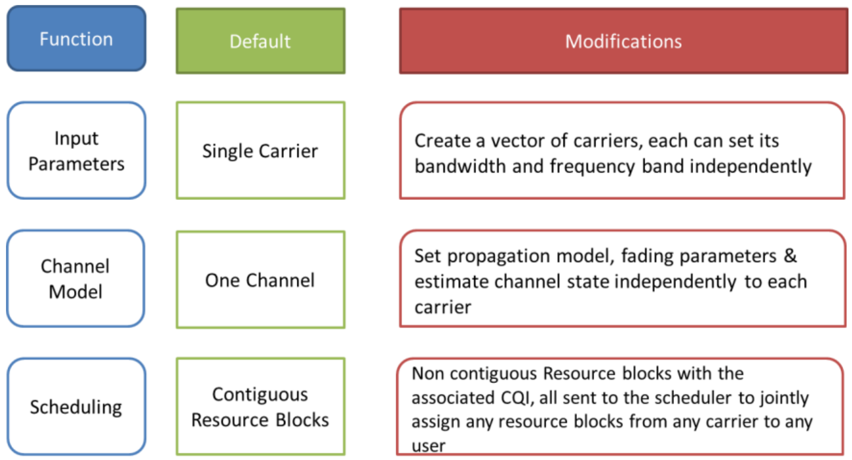

Figure 16: High-level description of modification done to the simulator to handle SA

4.1. Setting up Parameters

As noted earlier, spectrum-aggregation technology aggregates more than one carrier. Each carrier has its own frequency band and bandwidth. The simulator allows the user to define a single value for the two variables frequency (f) and bandwidth (B) both in MHz. Instead, we modified the simulator to accept multiple values for both variables, in which each pair represents values for a single carrier. Thus, if we assume as before that there are N carriers, the new frequency and bandwidth variables will be defined as follows:

Equation 7

$$f = [f_1, f_2, \dots . f_N]$$

where f_i represents the frequency band in MHz for the i-th carrier.

Equation 8

$$B = [B_1, B_2, \dots\ B_N]$$

Similarly, B_i represents the bandwidth in MHz for the i-th carrier. Then, the total bandwidth for the system will be defined as:

Equation 9

$$B_{tot} = \sum_{i=1}^{N} B_i$$

Since bandwidth in LTE standard is defined as:

Equation 10

$$B = 12 N_{RB} \Delta f$$

Where N_{RB} the number of resource is blocks and Δf is the subcarrier spacing which is set to be 15 kHz. In our modified simulator, number of resource blocks will be defined as:

Equation 11

$$N_{RB} = \sum_{i=1}^{N} N_{RB}^{i}$$

Where N_{RB}^{i} the number of resource blocks for the i-th carrier. This definition assumes that we can virtually stack all resource blocks belonging to multiple carriers next to each other to make the total bandwidth virtually contiguous.

In addition, other variables that will be affected due to the use of multiple bands carriers include transmit power and antenna gain. As earlier done to the frequency and bandwidth variables, we modify them in the simulator from scalars to vectors in order to be able to accept a unique value for each carrier the system uses.

4.2. Network Layout

4.2.1. Creating Set of eNodeBs

The simulator will generate a small LTE network with a number of cells, each with its eNodeB in the center based on specification of the following parameters:

– Inter eNodeB distance: specify the minimum distance between closest basestations, and

– Number of eNodeB rings: specify the number of eNodeB in the network.

Setting the inter eNodeB distance to 500 meters and the number of rings to 2 (6+12 neighboring cells) will allow the simulator to plot the following map.

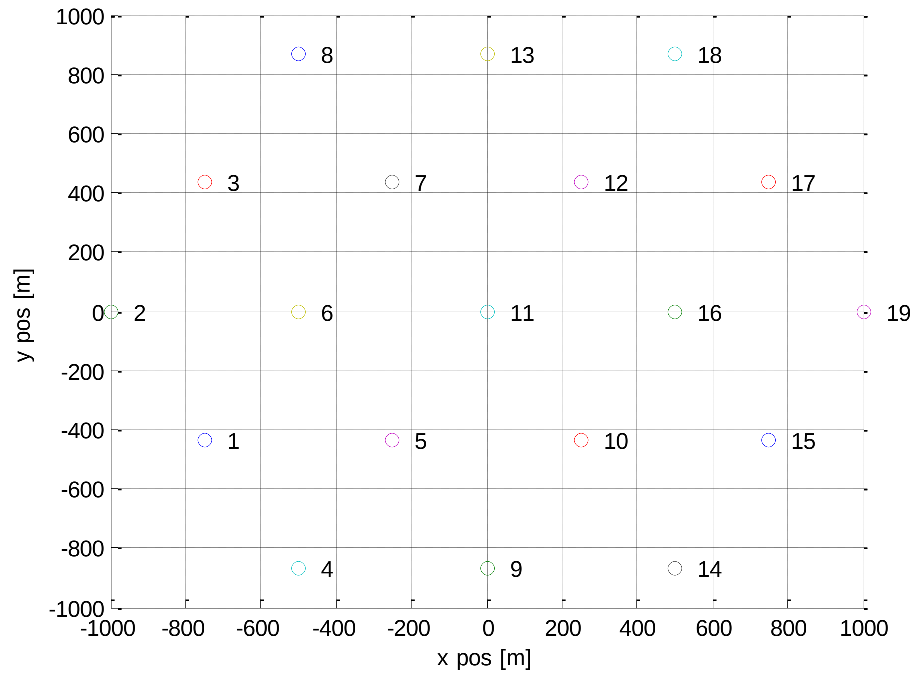

Figure 17: Scatter plot of hexagonal set of eNodeBs

4.2.2. Creating UEs

The simulator will place UE across the cells based on the value of the following parameters:

– Number of UE per eNodeB: specify number of UEs within the cell,

– Speed of UE: specify speed at which the UEs move in km/h, and

– Distribution of UE: how the UEs are generated over the Region of Interest (ROI).

Setting the number of UE per sector to 10 (3 sectors per cell) with constant UE per cell assuming fixed UEs will allow us to plot the map below.

We have to point out that eNodeB and UE generations required no modification, since they are unaffected by carrier frequency band or bandwidth, and they need to be executed only once as the original simulator does.

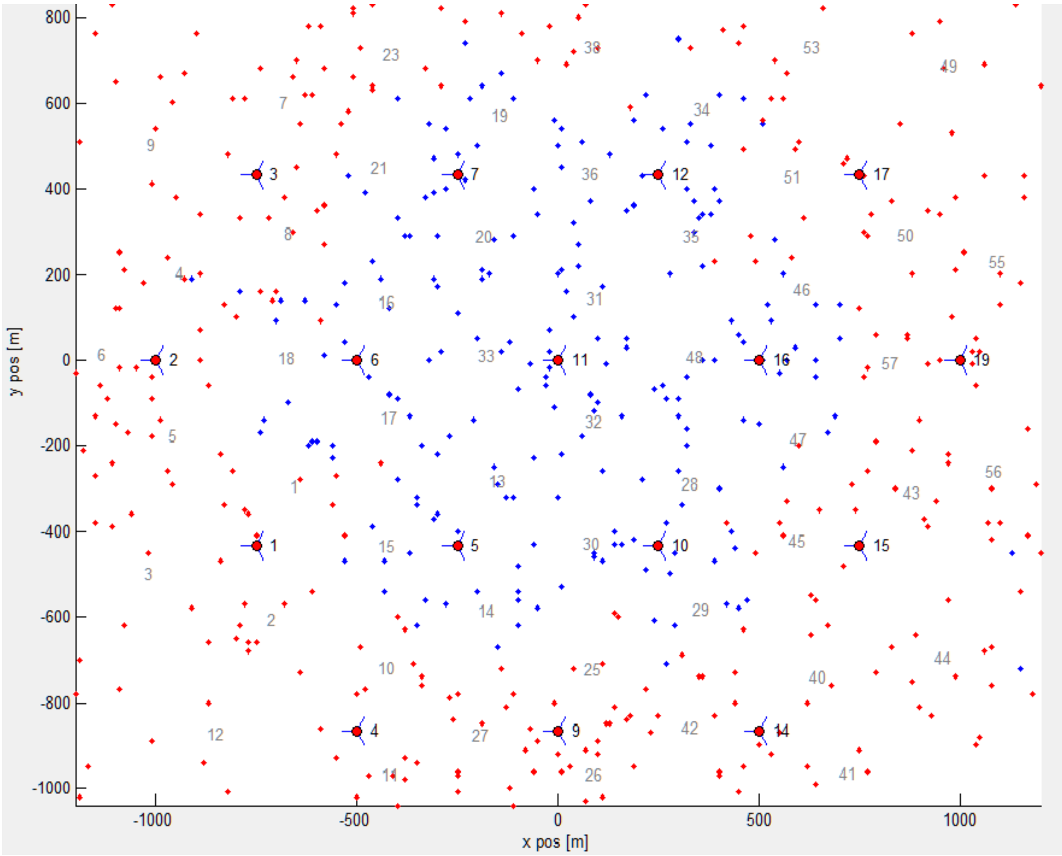

Figure 18: Scatter plot for UEs

4.3. Link Measurement (Channel Quality)

Then, the simulator will estimate the channel state information across the cell by calculating the path loss and fading maps for that cell. Path loss and shadow fading are calculated across the cell to generate network maps for each frequency carrier. In the modified simulator, the process is repeated for each frequency carrier, so each carrier will have its path loss, shadow fading and small-scale fading maps.

4.3.1. Path Loss Network Map

To calculate the path loss map across the cell, the simulator needs to first identify the following parameters:

- the frequency band of the carrier,
- the environment setting: urban, suburban or rural,
- the heights of the antennas,
- the path loss model: to specify which path loss equation is to be used, as discussed in the analytical overview section.

The simulator uses these settings along with the specifications of network layout generated earlier to start the calculation of path loss. The simulator uses the following steps to estimate the path-loss map:

- *Take as input the generated network map that shows eNodeBs layout*
- *For each eNodeB; save the selected frequency, environment settings and path loss model*
- *Generate distance matrix to estimate path loss at different positions across the map*
- *For each eNodeB; calculate pathloss using the equation of the chosen macroscopic pathloss model*

The last step is the only step that has been modified in the simulator to handle spectrum aggregation over multiple carriers. It now runs multiple times, once for each frequency band selected and generate and save multiple path loss maps.

Finally, the simulator will generate pathloss maps based on these calculations; one map for each frequency carrier. This map is generated by applying the path loss equation at different distances from the attached eNodeB. So, at any given position (x,y), there are estimated pathloss values of

$L_{P,\,b_i,u_j}$, where b_i donates eNodeB ($i = 0$ represents the attached eNodeB, $i = 1, \ldots N$ represents interfering eNodeB) while and u_j donates the position.

In Figure 19, below, path loss values for attached eNodeB are shown across the cell for two carriers: 700 MHz and 2600 MHz, respectively. The values of path loss for neighboring eNodeB's will be relevant when we do the budget-link calculation to estimate the interfering signal.

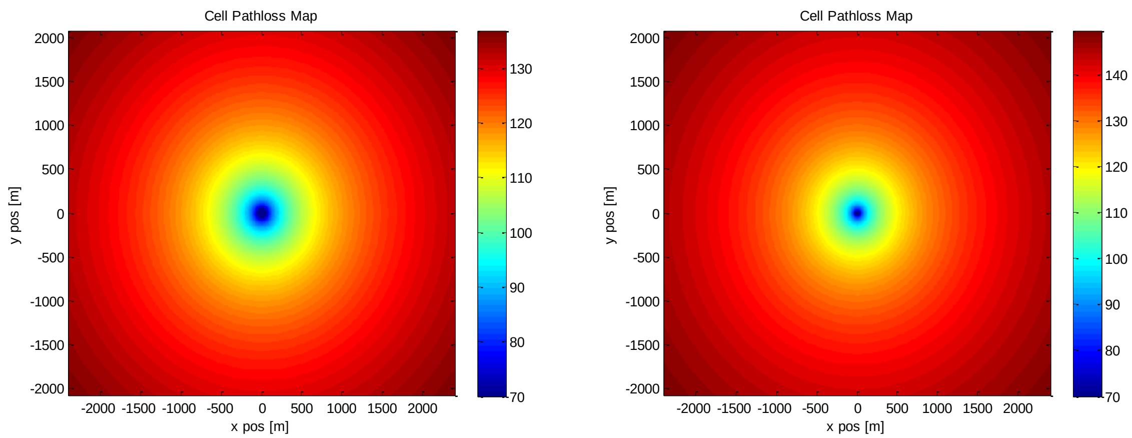

Figure 19: Cell pathloss maps for 700 MHz and 2600 MHZ carriers, respectively, in urban environment

Note that all plots in this chapter will be for systems in an urban environment. To avoid repetition and excess number of figures, plots for a system in suburban and rural environments are presented in Appendix C. In general, systems, in all environments, follow the same trend but at different scales.

4.3.2. Shadow Fading Network Map

Shadow fading represents the irregularities in geographic terrain that can affect the path loss. The simulator takes the following parameters:

- Mean and standard deviation: shadow fading can be approximated by a probability distribution like lognormal or two-dimensional Gaussian process.
- Inter-site shadow fading correlation: which represents the correlation between the sectors in a site.

For each frequency carrier, shadow fading is introduced as a Gaussian process with spatial correlation and with the use of inter-site correlation. This fading makes the user experience a slowly changing pathloss.

In this simulator, the shadow fading map generation is based on the following presumptions:

- *Take as input the generated network map that shows eNodeBs layout*
- *For each eNodeB; Shadow fading is log-normally distributed with mean 0 dB and standard deviation between 7 dB (for 700 MHz carrier) to 10 dB (for 2600 MHz carier). The Mean could be between 20 dB (for 700 MHz carrier) and 22.3 (for 2600 MHz) if we considered penetration loss in addition to the shadow fading.*
- *Correlation between eNodeB's shadow fading is fixed to 0.5*
- *For each NodeB; using the equation [*$Random\ matrix\ =\ mean\ +\ std *$ $randn\ (Ny, Nx)$*] generate a Gaussian map*
- *Calculate cross correlation between the generated Gaussian noises by computing the correlation coefficients between any two eNodeB's*
- *Calculate cross correlation between the generated shadow fading maps*

Similar to the path-loss map generation, we modify the simulator to generate and save a shadow-fading map for each frequency carrier as shown in Figure 20, below, such that at any given position (x,y), there are estimated shadow fading values of $L_{S,\, b_i, u_j}$, where b_i donates eNodeB ($i = 0$ represents the attached eNodeB, $i = 1, \ldots$ represents eNodeB's correlated with) while u_j donates the position.

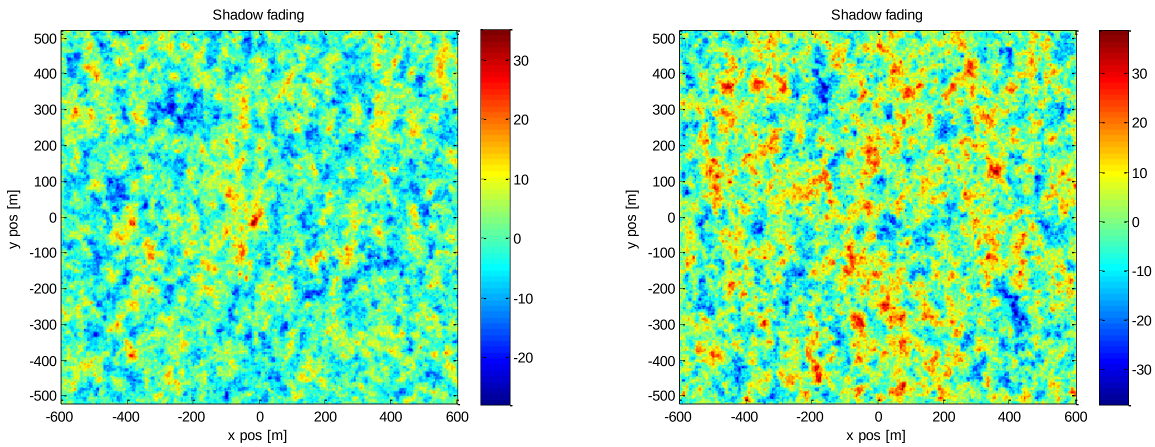

Figure 20: Cell shadow fading maps for 700 MHz and 2600 MHZ carriers, respectively, in urban environment

4.3.3. Small-Scale Fading and Channel modeling

Small-scale fading is a time-dependent process. It represents a trace of fading parameters showing the time variant behavior of the channel between the eNodeB and the UE like multipath fading and time dispersion due to mobility. It is modelled in the simulator as a one-dimensional random function of time. It takes the following parameters:

- Type of channel model: determine power delay profile (PDP) that specifies the multipath fading channel characteristics.
- UE speed and whether it's vehicular or pedestrian
- System bandwidth
- Trace length: to specify the channel trace in seconds

Then, the simulator takes the above parameters to generate the fast fading coefficient as follows:

- *Obtain a vector of average power parameters (in dB) and a vector of relative delays (in second) for the channel model chosen*
- *Load only the same channel parameters for each UE and eNodeB*
- *Generate fast fading coefficients for the simulation using the Rosa Zheng model* [77]

We modified the simulator in order to be able to generate multiple fast fading traces, one for each carrier. Channel Model types implemented in the simulator include 4G extended ITU channel models and Winner II+-based channel model. Based on the transmission mode, these estimated channel coefficients will be represented as a coefficient ${h_0}^2$ multiplied by the received signal power, and coefficient ${h_i}^2$ $(i = 1, \dots, N)$ multiplied by the *i-th* interfering signal power, as we will see in next section. We can produce a channel trace with a length of up to 10 seconds which would allow simulation runs for 10,000 TTIs.

4.3.4. SINR Calculation

To estimate the signal to interference and noise ratio (SINR) for each UE, the simulator will take the following parameters:

- Antenna gain
- eNodeB transmission power

Assuming an omnidirectional antenna with a Single-Input Single-Output (SISO) transmission mode, SINR for a given subcarrier and user u_j can be written as:

Equation 12

$$SINR_{u_j} = \frac{|h_0|^2 L_{P,\, b_0,u_j} L_{S,\, b_0,u_j} P_{t,b_0}}{\sigma^2 + \sum_{i=1}^{N} |h_i|^2 L_{P,\, b_i,u_j}\, L_{S,\, b_i,u_j} P_{t,b_i}}$$

Where:

- P_{t,b_i} is the eNodeB transmitting power, at *i=0* is the desired signal
- σ^2 is the receiver noise
- N is the number of interfering eNodeB’s

The modification done to the simulator in this part allows the calculation and saving of multiple SINR’s for the same user for subcarriers that belong to different frequency carriers.

Figure 21, below, show SINR distributions for two carriers at two inter-site distances. For the 2600 MHz carrier, the SINR mean across the cell drops from 9 dB to -9dB as we increase the inter-site distance from 500 m to 5 km, while the drop is only 4 dB from 9 dB to about 5 dB for the 700 MHz carrier. We can observe that at a low inter-site distance both frequency carriers have almost identical distributions.

.

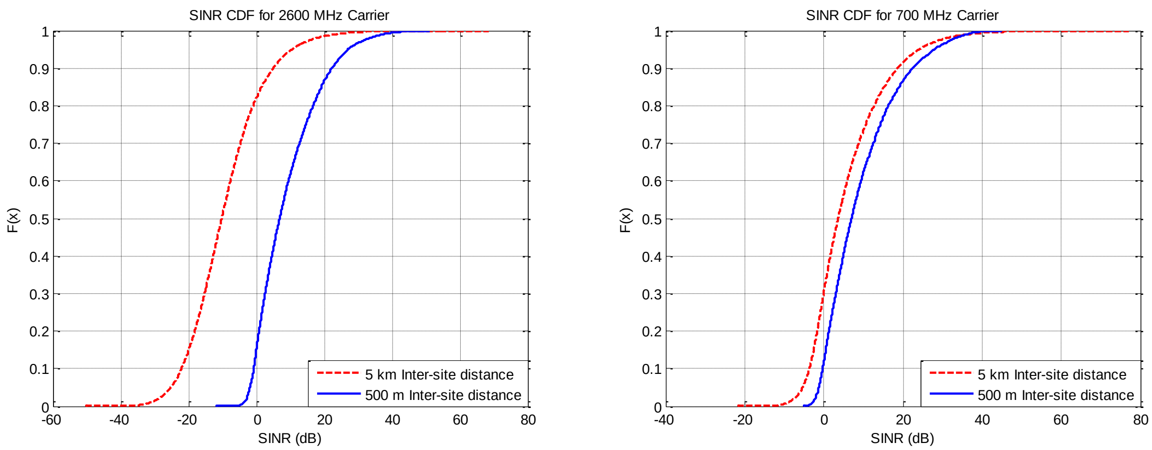

Figure 21: SINR distributions as inter-site distances change in urban environment

When we combine subcarriers from both frequency bands, we end up with an SINR distribution that has almost 0 dB for the 5 km inter-site distance, an improvement of about 8 dB over the system with all subcarriers in the 2600 MHz band exclusively.

To more closely investigate these results with some examples, we set a theoretical limit $SINR_{u_j} \geq S_R$, such that at the minimum SINR requirement ($SINR_{u_j} = S_R$) we have the maximum distance (d_{max}). The value of d_{max} is equivalent to maximum allowable path loss, or the coverage probability target which is usually set to 90% [78]. Figure 22, below, shows the estimated maximum distance for different frequency bands, assuming parameters are provided in [79],which states that -7.2 dB is the minimum SINR requirement for LTE technology [78], [80].

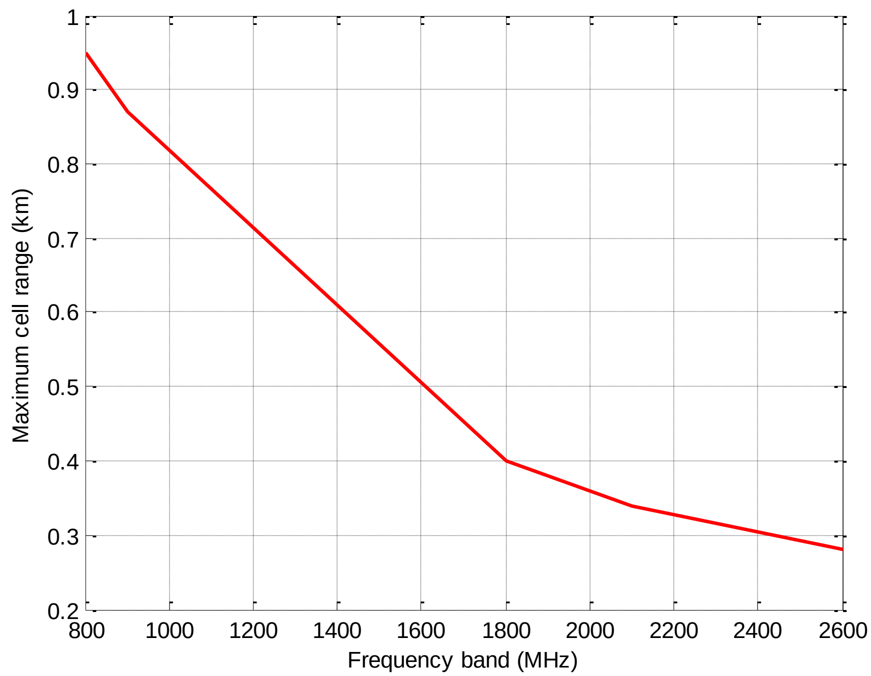

Figure 22: Cell ranges based on Okumura-Hata and COST 231-Hata propagation models in urban environment

The desired coverage probability function defines the probability that the sum of the path loss and the shadowing fading (plus penetration loss) to be satisfied. Based on values obtained from calculation in [78], this probability can be expressed as:

Equation 13

$$\varphi_{e,f} = \Pr[L_P(d) + X \leq L_{P,max} + L_{S+pn,margin}]$$

Where:

- e is environment
- f is frequency
- $L_P(d)$ is the path loss at distance d

– $L_{P,max}$ is the value of the maximum allowable path loss in dB

– $L_{S+pn,margin}$ is the marginal value of shadowing and penetration loss in dB

Figure 23, below, shows plots for coverage probability for users at the cell-edge, for six different systems with different inter-site distances (d_{IS}). Each system has 20 MHz (1200 subcarriers); the first five all have subcarriers in the same band (800, 900, 1800, 2100 and 2600 MHz) while the sixth system has 240 subcarriers in each one of these bands. This example shows the impact of the frequency band of allocated carriers, all of which could be in high frequency bands, low frequency bands or a combination of multiple bands.

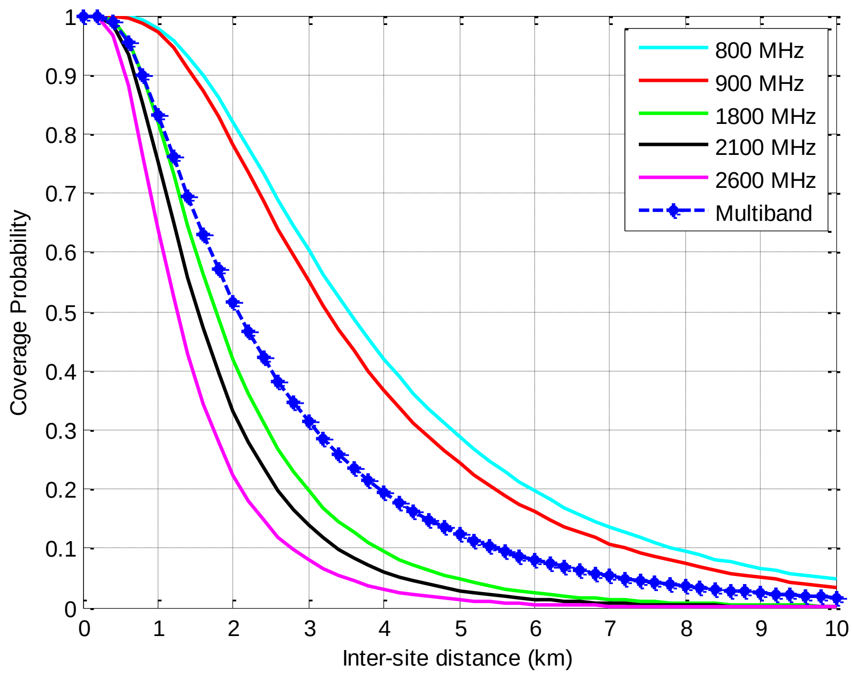

Figure 23: Coverage probability for a user at the cell-edge as frequency band and inter-site distance change in urban environment

Finally, this is how the distribution of SINR would like with a given 3 sectors-cell for the two carriers 700 MHz and 2600 MHz.

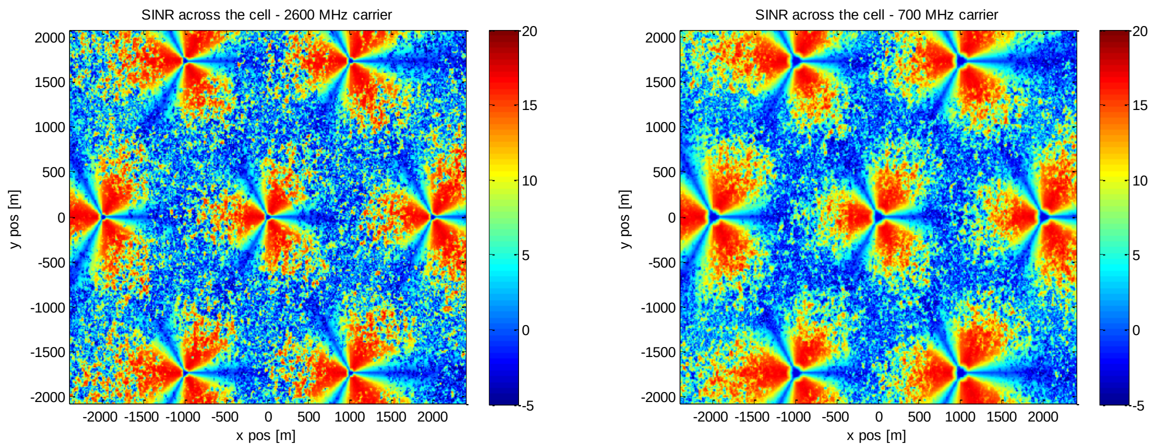

Figure 24: SINR throughout the cell in urban environment

4.4. Link Performance

After budget calculation, mapping from SINR (in dB) to capacity (in bps) need to be performed to allow the scheduler to assign spectrum resources properly in order to meet users demands.

4.4.1. Theoretical Capacity

Theoretically, capacity is upper-bounded by the very well-known Shannon limit:

Equation 14

$$C = BW \log_2(1 + SINR^L)$$

Where BW is the usable bandwidth in Hz and $SINR^L$ is a linear power ratio. Usable bandwidth in LTE requires consideration of correction factors as follows:

Equation 15

$$BW = B.CP_R.RF_R.SS_R$$

Where B is defined earlier in section 4.1, LTE bandwidth, which is dependent on the number of RBs (N_{RB}). CP_R is the Cyclic Prefix ratio which is defined as:

Equation 16

$$CP_R = 1 - \frac{2\ CP.CP_S}{f_s.TTI_l}$$

Where:

- CP is the cyclic prefix which is set to be 6 in the normal case
- CP_S is the cyclic prefix sample length which is dependent on the number of RBs
- f_s is the sampling frequency which is defined as the subcarrier spacing (15 kHz) multiplied by FFT points; and
- TTI_l is the length of TTI which is set to 0.001 seconds

While RF_R is the reference system ratio which is the ratio of the reference symbols to the total subframe symbols, and SS_R is the synchronization system ratio where 72 symbols are used for synchronization every 5 subframes.

We can calculate the CDF of the theoretical cell average capacity by calculating the value of C for each SINR value we have from the link measurement subsection, cf. Figure 25 below.

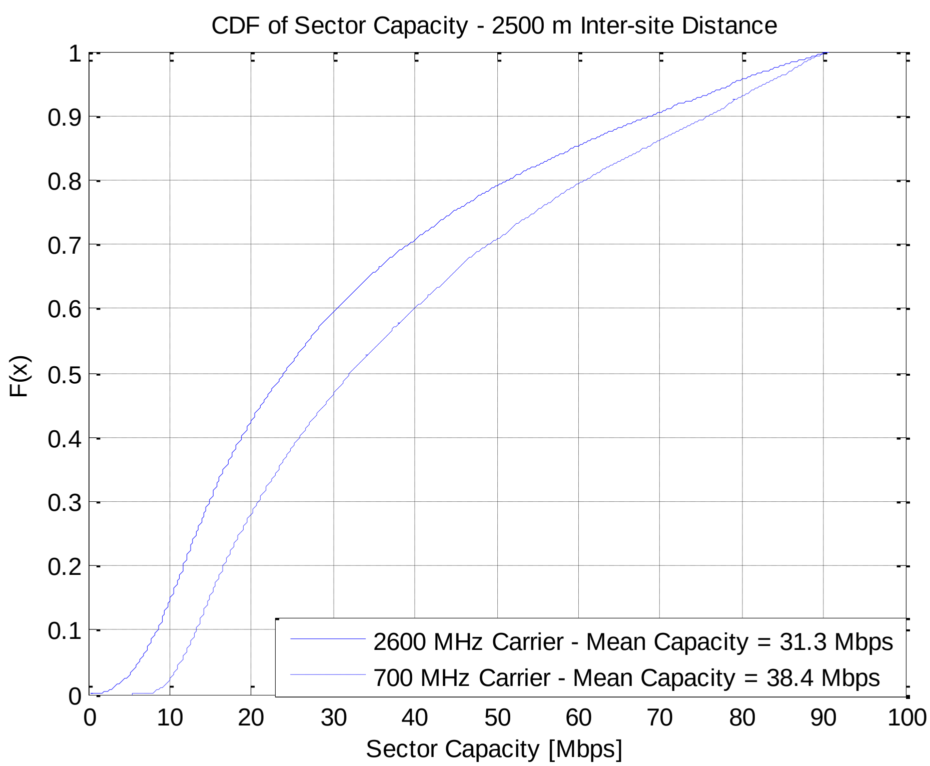

Figure 25: Sector Capacity based on Theoretical Calculation for SISO system in urban environment

4.4.2. SINR to Bit Mapping

LTE networks are designed to target a Block Error Rate (BLER) threshold that shouldn't be exceeded. The BLER is directly proportional to the spectral efficiency (b/s/Hz) and inversely proportional to the SINR, as shown in the Figure 26, below, for a SISO system. Thus, in order to reduce the BLER to the target level, either the SINR has to be increased or the modulation and coding scheme (MCS) has to be decreased.

.

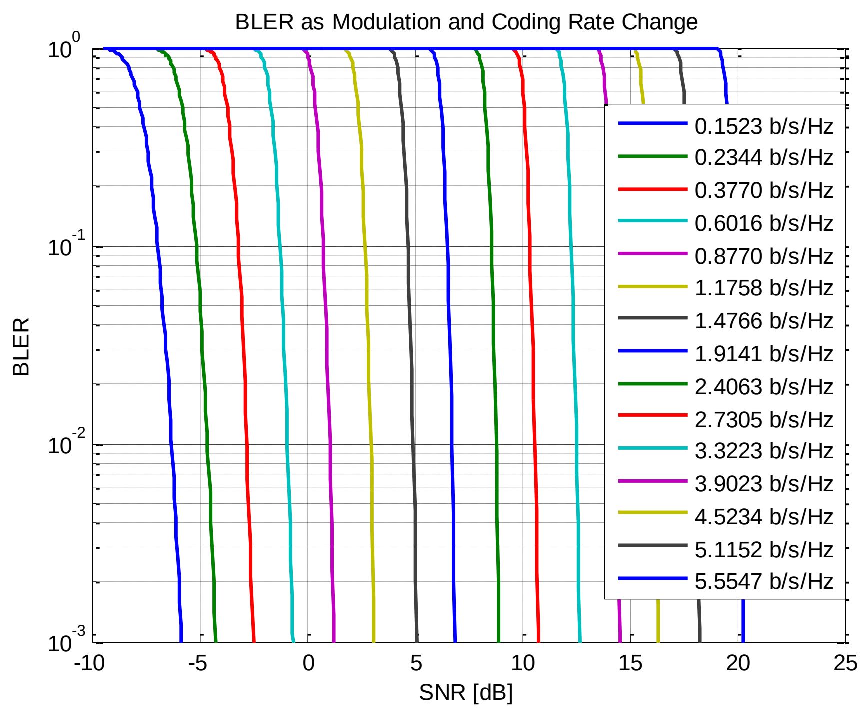

Figure 26: BLER as function of SINR and spectral efficiency

These BLER curves are abstracted from the measurement and analysis of the LTE link level to be used to map the SINR into spectral efficiency. The Channel Quality Indicator (CQI) has values ranging from 0 to 15. As Figure 27, below, shows, the mapping function will assign a given UE a CQI value based on its SINR. Then, the CQI values as a group will allow eNodeB to send to the UE at certain bit rates, as shown in the previous figure, to maintain the target BLER, which is 10% in this mapping.

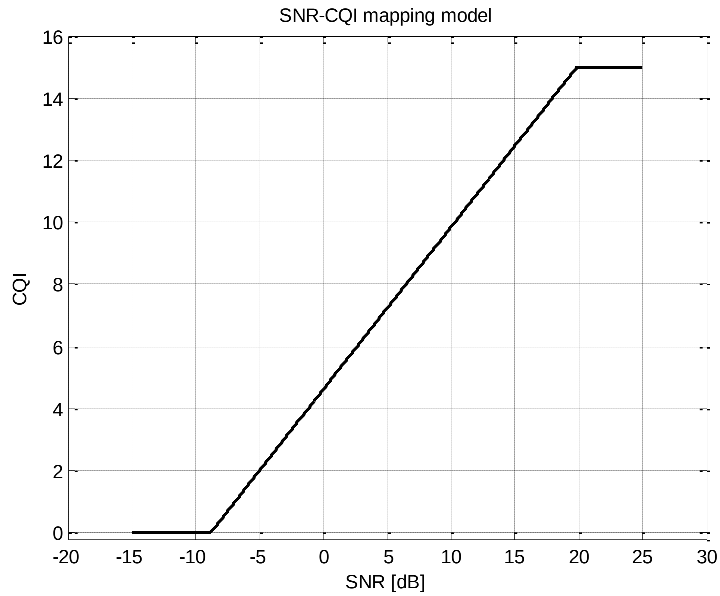

Figure 27: SNR-CQI mapping function

The last figure shows a typical CQI distribution across the cell. Due to the difference in SINR density between the two carriers, we can see with the 2600 MHz carrier more UE's are assigned lower CQI's.

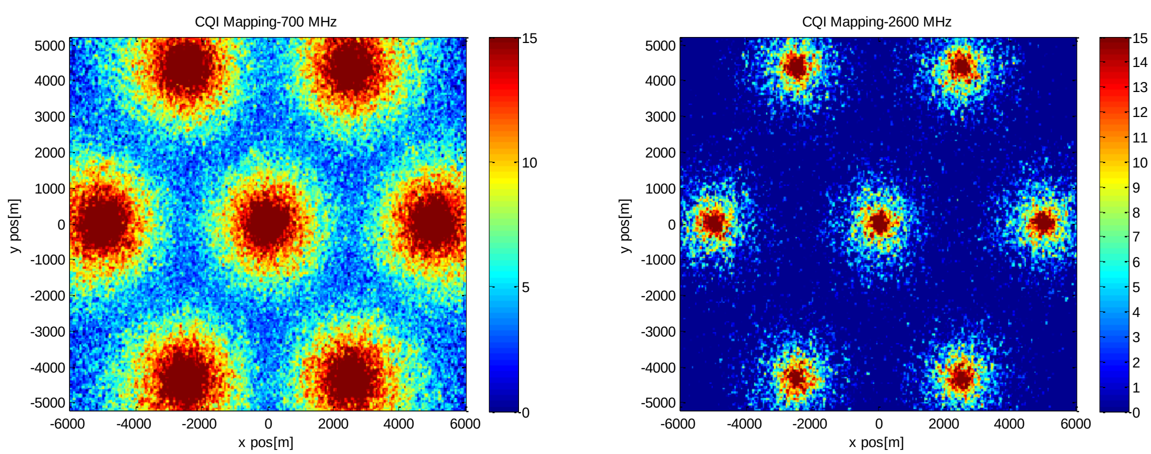

Figure 28: CQI mapping across the cell for two frequency carriers

While we did no modification on this part of the simulator, the process of assigning CQI values to carriers for users was affected because of the introduction of multiple carriers. We will discuss this in the next section, on initialization and feedback.

4.5. Initialization and Feedback

The initialization process simply means allowing UE's and eNodeB's to read all related information that was estimated by the simulator and saved earlier in different network maps. Then, the parameters that have been initialized in before the first simulation run will be updated following each subsequent run based on changes in the UE location (which affects SINR), in traffic, and in small-scale fading.

The downlink carrier is represented here as a time-frequency resource grid consisting of Resource Blocks (RB). Without going into details of LTE literature here, the eNodeB scheduler must assign these time-frequency resources to different users within the cell based on different factors, including the CQI assigned to that UE based on its SINR. The simulator saves a single SINR value for each UE with the carrier after applying path and shadowing losses. After applying fast fading because it is a frequency-time variant, a different CQI value might be assigned to each group of resource blocks within that carrier. Because in the system we simulate we have multiple carriers, we modified the initialization process to allow UEs and eNodeBs to read from multiple maps that have been generated and to store multiple CQI values, one for each set of resource blocks. Moreover, we introduced an indicator that identifies which carrier each RB belongs to. This could be helpful to processes like scheduling.

In summary, the simulator will carry out the following parameters initializations (some of which will be updated for each simulation loop based on feedback):

- *UE Initialization: for each UE;*
    - *Set the fast fading from eNB to the attached UE based on the selected channel model*
    - *Give the UE access to the pathloss map and shadow fading map*
    - *Give UE access to the RB gird within the carrier (modified to allow UE access multiple RB grids, one for each carrier)*
- *Specify the feedback channel delay time to synchronize updating the parameters when the simulation loop starts*
- *Give the eNB schedulers access to the attached UE channel information and traces*

4.6. Traffic

There are different traffic models that can be used in the simulation, as shown in the table below [81].

Table 8: Traffic models

Traffic Model	Description
Full buffer model	A simplified version of the traffic received/transmitted by a user in a data session. The number of users in the cell is constant and the buffers of the users' data flows always have an unlimited amount of data to transmit
Finite buffer (FTP traffic model)	A best-effort model. A user is assigned a finite payload to transmit or receive when it arrives, and it [Q: what is "it"?]leaves the system after the payload transmission or reception is completed. Multiple users within the network are not active simultaneously.
HTTP traffic model	An interactive traffic model where a web-page consists of a main object and embedded objects. Burst-traffic model is a simplified model of HTTP traffic with a fixed packet size that is used to save simulation time.
Video Streaming	Each frame of video data arrives at a regular interval T determined by the number of frames per second. Each frame is decomposed into a fixed number of slices, each transmitted as a single packet. The video encoder introduces encoding delay intervals between the packets of a frame.
Gaming	an interactive real-time model. A mobile network gaming user is in outage if the average packet delay is greater than 60 ms. The average delay is the average of the delays of all packets, including the delay of packets delivered and the delay of packets dropped

There are no changes done to this part of simulator. As recommended by 3GPP guidelines [35], full buffer and finite buffer models are mainly used to test performance.

Full Buffer traffic is modeled in the simulator mainly by fixing the number of active UEs and assuming buffers of the users' data flows always have unlimited amounts of data to transmit. Finite Buffer Traffic is simulated with Poisson UE arrival rate (λ) with a fixed finite buffer of (X) Mbits payload for each UE. The offered load per cell can then be defined as:

Equation 17

$$L = \lambda X$$

Assuming there are K users in the system, traffic intensity can be measured as [47]:

Equation 18

$$\lambda_T = \lambda K$$

4.7. Scheduling and Carrier Selections

In the original simulator, the scheduler applies its algorithm directly to the single carrier available by assigning different resource blocks to different users. Introducing multiple carriers requires a careful modification to the simulator to deal with it correctly. In the initialization discussed earlier, each resource block has an index that identifies which carrier the RB belongs to. This is then used in scheduling, as we will see in next subsections.

4.7.1. Joint Scheduling for Spectrum Aggregation

As explained earlier, spectrum-aggregation capability should allow us to assign resource blocks from multiple carriers to the same user simultaneously. This means that the scheduler will effectively see only one single carrier that has resource blocks equal to the sum of all resource blocks from all the carriers. As shown in Figure 29, below, we can stack all the resource blocks next to each other to represent the virtual contiguity the schedule sees. After this, the scheduler applies its scheduling algorithm to assign resource blocks to specific users. This shows that no direct modification needs to be done to the scheduling process in the original simulator in order to perform joint scheduling.

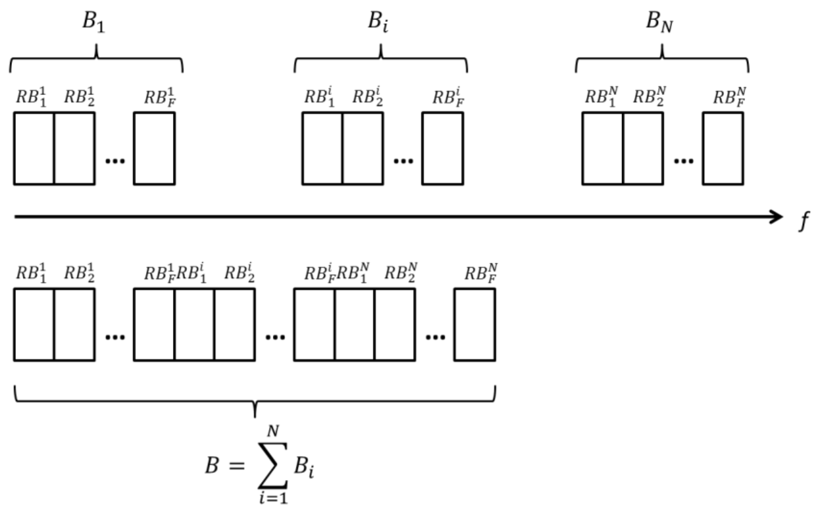

Figure 29: Stacking all subcarriers to create virtual contiguity for the joint scheduling

4.7.2. Carrier Selection for Independent Carriers

In independent carrier operations, the scheduler can assign to a given user resource blocks from only a single carrier. This requires us to make scheduling a two-step process:

- Step 1: select a carrier for a given user
- Step 2: assign resource blocks within that carrier

We perform the first step to the simulator by introducing an algorithm that select a carrier for each user based on the UE's location, CQI and load in each carrier. Here are the steps of the simple algorithm:

- *Estimate the average CQI for each UE j across all N carriers as:* $CQI_{ave}^{j} = \sum_{j=1}^{N} \frac{CQI_j}{N}$
- *Set a threshold CQI value (*CQI_{th}*) to identify cell edge user, such that user i is identified as cell edge user if:* $CQI_{ave}^{j} < CQI_{th}$
- *For all UEs:*
    - *If* UE_j *is cell edge user, select the carrier i such that:* $f_i \geq \{f_1, f_2, \dots f_N\}$
    - *Otherwise, select carrier with lowest number of users*

4.7.3. Scheduling Algorithms

There is no modification to this part of the simulator. After we form a single queue for joint scheduling in SA or select a carrier for each user and form multiple queues in IC, we apply a scheduling algorithm to assign RBs to users. Many scheduling algorithms for SA have been proposed; Cross-CC PF [49], which collects users previous throughput information and selects CCs based on users' SA capability. It increases fairness and exploits SA advantage. User grouping PF [51] divides users according to how many CCs they can be served by, then starts selections. In general, there is a trade-off between performance and fairness when designing a scheduling algorithm. For example, an algorithm that simply maximizes throughput would assign most of the resource blocks to devices that are closest to a cell tower, and thus can get a higher data rate with any given resource block, while devices at the edge of the cell may starve. This disparity could be even greater in an inter-band scenario, where devices close to the cell tower dominate use of the low-frequency bands.

For this simulation, we choose to apply the well-studied Proportional Fair (PF) scheduling algorithm [83] [84]. With this scheduling algorithm, users compete for resource blocks not based on their requested rates exclusively. Instead they compete after normalization by their respective average throughputs. The user with better channel quality will have a higher average throughput.

4.8. Simulation Loop

The path loss and shadow fading are position-dependent which makes them time-invariant. The simulator will generate these two maps for each frequency carrier and save them to be used for the rest of the simulation. They are assumed to be maintained constant for each UE, but fast fading is updated every TTI independently for each frequency carrier based on the chosen channel-model parameters. As shown in the Figure 30, below, the simulation loop starts after each UE is initialized, and it will run TTI times. Within the loop, the algorithms of the chosen traffic model(s) and scheduling assignments will be accessed for each TTI round. Information from the generated network will be available for each run, first through UE initialization and then by being updated periodically as feedback to the UE to replace information stored during initialization. As seen here, no modification to the simulation loop is needed to deal with multiple carriers. Instead, each element of this loop (i.e., input parameters, path loss map, scheduler, etc.) has been already modified to handle multiple carriers.

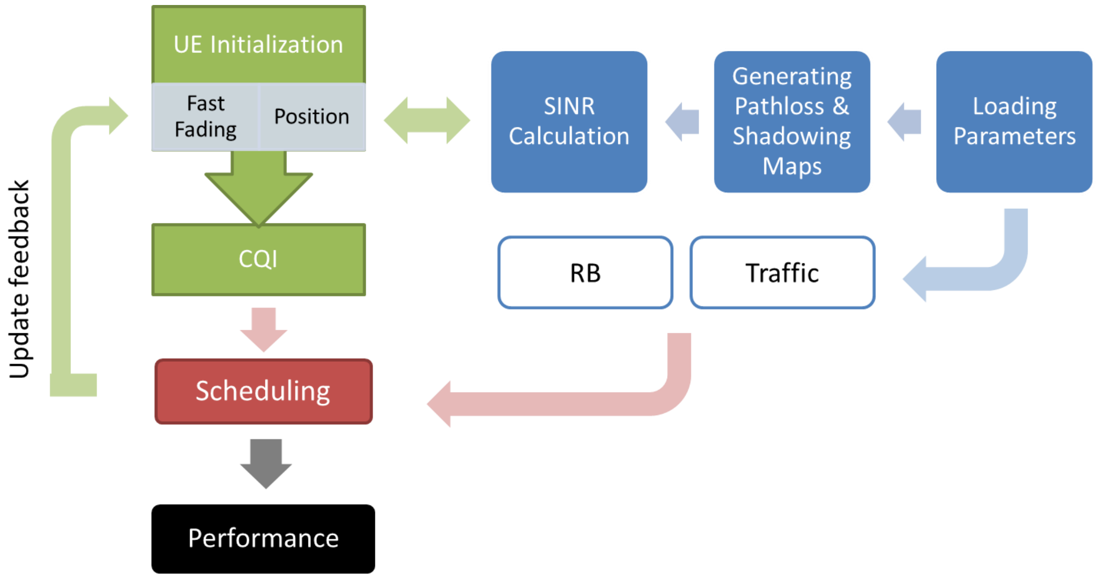

Figure 30: Simulation loop (on left)

4.9. Measuring Performance

Different metrics for the performance can be measured. At the end of the simulation, the simulator will provide all UE and eNodeB traces, which can then be used to measure these metrics.

4.9.1. Throughput

The simulator allows us to estimate the throughput for any user *k* using the following formula:

Equation 19

$$T_{UE}^{k} = \frac{\sum_{m=1}^{M} b_m^k}{M^{*}.T}$$

Where:

- M is the total number of TTI's and $M^{*}$is the number of TTI's at which user k transmit data
- b_m^k is the number of bits user k transmits at TTI = m

- T is the length of TTI in seconds

Having estimated average throughput for each UE, we now have a distribution of throughputs within a given cell. We can thus estimate the (average UE throughput) by estimating the mean of the distribution, the (peak UE throughput) by estimating the 95% percentile and the (edge UE throughput) by estimating the 5% percentile. In addition, the average system throughput can be measured with the following formula:

Equation 20

$$T_{Cell}^{ave} = \frac{\sum_{k=1}^{K} \sum_{m=1}^{M} b_m^k}{M.T}$$

Where: K is the total number of users in that cell. Throughput is usually measured when applying full buffer traffic. The finite buffer traffic model can be used to measure throughput at different density levels of users.

4.9.2. Fairness

Fairness is another metric that measures system performance. This index measures the equality of allocating RBs to UEs. Thus, if the eNodeB assigns RBs to K users, such that user k will have average UE throughput of T_{UE}^{k} , then fairness index can be defined as [83]:

Equation 21

$$FI = \frac{\left|\sum_{k=1}^{K} T_{UE}^{k}\right|^2}{K \sum_{k=1}^{K} {T_{UE}^{k}}^2}$$

When $FI = 1$, this means the system is 100% fair. This metric is important to test how fair the system is to users with low channel quality at the edge of the cell. Usually, such a measure is used to compare scheduling algorithms; however, it will be used in our analysis to compare SA and IC systems that use frequencies from multibands where cell edge users are sensitive to frequency bands.

5. Inputs and Assumptions

5.1. Main Inputs

Table 9, below, shows the main input assumptions concerning the allocated spectrum carriers and the way they are being operated. While the total bandwidth is set to B MHz for each network, the differences in the number of fragments, their frequency bands and whether they are aggregated or operated independently will create the five different scenarios we will simulate. Many of these assumptions and other assumptions to follow are either recommended by 3GPP guidelines [35] for simulating LTE systems or are default values as assumed by the Vienna Simulator.

Table 9: Main inputs related to frequency bands

Total bandwidth	20-80 MHz	
Block bandwidth	5, 10 and 20 MHz	
Number of fragments	From 1 to 5 blocks.	
Transmit power	43 dBm for 5 MHz bandwidth carriers, and 46 dBm for 10 and 20 MHz bandwidth carriers [35]	
Frequency Bands	700 MHz	2600 MHz
Antenna Gain	12 dBi [58]	15 dBi
Path loss model	Okumura-Hata [58]	COST 231-Hata
Shadow fading STD	8.8 dB [79]	10 dB

5.2. Variable Inputs

We vary some network parameters depending on the target output in order to see the impacts.

5.2.1. Traffic Models

Depends on the output we are looking for, we alternate between finite buffer and full buffer traffic models. For finite buffer model, we assume a fixed payload size of 2 Mbit and variable Poisson arrival rate.

5.2.2. Environment

The environment could be rural, suburban or dense urban. Changing this input will affect the propagation models and population density.

5.2.3. Active users

We vary the number of users from 10 to more than 200 users based on the selected environment. We also change the arrival rate for the finite buffer traffic model.

5.2.4. Inter-site distance

We vary the inter-site distance from 200 m-10km. Depending on the scheduling, users at the cell edge will be affected the most.

5.3. Fixed Assumptions

Table 10, below, shows constant parameters of the network that are inserted as inputs to the simulator. The values are based on 3GPP guidelines mentioned earlier

Table 10: Constant input assumptions and system configuration

Antenna configuration	2x2 MIMO	Feedback channel delay	3 TTI
Transmission Mode	CLSM	SINR averaging algorithm	MIESM
TTI length	0.001 s	Sectors per cell	3
Simulation Time	10,000 TTI	UE antenna gain	0
RB Bandwidth	180 kHz	Channel model	Winner II+
Noise figure	9 dB	Channel Trace length	5 s
Thermal noise density	-174	Coupling loss	20 dB
UE distribution	Uniform	UE speed	5 km/h
Antenna azimuth offset	30	Site height	20 m
Antenna downtilt	8	Receiver height	1.5 m

6. Results and Discussion

As per the scenarios listed earlier and the assumptions made in the previous section, we ran the simulation trying to test the impact of SA and the use of multiple bands on the wireless network performance. The simulation scenario is a 3GPP Macro-cell case with 19 sites and 3 sectors per site in keeping with 3GPP guidelines. We focus mainly on measuring the relative throughput gain and loss for each scenario. This is because throughput will be the main metric that we will use in subsequent chapters' analyses. In this section, all results are for urban environment systems. To avoid plotting many figures and because they show comparable results to urban but at different scale, suburban and rural environment systems results will be reported in Appendix C.

6.1. Throughput

We simulate three different sets of scenarios: contiguous spectrum (two scenarios), non-contiguous independent carriers (three scenarios) and non-contiguous spectrum aggregation (three scenarios), as we described them earlier in section 3.1. In the case of non-contiguous carriers, we assume the system has two carriers, each with a 10 MHz bandwidth, while the contiguous carrier is assumed to have a single 20 MHz bandwidth. We assume full buffer traffic with 20 users per sector in an urban environment. We run the simulation for the total of eight scenarios at different inter-site distances ranging between 500 m and 7 km. In addition, we don't assume any need for an extra guardband other than the built-in LTE guardbands for both contiguous and fragmented systems. This assumption made the intra-band SA scenarios cases have the same exact performance of the contiguous two scenarios, when we ran the simulation long enough. Therefore, we will not plot the two intra-band SA scenarios in the coming few figures. Figures 31 and 32, below, show the average system throughput and average UE throughput, respectively.

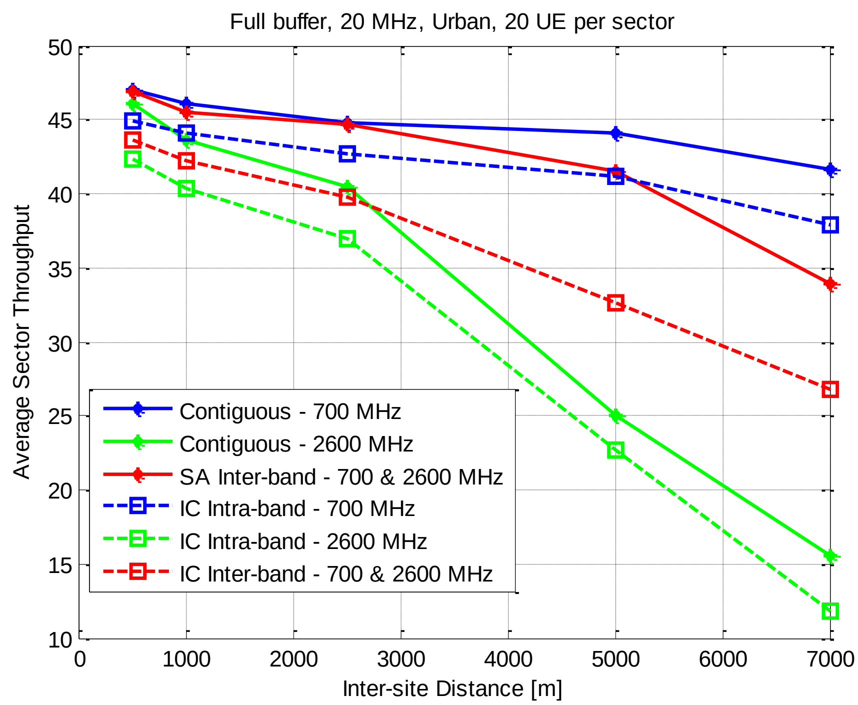

Figure 31: Average system throughput (Mbps) as inter-site distance changes

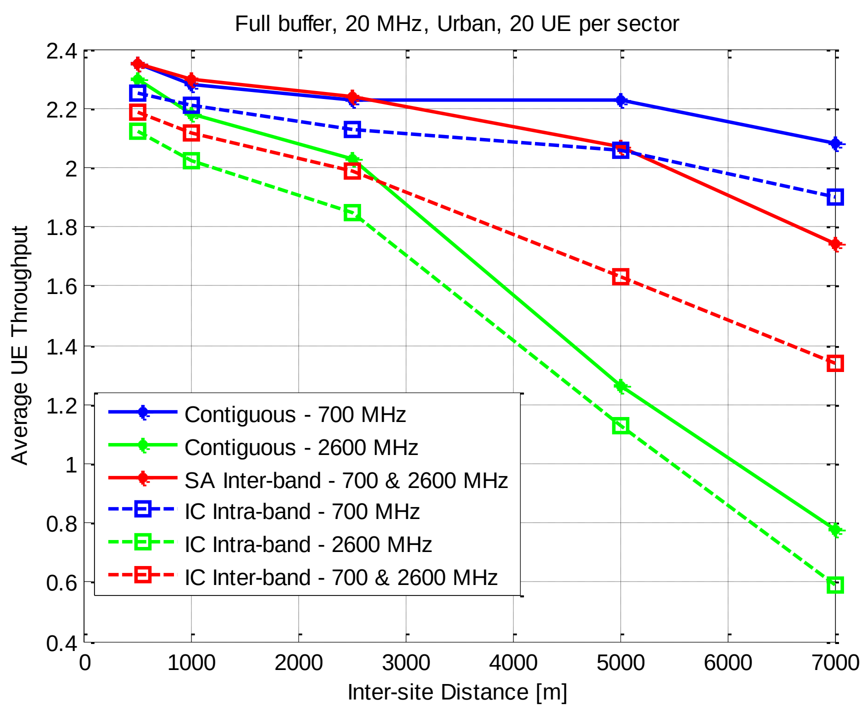

Figure 32: Average UE throughput (Mbps) as inter-site distance changes

First, we perform a series of simulation runs in order to obtain high confident results. Although repeating the simulation 100 times could be good enough as per 3GPP guidelines, we repeat it 1000 times which is sufficient to get robust results when compared to 500 times repetition. Because the channel is fast-fading and the simulation time is much longer, confidence intervals are very small. The different plots show that at short inter-site distances, below 1 km, the difference in path loss between different frequency bands has an insignificant effect on throughput. This is because users are close enough to the eNodeB to be served by both frequency carriers at relatively close SINR. At these small distances, we observe little gain for SA systems of around 7% over IC systems. This gain can be attributed to the larger multiuser diversity of these systems, which gives the scheduler more carriers to choose from for each UE. By continuing to compare systems that use the same frequency carriers but differ operationally, we note that the throughput gain increases to about 40% at 7 km inter-site distance. This is because the multiuser diversity becomes more significant as user density decreases within a cell as a result of the increase in inter-site distance. We also see that as the distance increases, frequency becomes a more significant factor, such that systems with only 2600 MHz carriers will have throughput equals to 35% and 45% of the throughput of systems using either only 700 MHz carriers or both types of carriers, respectively. In addition, inter-band systems have an extra advantage of frequency selective scheduling gain.

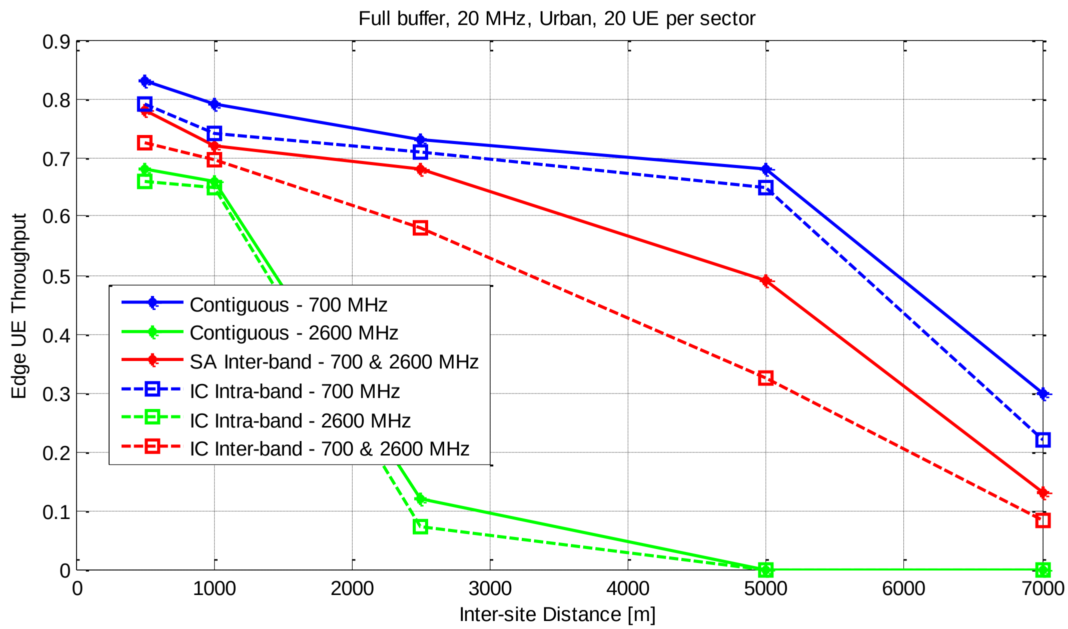

Figure 33: Throughput (Mbps) for UE at the cell edge

Looking at the edge of the cell UE throughput (Figure 33, above), we can see that systems with carriers only in the 2600 MHz range will stop serving edge UE beyond approximately 3 km of inter-site distance, while systems having access to a 700 MHz carrier will be able to serve edge UE beyond as much as 7 km of inter-site distance. As with the average UE throughput, edge UE throughput shows some gain over IC when SA is in use. This improvement is not as large as before because both systems will ultimately assign users to the 700 MHz carrier only.

When we fix the inter-site distance at 3 km and vary the user density per cell, we observe a number of differences in average UE throughput for each system, as Figure 34, below, shows. Moving from the 700 MHz to the 2600 MHz systems produces a gain of about 50% in throughput due to the advantage the lower frequency band has in wave propagation characteristics. We now re-plot this figure with only two scenarios where one uses SA and the other uses IC on inter-band frequency, as Figure 35, below, shows. Again, the SA system shows approximately a 20% gain over the IC system due to multiuser diversity, which decreases as density increases. To study the diversity more closely, we change the traffic model to a finite buffer with a fixed payload size of 2 Mbit and variable Poisson arrival rate. Since 1,000 TTI is equivalent to 1 s of time, which arguably might not be enough to measure the performance based on 2 Mbit payload of data, we increase the simulation runs to 10,000 TTI. This significantly slowed the simulation but it doesn't show significant improvement in the results, which allow us to claim that 1000 TTI should be enough to measure performance at the finite buffer case.

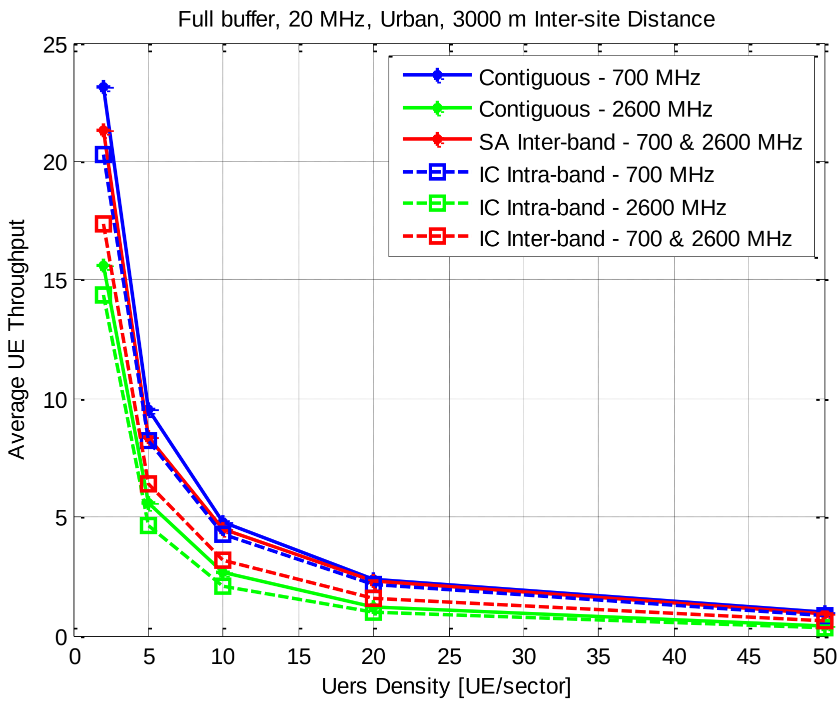

Figure 34: Average UE throughput (Mbps) as user density changes

Figure 36, below, shows that multiuser diversity combined with trunking efficiency resulting from joint scheduling provides the SA system with a gain in throughput starting from around 40% at the low arrival rate and decreasing gradually until it disappears altogether as active user density becomes significant. This confirms previous results showing that multiuser diversity gain diminishes when user density increases.

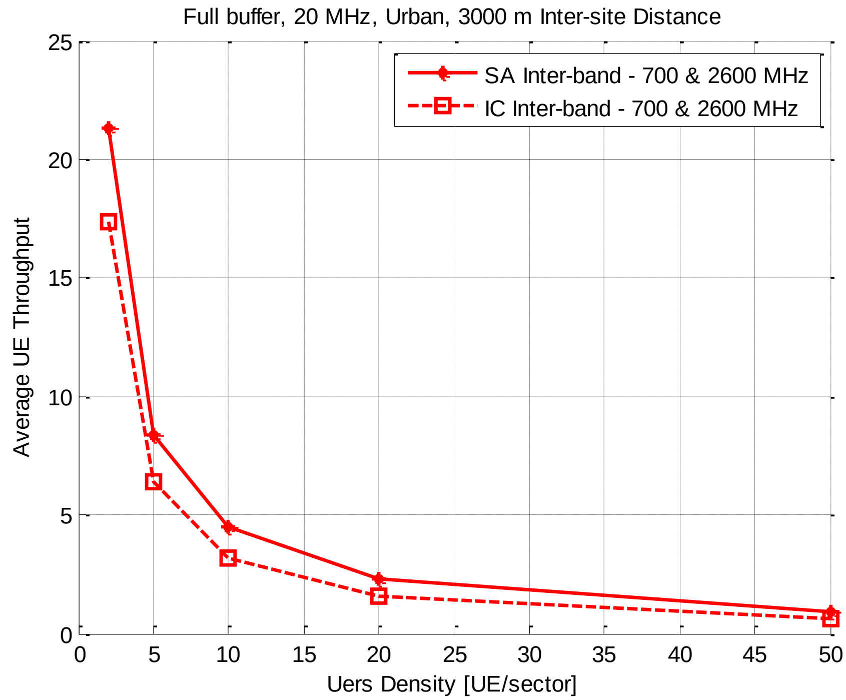

Figure 35: Re-plot of two inter-band scenarios from the previous figure

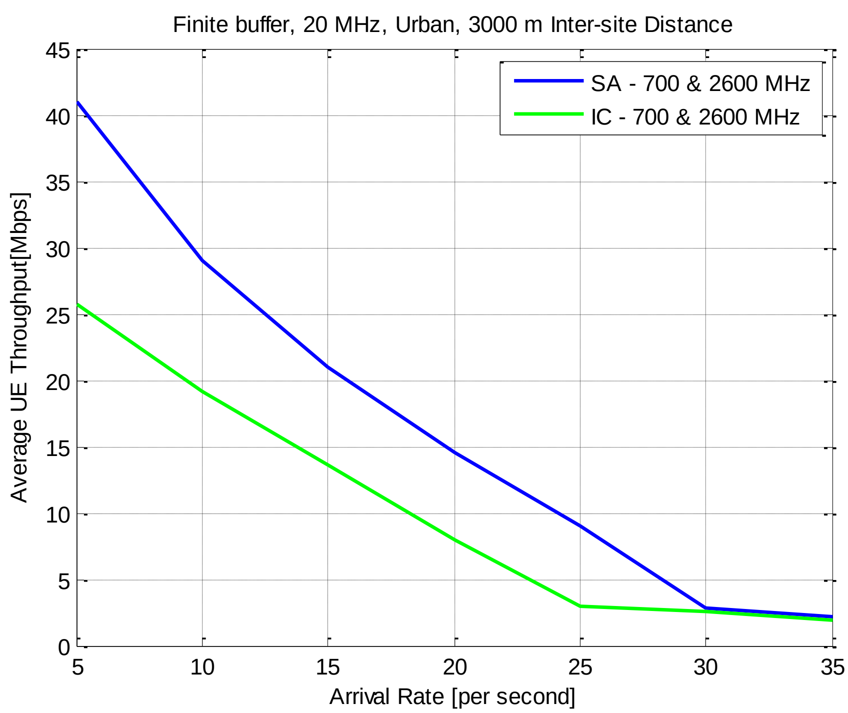

Figure 36: Average UE throughput for finite buffer traffic

Finally, looking the peak UE throughput in Figure 37, below, we can see that contiguous (not plotted) and SA systems will have at least double the peak rate that can be achieved by IC systems at cells with low density. As the IC system has access to only a more fragmented spectrum, it will experience less peak UE throughput. As the user density increases, these differences become less significant because the peak UE throughput is small due to users sharing RBs. Note that frequency bands are less of an issue in peak UE throughput simulation because this analysis focuses only on users in close proximity to eNodeB.

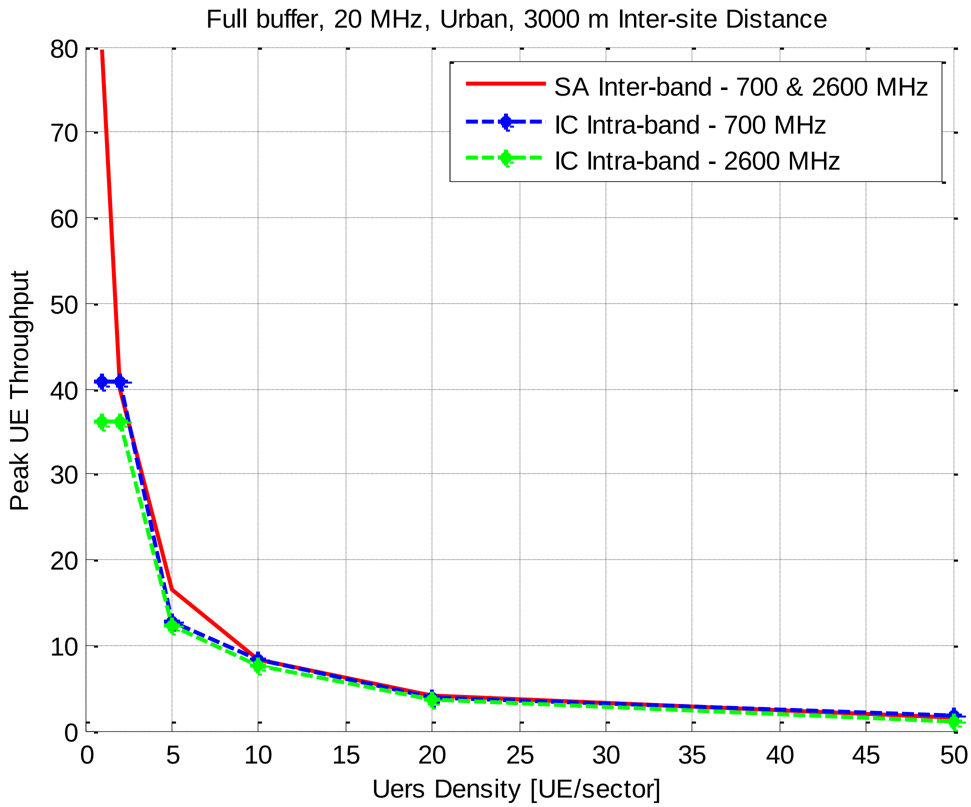

Figure 37: Peak UE throughput (Mbps) and impact of fragmentation

6.2. Fairness

To provide another measure that can help us understand the performance of these different network scenarios, we try to measure the fairness for each scenario. Figure 38, below, shows that the possibility of equal access is significantly affected by the frequency band(s) each system can access as inter-site distance increases. While all systems have similar fairness indicators (between 0.7 and 0.8) when the cell radius is small, systems that utilize only 2600 MHz will have a low fairness rating as the cell gets larger because users at the edge of the cell cannot be served. Having access to a lower frequency band carrier is necessary to maintain good service; otherwise, the operator will be forced to build more cells with small radii.

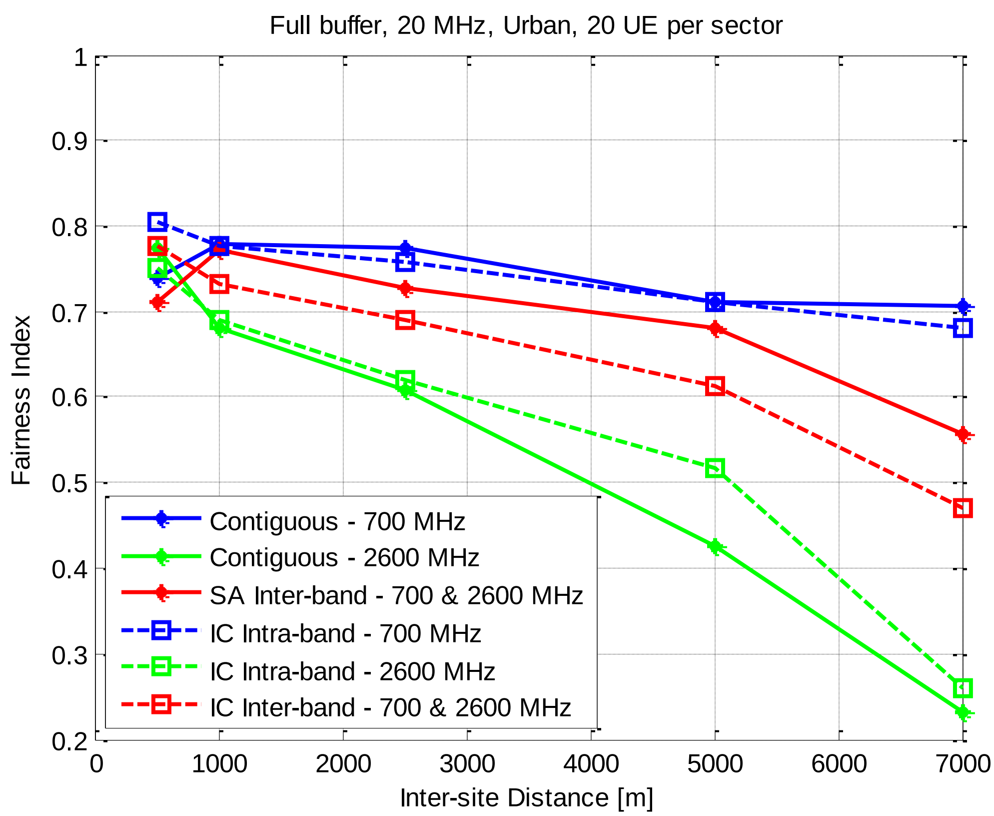

Figure 38: Measuring fairness for different cell sizes

6.3. Conclusion

Results from analysis in this chapter show that intra-band SA and contiguous carrier systems that use the same frequency band will achieve the same performance in an LTE system as long as no additional guardband is needed to avoid interference with adjacent channels. Also, an SA system will have better performance than an IC system due to multiuser diversity and scheduling gains. These gains are more significant when the user density is low and the system isn’t crowded. This applies to both full- and finite-buffer traffic models. We note that having access to a lower-frequency band carrier is necessary to maintain reasonable performance when inter-site distances are fairly large. Otherwise, cell sizes will be limited and can't be expanded.

In conclusion, this chapter measured the impact of spectrum aggregation technology on LTE network performance and how this impact is affected by spectrum allocated to the operator. We show that the use of SA technology with non-contiguous carriers in multiple bands can result, at some inter-site distances, in a performance level which is close to the best case scenario of using contiguous spectrum allocated in a relatively low frequency band.

III. QUANTIFYING THE IMPACT OF SPECTRUM AGGREGATION ON RADIO EQUIPMENT

When we estimate the NPV of cost of building out a greenfield network in the next chapter, radio equipment cost is part of the total cost. So, we start with this brief chapter to estimate the increase in equipment cost when produced to have spectrum aggregation capability. First, we define our research question then we provide technical background information on LTE equipment and the use of spectrum aggregation. After that, we discus proposed methods to quantify the additional cost due to SA and we present the collected data. Finally, we discuss the projected results.

1. Research Question

In this brief chapter, we try to answer the following question: how does the technical impact of spectrum aggregation affect the cost of radio equipment?

2. Background

User equipment generally consists of numerous components, which are shown in the first figure below. The second figure shows the architecture of eNB. These two figures illustrate the fact that user and basestation radio equipment are composed of many chipsets and hardware parts. However, the main blocks that we focus on in the analysis because they are most likely to be affected by CA are the baseband and the RF components [84], [85], [86], [87].

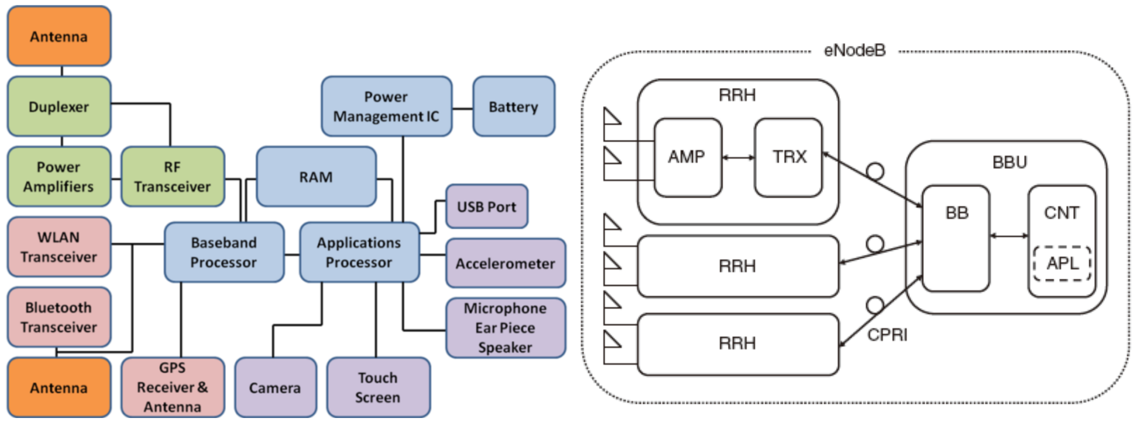

Figure 39: Simplified block diagram of UE components [87] and eNB hardware architecture [88]

These are the blocks that expected to be impacted by SA and their functions:

– Baseband Processor: collects the received data from the RF transceiver and extracts the raw data through demodulation and other signal processing such as IFFT

– RF Transceiver: converts the signal from RF frequency to baseband (0 Hz)

– RF Front End Module Components:

  - Power Amplifier: provides gain to the generated RF signal
  - RF Filters: duplexers, low-pass and band-pass filters
  - RF Switches: route the RF signal to enable multiple operating modes and frequency bands
  - Tuning: tunable components that adjust impendence to maximize power delivery
  - Antenna: radiates and captures RF signals

2.1. Technical Impact of SA on Radio Equipment

An LTE-Advanced terminal with reception and/or transmission capabilities for carrier aggregation should simultaneously receive and/or transmit signals on multiple component carriers [33]. Non-contiguous spectrum aggregation has an impact on the design of radio equipment as it requires modifying its wireless parts to accommodate the multi-channel aggregation. Based on 3GPP Technical Reports [89], [33] and [74] which consider possible transmitter and receiver structures used to handle CA over noncontiguous carriers, Figure 40, below, shows high-level concept designs for SA transceivers in which multiple parallel transceivers for aggregated frequency bands are used.

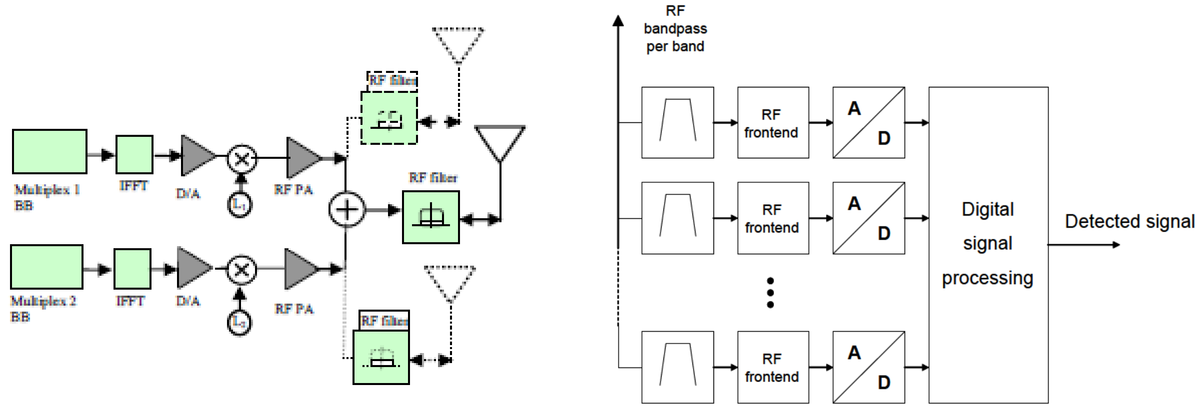

(a) TX Architecture [89], [33]

(b) RX Architecture [90]

Figure 40: Two basic transceiver concepts to handle SA

The changes that SA introduces in transmitters and receivers can affect the following components:

A. RF Transceiver: must be able to handle multiple signals from multiple bands. Multi-carrier signals can't be treated as a single signal; therefore multiple transceivers are required as shown in the figures above.

B. RF front ends: multiple RF chains must be able to handle multiband and CA.

   - Power Amplifier: while a single very wide band PA has lower efficiency [84], the use of multiple PAs could deplete the battery.

- Filters: filter requirements differ according to the band [91], [92] and so requires the installation of both multiple filters and multiple switches.

C. Antenna: There is tradeoff between volume and performance when multiple antennas or a very large band antenna with many antennas are required. Antenna switches and matching tuners can offer flexibility and improve signal strength across a wide range of frequencies or be configured for different bands, but this could decrease performance.

D. Baseband Processing: This should be designed to receive information from multiple channels (multiple data streams) simultaneously and convert them into a single stream, so multiple FFT IC chips are required [93]. Baseband must be capable of processing more than 150 Mbps, the minimum requirement for LTE CA functionality listed in Release 8 [10].

The UE is more of a concern than the base station or eNodeB because of the limitation of UE elements such as the power amplifier and filter to handle and aggregate multiple bands simultaneously, as these changes could impact power consumption, efficiency and cost.

2.2. SA Implemented Chipsets

In June 2013, South Korea's SK Telecom announced the launch of the first commercial LTE CA service [10], which aggregated 2 carries to enable peak speed of more than 200 Mbps. Other operators and chip manufactures announced that by 2015, they would have equipment commercially available that could aggregate 3 CC in order to reach a downlink speed of 300 Mbps [14], [94] and in May and June of 2014, tests of SA were conducted by multiple operators in different countries. SingTel and Ericsson initially deployed LTE-A with CA to reach an increased peak rate of up to 300 Mbps. Expansion of the deployment is subsequently expected as consumer devices supporting LTE-A become more widely available [95].

2.2.1. Current Implemented Chipset

Since Qualcomm is the leading original equipment manufacturer (OEM) for LTE systems, we discuss their most recent chipsets that accommodate carrier aggregation. The following diagram shows basic blocks for the chips made to be used with CA.

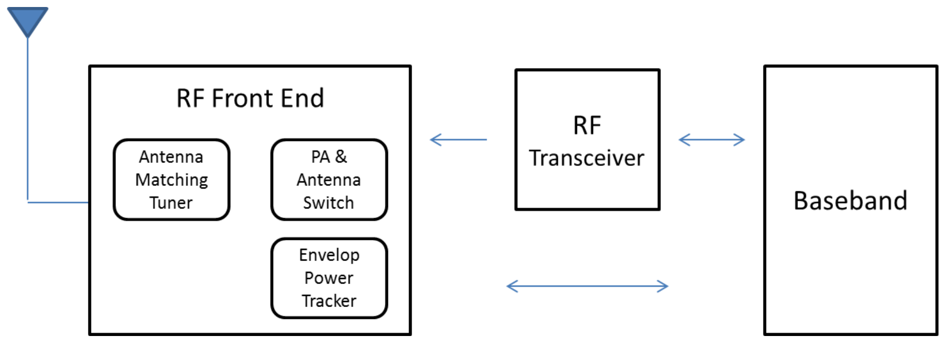

Figure 41: Diagram for Qualcomm Chipsets introduced to accommodate CA

a) RF Front End

In the second half of 2013, Qualcomm introduced the RF360 frontend solution: a family of chips including: power amplifiers, an antenna switch, an antenna matching tuner, and an envelope tracker. This chipset designed to reduce band fragmentation in LTE-Advanced CA and to help device manufacturers more easily develop multiband [98]. The RF360 front-end solution allows device makers to easily customize LTE advanced products for different band combinations by offering design flexibility and simplifying routing for 2 or 3 CC aggregations to support these band combinations. The first generation which allows more band combinations was announced in the second half of 2014.

b) RF Transceiver

The RF front-end solution is paired with the Qualcomm transceiver to achieve CA. Table 11, below, shows different generations of multiband transceiver chips that can accommodate different CC aggregations.

Table 11: Qulacomm RF Transceivers

Chip Name	Released	New Functions
WTR1625L & WFR1620	2H 2013	support multiband
WTR4905 WTR2955	2H 2014 1H 2015	- single chip - support up to 40 MHz 2-carrier aggregation on a single chip - Release 8 CA band combinations
WTR3925	2H 2014	- supports next generation LTE-A wideband CA - support up to 40 MHz 2-carrier aggregation on a single chip - more CA band combinations (release 10) [97]
WTR3905	2H 2015	add support for combining another carrier with WTR3925 to achieve 3-carrier aggregation

c) Baseband Processing

Qualcomm released and announced multiple generations of baseband processors and modems that meet different releases of LTE including the capability to handle CA with high data rates. Different LTE releases specify required downlink data rates. Release 8 requires 150 Mbps (UE Category 4), Release 10 requires 300 Mbps (UE Category 6) and Release 11 requires 450 Mbps (UE Category 10), all for downlink. Table 12, below, lists chipsets produced to handle LTE wideband and CA.

Table 12: Qualcomm Baseband and Modem Chips

Chip Name	Released	New Functions
Snapdragon 800 processor paired with Gobi 9x25 modem	2H 2013	supported aggregation of two 10 MHz carriers enabling peak data rates of 150 Mbps (Cat 4) [97]
Snapdragon 210 Processor with 4G LTE World modem	1H 2015	two 10 MHz Carrier Aggregation (CAT4 speeds of up to 150 Mbps) [98]
Gobi 9x35 modem	1H 2014	aggregate two 20 MHz carriers enabling a peak data rate of 300 Mbps (Cat 6)
Snapdragon 810 processor	2H 2014	CAT6 speeds of up to 300 Mbps with support for up to 3x20 MHz carrier aggregation on LTE FDD and LTE TDD
Gobi 9x45 Modem	2H 2015	supports carrier aggregation up to 60 MHz 3x CA for downlink speeds of up to 450 Mbps (Category 10)

2.2.2. Chipsets for Future Requirements

So far, the specifications only support carrier aggregation in a limited number of frequency bands which limit the complexity of UE design [101]. Release 10 supports intra-band contiguous aggregation in FDD band 1 and TDD band 40 and also supports inter-band aggregation in FDD bands 1 and 5 with 20 MHz total bandwidth. In each LTE release, a CA bandwidth class is defined for each of its supported bands or band combinations. The CA bandwidth class states the number of component carriers that the mobile supports and the total number of resource blocks that it can handle. Release 11 defined 28 possible band combinations with up to 40 MHz in total bandwidth. Release 12 defined more than 50 band combinations with up to 3 inter-band CCs aggregation and 60 MHz of bandwidth. Future releases will define more combinations in order to reach the ultimate 3GPP goal of aggregating up to five carriers to produce a total bandwidth of 100 MHz with a wide range of spectrum bands and bandwidth combinations enabling flexible configurations [102].

Although a chipset maker like Qualcomm has been able to provide chips with CA capabilities, those chipsets are still limited to a small number of bandwidth configurations, defined in LTE releases 10 and 11 [10], [75], [9]. More work will need to be done to make ICs that are capable of aggregating more CCs with a variety of bandwidth combinations.

On the other hand, device manufacturers need to coordinate their efforts with operators in different markets to know when LTE-A with CA is implemented and at which frequency bands, since current chip designs are not global and might not be utilized in every market. Early adopters of CA might produce regional-specific designs and this might make some operators think CA might now be feasible but not yet practical [101]. For example, manufacturers of Samsung Galaxy S5 LTE-A, which was released in mid-2014 in South Korea, might not be released in many other markets since LTE-A and CA have not yet been adopted.

3. Modeling the Analysis

So far, we've discussed the possible technical impacts of CA on radio equipment based on the design proposed by 3GPP. Going into further technical details is beyond the scope of this chapter, which is meant to quantify the expected increase in the cost of radio equipment. The resulted impact would contribute to the network costs, which will be discussed in next section. The impact on equipment due to CA [9] is summarized in Figure 42, below.

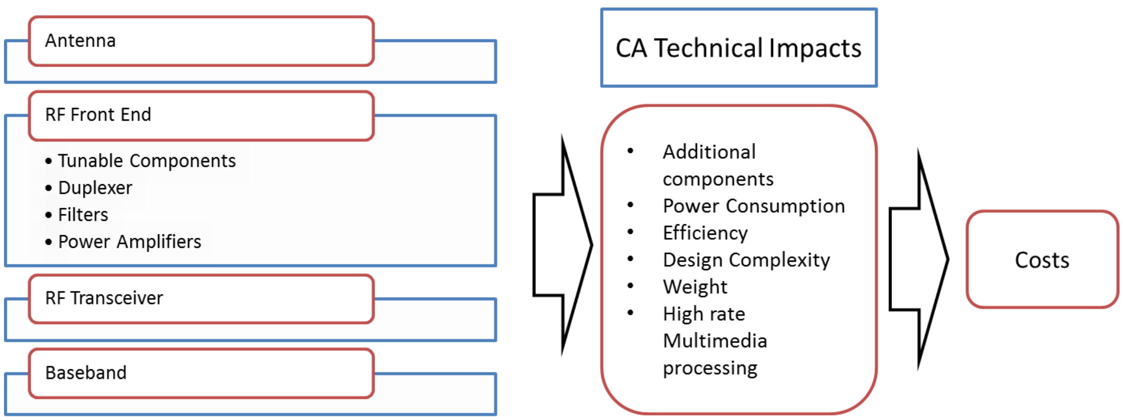

Figure 42: Components that might be affected by SA

Our main task is to quantify the projected cost of these CA impacts on equipment. Conceptually, these changes would result in the following additional costs [102]:

– RF component costs: the need for additional components

– RF performance costs: the loss in efficiency and increase in power consumption

– RF associated engineering costs: for more complex chip designs

– Baseband costs: for higher processing capabilities

We should also note also economy of scale could affect the cost of devices, which is volume dependent. However, these exact costs are only known to chip and device manufacturers.

Moreover, the manufacturing costs and selling prices of the different IC chips are considered proprietary information.

Different websites like (www.technology.ihs.com) and (www.teardown.com) do cost-teardown analysis for wireless devices including LTE equipment. This method breaks down all the IC chips within a given device and estimates the cost of each IC and part in dollars, Appendix E shows an example. Our cost analysis will use the data available from cost teardown estimates in order to project the CA cost of equipment, in the following methods:

a) Parameterization

We compare Tx/Rx architectures of conventional LTE equipment and CA-based equipment as proposed by 3GPP. The latter would require adding an RF chain and baseband ICs to handle the additional bands. The number of extra ICs depends on how many carriers can be aggregated. Based on the data we collected for IC cost, we can estimate the additional CA cost based on the number of CCs it can accommodate changes [4]. This method produces a linear relation between the cost and the number of CCs. With this method we follow two distinct approaches:

i- Multiple basebands: we assume that an additional chain of RF components and baseband processor will be needed for each additional carrier to be aggregated.

ii- Single baseband: we assume that for each additional carrier to be aggregated, an additional chain of RF components will be needed, but the baseband chip will remain one that is upgraded to handle higher data rates. As per LTE UE categories, a 2 CC aggregation will require a baseband that can support a 150 Mbps downlink, and a 5 CC aggregation will require a baseband that supports 1 Gbps.

b) Prediction

From Table 11 in Section 2.2.1 indicates that different chipsets that can perform 2- and 3-CCs aggregations are already available. We compare the cost of these chipsets to conventional ones that operate on a single band. Based on this comparison, we can project the cost of these ICs will be, as more CCs will need to be aggregated with more band combinations. This projection can used to adjust the results from the previous estimate.

4. Input Data

As mentioned earlier, we collected data about LTE devices from multiple cost-teardown websites in order to know the relative cost of the components that could be affected by spectrum aggregation to the total cost of the wireless device. Figure 43, below, shows the relative costs of the RF transceiver, the RF front end and baseband chips for a number of devices. As we show in the data tables showing additional details, in Appendix E, we investigated chip modules to make sure all the components in the figure are conventional and don't support CA. Figure 43 shows that these components cost $29 in a conventional LTE device on average, and the baseband is responsible for more than 50% of that cost.

Moreover, we searched for more recent LTE devices that had started implementing LTE Release 8 (Categories 3 and 4) and Release 10 (Category 6) specifications. These releases are the ones that require multiple LTE-band support and CA with limited combinations. The second figure below, Figure 44, shows the cost teardown for three such devices.

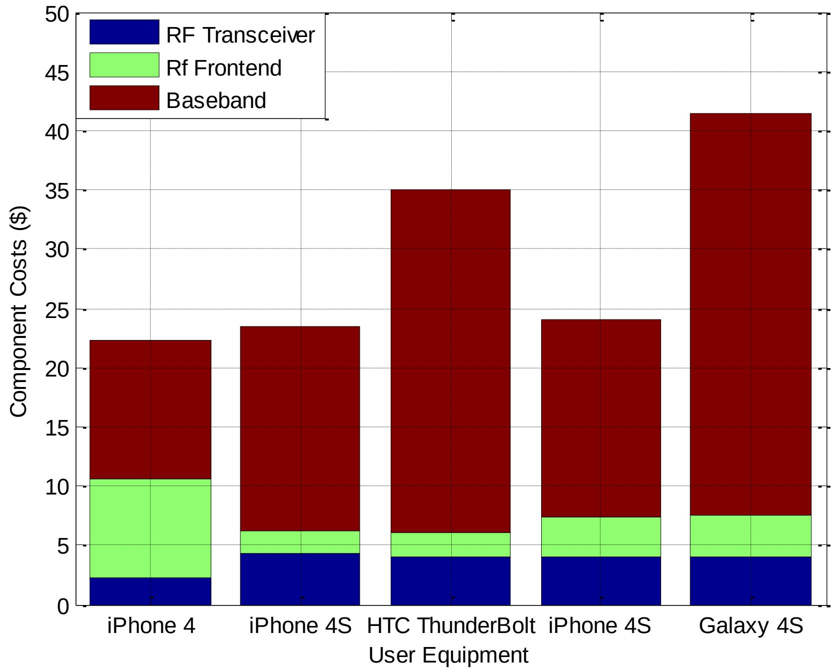

Figure 43: Teardown of LTE devices components costs (based on data from teardown.com and technology.ihs.com)

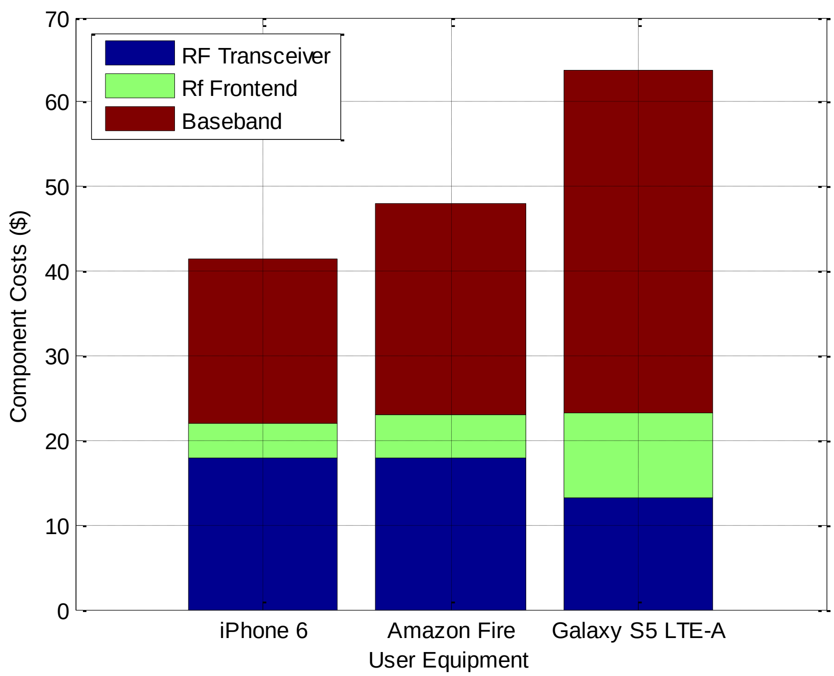

Figure 44: Teardown of recent Releases LTE-A devices components costs (based on data from teardown.com and technology.ihs.com)

We can see that the components in question have cost that composes, on average, $50. This is attributed to the increase in transceiver cost needed in order to handle more bands. In the iPhone 6 and Amazon Fire which can aggregate two carriers, two chips are needed for the transceivers to handle multiband, as explained in subsection 2.2.1. The transceiver cost becomes less in the Galaxy S5 since it uses a single WTR3925 chip although it could aggregate up to 3 carriers with addition of extra chip. We can also see that the baseband processor paired with the modem will be more costly, as they are required to handle 100-, 150- and 300-Mbps downlink data rates for LTE categories 3, 4 and 6 respectively. Because there are many more band combinations in Release 10, the RF front end solution in the Galaxy S5 LTE-A will require more components and consequently increase the costs commensurately.

5. Results and Discussion

Based on the first set of input data shown in Figure 43, in conventional LTE equipment that meets LTE UE Category 2 requirements, the cost of baseband and RF components compose about $29 (70% baseband, 15% RF transceiver and 15% RF front end). We follow the first parameterization method we described earlier, in Section 3. Figure 45, below, has a linear increase in equipment costs because of our assumptions of an additional RF chain and baseband IC were needed for each added carrier to be aggregated. In a second approach, we assumed baseband will need to be upgraded only when more carriers are aggregated. In this case, we do the parameterization for the baseband cost based on the data rate it has to support as more carriers are aggregated (e.g., 150 Mbps for a 2- carrier aggregation, and 1 Gbps for a 5-carrier aggregation).

We note in the Figure 45 that LTE radio equipment might increase between $20-29 for a two-carrier aggregation and between $74-118 for a five-carrier aggregation.

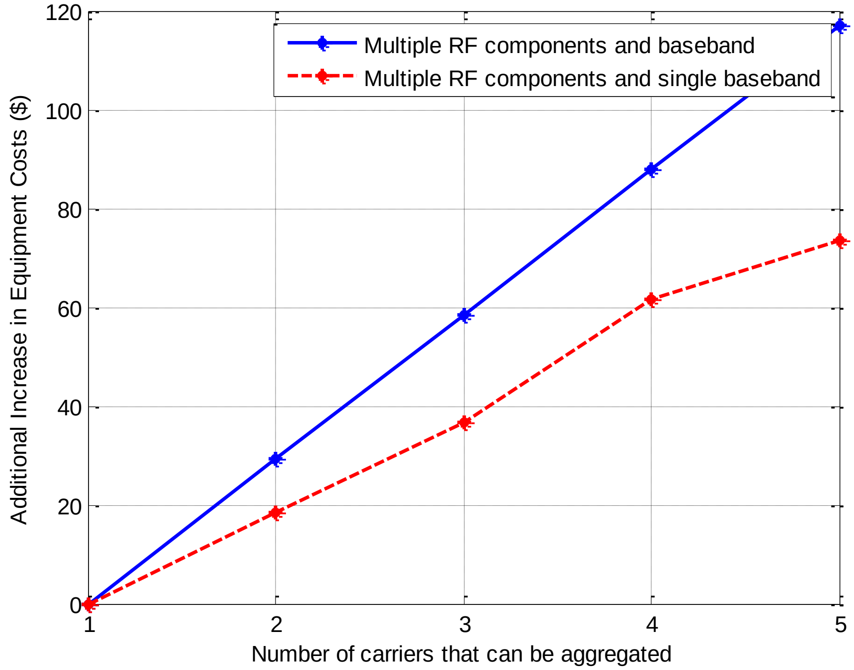

Figure 45: Projected increase in radio equipment cost due to CA

To make more precise predictions, we now use the second set of collected data (Figure 44) from the first generation of chipsets that were designed to handle CA. Since these existing chipsets were made to handle only 2 CC with the possibility of adding a third carrier and up to 300 Mbps, we regress the available data to predict how much the cost increase will be for more carriers to be aggregated and a higher data rate to be supported. Simple regression results based on two models are shown in Table 13, below, where X_i represents the number of aggregated carriers. Both regression analyses show that the two models' coefficients differ significantly from 0 at 5% level. They both have good coefficients of determination values which mean the regression approximated data well.

Table 13: Regression results for increase in equipment costs

Regression Model Coefficients	P-Value	R^2
$\widehat{Y_i} = -18.08 + 17.21X_i$	0.019	0.96
$\widehat{Y_i} = -2.23 + 29.89 \log X_i$	0.048	0.91

Figure 46, below, shows plots for the two regressions. The predicted linear relation has values that are very close to the second parameterization analysis we plotted earlier above, as it shows between a $16-68 increase in equipment cost. The linear-log relation predicts an increase of only about $45 when five carriers are aggregated.

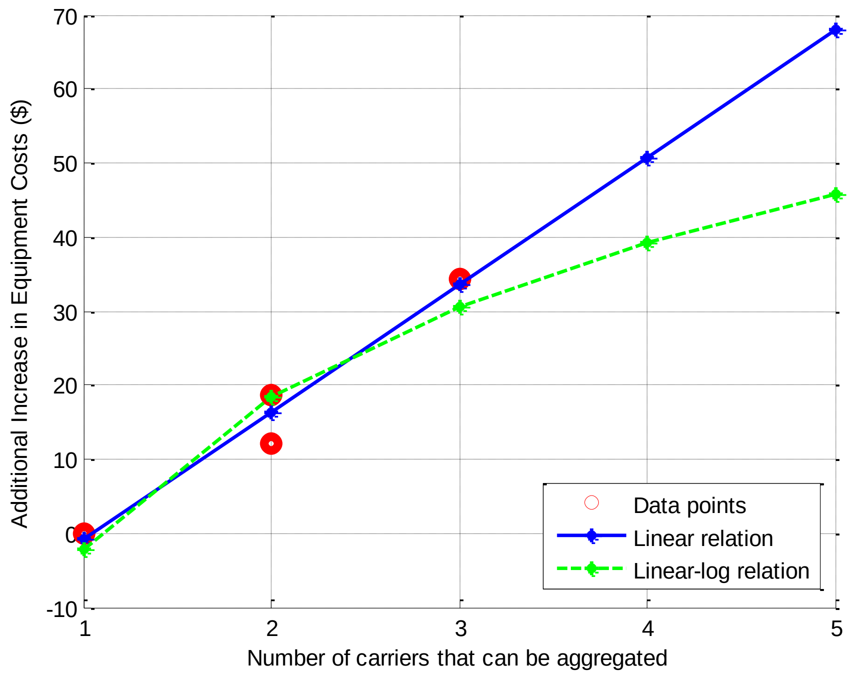

Figure 46: Predicted increase in radio equipment cost based on simple regressions

We can summarize the results from these different analyses in the Table 14, below. Average, minimum and maximum values will represent the range of uncertainty in our predictions. These results will be used in the next chapter's analysis to represent a part of SA costs on networks, and the range of values can be used when we do a sensitivity analysis.

Table 14: Summary of results

Number of carriers	2	3	4	5
Predictable increase ($)	20	35	50	68
Minimum increase ($)	18	31	40	45
Maximum increase ($)	28	60	87	115

IV. IMPACT OF FREQUENCY AND SPECTRUM AGGREGATION ON CAPACITY AND BUILD-OUT COST OF CELLULAR NETWORKS

In this chapter, we analyze the implications of spectrum aggregation and spectrum allocated on a large-scale network to assess the costs and benefits for cellular operators when building out a greenfield network. We compare different cellular network scenarios that differ from each other by spectrum allocated and their use for spectrum aggregation technology. This chapter investigates the impact of those two variables on these different network scenarios. First, assuming a pre-determined level of throughput required, we build out the networks for each scenario and estimate the required infrastructure cost for network roll-out. Second, assuming a pre-determined network infrastructure, we estimate the cell throughput supported in each scenario. Results show that inter-band spectrum aggregation could be almost as good as the best case scenario where the operator is allocated a contiguous spectrum in relatively low frequency band.

1. Research Questions

In this part of this research we address the following questions:

- What is the impact of using spectrum aggregation on the cost of building out a mobile network?
    - What is the cost of building out a greenfield mobile network that is required to: cover about 50% of the United States, have the capacity to meet users' traffic demands and maintain an acceptable quality of service for the following operators:
        - *a network that uses contiguous carriers within a single band;*

        - *a network that uses non-contiguous carriers independently, i.e., an independent-carriers operation in which carriers are fragmented either across multiple bands or within a single band; and*
        - *a network that uses non-contiguous carriers by aggregating them into a spectrum-aggregation operation that operates either across multiple bands or within a single band.*
    - How does the network build-out cost change as wide area network inputs such as the type of environment, market share and/or population density change?
- What is the benefit of spectrum aggregation on an existing mobile network?
    - What is the impact of using SA on the operator's ability to support higher throughput for users?
    - What is the cost effectiveness of each network scenario listed above?
- What is the impact of SA on allowing more access to emerging future broadband services?
    - What is the impact of SA on achievable peak user throughput?
    - How does the peak user throughput change as we vary the spectrum portfolio allocated to an operator with regard to block fragmentation?

2. Background

2.1. Review of Wide Network Modeling

The main contribution of this chapter is analyzing the impact of spectrum aggregation on a greenfield cellular network in terms of its build-out costs and total delivered capacity. To perform a technical-economic analysis for an LTE network, a country or a region of a country is usually used as the assessed coverage area. The regions studied in past research are Spain [103],

[104], the United Kingdom [105], [106], Argentina, Chile, and Colombia [107], Sweden [108] and the United States [109]. The general approach has been to use given traffic demand parameters as inputs and the cell radius required to fulfill these traffic requirements as outputs. The total number of cells required to cover the target area is estimated, taking into account the fact that the cell radius change as we move across the map due to changes in geography and population. This dimensioning process allows us to assess the total network-related costs that would be required by a specific operator based on a cost model, as shown in Figure 47, below.

In other words, the dimensioning for a network to estimate the number of cells needed is based on knowing a single cell's capacity requirement and then determining coverage requirements based on that. Different papers discuss the theory of LTE radio planning, which deals with these two issues [110]. The paper in [111] deals with coverage-limited and capacity-limited dimensioning of HSPA based beyond 3G networks. The coverage-limited dimensioning is based on determining the maximum cell radius versus the minimum required bit rate guaranteed at a given probability of cell coverage. On the other hand, capacity-limited dimensioning methods are based on different scheduling techniques. Although coverage estimates can be done based on both uplink and downlink channels, most papers calculate this based on downlink only, which yields a reasonable approximation for coverage [112]. Figure 47, below, contains a flow chart showing an example of wide-network modeling [103].

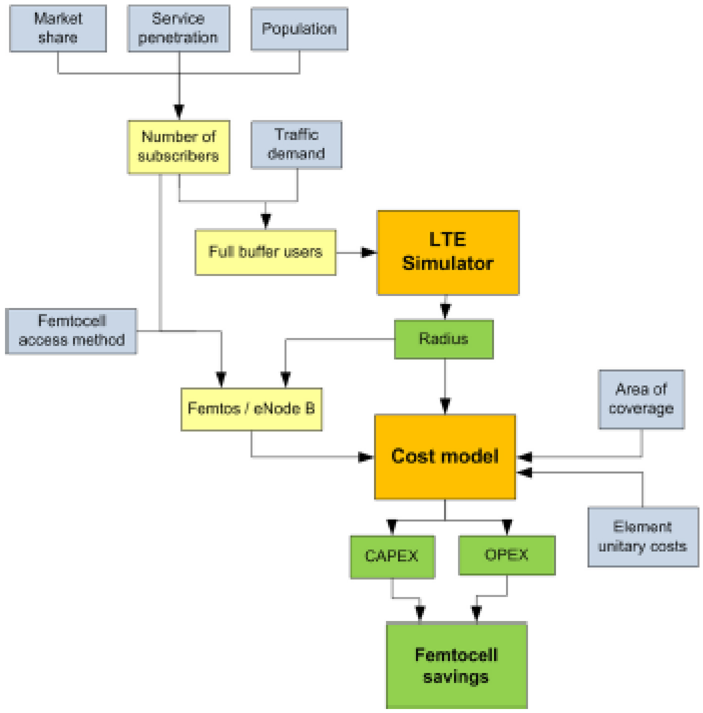

Figure 47: Flow diagram for dimensioning process used in [103]

While capacity and coverage analyses are usually done based on conventional base stations in the center, adding relay nodes to the cell could change the results by decreasing the number of cells required in certain cases [113]. Furthermore, many earlier studies, e.g. [114], [115], focus their research on planning and capacity-coverage for cellular network estimation by using a variety of techniques to reach accurate results.

In the papers mentioned above, the cost modeling is presented as a straightforward process after the number of cells required to cover the reference country region has been determined. Different papers, e.g. [116], [117], [118], suggest cost elements for the deployment of a greenfield cellular network.

2.2. Multiband and Cell Coverage

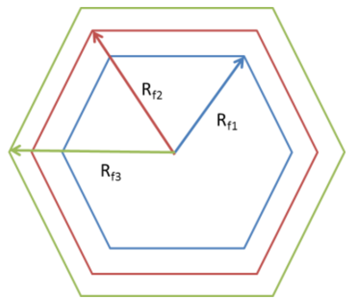

Figure 48: An example showing the design complexity when multiple bands are aggregated.

In general, in scenarios that use carriers from multiple frequency bands, estimating the coverage of the entire network requires consideration of multiple factors. Let's assume the inter-site distance is less than twice the maximum radius of the higher frequency band. In Figure 48, this means: $d_{IS} \leq 2R_{f1}$. Then, theoretically, all users can be served by all carriers, and from a planning point of view, this cell will be similar to a single-carrier cell. If $d_{IS} > 2R_{f1}$, then users near the cell edge won't be served by f_1 (or similarly if $d_{IS} > 2R_{f2}$, then the users near the cell edge won't be served by f_1 and f_2), and those users will experience low $SINR$ for the third carrier f_3 as well. This case makes cell planning more challenging. As we will see in the next section, simulation analysis results from Chapter II will be used to provide more accurate cell planning, based on a specific performance requirement.

3. Modeling the Analysis

3.1. Investigated Scenarios

In this chapter's analysis, we run the same five network scenarios from Chapter II, which differ with respect to spectrum holdings and the way they are operated. The only difference in the current investigation is the size of the network simulated. While in Chapter II, the analysis was based on a small-scale network, which was adequate to simulate the network's technical performance as per 3GPP recommendation about simulating LTE systems, the technical-economic analysis in this chapter will be based on a large-scale network.

Estimating the costs of a mobile network depends directly on the number of cells, which, in turn, depends on features of the coverage area and its population density. Therefore, doing the analysis over a small-scale sample network won't enable an accurate estimate of costs or returns, given that operators build out wide area networks. Instead, we simulate the real operator scenario that covers 50% of United States area.

3.2. Analysis Formulation

Our analysis is categorized into two main types:

i. Cost Analysis: assuming a pre-determined level of throughput required, we estimate the required infrastructure for each scenario; and

ii. Capacity Analysis: assuming a pre-determined network infrastructure, we estimate the cell throughput supported in each scenario.

Based on these two engineering analyses, we run an economic analysis to quantify their technical outputs in monetary terms. In analysis (i), we quantify the resulting required infrastructure in terms of network costs. In analysis (ii), we quantify the resulting throughput that can be supported in terms of total capacity, as shown in Figure 49. In addition to network simulation, the resulted costs of equipment due to SA impact from Chapter III would contribute to the network costs.

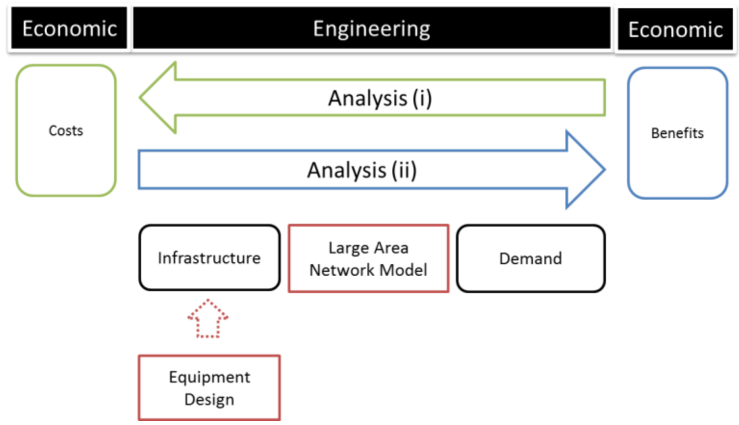

Figure 49: Main blocks showing overview of the analysis

3.3. Large Network Modeling

The cost of a nationwide network primarily depends on the number of cells that the operator needs to build in order to meet specific coverage and capacity requirements. Conversely, the capacity of a network depends primarily on the number of cells in any given region. Thus, we must develop models that show the relationship between capacity, number of cells, and cost, without determining the precise location of every tower.

To simplify the problem, as in [111], [119], [121], [122], we divide the area served by the cellular provider into H regions, and we assume that users are uniformly distributed within each region, although different regions may have very different population densities. Moreover, we assume that each region is large compared to a cell, so the inter-site distance can be roughly constant between adjacent cell towers, and we can estimate the average cell size in the region without consideration of the size or the shape of the region.

For each region h, we define the following:

- A_h is the area of the h^{th} region in km^2.

- N_h is the number of that region's active users which depends on the population, operator's market share and wireless service penetration within the region.
- I_{SD}^h is the inter-site distance in the region in km.
- T_h is the active user throughput in the region, which could be the peak, average or edge user throughput.

We define the users' density in the region as:

Equation 22

$$D_h = \frac{N_h}{A_h} \qquad \text{(in user/km}^2\text{)}$$

Users' density in region h can be expressed in (users/cell) as well:

Equation 23

$$D'_h = \frac{N_h}{CL} \qquad \text{(in users/cell)}$$

Where CL is the number of cells which can be expressed as [112]:

Equation 24

$$CL = \frac{A_h}{\frac{3\sqrt{3}}{8} {I_{SD}^h}^2}$$

In addition, the active user throughput in the region (which we calculate based on the simulation described in Chapter II) is dependent on, among other factors, both inter-site distance and user density; i.e.

Equation 25

$$T_h = f(I_{SD}^h, D_h, \dots .)$$

Therefore, the two proposed cost and capacity analyses introduced earlier are exclusively dependent on the two main variables: inter-site distance and throughput, as will be explained in detail in the next two subsections.

3.3.1. Cost Analysis

This analysis sets the minimum required value(s) for T_h, and then searcesh for the maximum possible I_{SD}^h". To estimate the cost of a wide-area cellular network that can achieve a given throughput per user, we must first determine the number of cell towers needed in each region to meet this performance requirement. The figure below shows the algorithm steps we follow to find the inter-site distance. First, we set a minimum user throughput requirement to be maintained in each cell [119], and we search for the inter-site distance in the network scenario that meets this requirement. This will decide the total number of cells required by the operator to cover the region. The search for the optimal inter-site distance will be done by running the small-scale simulation model at different values until we reach the maximum possible inter-site distance that meets this constraint. This can be expressed as:

Equation 26

$$\max_{x} \; I_{SD}^h$$

$$\text{S.T.} \quad T_h \approx \alpha$$

$$I_{SD}^h \leq R_{max}^f$$

Where α is a value that we set to represent the minimum user throughput requirement and R_{max}^f is the maximum inter-site distance in a coverage-limited region for a particular frequency band f. It is set at 30 km for the 700 MHz band and 10 km for the 2600 MHz band [122].

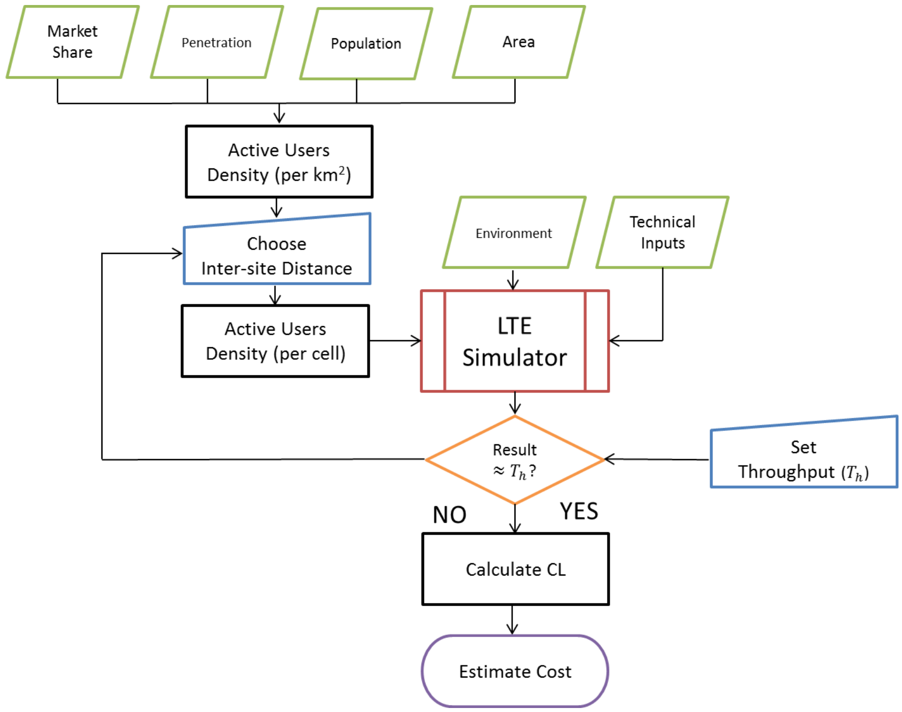

Figure 50: Algorithm for cost analysis

The final output estimated will be the number of cells that need to be built to meet this requirement. The build-out cost can be calculated by estimating the average cost of a cell and multiplying that by the resulting number of cells required. The cell cost is composed of two parts: the site cost and the equipment cost. The latter was analyzed in Chapter III to measure the SA impact on it and results from that analysis will be used in this chapter.

In this analysis, it's necessary to set the throughput requirement that we need to meet. We can set peak, average or edge UE throughput as a measure for the quality of service required. Mainly, we assume the targeted average UE throughput at the peak hour to be 2 Mbps [2]. We assume on average 50% of this operators' subscribers' UE are active at the peak hour in the coverage area.

Shortly before the completion of this thesis, we realized that a traffic intensity of 50% of subscribers sending 2 Mbps simultaneously in the peak hour, when scaled to an entire month of activity, is equivalent to 180 GB/user/mo. This number is more than 20 times the likely near future (2018-2019 time frame) forecast traffic of 9GB/user/mo. While the same traffic inputs were used in calculating the relative costs of all scenarios, it is unlikely that costs for every scenario scale in the same way with increased traffic. In particular, a lower traffic assumption (*i.e.* fewer active users in the peak hour) should imply fewer capacity-limited cells, relative to coverage-limited cells. This in turn may accentuate the value of low frequency spectrum. We present the results here using this unrealistically high traffic level, but future publications will use a revised traffic assumption. The Capacity analysis described in the next section is also affected by our overlarge traffic assumption

We assume the net present value of costs required to deploy a cell site to be $ 1 million on average [123], [124]. Finally, when we add the net present value of cost of UE devices, we assume the operator subsidizes the UE devices for 70% of the customers every 2 years while the rest are contract free customers. We also assume the LTE UE device costs the operator an average of $400.

3.3.2. Capacity Analysis

This analysis assumes fixed specific values for I_{SD}^{h}, and find the resultant T_h in the cell. Figure 51, below, shows the algorithm steps we followed to find the throughput. In this analysis, we have an existing nationwide network with a pre-determined inter-site distance in any region h. We run the LTE simulation to estimate capacity for each network scenario. The output is in the form of the total capacity or throughput that can be supported in each cell across the network. Since our analysis is a supply-side analysis, it doesn't account for subscriber' behavior, which would be included in a demand-side analysis. The average revenue per user (ARPU) can't be treated as a fixed value since it changes as traffic increases. Instead, we will quantify the benefits of the increase in the capacity supported in terms of increased cost effectiveness (measured in unit delivered data rate per unit cost).

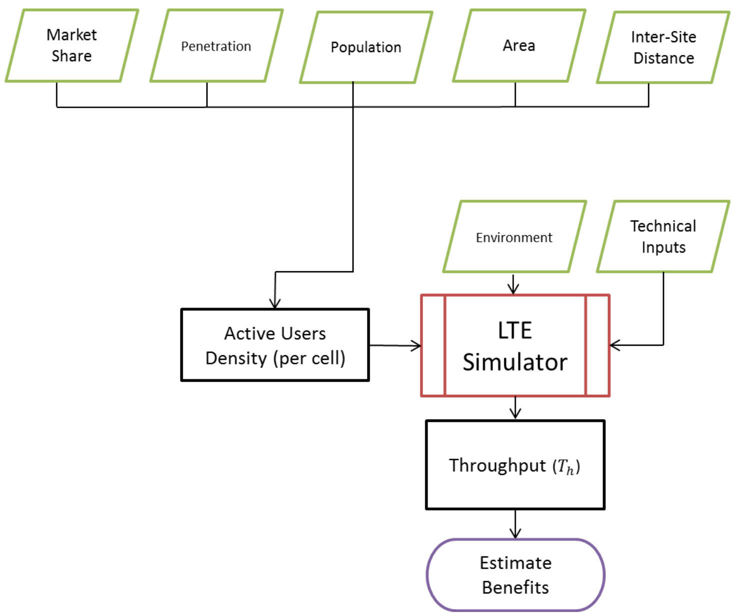

Figure 51: Algorithm for capacity analysis

In this analysis, we have an existing network infrastructure with predetermined inter-site distances as per Table below. The inter-site distances were selected to be similar to those that were found to minimize cost in the previous analysis in Section 3.3.1.

Table 15: Inter-site distances for the existing network

Region	Inter-site Distance
Super Dense Urban	500 m
Dense Urban	1.25 km
Urban	2.5 km
Suburban	5 km
Rural	8 km

4. Other Inputs and Assumptions

4.1. Population, Area and Environment

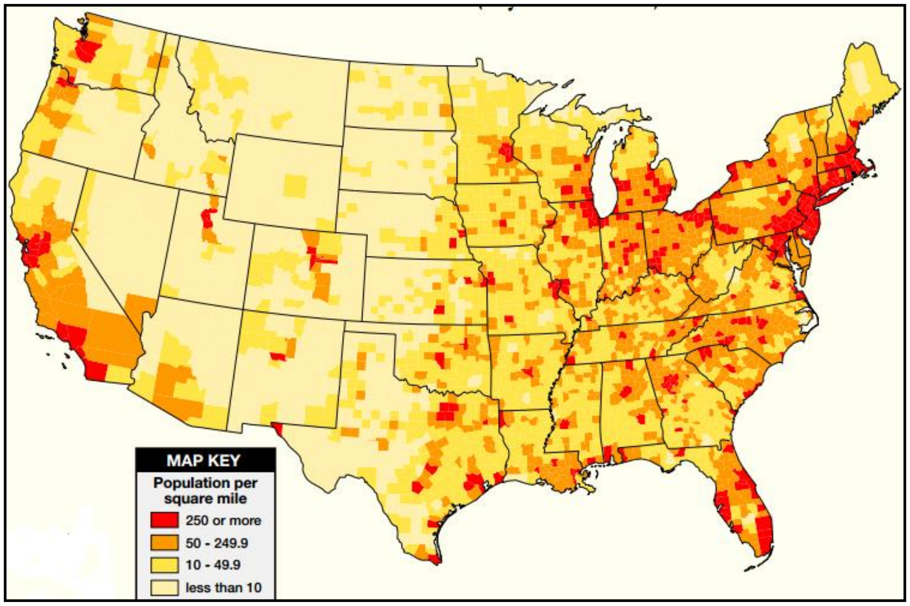

Figure 52: US population density by county. Figure from census.gov

The population density (POP/km^2) varies across the geographical map of the United States as seen in the census map above. Population density can be measured county by county where we can assume the population is uniformly distributed within each county [13]. Although each county has a distinct population density, like the map we categorize each county into one of five categories based on its population density. We define cutoff values $\{x_i,\ for\ i = 1, \dots 5\}$ to decide which category the county belongs to. We identify the following five types of regions based on population density: Super Dense Urban (population density > 1,500 pop/mi^2), Dense Urban (> 1,000 pop/mi^2), Urban (> 250 pop/mi^2), Suburban (> 50 pop/mi^2) and Rural (> 10 pop/mi^2). Then, each category will have a total area (the sum of all its counties' areas) and a total population (the sum of all the counties' populations) as Figure 53 shows. The super dense urban region, which represents 0.1% of the area with about 8% of the population, isn't shown in the figure because of scale.

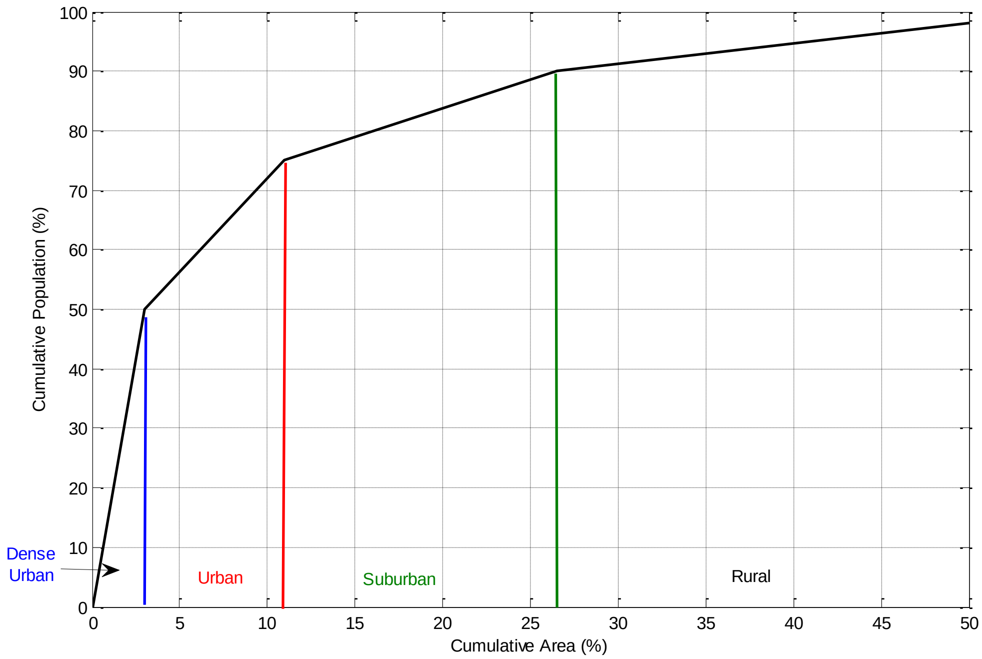

Figure 53: Breakdown of US area into five types of regions

Furthermore, taking the exact population density for each county would require us to run the wide-area model including the LTE simulator more than 3,000 times in order to estimate the number of cells and user throughput; this would be impractical given the amount of time the simulator takes for each run. Instead, we set the population density in all counties in one type of region at the average population density across counties in that region. As Figure 54, below, shows there will be a quantization error due to this approximation.

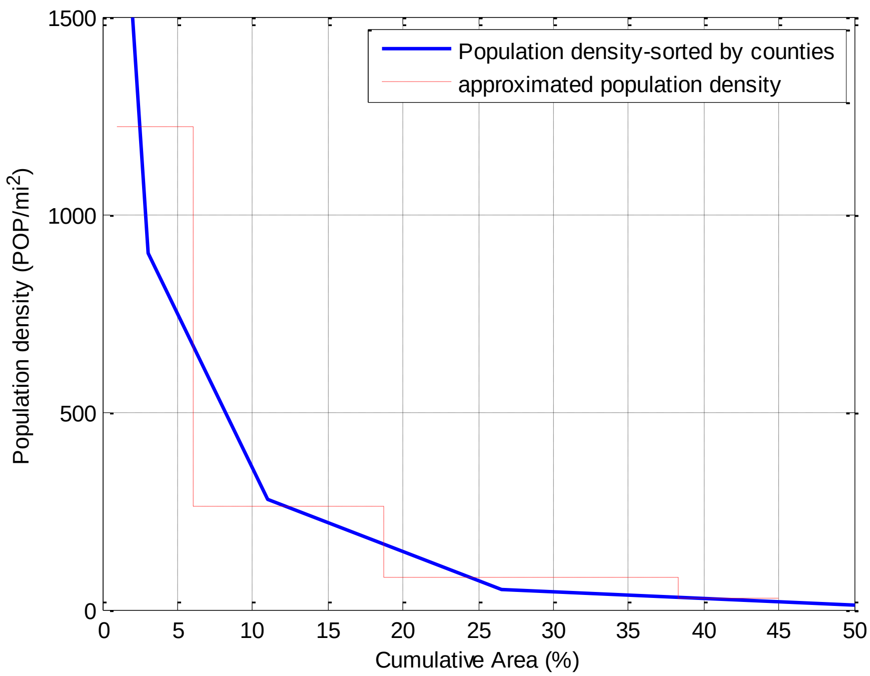

Figure 54: Averaged population density across each region type (plot is approximated)

However, we should point out that our analysis in this chapter mainly involves doing a comparison between network scenarios and finding out the relative change in costs rather than finding out the absolute values of these costs. This type of approximation would affect all scenarios equally. Similar methodologies for approximating population density across maps have been discussed earlier in a number of papers [104], [105]. [106], [119], [111],

We should note that rural regions that have population density lower than 10 pop/mi^2 were not assumed within the coverage target. The targeted area composes 50% of the US region and 98% of the total population.

4.2. Market Share and Spectrum Holdings

It is assumed that the operator targets 10% of subscribers within the operator's coverage area. The operator is assumed to have 40 MHz of spectrum (20 MHz for the downlink).

4.3. Technical Assumptions

We make the same assumptions as in Section 5 of Chapter II, where we simulated the LTE network. We assume it's, a full buffer traffic network with 3 sectors per cell. Bandwidth and spectrum fragmentation are variables that are adjusted to view their effect on results.

4.4. LTE Simulation Result

This is done by building on previous technical simulation we have done in [16] which simulated the relationship between performance and cell size for the investigated scenarios. We use model developed in that paper to generate results that help us build the nationwide LTE network.

5. Results and Discussions

In the following subsections, we plot and explain the results obtained in our analysis. First, we show the cost-analysis results, then the benefit-analysis results, and finally we discuss SA implications.

5.1. SA Costs

We applied our cost analysis to all eight scenarios we introduced earlier, searching for maximum inter-site distances between eNBs that still maintain the targeted average UE throughput as per all assumptions discussed in the previous section. We assumed all scenarios have a total of 20 MHz bandwidth for the downlink. Before we show the results, we have to explain that we are interested in relative difference in costs between the scenarios we are comparing, not the cost absolute numbers. The absolute value of cell sites needed is sensitive to the assumptions that needs to be met, i.e. minimum data rate, population density, maximum range…etc. Therefore, we look at the increase or decrease in cell sites of a scenario relative to a base scenario, this would limit the impact of these assumption to a certain point. Because of our unreasonably high traffic assumption, (as noted in Section 3.3.1) our. results show the 700 MHz base scenario will need to have about ~ 400,000 cell towers to meet full coverage and capacity requirements. This number exceeds the present total number of cell sites for *all* operators in the U.S. This in turn inflates the total costs to exorbitant values. By showing results relative to a base scenario, we can focus on the relative differences, rather than absolute cost numbers.

As Figure 55, below, shows, 700 MHz operators will have the lowest cost whether for contiguous 20 MHz, two 10 MHz independent carriers or for two 10 MHz aggregated carriers. The 700 MHz SA would have a very slight increase over the contiguous case due to the SA impact on LTE equipment. This would be an increase of less than 10% over the independent carrier case due to lower multiuser diversity, which would decrease the efficiency of using the spectrum. For this case, we had to decrease the inter-site distance to maintain the required average UE throughput and, consequently, be able to build more sites. The same applies to the three 2600 MHz scenarios. The 2600 MHz scenarios cost twice as much as the 700 MHz scenarios due to the propagation characteristics which require the former system to build almost twice as many sites as the latter. Having a system that uses both bands would cost more than the 700 MHz systems but less than the 2600 MHz systems alone. Such a system would allow for frequency selective diversity, and if these two bands are aggregated, multiuser diversity will increase, resulting in better performance and consequently less cost.

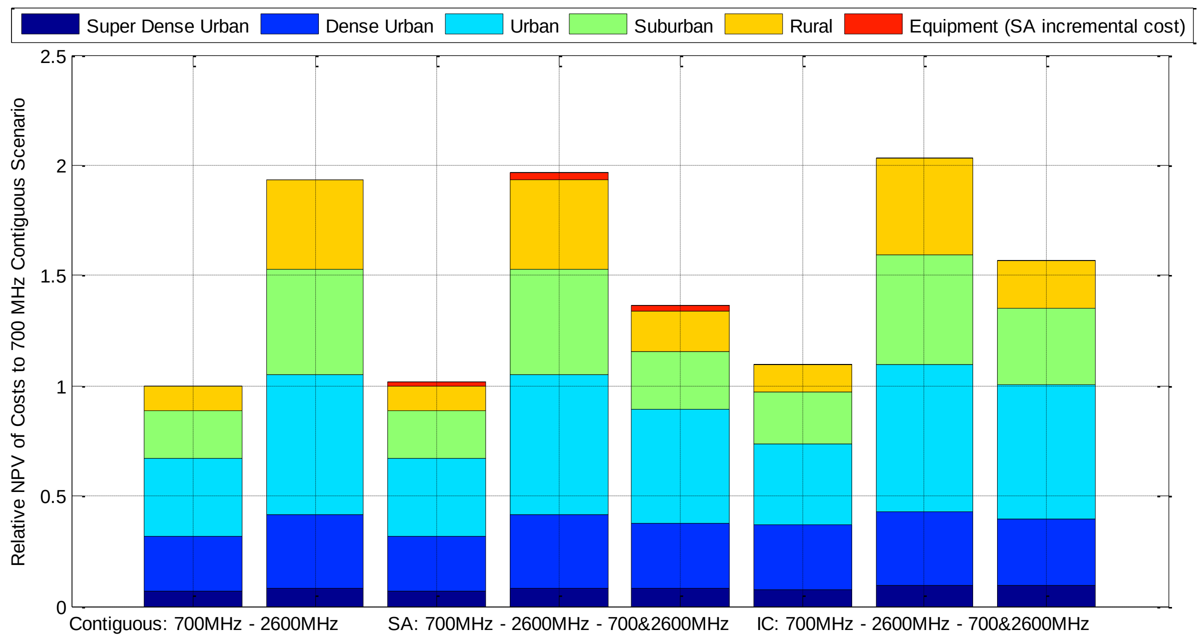

Figure 55: NPV of costs for the different scenarios (relative to the 700 MHz contiguous scenario)

The increase in equipment cost represents a minor percentage of the total cost. If we change the expected increase in equipment costs from $29 to the maximum projection of $118 as per the results included in Chapter III, we see the cost above becomes more significant and represents an increase of approximately 20% in SA scenarios. However, cost in the inter-band SA system is still at least 30% less than in the contiguous 2600 MHz scenario. We should note that the maximum increase projected in previous chapters was based on aggregating five carriers, while in these scenarios only two carriers are aggregated, so the equipment cost will be much less and closer to the earlier figure.

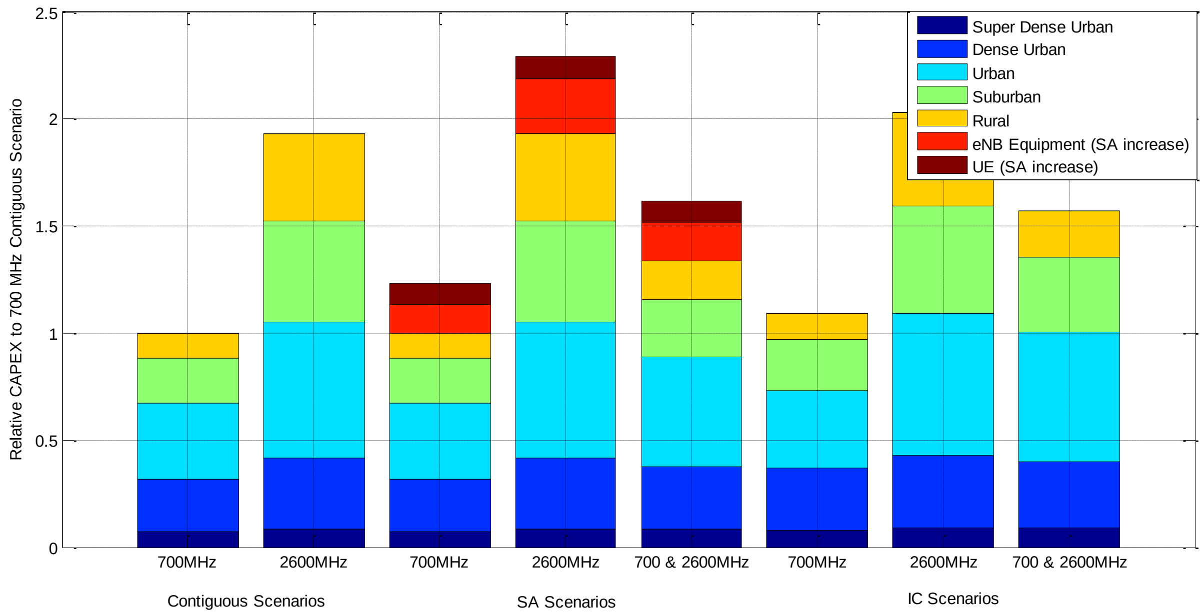

Figure 56: Impact of increasing SA equipment cost

If we change the throughput requirement to be based on maintaining the minimum target for edge UE of 0.1 Mbps, we can see in Figure 57, below, that the ranking will be the same. Although all operators will have to build more sites than in Figure 55, mainly in suburban and rural areas, to maintain the edge UE requirement, the 2600 MHz systems will be required to build more sites by 20-30% while the 700 MHz systems increase in sites needed to be built by less than 10% (because we normalize cost to the 700 MHz base scenario, the increase doesn't show in the figure).

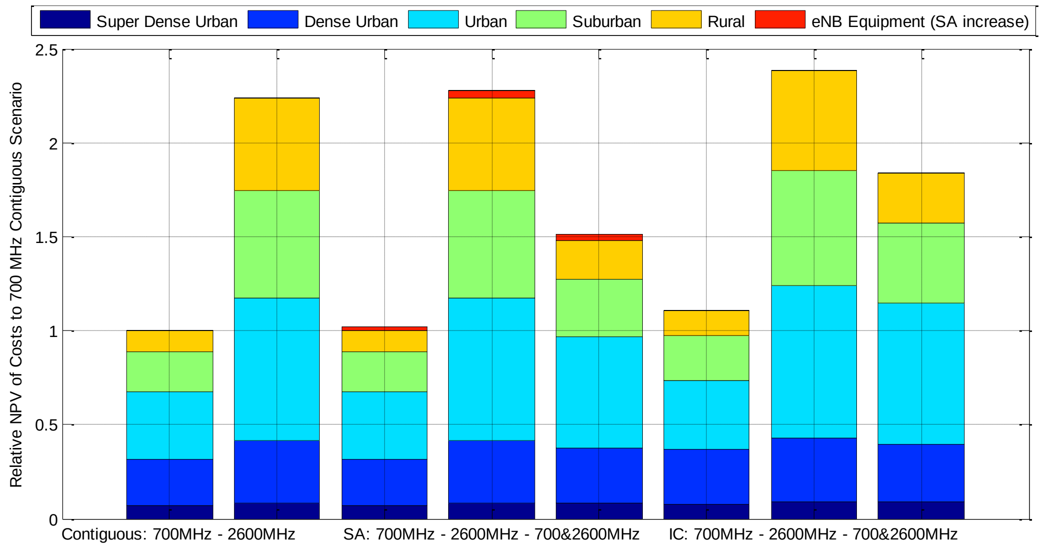

Figure 57: Impact of changing requirement to meet edge UE minimum throughput

5.2. SA Capacity

In the second set of results, we did the reverse analysis. We assumed there is an existing network that has a known net present value of cost and we need to compare the difference in performance between scenarios. We measure performance as total capacity, which is the sum of average cell capacity over all cells in the network. Figure 58, below, shows that the largest total capacity is shown by the 700 MHz contiguous and intra-band SA systems, which is expected. The inter-band SA system delivers capacity at least as great as the 700 MHz intra-band IC system, while the 2600 MHz systems have the lowest capacity.

Although all the eight system scenarios have the same network infrastructure and thus the same network cost, the SA systems incur extra cost due to SA equipment cost. To put both benefits (total capacity delivered) and total combined costs into perspective, we divide them by each other. The resulting cost effectiveness in (bps/$) is shown in the Figure 59, below.

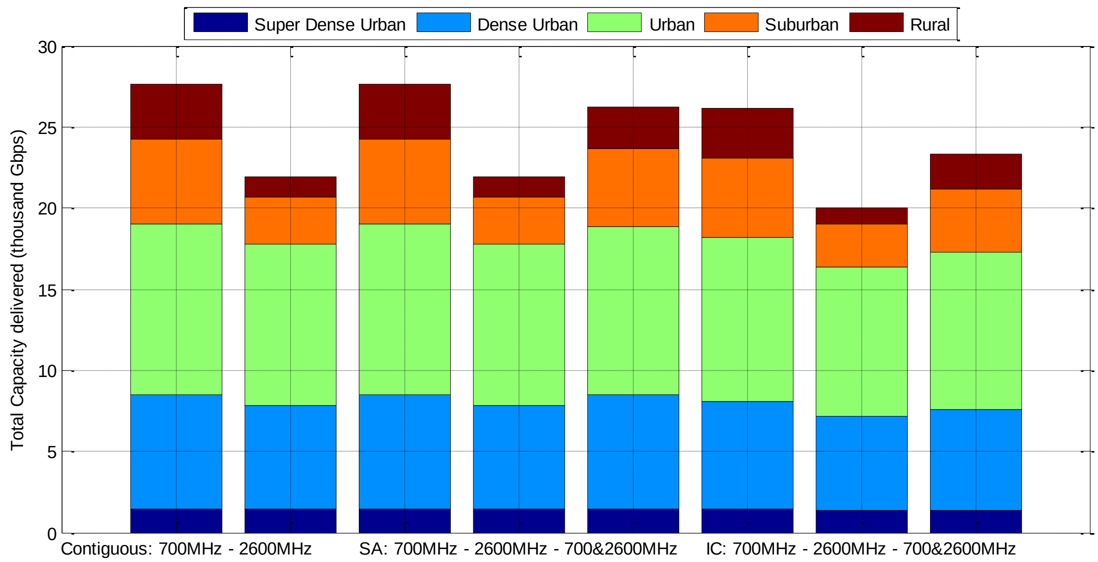

Figure 58: Total capacity delivered by each scenario

.

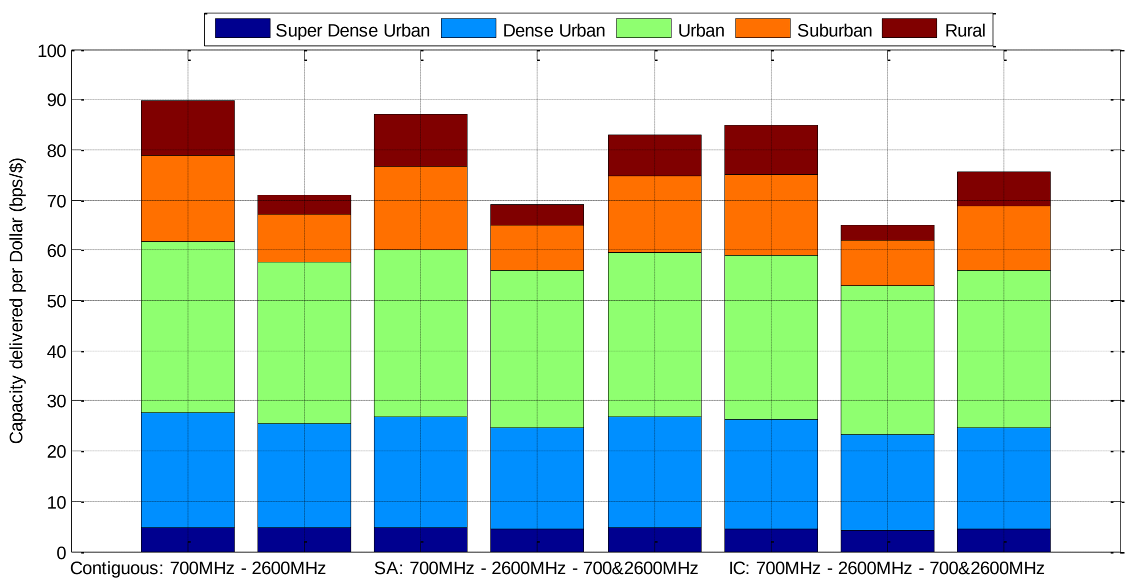

Figure 59: Comparing scenarios with respect to cost effectiveness (measured in bps/$)

As expected, the exclusive use of 700 MHz provides the highest capacity per cost in (bps/$) for operators, while the 2600 MHz scenarios will require a greater investment for each 1 bps delivered. Although the intra-band SA systems have the largest cost due to the cost of added equipment, we can see that the delivered capacity per dollar is greater with this scenario than with the two intra-band independent carriers. Furthermore, the inter-band systems are more cost-effective than the higher frequency band systems. The inter-band SA system is almost as cost-effective as the 700 MHz IC system; it delivers a little bit more capacity but it costs a little bit more. Using SA instead of IC produces an increase of about 5-7 bps delivered per dollar.

5.3. SA Impact on Broadband Access

As discussed in section 6.2 of Chapter II, the peak UE rate for low-density cells is much higher in the SA system than in the IC system. As the spectrum available becomes more fragmented, the advantage of SA becomes more evident, as Figure 60, below, shows.

Using the LTE simulator from Chapter II, we simulate a very low density cell with 3 UEs per cell (1 UE/sector). Also, it is a very small cell, with a 0.5 km inter-site distance, so the user is very close to the eNB. In addition, full buffer traffic is assumed to utilize as many RBs as possible. Scenario 1 assumes the users have SA capability, but with Scenario 2, carriers operate independently. We consider five scenarios, where the available spectrum is different in each. In the first, there is one 20 MHz block, so with or without SA, users experience identical peak throughput. In the second scenario, there is both a 20 MHz block and a 5 MHz block, the latter of which only the SA user can utilize to increase the peak throughput. In the remaining scenarios, the total bandwidth is fixed at 25 MHz, but that bandwidth is broken up in different ways: 10 + 10 + 5 MHz, 10 + 5 + 5 + 5 MHz, and 5 + 5 + 5 + 5 + 5 MHz As the 25 MHz of spectrum becomes more fragmented, the difference in achievable throughput for this user becomes greater.

This example shows that when low-bandwidth spectrum resources are available, they can be utilized more efficiently when SA is used. This will allow more users access to broadband applications that require a high peak rate, such as video streaming.

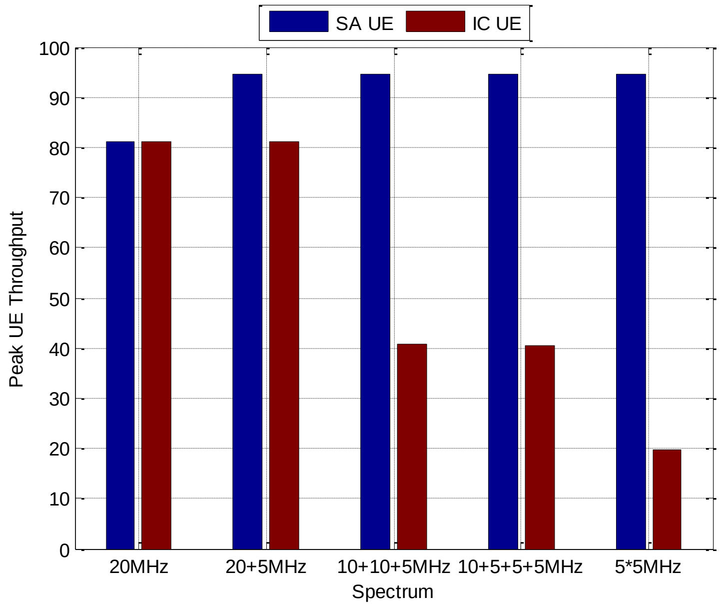

Figure 60: Peak Throughput for a single SA and IC user per sector

5.4. Conclusion

In the summary, analysis in this chapter showed the following:

- The inter-band SA network system might increase the expenditures required for a nationwide network by about 30% as compared to a 700 MHz network of the same bandwidth. On the other hand, this system would save about 50% of the cost of a 2600 MHz network.
- The inter-band SA network will be less cost-effective (measured in bps/$) than the 700 MHz scenario but more cost-effective than the 2600 MHz scenario.
- SA scenarios would show improvement in costs and benefits over IC scenarios.

- Although operators can build out networks at the lowest cost if they have contiguous low-frequency spectrum, it is almost as cost-effective for them to use a mix of low-frequency and high-frequency spectrum with inter-band SA. This is important because there is not enough spectrum at the lower frequencies to support all traffic for all operators, but all operators could realistically hold some low-frequency spectrum.
- SA technology will allow more access to broadband applications that require a high peak rate. Its advantage becomes especially significant when the spectrum is more fragmented.

V. CASE STUDY: CONVERTING TV CHANNELS TO CELLULAR USE

Having looked at the costs of spectrum aggregation technology when building out a greenfield wireless network, we now compare the use of spectrum aggregation technology with the conventional option of refarming spectrum to aggregate available spectrum fragments physically. For historical reasons, most countries have a block of spectrum that regulations say can be used for TV but cannot be used for cellular. Studies show it is technically possible to allow a channel to be used for TV in some places and cellular in others. Moreover, there may be more spectrum in a TV band than is needed for TV. We expect this to happen in the US soon as a result of an incentive auction [125]. It can also happen when TV technology changes, as we saw in the digital transition. When this occurs, there is choice between assigning licenses with smaller bandwidth or repacking and assigning licenses with larger bandwidth.

In this chapter, first, we define the research questions followed by background information on spectrum repacking. Then, we explain the modeling approach and all associated assumptions. Finally, we plot some results and discuss our findings from this comparison.

1. Research Questions

The fifth chapter of this research asks the following question:

Can the technology enabling spectrum aggregation be an economical alternative to the physical aggregation (repacking) of fragmented blocks of spectrum?

- What is the build-out deployment cost of a greenfield network that uses fragmented spectrum blocks across the UHF TV band and spectrum aggregation technology as compared to a network that uses a contiguous spectrum created through repacking?
- What is the cost of repacking the spectrum to make it contiguous?

2. Background

2.1. Review on TV Bands

Because of the interference protections set by regulators between TV many TV channels in each market remain unallocated to any stations, and this results in what is known as "TV white spaces [122]." Many papers have tried to quantify the total unused spectrum and capacity of white space [123], [124]. Such quantification depends on the technology to be used, e.g. fixed or mobile, and its technical characteristics.

Several extended studies--e.g., [125], [126], [127], [128], [129], and [130], have researched the possibility of cellular and broadcasting systems co-existing in the same band. Results vary, with some concluding that it is possible, while others, taking a more conservative stance, conclude that it is not feasible. The analyses also discuss likely co-channel and adjacent-channel interference between the two systems, and note the need for measures to mitigate interference.

Additional studies focus on TV stations' relinquishing part or their entire spectrum--either through incentive auction [131], or by sharing it--in order to increase the total spectrum that could be utilized for services such as cellular phone service [132]. However, when this available spectrum is fragmented across the band, the band might need to be reallocated to create a contiguous spectrum. An additional possibility is the use of SA over the TVWS, which, as discussed in this paper [133], shows that the proposed aggregation system would result in a net throughput gain.

The former approach of refarming spectrum by assigning TV stations to new channels would, it's been shown, most likely result in additional costs [134], [135] and [136]. This increase could either be paid by incumbent users in order to relinquish the spectrum, or it could be moved to another band. In the first case, compensation might be paid by the incumbent in order to relinquish part of the spectrum and meet its communication needs through other means such as wired networks. In the second case, the costs would pay for allocating a new spectrum band for the incumbent to use and upgrading its equipment in order to operate in the new band. However, all these costs vary greatly, depending on the incumbent user(s), whether the station is public or commercial, whether a mobile or fixed broadcasting service is being used, and so on.

In general, these costs occur as a result of the delay that operators incur while waiting for the required spectrum to be cleared of incumbent users. Historical data shows that the transition time required for reallocating spectrum and changing necessary regulations has taken from 6-13 years, with an average of 9 years [1]. This delay, in turn, requires the operator to increase the cellularity needed to meet growth requirements while also waiting for the spectrum to be made available, assuming that the operator cannot handle extra traffic without upgrading its network.

2.2. Analytical Overview

LTE could be operated over frequency bands between TV stations [137], [138]. When converting the use of TV channels into mobile systems, interference mitigation measures must be taken first. Some studies have found that the two services can coexist in the same band but not necessarily efficiently [139]. However, the white spaces of spectrum, which could potentially be used for mobile services, can be made available by either:

- relaxing interference constraints [131]; or
- TV stations giving up their spectrum channels through incentive auctions [134]

Either way, the freed-up channels are generally fragmented across the TV spectrum. They can be utilized as fragmented as they are, or the spectrum can be repacked by reassigning the remaining TV channels in order to repack the freed spectrum to make a contiguous wide band. The general cost of refarming spectrum depends on two main factors:

– the cost of providing the incumbent user of the adjacent band with compensation in order to change its frequency of operation, and/or
– the cost of the transition time that must pass before the band is cleared (i.e., the opportunity cost).

3. Modeling the Analysis

3.1. Scenarios Investigated

Since broadcast TV requires large distances between TV coverage areas for channel-interference protection, a TV viewer in any given location can only receive TV signals over a fraction of the total spectrum allocated to broadcast TV [131]. Moreover, while the amount of TV allocated to television must be enough to accommodate the largest television-viewing markets such as New York City, there are considerably fewer television stations in most markets. As a result, a median of 15 out of 37 UHF 6-MHz channels are assigned to a TV station in the largest 10 markets (out of the 210 designated market areas). It is possible to make some of these TV channels available for cellular, either by reducing the number of channels used for TV as would occur through incentive auctions, or by reducing the coverage areas of some TV stations. The resulting freed 6 MHz channels could be located at any frequency across the spectrum band 470-698 MHz in each market. We consider two options for how this spectrum can be allocated to cellular network:

A. by using the fragmented blocks and spectrum aggregation technology; or
B. by aggregating or repacking allocated spectrum in each market physically by reallocating spectrum for TV stations in order to form a contiguous wider block of the freed spectrum, as shown in the Figure 61, below.

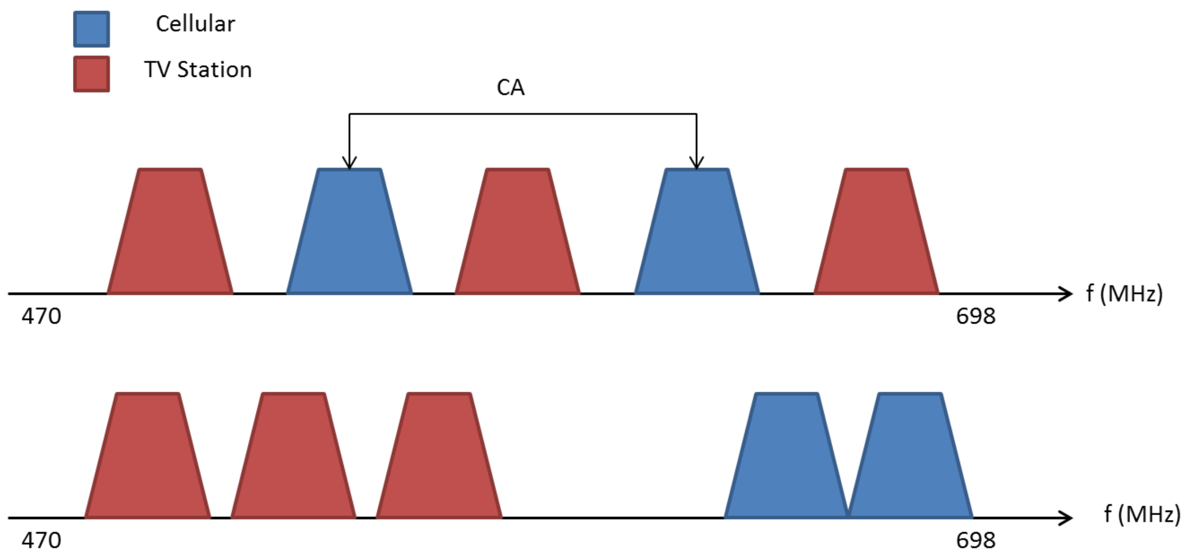

Figure 61: Option A: use of SA, Option B: spectrum repacking

3.2. Analysis Formulation

The freed channels being available, we now compare the costs of the two alternatives mentioned above. Then, we repeat the cost analysis from Chapter IV to estimate the network costs of both scenarios, A and B. Additional costs will be included with scenario B in order to attain the repacked contiguous block of spectrum that we began with. This cost is based on how many TV stations need to be reallocated new spectrum channels in each market. This reallocation cost will be estimated separately and then added to the total cost of this scenario, as the flow diagram in Figure 62, below, shows.

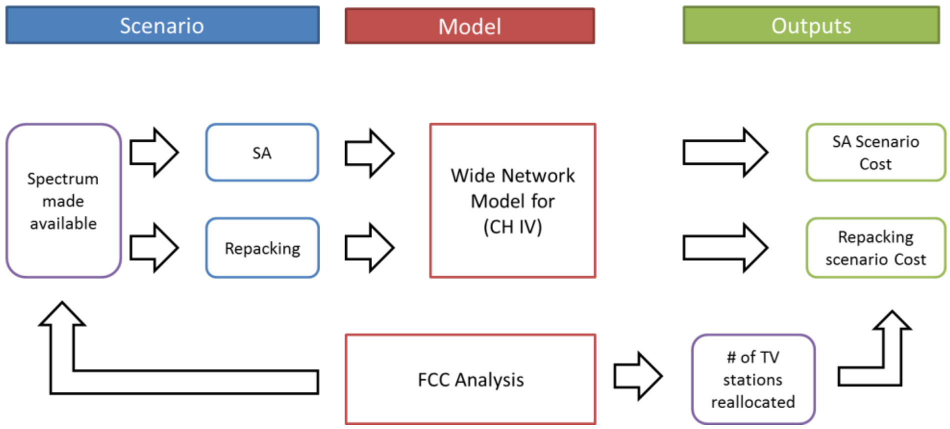

Figure 62: Simplified flow diagram of the proposed analysis

3.3. Analysis Models

3.3.1. Spectrum Repacking

Our assumptions about spectrum availability and repacking in this case study are largely based on a simulation study [137] conducted by the FCC in the context of the incentive auction [127]. Through this incentive auction, some TV stations would voluntarily relinquish spectrum, and then the FCC would repack the TV stations that remain in the UHF band. The first step frees a number of 6 MHz channels in the 600 MHz band, and the second step creates a contiguous block of spectrum for broadband from these fragmented channels. In their simulation study, the FCC created 100 unique repacking scenarios using the approach described in [140]. For each scenario, they estimated the total MHz of spectrum that could be cleared after repacking, and the percentage of stations for which some adjustment or repacking would be required. We use these results to determine spectrum availability. Without repacking, blocks in the fragmented spectrum are assumed to use a 0.5 MHz guard band at both edges of each 6-MHz channel for interference protection [125], [126], [127], as shown in Figure 63. With repacking, only one guard band of 4-6 MHz is needed at the edge between the contiguous spectrum and the nearest TV station [141] .

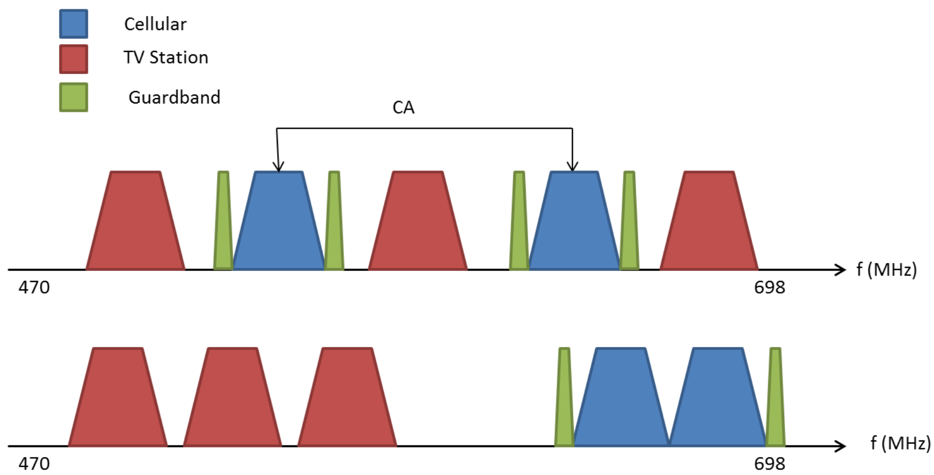

Figure 63: The two options with guardbands

3.3.2. Cost Modeling

The cost estimates for the cellular network in both contiguous and fragmented spectrum use the methodology developed in Chapter IV. The repacking cost equals the product of the number of stations that must change frequency and the cost per station, where the latter includes the following elements:

- costs for the TV station that are assigned a new channel, including costs for transmitters, antennas, and feed lines; and
- payment to the broadcaster for transition management

We collected information about these costs from interested parties responding to an FCC NPRM [141], mainly CTIA and NAB, which estimated costs based on data from FCC repacking scenario, as will be seen in the next section about input and assumptions.

4. Inputs and Assumptions

We use the same network model and apply the same technical and cost assumptions used in the cost analysis performed in previous chapter (Section 3.3.1 and Section 4) when running the network scenarios. **Because, as noted in the previous chapter, the user traffic assumptions are much too high, the total system costs calculated in both scenarios will also be unrealistically high. However, the relative values will still be of interest.**

We also use the following assumptions based on data about spectrum repacking:

- In every market area, 14 6-MHz TV channels (or a total of 84 MHz) are cleared
- None of the 14 are contiguous
- 7 channels each used by cellular operators for upstream/downstream
- Two operators want to build out a greenfield network. Each targets a 20% of population and has data rate need to be met

For scenario A (SA, No Repacking)

- Two additional 0.5 MHz guard bands taken from each 6 MHz channel is required so the total spectrum available for LTE is 70 MHz. [141]
- Radios support variable separation between upstream and downstream of frequency pairs because the allocated spectrum could be anywhere across the band.
- The cleared channels could be located anywhere between 470 MHz and 698 MHz, so we assume half are located in the lower band and half in the upper band

For scenario B (Repacking, and No SA)

- A 4 MHz guard band between the system and the nearest TV station, so a total of 80 MHz will be usable for cellular [142]
- 1,000 TV stations will need to change channels due to repacking at an average cost of $900,000 per station [142]
- The cleared spectrum is in the upper end of the 600 MHz band

5. Results and Discussions

As explained in section 4, the total cost of repacking would be about \$1 billion, significantly less than the \$1.75 billion included in the FCC's Spectrum Relocation Fund. Running the same network cost analysis as described in Chapter IV on the two scenarios and adding the repacking cost produces the results shown in Figure 64, below. Because of the need for extra guard bands between the LTE system and the broadcasting system (as explained earlier in this chapter), the SA scenario requires more spectrum for the guard band, leaving less for data utilization. In Scenario A, the spectrum is fragmented within the TV UHF band creating more neighboring TV stations than in Scenario B, where all stations are packed on one side. This (called cost of fragmentation) seen in the SA scenario requiring the building of more infrastructure in order to meet the capacity requirement. Although some fragments in Scenario A were assumed to have a frequency around 470 MHz, which has better propagation characteristics, this wasn't significant enough to reduce the cost due to less spectrum utilization.

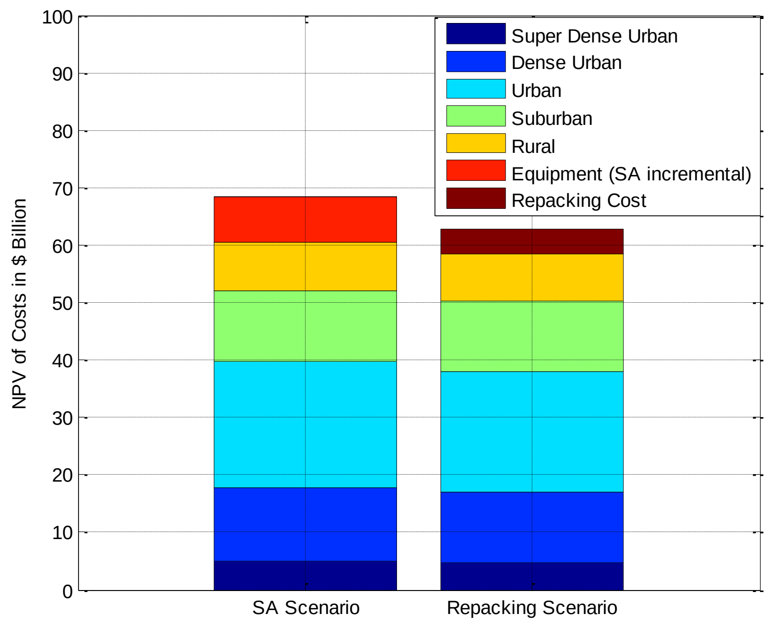

Figure 64: NPV of costs of the two scenarios

The difference in the cost of building out the two networks **[using our excessive traffic assumption]** is about $2 billion. **Under a more realistic traffic assumption, the total costs, and the difference in costs would be even less.** Even $2 billion is small enough that it is still possible for costs to be lower with SA than with repacking. For example, if the incremental cost of SA equipment turns out to be negligible and the repacking cost is at its projected maximum value, then scenario B will still cost more than Scenario A, as the figure below shows.

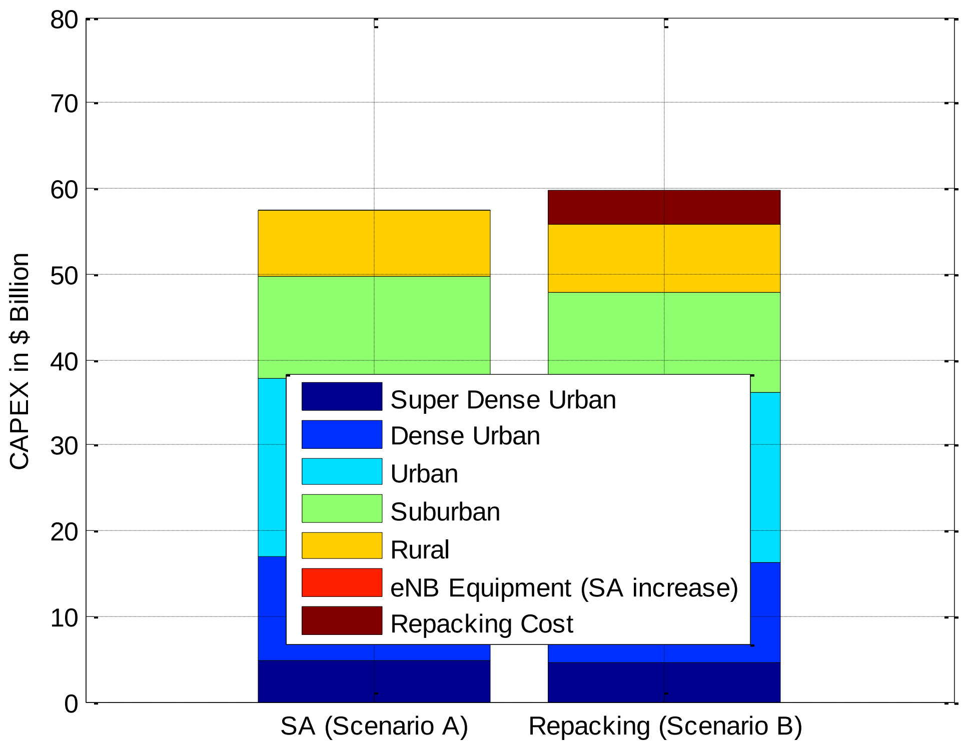

Figure 65: Costs when assuming SA has no equipment cost and repacking at maximum cost

However, if we assume the highest value for estimated increase in equipment costs due to SA, Scenario A will again have higher cost. This confirms that spectrum fragmentation, which creates the need for more guard bands under our current assumptions, has a significant cost. If we instead assumed that an LTE system would not cause or be victim of harmful interference from a broadcasting system in an adjacent channel, this would remove the need for these extra guard bands and equalize costs of the two scenarios, as both are capable of utilizing all 40 MHz. This question of whether SA is more cost-effective than repacking would then depend on the cost of the SA equipment itself and the cost of repacking, rather than the impact on infrastructure costs. In this analysis, the first ranges between $1.5 and 8 billion, and the latter varies between $1 and 4 billion.

6. Conclusion

We cannot reach a general conclusion from these results as to whether SA is more cost-effective than refarming, because the results are sensitive to critical input assumptions for which we need improved estimates. However, even with the assumptions we made about LTE systems being able to coexist with broadcasting system with 0.5 MHz separation, SA would cost more than repacking. This could indicate that repacking might be the cost-effective solution.

If the neighboring systems were LTE systems, the cost of fragmentation would be 0 because it would have its own built-in guard band that would comprise 10% of the spectrum no matter how fragmented the spectrum as a whole is. We can say that SA would be a cost-effective alternative to refarming when we have all LTE systems coexist in the same band.

.

VI. EMPIRICAL STUDY REGARDING SPECTRUM AUCTIONS

Before we comment, in the next chapter, on the impact of spectrum aggregation technology on spectrum economics, we now address, in this chapter, the willingness of wireless operators to pay for spectrum. SA enables virtual contiguity between non-contiguous carriers, which might affect the premium value of wide contiguity in auctioned blocks that was seen at auctions in the past. The objective of this chapter is to investigate if there is any evidence that operators might value a unit of spectrum in ($/MHz-POP) differently depending on the bandwidth of the block and the frequency band. Such evidence could help us to project the impact of SA on spectrum economics and valuation, which will be discussed in the next chapter.

We start this chapter by first defining our research question, and then reviewing previous work on spectrum auction analysis. Next, we explain our modelling approach used to analyze data from multiple auctions. Then, we review the data we collected for spectrum auctions. And, finally, we show and we discuss the results of our analysis.

1. Research Questions

This brief chapter tries to answer the following questions:

What factors impacted operators' WTP for auctioned spectrum blocks?

- How did operators' WTP for auctioned spectrum blocks change based on the block size?
- How did the use of WTP change based on the frequency band?
- How did the use of WTP change between 2001 and 2014, as technology changed from 3G to 4G?

2. Background

In this section, we discuss previous work that explores the relationship between auction prices and variables that might influence these prices, especially the frequency and bandwidth of auctioned spectrum. Many papers did empirical studies of spectrum auction data. Logarithmic regression models were used to analyze FCC auction 73 results in the 700 MHz band in 2008 [143]. The model introduced a dummy independent variable that represents adjacency, i.e. it equals to 1 when auctioned block is located adjacent to another block in the 700 MHz band auctioned earlier by the FCC. Analysis shows that those bidders who have access to a license in the adjacent block offered the highest bid for the auctioned block. Extensive empirical research studies were done on samples of national 3G spectrum auctions for the period 2000-2007 [144], [145], [146]. Econometric models were used to identify the factors that affect auction revenues. More econometric analysis of 3G auction spectrum valuation has been done [147]. It examines the factors affecting the price and the auction design. Similarly, linear regression analysis for all mobile licenses sold in an auction was done to investigate all independent variables affecting price paid by bidders in different 3G auctions [148]. Different econometric analysis was conducted to examine the Canadian AWS auction in 2008 [149]. The focus of this study was investigating the impact of designing the auction such that 40 MHz of spectrum was set-aside for new entrants exclusively. Results showed that the proposed design, which was meant to increase competition in the market, lowered the auction efficiency. This auction is considered a good example of how the regulator policy goals (increasing competition) can be reflected in auction design [150].

Finally, some review papers like [151] discuss the benefits of larger spectrum blocks in term of increasing trunking efficiency, inter-cell distances and deploying broadband systems and it argues qualitatively that such a block has high value for operators.

In conclusion, while some work has been done to investigate the impact of frequency on auction price, no extensive analysis has been done to measure the impact of block size. In this chapter, we use the comparable econometric analysis approach to examine spectrum auction data and the variables that affect spectrum valuation. Particularly, we look for empirical evidence about the impact of block size and frequency bands on valuation.

3. Input Data

We collected 3G spectrum auction results in different countries from economic consultancy service DotEcon and recent 4G auction results from both the news and regulator websites that we list in Appendix F. Our resulting database shows the price of the winning bids on different spectrum bands auctioned in different countries and at different times. The data provided included the following information:

- Country: Data were collected from 51 different countries. A few of these countries awarded some licenses to run "beauty contests" (a type of administrative licensing) instead of running auctions. Also, a significant number of these countries had only a small number of auctions, which might not have yielded statistically significant results when data analyses were run because of the limited number of observations.
- Bandwidth of licensed block: These ranged between 5 and 60 MHz for a single license.
- Population covered by the license: Small countries usually auctioned nationwide licenses, which made this factor the most fixed among all data points for that auction.
- Duration of the license: This was generally for 10 or 20 years.

- Date of the auction: Most of the auctions took place between 2000 and 2010. Some new data from recent auctions were added; however, quite a number of these auctions were Combinatorial Clock Auctions. That means the bidder placed a bid on multiple licenses that combined both multiple frequency bands and multiple blocks with different bandwidths. These observations were not useful for our analysis since our focus was on finding the impact of frequency bands and the size of spectrum blocks on bidders' WTP.
- Frequency band: This included frequency bands between 700 MHz and 2.6 MHz
- Price: The data provides both the winning bid price and the reserve price. Sometimes they were equal which may have indicated a lack of competition in the auction.

This data was also missing some information about variables that could affect the auction outcomes:

- Paired or unpaired: Most operators prefer paired for FDD operations over TDD spectrum that requires synchronization with neighboring systems. We tried to fill this information gap by finding some recent auctions that were documented on regulator websites or in other references.
- Population density: Information on the population served was also often lacking. Rural areas were less preferred by operators due to the high cost of covering a significant amount of area with fewer paying customers.
- Winner's current holding of spectrum: There was no information about the operator that might indicate whether the bidder was a new entrant or an existing operator and whether it explained the bidder's WTP for a specific band or block.
- Auction rules: The spectrum cap is a very significant factor on auction outcomes. Some bidders have access to only certain licenses due to cap restrictions. This was the case for a

Canadian auction where only new entrants could bid on specific licenses. In addition, we searched regulators' websites for other information about policies that might affect the bidding in auctions.

In addition to these two types of input data, when we were about to run an analysis across different auctions, we collected facts about the market during the time of the auction, including the:

- Number of operators in the market: This served as a measure of the competitiveness within that market.
- Number of licenses in auction: Along with the reserve price, this served as an indicator of how competitive the auction was.

Table 17, below, summarizes the multiple data sets that we selected from the database for the regression analyses.

Table 16: Data sets from auction database

Country	Auction Year	Frequency band	Bandwidth	Number of licenses	Note
Australia	2001	2.1 GHz	5 – 10 MHz	48 regional	No bidder was permitted to acquire more than 2 x 15 MHz in the same area
	2013	700 MHz and 2.5 GHz	10-40 MHz	9 national and 14 regional	This was a combinatorial clock auction, where bidders bid on a package with multiple bands and block sizes
Germany	2000	2 GHz	10 MHz	6 national	No bidder was allowed to acquire more than 2x15 MHz
	2010	800, 1800,	5-14.2 MHz	41 national	

		2100 and 2500 MHz			
United States	2006	2.1 GHz	5-10 MHz	1122 regional	
	2008	2.1 GHz	5-10 MHz	35 regional	
Canada	2008	2.1 GHz	5-10 MHz	292 regional	Some bands were open to new entrant bidders only
	2014	700 MHz	5-6 MHz	98 regional	
United Kingdom	2000	2 GHz	10 MHz	5 national	
	2012	800 MHz and 2.6 GHz	5-35 MHz	5 national	Some bidders bid on both bands as a package (CCA format)
Brazil	2007	2 GHz	10-30 MHz	36 national	
	2012	450 MHz and 2.5 GHz	10-20 MHz	4 national	This auction included a spectrum cap of 80 MHz per operator.
	2014	700 MHz	10 MHz	6 national	

4. Modeling the Analysis

4.1. Independent Variables

Spectrum auction results provide us with the market price for an auctioned block of spectrum. Our dependent variable price (*P*) is dependent on different factors related to the block of spectrum, the license and the auction. If we look at results of a specific auction that took place in a given country, it's apparent that the spectrum market price is dependent on the following variables:

- Duration of the spectrum license (*DL*);
- Population of the license area (*Pop*);

- Area per capita, a measure of population density in the license area (*Apop*). This variable might be necessary if the spectrum licenses being auctioned were for different regions with different population densities.
- Bandwidth of the auctioned block (*BW*). Available auction data indicated that each auction usually offered, at the most, two different bandwidths of auctioned blocks that could be represented as a dummy variables of 1, if a larger block, or 0, if a smaller one.
- Frequency band of the auctioned block (*Band*). Also, each auction usually offered , at the most, two different frequency bands of auctioned blocks that could be represented as dummy variables of 1, if a lower frequency band, or 0, if a higher one. Otherwise, it would represent the inverse of the frequency band since we expect $P \propto \frac{1}{Frequency}$ so we get a positive coefficient.
- Paired or unpaired spectrum (*Mode*). This can be represented as dummy variable, which would be 1, if paired, and 0, if unpaired.
- Wireless technology (Tech): 3G operates on specific bands, buy operators mostly prefer 2.1 GHz. From approximately 2000-2010, when bands like 800 and 1800 MHz were auctioned in some European countries, they could be utilized for GSM. Thus, we will represent this as a dummy variable to account for technology effect.
- Auction policies that control bidding for some parts of the auctioned spectrum.

To run regression for all auctions over multiple years, instead of running multiple tests, each for just one specific auction, we attempted to control more variables due to the differences in the spectrum market at the different times auctions were held. The following variables, thus, require further consideration:

– Time of the auction (*YR*): We added to the regression equation dummy variables (*YRs*) one of which would be 1 in the auction year while the rest were 0. We observed auctioned blocks of both large and small sizes to see how the coefficients for the years' variables changed from 2001 to 2014.

– Ratio of winners to bidders: This variable measured competition in the auction (*Comp*). Another definition would be the ratio of the reserve price to the winning price. A third measure would be the number of licenses in that auction.

– Number of operators in the market (*MNO*).: Since this number might affect the spectrum price inversely, the inverse can serve as a measure of competition in the market.

4.2. General Analysis of the Data

To test the data, we used the simplest ordinary least squares (OLS) regression model to estimate the relationship between price and the two most important variables, the amount of spectrum and the population, as the following:

Equation 27

$$P_{i,b} = \alpha_0 + \alpha_1(POP_i \times BW_b)$$

Where:

- i is the geographic area
- b is the auctioned block

This is the most obvious model because spectrum prices are usually expressed in ($/MHz-POP). Running this regression on all the data sets would reduce the explanatory power of the model R^2 due to many variations between countries with regard to currency and other factors. When we apply this test to the largest set of data on a single country (the U.S., 1,122 observations), it shows a statistically significant result at the 5% level with $\alpha_1 = 0.73$, $R^2 = 0.85$, leaving 15% of the price variation unexplained, as expected. In the next section, we present multivariable models that allow analysis of variables independent from each other.

4.3. Hypothesis

We test the following null hypotheses:

A. "the price per MHz-pop is independent of the block bandwidth size"

B. "the price per MHz-pop is independent of the frequency band"

C. "the price per MHz-pop hasn't changed over time with respect to block size"

4.4. Regression Models

Our mission is to try to analyze the two independent variables that we are concerned about and their impact on price: i.e., block size and frequency band. From the simple linear model in the previous subsection and from literature, we know that auction price is significantly dependent on bandwidth: the larger the block bandwidth, the higher the price operators are willing to pay. What we wanted to know next is the impact of the block size or bandwidth on operators' valuation for a unit of spectrum in ($/POP-MHz). Similarly, we want to know if their valuation for such a unit is affected by the spectrum's frequency band.

4.4.1. Model 1

To test the null hypothesis A, we start with the following equation:

Equation 28

$$PMHz_{i,b} \approx POP_i^{\beta_1} \times BW_b^{(1+\beta_2)}$$

Where *PMHz* is the price per MHz. We want to know if the price per unit of spectrum is dependent linearly on bandwidth. If $\beta_2 = 0$, then the unit price is independent of block size; otherwise we can reject the null hypothesis. Taking logarithm of both sides:

Equation 29

$$ln(PMHz_{i,b}) = \beta_0 + \beta_1 ln(POP_i) + (1 + \beta_2) ln(BW_b)$$

4.4.2. Model 2

Instead of the logarithmic relation between price and bandwidth, we propose a different linear model:

Equation 30

$$PMHz_{i,b} = \beta_0 + \beta_1 POP_i + \beta_2 BW_b$$

Again, we reject the null hypothesis A if $\beta_2 \neq 0$.

4.4.3. Model 3

As discussed before, regressing price on bandwidth and population only would leave unexplained variation in price. Instead, we try to include more variables in a different regression model to test block size and frequency band relation to price per MHz, as follows:

Equation 31

$$PMHz = \beta_0 + \beta_1 Band + \beta_2 BW + \beta_3 Mod + \beta_4 DL + \beta_5 POP + \beta_5 Tech$$

We reject the null Hypothesis A if $\beta_2 \neq 0$, and the null Hypothesis B if $\beta_1 \neq 0$. The third variable is a dummy variable. The fourth and fifth variables can be ignored when they are all equal for all licenses in a particular auction. We add the last variable in case there were multiple bands being auctioned and some of them could be used for GSM or 3G exclusively at that time. We can add more variables as needed--for example if we know there is a cap limit on some bidders who can’t bid for some licenses because of it.

4.4.4. Model 4

In this last model, we run regression across more than one auction taking place in the same country but at different times. The model will be similar to model 3 but with more variables:

Equation 32

$$PMHz = \beta_0 + \beta_1 BW + \beta_2 Band + \beta_3 Mod + \beta_4 DL + \beta_5 POP + \beta_5 Tech + \beta_6 Comp + \beta_7 MNO + \beta_8 YR$$

The purpose of this is to test null hypothesis C, if $\beta_8 \neq 0$, we can reject the null hypothesis. More specifically we want to know if smaller fragments of spectrum became more valuable over time. So, we need to analyze β_1 and note how it changes over time.

5. Results and Discussion

In most country cases, we try to show results for regressions based on models 1 and 2. Model 3 and 4 are only applied when we have unexplained variables effect. So, discussed results will be based on different models depending on the collected data set for each country.

5.1. Australia

The 2001 Australian auction for 2.1 GHz spectrum contains 48 observations with the following statistics about unit price:

Table 17: Statistics from Australian auction in 2001

Bandwidth	Mode	Mean (AUS \$/MHz-POP)	Std (AUS \$/MHz-POP)
5 MHz	Unpaired	0.1424	0.0310
5 MHz	Paired	1.0760	1.4116
10 MHz	Paired	0.6593	0.0614

However, this doesn't mean paired 5 MHz blocks were seen as more valuable by operators than a paired 10 MHz block, because there were two observations (out of 25) which showed a very high value, and when removed, the 5 remaining MHz mean would be around 0.63 AUS$/MHz-POP. Thus, we apply the first three regression models, with only variable (Mode) being added to model 3 since all other variables in the auction were fixed. Results are shown in the table below.

Table 18: Regression results for Australian auction

	Model 1	Model 2	Model 3
β_2	1.43	163,127	81,806
$P-value$	2.74×10^{-11}	2.3×10^{-5}	0.093
R^2	0.88	0.87	0.88

We can see that all three models have a high R^2 value. While the first two models show statistically significant results at a 1% level that allow us to reject the null hypothesis and provide evidence that valuation per unit is dependent on block size, the third model shows it only at the 10% level. This was expected because we included a dummy variable (Mode) in the model. The unpaired spectrum has much less value than paired channels regardless of the bandwidth. In this auction, all unpaired blocks were small, so in the first two models, its low valuation was attributed to the block size, while actually it was because of its operation mode.

In the 2014 auction, a combinational clock auction format was followed. This meant that the Australian Communication and Media Authority (ACMA) alone knew the total amount that each bidder paid for their package of spectrum (i.e., a combination of spectrum in the 700 MHz and 2.5 GHz bands). It was not possible to determine how the total price paid by any bidder was split between the spectrum it acquired in the 700 MHz and 2.5 GHz bands, nor could this be determined for the block sizes. However, ACMA set reserve prices in the 700 MHz band at AUS$1.36/MHz/pop and in the 2.5 GHz band at AUS$0.03/MHz/pop. This shows that ACMA expected operators to value a unit of spectrum more highly when it was in a lower band.

5.2. Germany

The 2010 German spectrum auction had 41 observations with the following statistics:

Table 19: Statistics from German auction in 2010

Bandwidth	Band (MHz)	Mode	Mean (€/MHz-POP)
5 MHz	2600	Unpaired	0.020
5 MHz	2600	Paired	0.022
5 MHz	2100	Unpaired	0.014
14.2 MHz	2100	Unpaired	0.005
4.95 MHz	2100	Paired	0.107
5 MHz	1800	Paired	0.025
5 MHz	800	Paired	0.726

Clearly this data set isn't a good example to test Null Hypothesis A because there are no different block sizes being auctioned that can be compared. For this reason, when we applied models 1 and 2, we ended up with a very small value for R^2, which indicates that variations in price cannot be explained by the block size variable alone. When we apply model 3 with variables for (Mode) and (Band), we get R^2 value of 0.965 and a large positive coefficient β_1 (multiplied by $\frac{1}{frequency\ band}$), which is statistically significant at 1% level. This shows that the unit price is highly dependent on the frequency band, and that we can reject the null hypothesis B.

For the year 2000 auction, 10 MHz paired channel in 2 GHz band had an average value of 5.12 €/MHz-POP. This is a much higher value than that of the 5 MHz paired channel in the same band in the 2010 auction. However, this is not statistically significant evidence given that there was a 10-year gap between the two auctions with different market players and many other factors that can't be captured by our proposed model 4.

5.3. United States

FCC auctions 66 and 78 for mostly advanced wireless system (AWS-1) spectrum had the following statistics:

Table 20: Statistics from the AWS-1 Auction

Bandwidth	Year	Mean ($/MHz-POP)	Std ($/MHz-POP)
5 MHz	2006	0.26	0.25
10 MHz	2006	0.18	0.19
5 MHz	2008	0.04	0.019
10 MHz	2008	0.10	0.072

Although the average value for 5MHz bandwidth blocks was larger than for 10 MHz blocks in 2006, when we ran regressions using model 1 and 2, we found that the larger block was valued more highly in both auctions, as the Table 21, below, shows.

Table 21: Results for regressions on AWS-1 auctions

Model & Auction	β_2	$P - value$	R^2
Model 1 (2006)	0.19	0.06	0.85
Model 2 (2006)	37,383	0.01	0.85
Model 1 (2008)	1.12	0.04	0.73
Model 2 (2008)	732.9	0.38	0.89

All, except the last test, show that the price per MHz is dependent on the block size. In addition, we tried to test null hypothesis C by comparing the results from both auctions to see if there was any evidence that valuation had changed over the two years studied. We added a dummy variable for the year 2008 and another variable as a measure for the competitiveness in the auction based on the number of bidders. No statistically significant results were shown.

5.4. Canada

The following table shows the average value per MHz-POP for two different frequency bands paid by each operator in two different auctions.

Table 22: Average prices paid in two Canadian auctions

Bidder	2 GHz (2008)	700 MHz (2014)
Bell Mobility Inc.	1.01 $/MHz-POP	1.05 $/MHz-POP
Bragg Communications Inc.	0.36 $/MHz-POP	0.65 $/MHz-POP
Rogers Communications Inc.	1.04 $/MHz-POP	4.32 $/MHz-POP
TELUS Communications Company	1.20 $/MHz-POP	1.78 $/MHz-POP

It shows that operators value a unit of 700 MHz band more than the 2 GHz band, that during 2014 the spectrum market became more competitive, or both. Unfortunately, we can't further analyze 2014 auction results because the information was in CCA format where the bidders bid on different licenses with different block sizes and modes simultaneously. For the 2008 advanced wireless system auction, we ran models 1 and 2 regressions to test the null hypothesis A, and results are shown in Table 23, below.

Operator	Model	β_2	$P-value$	R^2
Bell	Model 1	0.60	0.002	0.87
	Model 2	32,903	0.09	0.93
TULES	Model 1	1.22	$1.6\text{x}10^{-24}$	0.85
	Model 2	20,505	0.21	0.92

Because there are many auction rules restricting who could bid on what license, we analyzed operators individually rather than analyzing across all licenses. Only two operators bid on licenses having different block sizes. When we use model 1, we can see there is statistically significant evidence that price per spectrum unit is dependent on the block size. This allows us to reject the null hypothesis A.

5.5. United Kingdom

In the 2000 3G spectrum auction, a unit of 2x10 MHz in the 2.1 GHz band was valued at an average of 3.7 £/MHz-POP. While in the 2013 4G spectrum, valuation by the same operators was about 10 times less for blocks in the 800 MHz and 2.6 GHz bands. However, 2000's high valuation was attributed to the design of the auctions at that time. In 2013, an 800 MHz band had an average price of 0.42 £/MHz-POP whereas the 2.6 GHz had an average price of 0.06 £/MHz-POP. Two of the five bidders made combinational package bids on spectrum from both bands.

5.6. Brazil

There is little information about blocks auctioned in 2007 in the 2 GHz band. The average price was 0.08 $/MHz-POP. However, it wasn't clear whether the block size had an effect on pricing. In the 2012 auction for 2.5 GHz band, the 20 MHz block had an average price of 0.044 $/MHz-POP while the 10 MHz blocks were valued at 0.025 $/MHz-POP. In the 2014 auction, 700 MHz carriers were valued at 0.194 $/MHz-POP on average. There was not enough observation to run regressions, but there appeared in these auctions a general trend that larger blocks were valued more per MHz-POP than the lower frequency bands.

5.7. Conclusion

Spectrum auctions prices are affected by many factors that can’t be controlled, especially when they are related to competition among bidders and their behavior during an auction. In this chapter, we analyzed available auction data in order to test three hypotheses, and on the basis of our findings, we can conclude the following:

- Based on statistically significant results from auctions in Australia, Germany, the United States and Canada, in addition to data observations in Brazil, the price per MHz-pop depends on the block bandwidth size: the larger blocks tend to have higher valuation per MHz-POP for bidders. This allows us to reject Null Hypothesis A.
- Based on statistically significant results from German auctions and data observations in Australian, Canadian and Brazilian auctions, the price per MHz-pop depends on the frequency band: the lower frequency bands tend to have higher valuations per MHz-POP for bidders and for regulators when setting reserve prices in auctions. This allows us to reject Null Hypothesis B.
- There is not enough evidence to conclude that operators changed their valuation for smaller block sizes over time. Analyzing data from multiple auctions across time requires more data than was available for this study. Operators change their strategies over time as the market and competition produce changes that could affect their spectrum preferences.
- Nevertheless, since SA technology would bring virtual contiguity, we predict that the premium paid by operators for larger blocks of spectrum could fall as the technology continues to develop. Furthermore, this trend could apply as well to frequency bands of supplementary carriers based on the operators' current holdings of spectrum. These projections will be further considered in next chapter using network models already developed.

- After we combine findings from this chapter with results from the next chapter, we will use them when we discuss policy implications to provide regulators with recommendation about policies including auction design.

VII. IMPLICATIONS OF SPECTRUM AGGREGATION ON SPECTRUM ECONOMICS

The objective of this chapter is to characterize the impact of SA impact on spectrum valuation. We use the findings from Chapters IV and VI as well as the wide-area network model for the analysis to be performed in this chapter. We start by defining our research questions and providing some background information on spectrum economics and valuation in general. Then, we discuss the method of analysis to be used and state our assumptions and inputs. Next, we plot results based on the analysis described, and finally, we the conclusions to be drawn.

1. Research Questions

This investigation will answer the following question:

- How does the impact of obtaining new spectrum on infrastructure cost depend on the frequency and bandwidth of the new spectrum, the spectrum already held, and whether spectrum aggregation is used? More specifically:
    - To what degree does the saving in infrastructure cost depend on the bandwidth of the additional spectrum?
    - To what degree does this cost saving depend on whether the additional spectrum is one wide block or a small fragment?
    - How much does this cost savings depend on the frequency band of the additional spectrum?
    - How much does the saving depend on whether part of the network's existing spectrum portfolio is of a low frequency band?

- What can we conclude about the valuation of spectrum blocks (as measured in $/MHz-POP) when SA is/isn't used? In other words, what is the impact of SA (as compared to IC) on the valuation of additional spectrum fragment(s) for a Greenfield network deployment?
- What can we say about the impact of SA on operators' valuation for spectrum in terms of block sizes and frequency bands? Does it remove the importance of spectrum physical contiguity?

2. Background

2.1. Literature Review

Spectrum valuation can be based on different economic methods. In addition to the common approach of analyzing spectrum auction results, as discussed in Chapter VI, another approach is to treat spectrum as a public utility and calculate the cost of recycling it--i.e., the cost of spectrum planning and administration [152].

The commercial value of radio spectrum is very dependent on two kinds of parameters: the cost of building the network and the profit that can be generated once it's built [4]. Thus, valuation can be determined by calculating the net present value of exploiting the spectrum over the entire license period. This is calculated by estimating the NPV of the operator's expected revenues minus costs. The revenue is dependent on the forecast of subscribers, services and ARPU, while costs are dependent on the sites and related costs. Revenue also depends on parameters that are related to individual operators' strategic choices, which vary greatly and might lead to speculative results if they are used to estimate spectrum value.

One method of valuation known as the substitution technique asks: "If the spectrum were not available, how could we deliver a similar service, and at what price?" [152]. This technique involves substituting bandwidth for cellularity and asks: for a given capacity, how much do cells with a given amount of spectrum cost? As spectrum bandwidth increases, cost per cell decreases. This saving can be used to value this spectrum [106] [108] [153], as we will see in Section 3.

2.2. Overview of the Impact of SA on Spectrum Valuation

Spectrum valuation can be impacted by physical characteristics of the spectrum, such as the following:

- Bandwidth: spectrum is valued per MHz; the larger the bandwidth the higher the value, as we saw in Chapter VI. This increase isn't necessarily linear, so wider blocks might be valued more per unit than smaller ones. The effective bandwidth, or the amount of data that can be transmitted over a spectrum block, is a related factor. If it were possible for a technology to increase spectral efficiency in order to carry more data this might reflect a higher spectrum value when such a technology were used.
- Coverage-area population: spectrum is valued per POP in the covered area.
- Frequency band: The frequency band that has the least path loss might be more valuable for operators serving coverage-limited areas. This higher valuation for lower-frequency bands was discussed in Chapter VI.
- Contiguity or adjacency: contiguous carriers can be valued more highly than fragmented carriers even if the bandwidth of both carriers is the same [143].

The use of SA technology can impact these physical characteristics. This might lead to equalizing values of spectrum in terms of block size, since SA enables virtual contiguity of fragmented small blocks. For this reason, it is expected that the technology will either reduce the premium of wide blocks or increase the value of smaller blocks, as we will investigate later in this chapter.

Applying this overview of spectrum value to assess possible impact of SA, we will now look at the projected SA effect on access to new broadband services (emerging applications that require a high data rate). The market value of the spectrum when used for mobile broadband applications is different from the value when it is used for other narrow band applications [1]. Broadband services in particular produces a high demand for wide contiguous spectrum which, as we saw in Chapter VI, might lead to higher WTP from operators. On the other hand, there is less of a demand from broadband operators for small fragments. There is a limited supply of wide contiguous spectrum to meet this demand. However, SA increases the amount of spectrum available by virtually aggregating small fragments, resulting in new equilibrium.

3. Modeling the Analysis

3.1. Investigated Scenarios

In this chapter analysis, we focus only on two network scenarios: an inter-band independent carriers scenario (IC) and an inter-band spectrum aggregation scenario (SA). Then, two other network scenarios, *IC'* and *SA'*, are introduced as duplicates of the IC and SA scenarios with one difference; the total bandwidth will increase to be $B + BW_a$ MHz, where BW_a is the bandwidth of the additional block of spectrum B_a that will be added to the network scenario we analyze.

3.2. Analysis Formulation

In this chapter, the wide-area network model scenario developed in Chapter IV is used to analyze the scenarios. Inputs to the model will be changed for two main variables: spectrum portfolio and minimum traffic requirement, as shown in the schematic diagram below. This change allows us to run various states of the scenarios being investigated in order to estimate network costs for each scenario. Then, based on the savings each time an additional spectrum is added, a methodology for spectrum valuation by operators can be formulated.

In addition, data analysis of mobile spectrum auction results from previous chapters that shed light on the relation between operators' WTP and various block sizes and frequency bands will be used for comparison with the scenario analysis. From the results of these two analyses, a more general conclusion about SA and spectrum valuation will be drawn

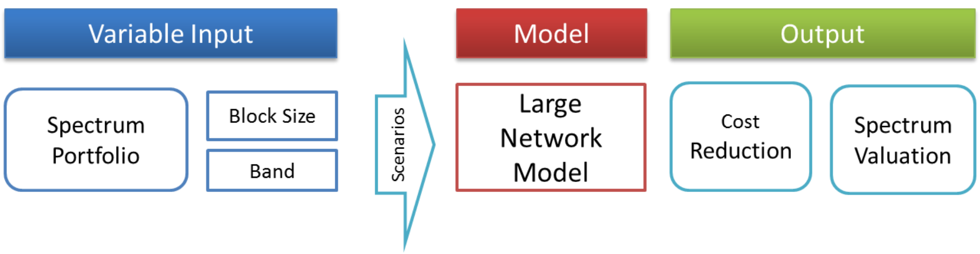

Figure 66: Simplified flow diagram of the proposed analysis

3.3. Costs Savings and Spectrum Value Estimation

Instead of estimating the NPV of costs and revenues, the cost-reduction scenario can be used to calculate the savings accruing from the deployment of additional spectrum for an operator with existing spectrum. This methodology assumes that the revenue will remain constant as the network produces the same capacity, but the extra spectrum will reduce network build-out cost.

To value the additional block of spectrum B_a MHz, we follow these steps:

a. find build-out network costs for the four scenarios *IC*, *SA*, *IC'* and *SA'*
b. find the cost reductions when independent carriers are being used by comparing costs of scenario *IC'* to *IC*, such that:

Equation 33

$$\Delta S_{IC} = NPVCost_{IC} - NPVCost_{IC'}$$

c. find the savings when spectrum aggregation is used by comparing the costs of scenario *SA'* to *SA*, such that:

Equation 34

$$\Delta S_{SA} = NPVCost_{SA} - NPVCost_{SA'}$$

Then, the reduction in the NPV of cost of building out a network by adding spectrum block (B_a) can be interpreted as a measure to valuate this additional bandwidth B_a per MHz-POP. We are interested in comparing the change in this value when independent carriers are used versus when spectrum aggregation is used. This comparison will show the impact of spectrum aggregation on valuation of an additional block of spectrum.

4. Inputs and Assumptions

In order to run multiple states for the four scenarios, we repeatedly change the following two specifications for both networks:

- Frequency band: we alternate the frequency bands for allocated blocks between higher and lower LTE frequency bands
- Allocated block size and number of fragments: we change the bandwidth of allocated blocks, which in turn varies the number of fragments, given that the total bandwidth is fixed at B MHz or $B + B_a$ MHz for the other two scenarios. This additional block B_a varies in size, too.

Table 23, below, shows values for these various inputs. We assume the networks we build have a minimum requirement of 2 Mbps average UE throughput as discussed in Chapter IV.

Table 23: Specifications for different scenarios

Main block Bandwidth (B)	20 MHz
Additional block bandwidth (B_a)	5 MHz
Fragments of the Main Block	1 (20 MHz), 2 (10+10 MHz) or 4 (4x5 MHz)
Spectrum operation	IC or SA
Frequency bands	700 MHz or 2.6 GHz
Data rate requirement	Average UE throughput of 2 Mbps

5. Results and Discussions

The set-up of the first scenarios assumes a system that utilizes 20 MHz for the downlink in the 700 MHz band. Of course, this system will have the build-out cost of a 20 MHz contiguous spectrum in the 700 MHz band. Because we are interested in knowing the change in cost and not the absolute cost, which is strongly dependent on a number of input assumptions, we make the 700 MHz contiguous spectrum our base scenario, and we assume it has NPV cost of $\$\,x$. Now, two scenarios will be presumed to have an additional 5 MHz in the same band, but it is not adjacent to the 20 MHz block. One of these two scenarios uses SA, and the other uses IC. Four more scenarios will have the same set-up with one difference; B_a will be presumed to be in the 2600 MHz band for two of them and in the 1800 MHz band for the other two.

Based on the cost analysis from Chapter IV, results show that adding 5 MHz in the 700 MHz to the base scenario reduces the cost by approximately 5%. Based on equations defined in Section 3, we can estimate the value of the additional spectrum in $/MHz-POP.

Cost savings is dependent on the total network cost (\$*x*). As first noted in Chapter IV Section 3.3.2, a too-high traffic assumption erroneously used in all of our modeling greatly increases total network costs. Because costs saving is dependent on the total network cost (\$*x*) the estimated spectrum value is much too high as well.. Thus, using the cost estimate of *x*=\$400 billion from Chapter IV, a 5% cost reduction would lead to a spectrum value of \$13/MHz-POPin the 700 MHz band, which is higher than the values from auctions shown in Chapter VI. If, for example, a more realistic traffic assumption had led to a network cost of say, *x*=\$80 billion, then the additional spectrum would be valued at approximately \$2.6/MHz-POP, which is close to recent auction prices in the U.S.

Since in this analysis we are interested in how spectrum value changes with other factors such as frequency, bandwidth, and whether SA is employed, we will plot spectrum values 'normalized', i.e. divided by a base scenario cost (\$*x*) arbitrarily set at \$80 billion, to reduce the impact of build-out cost to the greatest possible extent and focus on the relative change. It should also be noted that the assumptions in Chapter IV will cause some parts of the country to be capacity-limited when they might otherwise have been coverage limited, at least at high frequencies. As such, we might expect the estimated value of low-frequency spectrum to be even greater than we show in this chapter, at least for a cellular carrier that does not already have some low-frequency spectrum. Despite these issues, we believe the relative comparisons of spectrum values are highly instructive, beginning with Figure 67, which shows how spectrum value depends on frequency, both with and without SA.

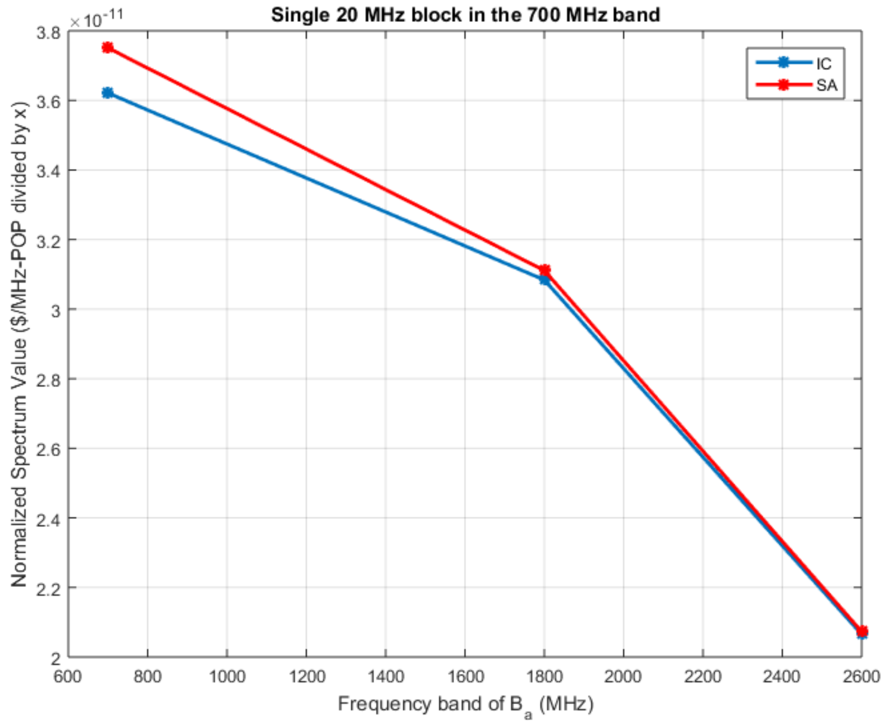

Figure 67: Interpreting reduction in build-out cost due to additional block as value projected for block by operator

That the 700 MHz block is always far more valuable than the 2600 MHz block, a result that is consistent with our findings in Chapter VI. This is because a 700 MHz carrier would increase capacity in both dense areas and rural areas and enable coverage in rural areas. Figure 67 also shows that SA makes spectrum more valuable, especially at lower frequencies, although the effect is modest compared to that of frequency. It may be that SA makes 5 MHz of spectrum more valuable in this case because SA increases the capacity that the additional spectrum will provide.

We repeated the same experiment using IC and SA, but with the main 20 MHz block (B) in the 2600 MHz band instead of 700 MHz, as shown in Figure 68. Clearly, in the 2600 MHz scenario, access to additional spectrum in the 700 MHz band would be highly valued since it would and greatly increase the operator's ability to reduce cellularity in coverage-limited areas, as well as providing the operator with extra capacity in populated areas. The operator with spectrum in the 2600 MHz band values low-frequency spectrum far more than the operator with spectrum in the 700 MHz, because the latter can already serve coverage-limited regions with fewer towers. We observe that SA would only slightly increase the operator’s valuation for a 5 MHz of spectrum. This can be explained by the fact that SA can utilize such a small block more efficiently, which leads to a reduced build-out cost.

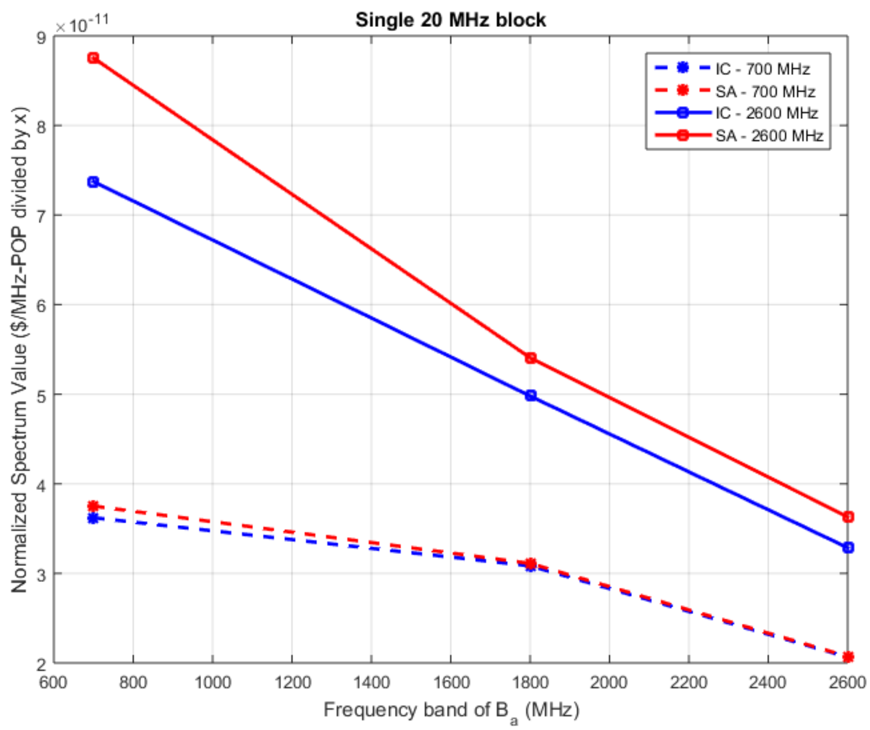

Figure 68: Projected value for spectrum by different scenarios

As shown in Figure 69, below, increasing fragmentation would increase the operator’s valuation for 5 MHz of spectrum when the operator uses SA. Similar to the trend we saw before, a 2600 MHz operator would value an additional carrier in the 700 MHz almost twice as highly as a carrier in the 2600 MHz band, while the 700 MHz operator would have a significantly lower valuation. It can also be observed that the operator with inter-band carriers has more moderate valuation for the additional spectrum with slower changes as its frequency increases than does the 2600-MHz operator.

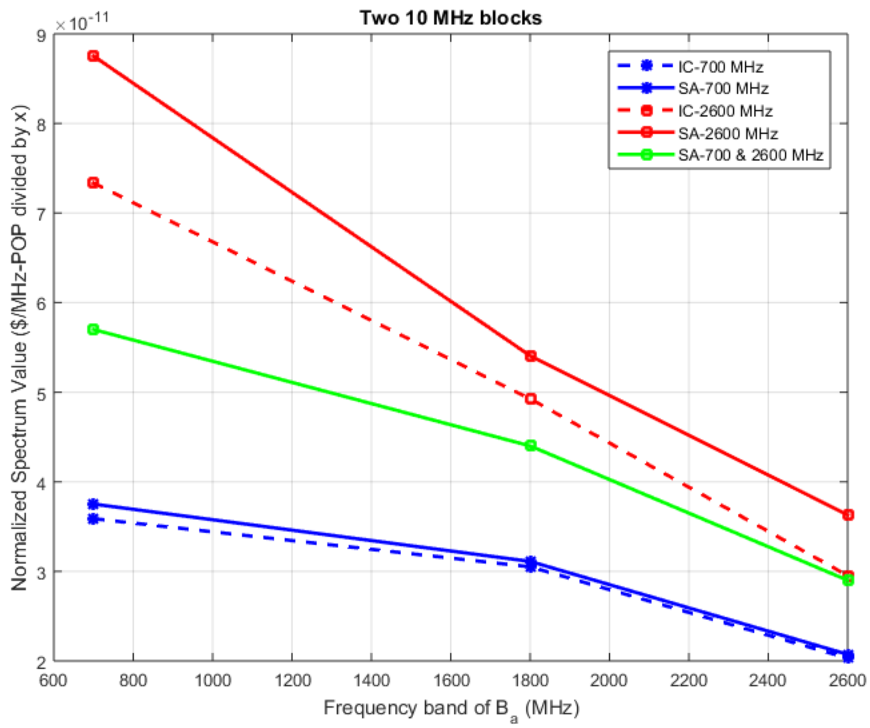

Figure 69: Projected value for additional spectrum added to two 10 MHz blocks of spectrum

In conclusion, we can summarize the findings from this and previous chapters as follows:

- The more spectrum an operator has access to, the less costly its network build-out will be.
- In general, an operator would value a wider block of spectrum with a higher value per MHz-POP over smaller fragments (This is consistent with our findings in Chapter VI). However, when the operator implements SA, the difference in valuation between the smaller and larger bands becomes less significant. This can be attributed to the technology's ability to fully utilize any fragment, pushing the valuation closer to that seen with the block bandwidth.

- If the additional block is in a low-frequency band, it will be more valuable than if it is in a higher-frequency band. However, this valuation depends on the user density: in areas with high user-density, it would be is lower, but in areas with low -user density, it would be higher. In areas with lower user density, coverage requirement would be the dominant factor in network build-out. Also, this valuation is highly dependent on the operator spectrum holding. If the holding contains only low-frequency blocks, its valuation for additional blocks in a low-frequency band won't be as high as if it has access to only higher frequency spectrum.

VIII. POLICY IMPLICATIONS OF SPECTRUM AGGREGATION

This chapter returns to the main general question we wanted to answer which is: "what is the policy impact of spectrum aggregation?" Based on findings from previous analyses in the thesis, we discuss the impact of the ability to use multiband spectrum and SA on spectrum policies. Regulators' policies in managing spectrum need to keep up with the changes in technologies. If a technology like SA could have changing effects on network costs, benefits and spectrum valuation, this should be met with policy changes as well.

1. Band Planning

Band plan involves determining the bandwidth of blocks to be allocated (assigned or auctioned) and the frequency separation between blocks designated for downlink and uplink.

1.1. Block Size

Some regulators in number of countries used to assign small blocks with narrowband channels for mobile operators to use in their voice services. As technology improves, spectral efficiency improves as well and low data-rate applications required even narrower channels. As high data rate applications emerge, a spectrum paradigm shift took place and wideband channels were needed by operators [154]. Since 3G systems were being deployed, operators were allocated large blocks of spectrum: paired 20 MHz bandwidth carriers or even more.

As analyses in this thesis showed and some papers discussed [151], large contiguous blocks of spectrum are preferred from the operators' point of view. Large blocks allow using the spectrum more efficiently and provide customers with better quality of service like higher peak rate. From regulators' point of view, larger blocks mean less access to a particular frequency band by fewer operators. This means less competition in the market.

Again, as we saw in the analysis of Chapter II, the introduction of SA technology would help the operators to overcome the technical barriers of using smaller blocks of spectrum; virtual contiguity delivered by SA increases efficiency and allow higher peak rate for users. Thus, SA might make multiple small blocks almost as equivalent as to a wide contiguous block. In addition, analysis in Chapter VII, show that under some assumptions, operators using SA would value-per-unit small block of spectrum almost as they value a unit of larger-block.

Based on that, regulators might consider creating band plans with the minimum usable block size instead of large blocks [155]. For example, in frequency bands designated for LMR, block sizes shouldn't exceed 5 MHz.

1.2. Frequency Separation

In FDD operation, the Tx/Rx frequency separation is needed to avoid interference between the two uplink and downlink channels [156]. Setting a minimum frequency separation, when band planning, is an issue for regulators. It is dependent on many factors including the used technology and the required duplex filtration to prevent interference [157], [158]. The bandwidth of duplex gap has a direct impact on the design of a duplex filter, which is the one of the most dominating RF components. A larger duplex gap can facilitate design of duplex filters with lower insertion loss.

While our analysis deals only with applying SA in the downlink, 3GPP will implement the technology in the uplink carriers too. As we‘ve discussed in Chapter III, filter design is a significant issue in making radio equipment capable of accommodating SA. Chip manufactures work on improving filter designs to allow devices aggregate many frequency carriers combinations. While this is beyond the scope of our study, the improved filter designs might relax the need for a minimum duplex gap in FDD communications. Future work can be reviewing the theory about filters and duplex gap to understand if the changes in design to enable SA to aggregate carriers in both ways would affect filters ability to receive and transmit on adjacent channels without self-interfering with the wideband receiver.

2. Spectrum Allocation and Assignment

Spectrum block can be allocated to specific use or services and then it is assigned to operators through different approaches, like auction. The regulator before approving the assignment or the spectrum license needs to insure the operator doesn't violate any regulations in effect like spectrum cap.

2.1. Spectrum Auction

Designing spectrum auction is discussed in many papers [159] - [167]. Given the different impacts that we've seen of SA, the technology is expected to have an impact on auction design as well. Assuming the regulator will create a band plan with small block sizes as recommended in section 1, here are further justified recommendations for spectrum auction:

- Auctioning smaller blocks most likely will not have negative effect on the auction revenue significantly. SA, as discussed in last two chapters, would maintain the per-unit value of small and large blocks close.
- Operators, especially new entrants, would like to have access to enough spectrum, i.e. multiple small blocks. Regulators could design the auction in a combinational clock format such that bidder can assemble the required bandwidth by bidding on multiple small blocks in one package. SA capability would work as a tool to be used by the operator to reach the large bandwidth needed to build out the network. As we've seen in

Chapter VII, this might make the operator to highly value small blocks in high frequency bands than before.

2.2. Spectrum Cap limit

A spectrum cap is meant to allow fair access to spectrum by all players in the market [168]. The conventional policy is to set a cap limit per the total spectrum allocated to an operator. In order to make the recommendation we provided about block size and spectrum auction work properly, spectrum cap per bands should be implemented. Setting spectrum cap per specific bands and whether lower bands should have more weight in such a regulation have been discussed lately [169], [170], [171]. The capability of SA technology will make such strict cap limit more plausible. Operators will be forced to access more bands if they want to increase their total bandwidth and SA will provide them with the required contiguity. Per-band cap limit could be applied more strictly in lower bands with small total bandwidth and high demands by operators.

3. Flexible spectrum management

Our recommendations about block size in band plans, spectrum auction and spectrum cap would increase spectrum fragmentation. Fragmentation couldn't be avoided even when regulators intention is to allocate wide blocks of spectrum due to different reasons we discussed in the first chapter. SA provides operators the chance to exploit it. For regulators, it is a chance to allow fair access to spectrum, increase competition, utilize all fragments of spectrum and generate revenue from auctioning them.

The technical advancement SA requires accessing spectrum with high flexibility and joining carriers with different bandwidths in different frequency bands could lead to more flexible management of the spectrum. Discussion about the need for more flexible spectrum management due to the flexibility that new technologies brought was presented in some policy papers, [154], [172], [173], [174]. For future work on SA impact on policy, here are some observations:

- Some high frequency bands only used when there is high demand (like the additional band discussed in chapter VII). Since there no enough blocks in some bands for every operator, regulator can assign them on shared basis. SA could make this type of allocation more practical by allowing the operator to aggregate them with other bands when need more capacity
- As spectrum blocks get smaller and non-contiguous, this could increase secondary market liquidity and encourage secondary trading (or even real-time secondary trading) for such blocks. The primary user of them would be more willing to trade or time-share them knowing that there is enough supply in the spectrum market to substitute the block she leased.

4. Illustrative Example on Spectrum Allocation

We present here an artificial example of a mobile market with different operators with different times entering the market. Along with what we learned about operators' valuation for different spectrum blocks in the previous two chapters, we vary regulator policy decisions with regard to block sizes in a band plan and applying spectrum cap per band, to see the joint impact of all these factors on the allocated spectrum to each operator. Then, we estimate the build out cost for each operator in each case and discuss the SA impact.

4.1. Market Variables

In a given, mobile market, we assume there is B MHz of spectrum in K bands such that spectrum band k has bandwidth B_k MHz and $\sum_{k=1}^{K} \mathrm{B}_k = B$ MHz. The market regulator allowed M mobile operators to enter the market. We fix these variables for a given market by assigning specific values to them as per the following table.

:

Table 24: assigning values to the market variables

Variable	Description	Assumed value
B	Total bandwidth	80 MHz
K	Number of frequency bands	4
B_k	Bandwidth of each frequency band	$B_1 = 20\ MHz$ in the 700 MHz band $B_2 = 20\ MHz$ in the 1800 MHz band $B_3 = 20\ MHz$ in the 2100 MHz band $B_4 = 20\ MHz$ in the 2600 MHz band
M	Number of operators	4

4.2. Assumptions on Operators

4.2.1. Entry to the Market

We assume Operator 1 has a chance of being allocated all of her 20 MHz first from any band she prefers. Then, Operator 2 and 3 will be allocated blocks simultaneously, i.e. Operator 2 will be allocated her first block then Operator 3 will be allocated a block and so on till they reach the 20 MHz cap limit. Finally, Operator 4 will be allocated the remaining 20 MHz. This arrangement will imitate the real situation of the time of entry to the marker; first entrant usually has an advantage.

4.2.2. Operators' Allocation Preferences

Moreover, based on analysis of previous chapters, we can predict operator's behavior with regard to WTP of different bands. Thus, we assume operators have utility function that value lower frequency bands more than high frequency bands and prefer contiguous blocks more than fragmented small blocks. Finally, let's define S_m (in MHz) as the total bandwidth assigned to operator *m* and S_m^k as the bandwidth assigned to operator *m* in band *k*; such that $\sum_{k=1}^{K} S_m^k = S_m$.

4.3. Policy Variables

The regulator wants to implement spectrum allocation policies to maximize competition between operators. One way to achieve that is to maximize the fairness index (*FI*) in access to available spectrum among operators which can be written as:

Equation 35

$$\max_{0 \le x \le B} FI$$

Where fairness can be written as:

Equation 36

$$FI = \frac{\left(\sum_{m=1}^{M} A_m\right)^2}{M \sum_{m=1}^{M} A_m^2}$$

Where A_m is a variable related to the allocated spectrum to operator *m*. For now, let's define A_m to be equal to the total bandwidth assigned to operator *m*; i.e. $A_m = S_m$. It's clear that when $S_m = \frac{B}{M}$ for all operators, F will be maximized to 1. Thus, based on the table above: $S_m = 20\ MHz$, for $m = 1,2,3,4$. The regulator has two policy variables that his objective function can be subjected to:

a. Block size (B_{size}) which specifies the block bandwidth in each band plan. We vary this variable between 20 MHz, 10 MHz and 5 MHz.

b. Spectrum cap limit per band *k* (B_{cap}^k) which specifies the maximum bandwidth to be allocated to operator *m* in band *k*, such that: $S_m^k \le B_{cap}^k$. We vary this variable between S_m (or 20 MHz, it means no per-band cap is applied), 10 MHz or 5 MHz

As we change those two policy variables, allocated spectrum to each one of the four operators in each band will change. All cases are shown in the table below. As per the assumption we made about operators' entry to the market and their preferences, Operator 1 will tend to acquire spectrum as low in frequency as possible and as contiguous as possible.

Table 25: Different spectrum allocations to operators, as regulator policy varies

	Policies restrictions	**Allocated spectrum**	**Total number of blocks (Fragmentation)**
Case 1	$B_{size} = 20\ MHz$ $B_{cap}^{k} \leq S_m$ (20 MHz)	$S_1^1 = 20$ MHz, $S_1^2 = 0, S_1^3 = 0,\ S_1^4 = 0$ $S_2^1 = 0, S_2^2 = 20\ MHz, S_2^3 = 0,\ S_2^4 = 0$ $S_3^1 = 0, S_3^2 = 0, S_3^3 = 20\ MHz,\ S_3^4 = 0$ $S_4^1 = 0, S_4^2 = 0, S_4^3 = 0,\ S_4^4 = 20\ MHz$	4
Case 2	$B_{size} = 10\ MHz$ $B_{cap}^{k} \leq S_m$(20 MHz)	$S_1^1 = 20$ MHz, $S_1^2 = 0, S_1^3 = 0,\ S_1^4 = 0$ $S_2^1 = 0, S_2^2 = 10\ MHz, S_2^3 = 10\ MHz,\ S_2^4 = 0$ $S_3^1 = 0, S_3^2 = 10\ MHz, S_3^3 = 10\ MHz,\ S_3^4 = 0$ $S_4^1 = 0, S_4^2 = 0, S_4^3 = 0,\ S_4^4 = 20\ MHz$	6
Case 3	$B_{size} = 10\ MHz$ $B_{cap}^{k} \leq 10\ MHz$	$S_1^1 = 10$ MHz, $S_1^2 = 10\ MHz, S_1^3 = 0,\ S_1^4 = 0$ $S_2^1 = 10$ MHz, $S_2^2 = 0, S_2^3 = 10\ MHz,\ S_2^4 = 0$ $S_3^1 = 0, S_3^2 = 10\ MHz, S_3^3 = 0,\ S_3^4 = 10\ MHz$ $S_4^1 = 0, S_4^2 = 0, S_4^3 = 10\ MHz,\ S_4^4 = 10\ MHz$	8
Case 4	$B_{size} = 5\ MHz$ $B_{cap}^{k} \leq 10\ MHz$	$S_1^1 = 10$ MHz, $S_1^2 = 10\ MHz, S_1^3 = 0,\ S_1^4 = 0$ $S_2^1 = 5$ MHz, $S_2^2 = 5\ MHz, S_2^3 = 5\ MHz,\ S_2^4 = 5\ MHz$ $S_3^1 = 5\ MHz, S_3^2 = 5\ MHz, S_3^3 = 5\ MHz,\ S_3^4 = 5\ MHz$ $S_4^1 = 0, S_4^2 = 0, S_4^3 = 10\ MHz,\ S_4^4 = 10\ MHz$	12
Case 5	$B_{size} = 5\ MHz$ $B_{cap}^{k} \leq 5\ MHz$	$S_1^1 = 5$ MHz, $S_1^2 = 5\ MHz, S_1^3 = 5\ MHz,\ S_1^4 = 5\ MHz$ $S_2^1 = 5$ MHz, $S_2^2 = 5\ MHz, S_2^3 = 5\ MHz,\ S_2^4 = 5\ MHz$ $S_3^1 = 5\ MHz, S_3^2 = 5\ MHz, S_3^3 = 5\ MHz,\ S_3^4 = 5\ MHz$ $S_4^1 = 5\ MHz, S_4^2 = 5\ MHz, S_4^3 = 5\ MHz,\ S_4^4 = 5\ MHz$	16

The last column of the table is an estimate of the resulting total number of blocks after all available spectrum allocated to the four operators. It is a measure of how fragmented the spectrum allocations are. It can be clearly noted that this measure is a function of both B_{size} and B_{cap}^{k}; the smaller their values are the more fragmented allocations will be.

4.4. Analysis Results

Using the model developed in chapter IV, we estimate the build-out cost for each of the four operators in each of the five cases presented in the table above. We assume all operators use SA. Results are shown in Figure 70, below. Here are a number of observations:

- In each of the five cases, each operator has access to contiguous 20 MHz, either physically wide block or virtually contiguous through the use of SA
- In each case, Operator 1 has the advantage of entering the market and be allocated spectrum first. This allows her to have lower cost than other operators by having a license in a lower frequency band. Operator 4 has the disadvantage of entering the market late. She never has access to the 700 MHz before case 5.
- When wide contiguous blocks can be allocated to individual operators and no spectrum cap per-band is enforced, the network costs differ significantly between Operators 1 and 4.
- As allocated block size gets smaller and spectrum cap per band gets lower, difference in build out costs among operators becomes less.
- SA makes more fragmented spectrum cost-effective to use as the technology removes or at least reduces barriers that make small fragments of spectrum less preferred, as we discussed earlier in sections 1 and 2.

- Looking at the different five case, regulator should consider creating combinational packages of spectrum like the ones in Case 5 rather than Case 1. The cumulative valuation of the four 5 MHz blocks in the 2600 MHz band by the four operators could be greater than or equal the single valuation of 20 MHz block in 2600 MHz by Operator 4.
- Although having access to a contiguous wide spectrum block in a lower frequency band like 700 MHz is the optimum case for an operator, from regulator's point of view, having smaller blocks to be allocated to operators and a low spectrum cap per each band will lead to fair access to available spectrum among all operators. In the fairness index defined earlier, instead of letting $A_m = S_m$, we let $A_m = Cost_m$. Different spectrum bands have different weights, or different value per unit.

Based on this new definition for *FI*, from Figure 71 below, we can see that the spectrum allocation strategy becomes fair as the regulator makes blocks small and applies a spectrum cap in each band. This allows access to all bands by all operators. If wide contiguous blocks were allocated to operators or less strict spectrum cap rules were implemented, the fairness index will be lower. The second curve shows the least fair scenario between Operator 1 and 4; without regulations the first entrant to the market will have much better access to valuable spectrum.

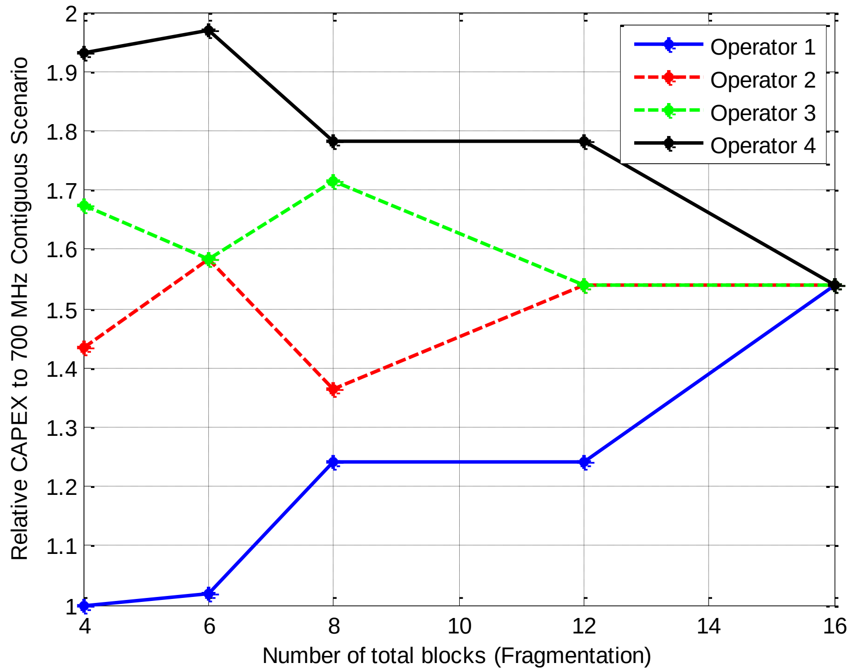

Figure 70: the build-out cost for each of the four operators in each of the five cases. We assume all operators use SA

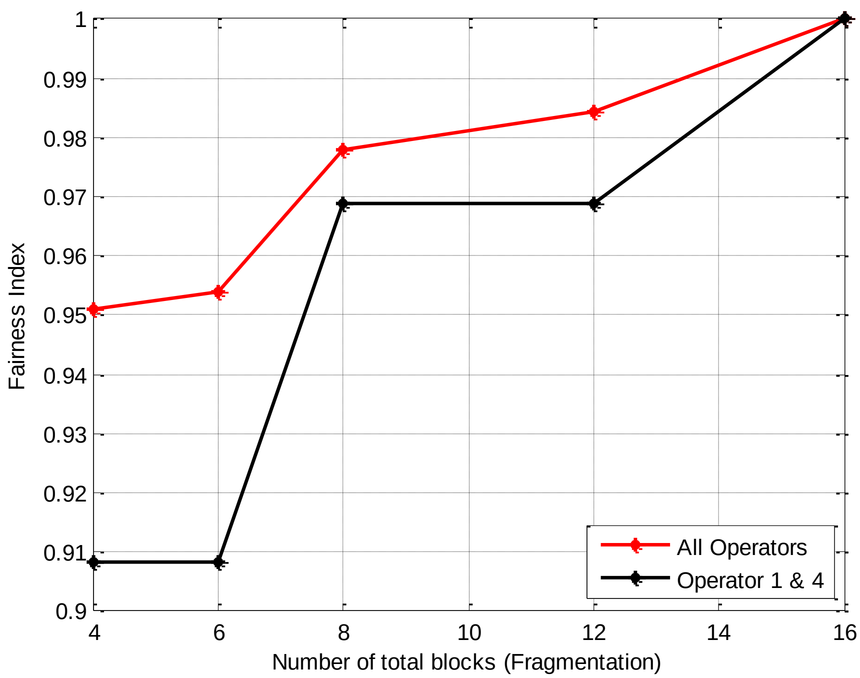

Figure 71: Fairness index as allocated spectrum blocks increase

Finally, the last figure, below, shows how the build out cost changes among the four operators when they operate carriers independently without SA. The build-out cost will be higher for each operator as we learned before due to the lower efficiency in operating the small fragments of spectrum. In addition, each operator will have much lower peak rate available for users.

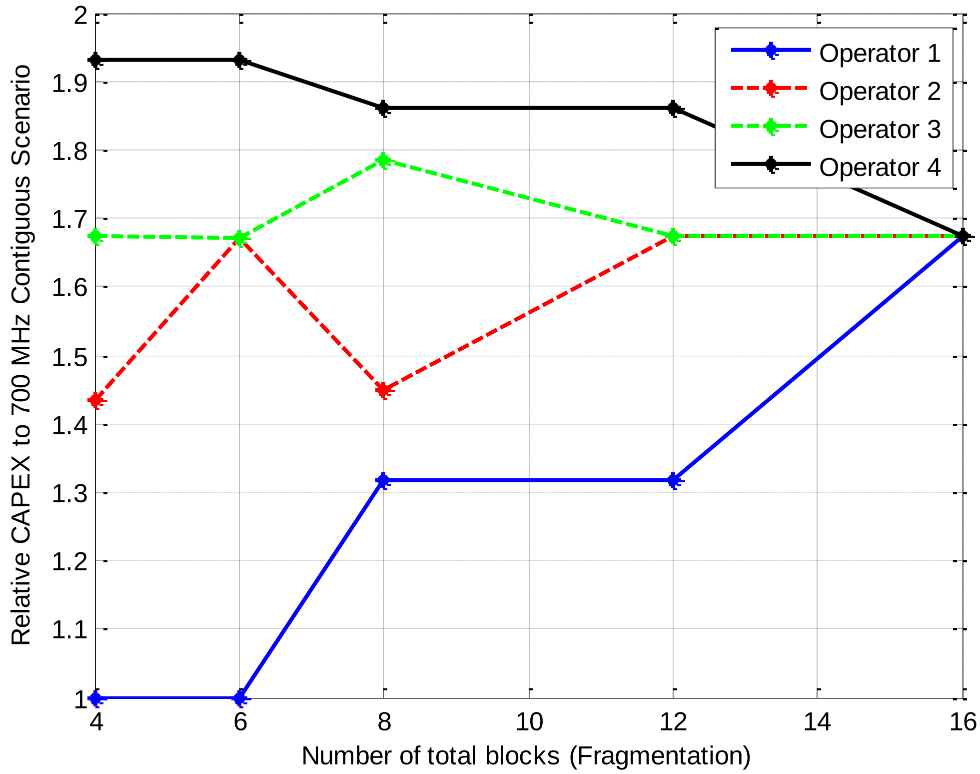

Figure 72: The build-out cost for each of the four operators in each of the five cases (IC operation)

IX. CONCLUSION

In this thesis, we performed different analyses to explore spectrum aggregation technology and understand its implications. First, we conducted technical analysis by simulating wireless networks with and without SA technology. Results showed that SA technology could improve, under certain assumptions, the network performance compared to independent carriers operation. In addition, SA facilitates the possibility of using multiple bands which could show improvement over only high-frequency systems. Based on this analysis, we analyzed the benefits and costs of the technology based on a wide-area network that has nationwide coverage. While SA could slightly increase the cost of building out such a network, it would reduce costs when compared to a network using IC. In addition, SA can provide more bps per $ and provide a higher peak data rate as spectrum becomes more fragmented. We test these results by applying the same model to a TV band case, and compare the feasibility of using fragmented spectrum in that band with SA versus the physical repacking of spectrum. Because of our assumptions with regard to guard band between LTE and TV systems, SA didn’t result in less build-out costs. However, under different assumptions, SA could be a cost-effective alternative to spectrum refarming. Then, we empirically studied the operators’ willingness to pay for blocks of spectrum and how this depends on bandwidth and frequency in multiple spectrum auctions. We found that there is a premium operators pay in order to have contiguous low-frequency band spectrum. Running the analysis for the nationwide network showed that SA might change operator’s valuation for spectrum blocks and it could reduce the premium they pay for wide blocks and improve their valuation for smaller ones. Finally, we wrapped up the thesis analysis by discussing some policy implications. We showed that if regulators allocated smaller blocks with a per-band spectrum cap, this could enhance competition between operators as it gives them fair access to spectrum.

REFERENCES

[1] FCC, "Connecting America: National Broadband Plan," 2010.

[2] Cisco, "Cisco Visual Networking Index: Global Mobile Data Traffic Forecast Update, 2012–2017," White Paper, 2013.

[3] B. Mitchell, "How Fast Does Your Network Need To Be?," [Online]. Available: http://compnetworking.about.com/od/speedtests/tp/how-fast-does-your-network-need-to-be.htm. [Accessed 18 November 2013].

[4] Shukla, Anil; Willamson, Brian; Burns, John; Burbidge, Eddie; Taylor, Alan; Robinson, David, "A Study for the Provision of Aggregation of Frequency to Provide Wider Bandwidth Services," QinetiQ Ltd, August 2006.

[5] B. Har-Even, "LTE spectrum fragmentation delaying LTE roll out report suggests," telecoms.com, 2 August 2011. [Online]. Available: http://www.telecoms.com/31428/lte-spectrum-fragmentation-delaying-lte-roll-out-report-suggests/. [Accessed 8 August 2011].

[6] FCC, "Annual Report and Analysis of Competitive Market Conditions With Respect to Mobile Wireless, Including Commercial Mobile Services," Sixteenth Report, FCC 13-34, 2013.

[7] J. Wannstrom, "Carrier Aggregation explained," 3GPP, June 2013. [Online]. Available: http://www.3gpp.org/technologies/keywords-acronyms/101-carrier-aggregation-explained. [Accessed 18 November 2013].

[8] P. Clarke, "Cognovo, R&S to demo LTE carrier aggregation," EE Times, 23 February 2012. [Online]. Available: http://www.eetimes.com/document.asp?doc_id=1266532. [Accessed 2 March 2012].

[9] K. Hill, "Test & Measurement: Carrier aggregation gains momentum," RCRWireless.com, July 2013. [Online]. Available: http://www.rcrwireless.com/article/20130628/test-equipment/test-measurement-spirent-carrier-aggregation/. [Accessed November 2013].

[10] M. Saadi, "LTE Carrier Aggregation: Motivations and challenges," informa.com, July 2013. [Online]. Available: http://blogs.informatandm.com/14501/lte-carrier-aggregation-motivations-and-challenges/. [Accessed August 2013].

[11] H. Lee, S. Vahid and K. Moessner, "A Survey of Radio Resource Management for Spectrum Aggregation in LTE-Advanced," *IEEE COMMUNICATIONS SURVEYS & TUTORIALS,* vol. ACCEPTED FOR PUBLICATION, 2013.

[12] Z. Shen, A. Papasakellariou, J. Montojo, D. Gerstenberger and F. Xu, "Overview of 3GPP LTE-Advanced Carrier Aggregation for 4G Wireless Communications," *IEEE Communications Magazine,* pp. 122-130, February 2012.

[13] A. Roessler, S. Merkel and M. Kottkamp, "Carrier aggregation – (one) key enabler for LTE-Advanced," ROHDE & SCHWARZ, 2012.

[14] S. Marek, "LTE-Advanced Status Report," FierceWireless, June 2014.

[15] K. I. Pedersen, F. Frederiksen, C. Rosa, H. Nguyen, L. G. U. Garcia and Y. Wang, "Carrier Aggregation for LTE-Advanced: Functionality and Performance Aspects," *IEEE Communications Magazine,* pp. 89-95, 2011.

[16] R. Ratasuk, D. Tolli and A. Ghosh, "Carrier Aggregation in LTE-Advanced," in *IEEE Vehicular Technology Conference*, 2010.

[17] K. Johansson, J. Bergman, D. Gerstenberger, M. Blomgren and A. Wallén, "Multi-Carrier HSPA Evolution," in *IEEE VTC*, 2009.

[18] K. Challapali, C. Cordeiro and D. Birru, "Evolution of spectrum-agile cognitive radios: first wireless internet standard and beyond," in *ACM Proceedings of the 2nd annual international workshop on Wireless internet*, 2006.

[19] M. Iwamura, K. Etemad, M.-H. Fong and R. N. a. R. Love, "Carrier Aggregation Framework in 3GPP LTE-Advanced," *IEEE Communications Magazine,* pp. 60-67, August 2010.

[20] H. T. Nguyen and I. Z. Kovacs, "Downlink Radio Resource Management for LTE-Advanced System with Combined MU-MIMO and Carrier Aggregation Features," in *IEEE Vehicular Technology Conference*, 2012.

[21] Samurai, "Spectrum Aggregation in Practice," Spectrum Aggregation and Multi-user MIMO: Real-World Impact, 2010.

[22] G. VIVIER, B. BADIC, A. CATTONI, H.-N. CHOI, J. DUPLICY, F. KALTENBERGER, I. Z. KOVÁCS, H. T. NGUYEN and S. SEZGINER, "Spectrum Aggregation: initial outcomes from SAMURAI project," in *www.FutureNetworkSummit.eu*, 2011.

[23] A. Cattoni, H. Nguyen, J. Duplicy, D. Tandur, B. Badic, R. Balraj, F. Kaltenberger and I. Latif, "Multi-User MIMO and Carrier Aggregation in 4G Systems: the SAMURAI Approach," in *Workshop on 4G Mobile Radio Access Networks*, 2012.

[24] M. Siebert, A. Mihovska, E. Mohyeldin, P. Nguyen, J.-P. Desbat, M. Mustonen and W. Mohr,

"Strategies and technologies for spectrum utilisation and sharing aspects of IMT," Wireless World Initiative New Radio – WINNER+, 2010.

[25] H. Li, S. Dehnie, V. Chakravarthy, Z. Wu, Y. Ma and D. Walter, "Spectrum Utilization Efficiency of Cognitive Radio Systems with Limited Sampling Capability: The Impact of Spectrum Non-contiguity," in *DySPAN*, 2012.

[26] E. Coffman, P. Robert, F. Simatos, S. Tarumi and G. Zussman, "Channel Fragmentation in Dynamic Spectrum Access Systems - a Theoretical Study," arXiv:1002.3084, 2010.

[27] Y. Li, S. K. Jayaweera and C. G. Christodoulou, "Wideband PHY/MAC Bandwidth Aggregation Optimization For Cognitive Radios," in *3rd International Workshop on Cognitive Incromation Processing*, 2012.

[28] W. Qiu, H. Minn and C.-C. Chong, "Enhanced Frequency Diversity Exploitation in Carrier Aggregation for LTE-Advanced Systems," in *IEEE Vehicular Technology Conference*, 2011.

[29] K. I. Pedersen, F. Frederiksen, C. Rosa, H. Nguyen, L. G. U. Garcia and Y. Wang, "Carrier Aggregation for LTE-Advanced: Functionality and Performance Aspects," *IEEE Communications Magazine,* pp. 89-95, June 2011.

[30] X. Cao, D. Xiao and C. Xiu, "Handover performance of relaxing SCell measurement period in LTE-A with carrier aggregation," in *Electric Information and Control Engineering*, 2011.

[31] I. Shayea, M. Ismail and R. Nordin, "Capacity Evaluation of Carrier Agreggation Techniques in LTE-Advanced System," in *International Conference on Computer and Communication Engineering*, 3-5 July 2012.

[32] H. Wang, C. Rosa and K. Pedersen, "Performance of Uplink Carrier Aggregation in LTE-Advanced Systems," in *IEEE Vehicular Technology Conference*, 2010.

[33] ETSI TR 136 912, "Feasibility study for Further Advancements for E-UTRA (LTE-Advanced)," 3GPP, 2012.

[34] 3GPP TR 25.825, "Dual-cell High Speed Downlink Packet Access (HSDPA) operation," 3GPP, 2008.

[35] ETSI TS 136 300, "LTE Overall description," 3GPP, 2013.

[36] C. Cox, An Introduction to LTE, Wiley, 2012.

[37] 3GPP TR 36.814, "Further advancements for E-UTRA physical layer aspects," 3GPP, 2010.

[38] Y. Wang, K. Pedersen, T. Sorensen and P. Mogensen, "Utility Maximization in LTE-Advanced Systems with Carrier Aggregation," in *IEEE Vehicular Technology Conference*, 2011.

[39] G. Galaviz, D. H. Covarrubias, A. G. Andrade and S. Villarreal, "A resource block organization strategy for scheduling in carrier aggregated systems," *EURASIP Journal on Wireless Communications and Networking,* 2012.

[40] O. Cabral, F. Meucci, A. Mihovska, F. J. Velez, N. R. Prasad and R. Prasad, "Integrated Common Radio Resource Management with Spectrum Aggregation Over Non-Contiguous Frequency Bands," *Wireless Pers Commun DOI 10.1007/s11277-011-0242-6,* vol. 59, pp. 499-523, 2011.

[41] Y.-L. Chung, L.-J. Jang and Z. Tsai, "An Efficient Downlink Packet Scheduling Algorithm in LTE-Advanced Systems with Carrier Aggregation," in *The 8th Annual IEEE Consumer Communications and Networking Conference*, 2011.

[42] Z. Ji-hong, L. Hui and Q. Hua, "A SPF-PF crossing Component Carrier joint scheduling algorithm," in *International Conference on Advanced Communication Technology*, 2012.

[43] X. Cheng, G. Gupta and P. Mohapatra, "Joint Carrier Aggregation and Packet Scheduling in LTE-Advanced Networks," in *IEEE Communications Society Conference on Sensor, Mesh and Ad Hoc Communications*, 2013.

[44] G. Yuan, X. Zhang, W. Wang and Y. Yang, "Carrier Aggregation for LTE-Advanced Mobile Communication Systems," *IEEE Communications Magazine,* pp. 88-93, February 2010.

[45] L. Zhang, K. Zheng, W. Wang and L. Huang, "Performance analysis on carrier scheduling schemes in the long-term evolution-advanced system with carrier aggregation," *IET Communications,* vol. 5, no. 5, pp. 612-619, April 2010.

[46] L. Chen, W. Chen, X. Zhang and D. Yang, "Analysis and Simulation for Spectrum Aggregation in LTE-Advanced System," in *IEEE Vehicular Technology Conference*, Anchorage, AK, 2009.

[47] L. Zhang, Y. Wang, L. Huang, H. Wang and W. Wang, "QoS Performance Analysis on Carrier Aggregation Based LTE-A Systems," in *IET International Communication Conference on Wireless Mobile and Computing*, 2009.

[48] H. Wang, C. Rosa and K. Pedersen, "Performance Analysis of Downlink Inter-band Carrier Aggregation in LTE-Advanced," in *IEEE Vehicular Technology Conference*, 2011.

[49] Y. Wang, K. I. Pedersen, T. B. Sørensen and P. E. Mogensen, "Carrier Load Balancing and Packet Scheduling for Multi-Carrier Systems," *IEEE TRANSACTIONS ON WIRELESS COMMUNICATIONS,* vol. 9, no. 4, April 2010.

[50] F. Meucci, O. Cabral, F. J. Velez, A. Mihovska and N. R. Prasad, "Spectrum Aggregation with Multi-Band User Allocation over Two Frequency Bands," in *IEEE Mobile WiMAX Symposium*, 2009.

[51] S. Songsong, F. Chunyan and G. Caili, "A Resource Scheduling Algorithm Based on User Grouping for LTE-Advanced System with Carrier Aggregation," in *International Symposium on Computer Network and Multimedia Technology*, 2009.

[52] Cellular Expert, "Cellular Expert for LTE Planning," [Online]. Available: ftp://ftp.systematics.co.il/GIS/2012/PDF/Cellular%20Expert%20for%20LTE%20Planning%20-%202.pdf. [Accessed 4 November 2013].

[53] H. Zarrinkoub, Understanding LTE with MATLAB, Wiley, 2014.

[54] Y. Gao, X. Zhang, D. Yang and Y. Jiang, "Unified simulation evaluation for mobile broadband technologies," *IEEE Communications Magazine,* vol. 47, no. 3, March 2009.

[55] L. Chen, W. Chen, B. Wang, X. Zhang, H. Chen and D. Yang, "System-Level Simulation Methodology and Platform for Mobile Cellular Systems," *IEEE Communications Magazine,* pp. 148-155, July 2011.

[56] G. Piro, L. A. Grieco, G. Boggia, F. Capozzi and P. Camarda, "Simulating LTE Cellular Systems: An Open-Source Framework," *IEEE TRANSACTIONS ON VEHICULAR TECHNOLOGY,* vol. 60, no. 2, pp. 498-513, 2011.

[57] Y. Li, F. Yu, S.-l. Zheng and C.-l. Yang, "LTE System Level Simulation with Matlab," in *Conference on Internet Technology and Applications*, 2011.

[58] J. C. Ikuno, M. Wrulich and M. Rupp, "System level simulation of LTE networks," in *IEEE Vehicular Technology Conference*, Taipei, Taiwan, 2010.

[59] C. Mehlführer, J. C. Ikuno, M. Šimko, S. Schwarz, M. Wrulich and M. Rupp, "The Vienna LTE simulators - Enabling reproducibility in wireless communications research," *EURASIP Journal on Advances in Signal Processing,* 2011.

[60] C. Mehlfuhrer, M. Wrulich, J. C. Ikuno, D. Bosanska and M. Rupp, "SIMULATING THE LONG TERM EVOLUTION PHYSICAL LAYER," in *17th European Signal Processing Conference*, 2009.

[61] "APT 700MHz - Best Choice for nationwide coverage," ZTE Corporation, 2013.

[62] S. S. Kale and A. Jadhav, "An Empirically Based Path Loss Models for LTE Advanced Network and Modeling for 4G Wireless Systems at 2.4 GHz, 2.6 GHz and 3.5 GHz," *International Journal of Application or Innovation in Engineering & Management,* vol. 2, no. 9, pp. 252-257, 2013.

[63] A. F. Molisch, Wireless Communications, Second Edition, Wiley, 2011.

[64] H. Salgado, M. A. Sirbu and J. M. Peha, "A Narrow Band Approach to Efficient PCS Spectrum Sharing Through Decentralized DCA Access Policies," *IEEE Personal Communications,* vol. 4, no. 1, pp. 24-34, Feb. 1997.

[65] Y.-S. Choi, J.-H. Wui and D. Kim, "Statistical Analysis of Adjacent Channel Interference in LTE Downlink," 2011.

[66] M. Aulama and M. Olama, "Coexistence Analysis of Adjacent LTE Systems," in *International Conference on Computing, Networking and Communications (ICNC)*, 2013.

[67] Z. Ruiming, Z. Xin, L. Xi2, P. Qun, F. Yinglong1 and Y. Dacheng, "Performance Evaluation on the Coexistence Scenario of Two 3GPP LTE Systems," in *IEEE Vehicular Technology Conference*, 2009.

[68] T. Cai and J. Deng, "COEXISTENCE STUDY AND INTERFERENCE ANALYSIS IN LTE NETWORKS," in *International Conference on Control Engineering and Communication Technology*, 2012.

[69] CSMAC, "INTERFERENCE AND DYNAMIC SPECTRUM ACCESS Subcommittee Final Report," COMMERCE SPECTRUM MANAGEMENT ADVISORY COMMITTEE, 2010.

[70] E. Kwerel and J. Williams, "The Spectrum Regulator's Dilemma in a Dynamic World: Limiting Interference without Stifling Innovation," in *A Conference held at the Information Technology and Innovation Foundation (ITIF)*, Washington, DC, 2010.

[71] ETSI TS 136 104, "Base Station (BS) radio transmission and reception," 3GPP, 2011.

[72] 3GPP TR 36.808, "Carrier Aggregation; Base Station (BS) radio transmission and reception," 3GPP, 2013.

[73] CEPT Report 41, "Compatibility between LTE and WiMAX operating within the bands 880-915 MHz / 925-960 MHz and 1710-1785 MHz / 1805-1880 MHz (900/1800 MHz bands) and systems operating in adjacent bands," ECC-CEPT, 2010.

[74] S. Jingfei, "Mitigating interference between LTE and 2G/3G networks," no. 53, pp. 44-46, 2009.

[75] 3GPP TR 36.823, "Carrier aggregation enhancements; Base Station (BS) radio transmission and reception," 3GPP, 2013.

[76] Ericsson, "Analysis of Carrier Aggregation in LTE-advanced," 3GPP TSG-RAN WG4, Seoul, Korea, 2009.

[77] Huawei, "Carrier Aggregation in Advanced E-UTRA," 3GPP TSG RAN WG1, 2008.

[78] Y. R. Zheng and C. Xiao, "Simulation models with correct statistical properties for Rayleigh fading channels," *Communications, IEEE Transactions on,* vol. 51, no. 6, pp. 920-928, June 2003.

[79] T. Janssen, R. Litjens and K. Sowerby, "Best before or still fine after? On an expiration date for spectrum sharing," TNO White Paper, 2013.

[80] H. Holma and A. Toskala, LTE for UMTS- OFDMA and SC-FDMA Based Radio Access, Wiley, 2009.

[81] W. Afrić and S. Z. Pilinsky, "UMTS LTE Downlink Cell Size Calculation," in *54th International Symposium ELMAR-2012*, Zadar, Croatia, 12-14 September 2012.

[82] NGMN Alliance, "NGMN Radio Access Performance Evaluation Methodology," White Paper, 2008.

[83] Z. Sun, C. Yin and G. Yue, "Reduced-Complexity Proportional Fair Scheduling for OFDMA Systems," in *International Conference on Communications, Circuits and Systems*, 2006.

[84] C. Wengerter, J. Ohlhorst and A. E. v. Elbwart, "Fairness and Throughput Analysis for Generalized Proportional Fair Frequency Scheduling in OFDMA," in *Vehicular Technology Conference*, 2005.

[85] R. Jain, D. Chiu and W. Hawe, "A Quantitative Measure Of Fairness And Discrimination For Resource Allocation In Shared Computer Systems," DEC Research Report TR-301, September 1984.

[86] W. Mueller, "RF Front End Components and Limitations," in *FCC Forum on the Future of Band Plans*, 2012.

[87] G. Tkachenko, "Integration and Multi-Mode/Band," in *FCC Forum on the Future of Band Plans*, 2012.

[88] J. Shamblin, "Filter Technology and its Impact on Band Planning," in *FCC Forum on the Future of Band Plans*, 2012.

[89] National Instruments, "RF Front End Testing with NI PXI," White Paper, 2013.

[90] K. Watanabe and M. Machida, "Outdoor LTE Infrastructure Equipment (eNodeB)," *FUJITSU Sci. Tech. Journal,* vol. 48, no. 1, pp. 27-32, January 2012.

[91] 3GPP TR 36.815, "LTE-Advanced feasibility studies in RAN WG4," 3GPP, 2010.

[92] A.-L. Bouaziz, J.-P. Desbat, J.-M. Kelif, H. Mennenga, A. Mihovska, W. Mohr, M. Mustonen and M. Siebert, "Aspects of WINNER+ Spectrum Preferences," Wireless World Initiative New Radio –

WINNER+, 2009.

[93] W. Mueller, "Some Trends In Multi-Band Multi-Mode RF Front End Components," in *FCC Forum on the Future of Band Plans*, 2012.

[94] B. Abbott, "Filter Components," in *FCC Forum on the Future of Band Plans*, 2012.

[95] G. Vivier, "Challenges for UE with Carrier Aggregation Capability," in *Future Network Mobile Summit*, 2011.

[96] Qualcomm, "Qualcomm Announces Fifth-Generation LTE Multimode Modem for Download Speeds of Up to 450 Mbps and Next-Generation Envelope Tracker for Optimized Power Consumption," 19 Nov 2014. [Online]. Available: https://www.qualcomm.com/news/releases/2014/11/19/qualcomm-announces-fifth-generation-lte-multimode-modem-download-speeds-450. [Accessed 27 Nov 2014].

[97] Ericsson, "SingTel unveils first live LTE-A 300 Mbps service in Singapore," 30 May 2014. [Online]. Available: http://www.ericsson.com/news/140530-singtel-unveils-first-live-lte-a300mbps-service_244099437_c. [Accessed 29 Nov 2014].

[98] A. Santos, "Qualcomm outs global LTE chip, claims a world first," engadget, 22 Feb 2013. [Online]. Available: http://www.engadget.com/2013/02/22/qualcomm-first-global-lte-chip/. [Accessed 7 Sep 2013].

[99] Qualcomm, "LTE Advanced—Evolving and expanding in to new frontiers," August 2014.

[100] Qualcomm, "Qualcomm Extends the Benefits of LTE and Carrier Aggregation to Entry-Level Smartphones and Tablets," 10 Sep 2014. [Online]. Available: https://www.qualcomm.com/news/releases/2014/09/10/qualcomm-extends-benefits-lte-and-carrier-aggregation-entry-level. [Accessed 29 Nov 2014].

[101] ETSI TS 136 101, "User Equipment (UE) radio transmission and reception," 3GPP, 2013.

[102] A. Morris, "Filtering Challenges," in *FCC Forum on the Future of Band Plans*, 2012.

[103] J. Lipsky, "Qualcomm Rides LTE to Cat 10," EE Times, 20 Nov 2014. [Online]. Available: http://www.eetimes.com/document.asp?doc_id=1324710. [Accessed 29 Nov 2014].

[104] G. Varrall, "RF Cost Economics for Handsets," RTT White Paper, 2007.

[105] Z. Frias and J. Pérez, "Techno-economic analysis of femtocell deployment in long-term evolution networks," *EURASIP Journal on Wireless Communications and Networking,* vol. 288, no. 1, 2012.

[106] S. A. Azcoitia, Á. M. Fernández and L. M. G. Verdura, "Using bottom-up LRIC models to calculate radio spectrum value for mobile operators," in *Conference on Telecommunications Internet and Media Techno Economics*, 2010.

[107] Ofcom, "LTE Technical Modelling Revised Methodology," 800 MHz & 2.6 GHz Combined Award – Technical modelling for competition assessment, 2012.

[108] P. Marks, K. Pearson, B. Williamson, P. Hansell and J. Burns, "Estimating the commercial trading value of spectrum," Ofcom, 2009.

[109] W. A. Leighton, "Measuring the Effects of Spectrum Aggregation Limits: Three Case Studies from Latin America," in *Available at SSRN: http://ssrn.com/abstract=1494371*, October 25, 2009.

[110] B. G. Mölleryd, J. Markendahl, Ö. Mäkitalo and J. Werding, "Mobile Broadband Expansion Calls for More Spectrum or Base Stations - Analysis of the Value of Spectrum and the Role of Spectrum Aggregation," in *European Regional ITS Conference*, 2010.

[111] R. Hallahan and J. M. Peha, "Quantifying the Costs of a Nationwide Public Safety Wireless Network," *Telecommunications Policy,* vol. 34, no. 4, pp. 200-220, May 2010.

[112] J. Salo, M. Nur-Alam and K. Chang, "Practical Introduction to LTE Radio Planning," White Paper, European Communications Engineering (ECE) Ltd, Espoo, Finland, 2010.

[113] A. Masmoudi and S. Tabbane, "Air Interface Dimensioning Techniques for Coverage and Capacity-Limited HSPA Based Networks," in *IEEE 17th International Conference on Telecommunication*, 2010.

[114] S. Abdul Basit, "Dimensioning of LTE Network," Helsinki University of Technology, 2009.

[115] R. Schoenen, W. Zirwas and B. H. Walke, "Capacity and Coverage Analysis of a 3GPP-LTE Multihop Deployment Scenario," in *IEEE ICC Workshop*, 2008.

[116] R. M. d. Moraes, "PERFORMANCE ANALYSIS OF WIRELESS NETWORKS," PhD Thesis - UNIVERSITY OF CALIFORNIA SANTA CRUZ, 2005.

[117] L. Zhang, "Network Capacity, Coverage Estimation and Frequency Planning of 3GPP Long Term Evolution," Master thesis - Linköping University, 2010.

[118] Nokia Siemens Networks, "Mobile broadband with HSPA and LTE – capacity and cost aspects," White Paper, 2010.

[119] R. Hallahan and J. M. Peha, "Quantifying the Costs of a Nationwide Broadband Public Safety

Wireless Network," in *36th Telecommunications Policy Research Conference*, 2008.

[120] Qualcomm, "The economics of mobile wireless data," White Paper, 2006.

[121] R. Hallahan and J. M. Peha, "The Business Case of a Nationwide Wireless Network that Serves both Public Safety and Commercial Subscribers," in *37th Telecommunications Policy Research Conference*, 2009.

[122] R. Hallahan and J. M. Peha, "The Business Case of a Nationwide Wireless Network that Serves both Public Safety and Commercial Subscribers," *Telecommunications Policy,* vol. 35, no. 3, 2011.

[123] R. Bendlin, R. Chen, A. Ekpenyong, Z. Lin and E. Onggosanusi, "Embracing LTE-A with KeyStone SoCs," Texas Instruments White Paper, October 2012.

[124] L. BELHOUCHET and H. E. EBDELLI, "LTE Overview – Design Targets and Multiple Access Technologies," in *ITU Workshop on 4G Systems*, 2010.

[125] Sector & Sovereign Research, LLC, "Quick Thoughts: Yes, Comcast, There is a Threat From Wireless Broadband," 9 Nov 2011. [Online]. Available: http://www.sector-sovereign.com/2011/11/quick-thoughts-yes-comcast-there-is-a-threat-from-wireless-broadband/. [Accessed 2 Dec 2014].

[126] G. BROWN, "LTE Base Stations & the Evolved Radio Access Network," HeavyReading, [Online]. Available: http://www.heavyreading.com/details.asp?sku_id=2308&skuitem_itemid=1151. [Accessed 3 Dec 2014].

[127] CTIA – THE WIRELESS ASSOCIATION, "REPLY COMMENTS : In the Matter of Expanding the Economic and Innovation Opportunities of Spectrum Through Incentive Auctions," FCC, 2013.

[128] Spectrum Bridge, "United States TV White Spaces: Usage & Availability Analysis," White Spaces Report, 2010.

[129] K. Harrison, S. M. Mishra and A. Sahai, "How much white-space capacity is there?," IEEE DySPAN, 2010.

[130] D. Grunwald, "How New Technology Turn a Spectrum Crisis into a Spectrum Opportunity," University of Colorado, Boulder , 2011.

[131] APT REPORT, "IMPLEMENTATION ISSUES ASSOCIATED WITH USE OF THE BAND 698-806 MHZ BY MOBILE SERVICES," APT Wireless Group Meeting, 2011.

[132] A. Guidotti, P. Grazioso, M. Barbiroli, C. Carciofi, D. Guiducci and G. & Riva, "Analysis of coexistence and mutual interference between mobile and digital television systems," *Revista S&T,*

vol. 19, no. 9, pp. 9-30, 2011.

[133] W. Li, J. Chen, H. Long and B. Wu, "Performance and Analysis on LTE System under Adjacent Channel Interference of Broadcasting System," in *IEEE 12th International Conference on Computer and Information Technology*, 2012.

[134] F. Moresi, "LTE per il mobile broadband: tecnologia, regolamentazione, ecosistema e mercato," Seminario AGCOM, 2012.

[135] A. Achtzehn, M. Petrova and P. Mähönen, "Deployment of a Cellular Network in the TVWS: A Case Study in a Challenging Environment," in *CoRoNet '11 Proceedings of the 3rd ACM workshop on Cognitive radio networks*, 2011.

[136] CEPT Report 23, "Technical considerations regarding harmonisation options for the Digital Dividend," ECC-CEPT, 2007.

[137] FCC, "Spectrum Analysis: Options for Broadcast Spectrum," OBI Technical Report No. 3, 2010.

[138] C. Bazelon, "The Need for Additional Spectrum for Wireless Broadband: The Economic Benefits and Costs of Reallocations," The Battle Group, 2009.

[139] Y. Dai, A. Cuffaro, J.-L. Gauvreau, R. D. Girolamo, A. Touag and A. Demir, "Dynamic Spectrum Management System Aggregating Non-Contiguous Spectrum over TVWS," in *CROWNCOM*, 2012.

[140] C. Bazelon, C. L. Jackson and G. McHenry, "An Engineering and Economic Analysis of the Prospects of Reallocating Radio Spectrum from the Broadcast Band through the Use of Voluntary Incentive Auctions," in *TPRC*, 2011.

[141] ECC REPORT 16, "REFARMING AND SECONDARY TRADING IN A CHANGING RADIOCOMMUNICATIONS WORLD," ECC CEPT, 2002 .

[142] J. A. Eisenach, "Spectrum Reallocation and the National Broadband Plan," *Federal Communications Law Journal,* 2010.

[143] C. GABRIEL, "Huawei runs LTE in white spaces," Rethink Wireless, 24 October 2011. [Online]. Available: http://www.rethink-wireless.com/2011/10/24/huawei-runs-lte-white-spaces.htm. [Accessed 29 October 2011].

[144] T. Parker, "T-Mobile 600 MHz study shows LTE can share channels with nearby TV stations," FierceWirelessTech, 18 December 2013. [Online]. Available: http://www.fiercewireless.com/tech/story/t-mobile-600-mhz-study-shows-lte-can-share-channels-nearby-tv-stations/2013-12-18. [Accessed 2014 February 1].

[145] ITU-R M.1767, "Protection of land mobile systems from terrestrial digital video and audio broadcasting systems in the VHF and UHF shared bands allocated on a primary basis," ITU-R Recommendation, 2006.

[146] FCC, "Analysis of Potential Aggregate Interference," 2013.

[147] FCC, "NOTICE OF PROPOSED RULEMAKING: Expanding the Economic and Innovation Opportunities of Spectrum Through Incentive Auctions," September 2012.

[148] G. S. Ford, T. M. Koutsky and L. J. Spiwak, "USING AUCTION RESULTS TO FORECAST THE IMPACT OF WIRELESS CarterfoneREGULATION ON WIRELESS NETWORKS," PHOENIX CENTER POLICY BULLETIN NO. 20, 2008.

[149] G. Madden, "Generalizing US Spectrum Experience, Discussant Paper for: US Wireless License Auctions: 1994-2009 by Thomas W. Hazlett," in *Australian Competition and Consumer Commission 2009 Regulatory Conference*, July 30, 2009.

[150] G. G. Madden, I. Saglam and A. Morey, "Auction Design and the Success of National 3G Spectrum Auctions," No 1002, Working Papers from TOBB University of Economics and Technology, Department of Economics, 2010.

[151] G. Madden and A. Morey, "A Global Analysis of Third Generation Mobile Telecommunications Market Entry," in *22nd European Regional ITS Conference*, 2011.

[152] E. Bohlin, G. Madden and A. Morey, "An Econometric Analysis of 3G Auction Spectrum Valuations," European University Institute, 2010.

[153] DotEcon Ltd, "Award of 800MHz and 900MHz spectrum," Update report on benchmarking, 2010.

[154] K. Hyndmany and C. F. Parmeter, "Efficiency or Competition? A Structural Econometric Analysis of Canada's AWS Auction and the Set-Aside Provision," February 2013. [Online]. Available: http://www.hyndman-honhon.com/hyndman/HP-AWS-Auction.pdf. [Accessed 11 1 2014].

[155] C. M. Dippon, "Regulatory Policy Goals and Spectrum Auction Design," NERA Economic Consulting, 2009.

[156] M. Roetter, "Spectrum for Mobile Broadband in the Americas: Policy Issues for Growth and Competition," On behalf of the GSMA, 2011.

[157] K. V. Bruwaene, "Estimating the Value of Spectrum," Belgium, 2003.

[158] R. Sweeta, I. Viehoffb, D. Linardatosc and N. Kalouptsidisc, "Marginal value-based pricing of additional spectrum assigned to cellular telephony operators," *Information Economics and Policy,*

vol. 14, pp. 371-384, 2002.

[159] N. Jesuale and B. C. Eydt, "Spectrum Paradigm Shift," *RadioResource Mission Critical Communications Magazine,* vol. 23, no. 3, pp. 83-91, March 2008.

[160] Technological Advisory Council, "FCC Thoughts on Future Band Plans," in *FCC Forum on the Future of Band Plans*, 2012.

[161] E. TEJEDOR, "Band Planning: UL-DL Frequency Seperation," in *FCC Forum on the Future of Band Planning*, July 2012.

[162] S. Hong, J. Mehlman and S. Katti, "Picasso: Flexible RF and Spectrum Slicing," in *Proceedings of the ACM SIGCOMM 2012 conference on Applications, technologies, architectures, and protocols for computer communication*, 2012.

[163] CEPT Report 31, "Technical considerations regarding harmonisation options for the digital dividend in the European Union," ECC-CEPT, 2009.

[164] C. Bazelon, "Pairing AWS-3 with the 1755 MHz Band is More Valuable than Pairing it with Frequencies from the 1690 MHz Band," The Brattle Group, 2011.

[165] P. Cramton, E. Kwerel, G. Rosston and A. Skrzypacz, "Using Spectrum Auctions to Enhance Competition in Wireless Services," SIEPR Discussion Paper, 2011.

[166] P. Cramton, "Auctioning the Digital Dividend," in *International Workshop on Communication Regulation in the Age of Digital Convergence: Legal and Economic Perspectives*, 2008.

[167] P. Cramton, "Why Large Licenses Are Best for the 700 MHz Spectrum Auction," Before the Federal Communications Commission, on behalf of Verizon Wireless, April 2007.

[168] P. Cramton, "Spectrum Auction Design," 2009.

[169] J. B. Baker, "Spectrum Auction Rules That Foster Mobile Wireless Competition," Before FCC, In the Matter of Policies Regarding Mobile Spectrum Holdings, March 2013.

[170] Tolaga Research, "The Emergence of Multi-band Spectrum Auctions," Spectrum Regulation Research, 2010.

[171] D. Sahota, "Sweden auctions 1800MHz spectrum," telecoms.com, 12 October 2011. [Online]. Available: http://www.telecoms.com/34652/sweden-auctions-1800mhz-spectrum/. [Accessed 12 October 2011].

[172] C. GABRIEL, "UK 4G auction delayed again but trials start," Rethink Wireless, 10 October 2011. [Online]. Available: http://www.rethink-wireless.com/2011/10/10/uk-4g-auction-delayed-trials.htm. [Accessed 1 December 2011].

[173] Arthur D. Little, "Mobile Broadband, Competition and Spectrum Caps," An independent paper prepared for the GSM Association, 2009.

[174] J. M. Peha, "Cellular Competition and the Weighted Spectrum Screen," in *41st Telecommunications Policy Research Conference (TPRC)*, 2013.

[175] J. M. Peha, "Updating the Spectrum Screen," Comments for Public Knowledge in the matter of The State of Mobile Wireless Competition, WT Docket No. 11-186, November 2012.

[176] Vodafone, "A spectrum policy to foster competitiveness, sustainability and cohesion," in *White Paper*, 2010.

[177] K. Tan, Y. He, H. Shen, J. Zhang and Y. Zhang, "Spectrum Virtualization Layer," Microsoft Research Asia, 2011.

[178] L. Doyle, J. McMenamy and T. K. Forde, "Regulating for Carrier Aggregation & Getting Spectrum Management Right for the Longer Term," in *DySPAN*, 2012.

[179] K. Tan, H. Shen, J. Zhang and Y. Zhang, "Enable Flexible Spectrum Access with Spectrum Virtualization".

[180] W. Wang, Z. Zhang and A. Huang, "Spectrum Aggregation: Overview and Challenges," *Network Protocols and Algorithms,* vol. 2, no. 1, pp. 184-196, 2010.

[181] 3GPP TR 37.804, "Study on UMTS/LTE in 900 MHz band and coexistence with 850 MHz band," 3GPP, 2012.

[182] 3GPP TR 37.801, "UMTS-LTE 3500 MHz Work Item Technical Report," 3GPP, 2011.

[183] ITU-R M.2134, "Requirements related to technical performance for IMT-Advanced radio interface(s)," REPORT, 2008.

[184] D. Bultmann and T. Andre, "Analysis of 3GPP LTE-Advanced Cell Spectral Efficiency," in *IEEE International Symposium on Personal, Indoor and Mobile Radio Communication*, 2010.

[185] O. IOSIF and I. BĂNICĂ, "Performance Analysis of Downlink LTE Using System Level Simulator," *U.P.B. Sci. Bull., Series C,* vol. 75, no. 1, pp. 111-122, 2013.

[186] FCC Public Notice, "Media Bureau Seeks Comment on Catalog of Eligible Expenses and other Issues related to the Imbursement of Broadcaster Channel Reassignment Costs," GN Docket No. 12-268, 2013.

[187] ETSI TS 136 211, "Physical channels and modulation," 3GPP, 2013.

[188] G. d. l. Roche and C.-C. Chong, "Bandwidth Dependency Channel Model: On the Impact to Carrier Aggregated Systems," in *IEEE WCNC*, 2011.

[189] C. M. Park, H. B. Jung, S. H. Kim and D. K. Kim, "System Level Performance Evaluation of Various Carrier Aggregation Scenarios in LTE-Advanced," in *International Conference on Advanced Communication Technology*, 2013.

[190] K. R. Manoj, "COVERAGE ESTIMATION FOR MOBILE CELLULAR NETWORKS FROM SIGNAL STRENGTH MEASUREMENTS," PhD Thesis - THE UNIVERSITY OF TEXAS AT DALLAS, 1999.

[191] CTTC, "LTE Simulator Documentation," Centre Tecnològic de Telecomunicacions de Catalunya, 2011.

[192] J. Zyren and W. McCoy, "Overview of the 3GPP Long Term Evolution Physical Layer," White Paper, 2007.

[193] Agilent Technologies, "Introducing LTE-Advanced," March 2011.

[194] A. Osseiran, J. F. Monserrat and W. Mohr, Mobile and Wireless Communications for IMT-Advanced and Beyond, John Wiley & Sons, Ltd, 2011.

[195] D. Astély, E. Dahlman, A. Furuskär, Y. Jading, M. Lindström and S. Parkvall, "LTE: The Evolution of Mobile Broadband," *IEEE Communications Magazine,* pp. 44-51, April 2009.

[196] M. BERGSTROM, "Analysis of Interference and Performance in Heterogeneously Deployed LTE systems," Master of Science Thesis - Stockholm, 2010.

[197] M. Kottkamp, "LTE-Advanced Technology Introduction," White Paper, 2010.

[198] T. Nakamura, "LTE-Advanced (3GPP Release 10 and beyond) - RF aspects -," FUJITSU LIMITED, Beijing, China, 2009.

[199] J. Parikh and A. Basu, "LTE Advanced: The 4G Mobile Broadband Technology," *International Journal of Computer Applications,* vol. 13, no. 5, pp. 17-21, 2011.

[200] S. Parkvall, A. Furuskär and E. Dahlman, "Evolution of LTE toward IMT-Advanced," *IEEE*

Communications Magazine, pp. 84-91, February 2011.

[201] Y. Wang, "System Level Analysis of LTE-Advanced: with Emphasis on Multi-Component Carrier Management," PhD Thesis - Aalborg University, 2010.

[202] Anritsu, "LTE Resources Guide," White Paper, 2010.

[203] Motorola, "Long Term Evolution (LTE): Overview of LTE Air-Interface," White Paper, 2007.

[204] P. Bhat, S. Nagata, L. Campoy, I. Berberana, T. Derham, G. Liu, X. Shen, P. Zong and J. Yang, "LTE-Advanced: An Operator Perspective," *IEEE Communications Magazine,* pp. 104-114, February 2012.

[205] Qualcomm Inc, "HSPA+ for Enhanced Mobile Broadband," White Paper, 2009.

[206] S. M. Duarte, "Analysis of Technologies for Long Term Evolution in UMTS," Master Thesis - Technical University of Lisbon, 2008.

[207] Freescale Semiconductor, "Long Term Evolution Protocol Overview," White Paper, 2008.

[208] Qualcomm Inc, "LTE Advanced—Leading in chipsets and evolution," August 2013. [Online]. Available: http://www.qualcomm.com/sites/default/files/document/files/wireless-networks-lte_advanced-leading_in_chipsets_and_evolution.v6.20130827.pdf. [Accessed December 2013].

[209] Y. Kakishima, T. Kawamura, Y. Kishiyama, H. Taoka and T. Nakamura, "Experimental Evaluation on Throughput Performance of Asymmetric Carrier Aggregation in LTE-Advanced," in *IEEE Vehicular Technology Conference*, 2011.

[210] M. Bennis, I. Cosovic, K. Doppler, P. Lunden, M. Siebert, A. Sorri, J. Vihriälä, E. Virtej and R. Walsdorf, "Initial Report on System Aspects of Flexible Spectrum Use," Wireless World Initiative New Radio – WINNER+, 2009.

[211] S. Wallsten, "Is There Really a Spectrum Crisis? Quantifying the Factors Affecting Spectrum License Value," Technology Policy Institute, 2013.

[212] INDEPEN, "AN ECONOMIC STUDY TO REVIEW SPECTRUM PRICING," AEGIS SYSTEMS AND WARWICK BUSINESS SCHOOL, 2004.

[213] Q. Song and W. Wang, "Research on Economic Evaluation Methodology for Radio Spectrum Resource Management," in *International Conference on Management and Service Science*, 2009.

[214] C. Doyle and M. Cave, "The Economics of Pricing Radio Spectrum," March 2004. [Online]. Available: http://userpage.fu-berlin.de/~jmueller/its/conf/berlin04/Papers/Doyle.pdf. [Accessed

12 August 2012].

[215] ITU, "Exploring the value and economic valuation of spectrum," Broadband Series, 2012.

[216] D. Robinson, A. Shukla, J. Burns and A. Atefi, "Resource Trading for Spectrum Aggregation and Management," in *IEEE DySPAN*, 2005.

[217] D. Webbink, "The Value of the Frequency Spectrum Allocated to Specific Uses," *IEEE Transactions on Electromagnetic Compatibility,* vol. Part II, no. 3, pp. 343-351, August 1977.

[218] T. R. Beard, G. S. Ford, L. J. Spiwak and M. L. Stern, "A Policy Framework for Spectrum Allocation in Mobile Communications," Phoenix Center Policy Paper No. 42, 2011.

[219] T. W. Hazlett and R. E. Mufioz, "A welfare analysis of spectrum allocation policies," *RAND Journal of Economics,* vol. 40, no. 3, pp. 424-454, 2009.

[220] R. Merritt, "Integrated chips fuel smartphone growth," EE Times, 19 April 2011. [Online]. Available: http://www.eetimes.com/electronics-news/4215273/Integrated-chips-fuel-smartphone-growth?pageNumber=0. [Accessed 20 November 2011].

[221] P. Viswanath, D. N. C. Tse and R. Laroia, "Opportunistic Beamforming Using Dumb Antennas," *IEEE TRANSACTIONS ON INFORMATION THEORY,* vol. 48, no. 6, pp. 1277-1294, June 2002.

[222] J. Peha, "Cellular Competition and the Weighted Spectrum Screen," in *Telecommunications Policy Research Conference (TPRC)*, 2013.

APPENDICES

Appendix A: Source code for LTE Simulator

Code for Input Parameters

```
%% Multibands
mfrequency       = [0.7e9 2.6e9];
mbandwidth       = [10e6 5e6];

%% C: General parameters

LTE_config.nTX           = 2;
LTE_config.nRX           = 2;
LTE_config.tx_mode       = 4;
%% Transmission parameters (used for the throughput calculation)
LTE_config.N_sym = 7;
for i=1:length(mbandwidth)
    LTE_config.bandwidth=mbandwidth(i);
    switch LTE_config.bandwidth
        case 1.4e6
            mN_RB(i) = 6;
            mfft_points(i) = 128;
            mCP_length_samples(i) = 9;
        case 3e6
            mN_RB(i) = 15;
            mfft_points(i) = 256;
            mCP_length_samples(i) = 18;
        case 5e6
            mN_RB(i) = 25;
            mfft_points(i) = 512;
            mCP_length_samples(i) = 36;
        case 10e6
            mN_RB(i) = 50;
            mfft_points(i) = 1024;
            mCP_length_samples(i) = 72;
        case 15e6
            mN_RB(i) = 75;
            mfft_points(i) = 1536;
            mCP_length_samples(i) = 108;
        case 20e6
            mN_RB(i) = 100;
            mfft_points(i) = 2048;
            mCP_length_samples(i) = 144;
        otherwise
            error('Bandwidth not supported');
    end
end
LTE_config.bandwidth=sum(mbandwidth);
LTE_config.N_RB=sum(mN_RB);
```

```
LTE_config.Ntot = LTE_config.N_RB*12;
LTE_config.fft_points=sum(mfft_points);
LTE_config.fs = 15e3*LTE_config.fft_points;
LTE_config.CP_length_samples=sum(mCP_length_samples);
switch LTE_config.nTX   % number of reference symbols
    case 1
        numb = 4;
    case 2
        numb = 8;
    case 4
        numb = 12;
    otherwise
        error('Not defined for %d TX antennas',LTE_config.nTX);
end
LTE_config.sym_per_RB_nosync = 12*LTE_config.N_sym - numb; % no
synchronization signals
LTE_config.sym_per_RB_sync = 12*LTE_config.N_sym -(numb+12); % take also
synchronization signals into account
LTE_config.scheduler_params.overhead_ref = numb;
LTE_config.scheduler_params.overhead_sync = numb+12;

for i=1:length(mfrequency)
    LTE_config.frequency=mfrequency(i);
.......

%% Give the schedulers access to al UE and all carriers
for c_=1:length(eNodeBs_sectors)

eNodeBs_sectors(c_).scheduler.set_UE_traces(simulation_traces.UE_traces);
end

networkPathlossMap_by_band(i,:)=networkPathlossMap;
UEs_by_band(i,:)=UEs;
eNodeBs_sectors_by_band(i,c_,:)=eNodeBs_sectors;



end % end of 'mfrequency' for loop
```

Code for Creating hexagonal set of eNodeBs

```
% Distance between BTSs
inter_bts_distance = LTE_config.inter_eNodeB_distance;
% Number of BTS rings in the network map
n_rings = LTE_config.nr_eNodeB_rings;

%total nr. of eNodeBs
% each ring consists of 6 NodeBs at the corners of the hexagon
% each edge then has "i-1" further NodeBs, where "i" is the ring index
% total_nr_eNodeB = sum(6*(1:n_rings))+1;
```

```
[tmp_gridx,tmp_gridy] = meshgrid(-n_rings:n_rings,...
    (-n_rings:n_rings)*sin(pi/3)); %regular grid
if mod(n_rings,2) == 0
    tmp_shift_idx = 2:2:2*n_rings+1; %shift all even rows
else
    tmp_shift_idx = 1:2:2*n_rings+1; %shift all odd rows
end

tmp_gridx(tmp_shift_idx,:) = tmp_gridx(tmp_shift_idx,:) + 0.5; %shift

rot = @(w_) [cos(w_),-sin(w_);sin(w_),cos(w_)]; %rotation operator
for i_ = 1:7
    %border of the network
    tmp_hex(i_,:) = ((n_rings+0.5)*rot(pi/3)^(i_-1)*[1;0]).'; %#ok<AGROW>
end

tmp_valid_positions =
inpolygon(tmp_gridx,tmp_gridy,tmp_hex(:,1),tmp_hex(:,2));
tmp_x = tmp_gridx(tmp_valid_positions);
tmp_y = tmp_gridy(tmp_valid_positions);

%% Create the eNodeB array
for b_ = 1:length(tmp_x)
    eNodeBs(b_)           = network_elements.eNodeB;
    eNodeBs(b_).id        = b_;
    eNodeBs(b_).pos       = [tmp_x(b_)*inter_bts_distance
tmp_y(b_)*inter_bts_distance];
    eNodeBs(b_).site_type = 'macro';
end
% Plot where the BTs are and add a text legend to know where are the BTSs
for b_ = 1:length(eNodeBs)

scatter(eNodeBs(b_).pos(1),eNodeBs(b_).pos(2),'MarkerEdgeColor','k','MarkerFa
ceColor','w');

text(eNodeBs(b_).pos(1)+6*networkPathlossMap.data_res,eNodeBs(b_).pos(2),num2
str(b_));
end

% Plot the center of the cells
for s_ = 1:length(eNodeBs_sectors)

text(cell_centers(s_,1),cell_centers(s_,2),num2str(s_),'HorizontalAlignment',
'center','Verticalalignment','middle','Color',0.75*[1 1 1]);
end

xlabel('x pos [m]');
ylabel('y pos [m]');
```

Code for Creating UEs in the Cells

```
%% Creating or loading UE position, depending on the configuration
% Create UEs according to the previously generated positions
UEs = network_elements.UE;
if (~use_UE_cache) || (use_UE_cache&&~cache_file_exists)
    for u_ = 1:size(UE_positions,1)
        % General UE settings that can be saved and re-used
        UEs(u_)      = network_elements.UE;
        UEs(u_).id   = u_;
        UEs(u_).pos = LTE_common_pixel_to_pos( UE_positions(u_,:),
networkPathlossMap.coordinate_origin, networkPathlossMap.data_res);

        % Generate a walking model for the user
        if isfield(LTE_config.UE,'walk')
            if strcmp(LTE_config.UE.walk,'SLvsLL')
                UEs(u_).walking_model = walking_models.SLvsLLWalkingModel; %
Since no angle is specified, a random one is chosen
            end
        else
            UEs(u_).walking_model =
walking_models.straightWalkingModel(LTE_config.UE_speed*LTE_config.TTI_length
); % Since no angle is specified, a random one is chosen
        end
    end
    if LTE_config.debug_level>=1
        fprintf('Saving UE positions to %s\n',LTE_config.UE_cache_file);
    end
    if use_UE_cache
        try
            if exist(LTE_config.UE_cache_file,'file')
                throw(MException('LTEsim:cacheExists', 'The cache file was
concurrently generated during another simulation run'));
            end
            save(LTE_config.UE_cache_file,'UEs','UE_positions');
        catch err
            fprintf('UE cache could not be saved. If needed, it will be
generated again in the next run (%s).\n',err.message);
        end
    end
```

Code for Generating Macroscopic Pathloss

For each carrier:

```
% Add the Antennas to the eNodeBs
s_idx    = 1;
eNodeBs = network_elements.eNodeB_sector; % Initialization
for b_ = 1:length(eNodeBs_sites)
    % Create the eNodeB_sector objects
    % Writing eNodeBs(b_).sectors(1) gave me an error. Maybe a bug??
    eNodeBs_sites(b_).sectors     = network_elements.eNodeB_sector;
    for s_ = 1:length(LTE_config.sector_azimuths)
        eNodeBs_sites(b_).sectors(s_)                =
network_elements.eNodeB_sector;
```

```
        eNodeBs_sites(b_).sectors(s_).parent_eNodeB = eNodeBs_sites(b_);
        eNodeBs_sites(b_).sectors(s_).id            = s_;
        eNodeBs_sites(b_).sectors(s_).azimuth       =
utils.miscUtils.wrapTo359(LTE_config.antenna_azimuth_offsett +
LTE_config.sector_azimuths(s_));
        eNodeBs_sites(b_).sectors(s_).max_power     = eNodeB_sector_tx_power;
        eNodeBs_sites(b_).sectors(s_).antenna_type  =
LTE_config.antenna.antenna_gain_pattern;
        eNodeBs_sites(b_).sectors(s_).nTX           = LTE_config.nTX;

        eNodeBs_sites(b_).sectors(s_).eNodeB_id     = s_idx;
        eNodeBs(s_idx)                              =
eNodeBs_sites(b_).sectors(s_);

        % Attach the correct antenna to the eNodeB

antennas.antenna.attach_antenna_to_eNodeB(eNodeBs_sites(b_).sectors(s_),LTE_c
onfig);

        % Create the macroscopic pahloss model that will be used
        if LTE_config.debug_level>=1
            fprintf('Site %d, eNodeB %d: ',b_,s_);
        end

        eNodeBs_sites(b_).sectors(s_).macroscopic_pathloss_model =
macroscopic_pathloss_models.generalPathlossModel.generateMacroscopicPathlossM
odel(...
            LTE_config,...
            LTE_config.macroscopic_pathloss_model,...
            LTE_config.frequency,...
            LTE_config.macroscopic_pathloss_model_settings);

        s_idx = s_idx + 1;
    end
end



macroscopic_pathloss_model =
macroscopic_pathloss_models.freeSpacePathlossModel(frequency);



        function obj = freeSpacePathlossModel(frequency)
            obj.frequency = frequency;
            obj.name = 'free space';
        end
        % Returns the free-space pathloss in dB. Note: distance in METERS
        function pathloss_in_db = pathloss(obj,distance)
            % Restrict that pathloss must be bigger than 0 dB
            pathloss_in_db =
max(10*log10((4*pi/299792458*distance*obj.frequency).^2),0);
        end
```

```
%% Create pathlossMap
networkMacroscopicPathlossMap                              =
channel_gain_wrappers.macroscopicPathlossMap;
networkMacroscopicPathlossMap.data_res                     = data_res;
networkMacroscopicPathlossMap.roi_x                        = roi_x;
networkMacroscopicPathlossMap.roi_y                        = roi_y;


function
calculate_pathloss_maps(LTE_config,eNodeBs,networkMacroscopicPathlossMap,vara
rgin)
            if ~isempty(varargin)
                elevation_map     = varargin{1};
                elevation_map_set = true;
            else
                elevation_map     = 0;
                elevation_map_set = false;
            end

            % Calculates the pathloss maps for a given eNodeB set (cell set)
            total_sectors          = length([eNodeBs.sectors]);
            data_res               = networkMacroscopicPathlossMap.data_res;
            roi_x                  = networkMacroscopicPathlossMap.roi_x;
            roi_y                  = networkMacroscopicPathlossMap.roi_y;
            roi_maximum_pixels     = LTE_common_pos_to_pixel( [roi_x(2)
roi_y(2)], [roi_x(1) roi_y(1)], data_res);
            roi_height_pixels      = roi_maximum_pixels(2);
            roi_width_pixels       = roi_maximum_pixels(1);
            distance_matrix        =
zeros(roi_height_pixels,roi_width_pixels,length(eNodeBs));
            cell_pathloss_data     =
zeros(roi_height_pixels,roi_width_pixels,total_sectors);
            sector_antenna_gain    =
zeros(roi_height_pixels,roi_width_pixels,total_sectors);

            site_positions     = reshape([eNodeBs.pos],2,[])';
            site_positions_pix = LTE_common_pos_to_pixel( site_positions,
[roi_x(1) roi_y(1)], data_res);

            % Generate distance and angle matrix
            position_grid_pixels      =
zeros(roi_height_pixels*roi_width_pixels,2);
            position_grid_pixels(:,1) =
reshape(repmat(1:roi_width_pixels,roi_height_pixels,1),1,roi_width_pixels*roi
_height_pixels);
            position_grid_pixels(:,2) =
repmat(1:roi_height_pixels,1,roi_width_pixels);
            position_grid_meters      =
LTE_common_pixel_to_pos(position_grid_pixels,networkMacroscopicPathlossMap.co
ordinate_origin,networkMacroscopicPathlossMap.data_res);

            %% Sector pathloss
            s_idx = 1;
            all_sectors   = [eNodeBs.sectors];
```

```
            eNodeB_id_set = [all_sectors.eNodeB_id];
            for b_ = 1:length(eNodeBs)
                distances                = sqrt((position_grid_meters(:,1)-
eNodeBs(b_).pos(1)).^2 + (position_grid_meters(:,2)-eNodeBs(b_).pos(2)).^2);
                distance_matrix(:,:,b_) =
reshape(distances,roi_height_pixels,roi_width_pixels);
                for s_ = 1:length(eNodeBs(b_).sectors)

                    if
isempty(eNodeBs(b_).sectors(s_).macroscopic_pathloss_model)
                        capesso_pathloss = true;
                    else
                        capesso_pathloss = false;
                    end

                    % Calculate macroscopic pathloss using the macroscopic
pathloss model from each eNodeB
                    if ~capesso_pathloss
                        cell_pathloss_data(:,:,s_idx) =
eNodeBs(b_).sectors(s_).macroscopic_pathloss_model.pathloss(distance_matrix(:
,:,b_));
                    else
                        cell_pathloss_data(:,:,s_idx) =
networkMacroscopicPathlossMap.pathloss(:,:,s_idx);
                    end

                    % Horizontal angle grid
                    angle_grid = (180/pi)*(atan2((position_grid_meters(:,2)-
eNodeBs(b_).pos(2)),(position_grid_meters(:,1)-eNodeBs(b_).pos(1)))) -
utils.miscUtils.wrapTo359(-eNodeBs(b_).sectors(s_).azimuth+90); % Convert the
azimuth (0°=North, 90°=East, 180^=South, 270°=West) degrees to cartesian

                    if
strcmp(class(eNodeBs(b_).sectors(s_).antenna),'antennas.kathreinTSAntenna')
                        % Although the elevation map and the site information
should have the same information, the elevation map info takes precedence
                        if elevation_map_set
                            eNodeB_elevation =
elevation_map(site_positions_pix(b_,2),site_positions_pix(b_,1));
                        else
                            eNodeB_elevation = eNodeBs(b_).altitude;
                        end

                        % Horizontal angle grid
                        horizontal_angle_grid   =
reshape(angle_grid,roi_height_pixels,roi_width_pixels);
                        horizontal_angle_grid_s =
utils.miscUtils.wrapTo359(horizontal_angle_grid);

                        % Vertical angle grid
                        vertical_angle_grid_el =
(180/pi)*(atan2(eNodeBs(b_).sectors(s_).tx_height + elevation_map -
eNodeB_elevation - LTE_config.rx_height, distance_matrix(:,:,b_)));
```

```
                        % Calculate antenna gain
                        sector_antenna_gain(:,:,s_idx) =
eNodeBs(b_).sectors(s_).antenna.gain(horizontal_angle_grid_s,
vertical_angle_grid_el, eNodeBs(b_).sectors(s_).electrical_downtilt,
eNodeBs(b_).sectors(s_).mechanical_downtilt);
                    else
                        % Calculate angle
                        theta_matrix =
reshape(angle_grid,roi_height_pixels,roi_width_pixels);

                        % Set sector_azimuth to (-180,180)
                        theta_matrix                        = theta_matrix + 180;
                        theta_matrix                        =
mod(theta_matrix,360);
                        theta_matrix                        = theta_matrix - 180;
                        sector_antenna_gain(:,:,s_idx) =
eNodeBs(b_).sectors(s_).antenna.gain(theta_matrix);
                    end

                    % Mapping between s_idx and b_/s_ pair

networkMacroscopicPathlossMap.sector_idx_mapping(eNodeBs(b_).sectors(s_).eNod
eB_id,:) = [b_ s_];
                    networkMacroscopicPathlossMap.site_sector_mapping(b_,s_)
= eNodeBs(b_).sectors(s_).eNodeB_id;;

                    s_idx = s_idx + 1;
                end
            end

            % Just in case...
            cell_pathloss_data(isnan(cell_pathloss_data) |
(cell_pathloss_data<0)) = 0;

            networkMacroscopicPathlossMap.pathloss(:,:,eNodeB_id_set) =
cell_pathloss_data - sector_antenna_gain;
        end
```

Code for Generating Shadow Fading

For each carrier:

```
    % Generate shadow fading
    if LTE_config.macroscopic_pathloss_is_model
        if LTE_config.debug_level>=1
            fprintf('Generating shadow fading\n');
        end
        switch LTE_config.shadow_fading_type
            case 'claussen'
                [LTE_config.roi_x LTE_config.roi_y] =
networkPathlossMap.valid_range;
                if LTE_config.debug_level>=1
```

```
                    fprintf('Generating Claussen space-correlated shadow
fading map\n');
                end
                networkShadowFadingMap =
channel_gain_wrappers.shadowFadingMapClaussen(...
                    LTE_config.shadow_fading_map_resolution,...
                    LTE_config.roi_x,...
                    LTE_config.roi_y,...
                    LTE_config.shadow_fading_n_neighbors,...
                    eNodeBs,...
                    LTE_config.shadow_fading_mean,...
                    LTE_config.shadow_fading_sd,...
                    LTE_config.r_eNodeBs);
            case 'none'
                [LTE_config.roi_x LTE_config.roi_y] =
networkPathlossMap.valid_range;
                if LTE_config.debug_level>=1
                    fprintf('Generating dummy shadow fading map (i.e. no
shadow fading');
                end
                networkShadowFadingMap =
channel_gain_wrappers.shadowFadingDummyMap(...
                    LTE_config.roi_x,...
                    LTE_config.roi_y);
            otherwise
                error('%s shadow fading type not supported. Only "clausse"
and "none" supported',LTE_config.shadow_fading_type);
        end
    end
            %% Calculate cross-correlation between eNodeBs
            num_eNodeBs = length(eNodeBs);
            % Fixed shadow fading correlation between maps
            r_eNodeBs = eNodeBs_ccorr;

            %% Generate cross correlated gaussian maps
            % The last one will be the original random one
            if length(varargin)==0
                a_n_random_matrix = mean + std*randn(N_y,N_x,num_eNodeBs);
                a_n_original_map = mean + std*randn(N_y,N_x);

                a_n_matrix = zeros(N_y,N_x,num_eNodeBs);
                for i_=1:num_eNodeBs
                    % Generate i gaussian maps based on an 'original' one
                    a_n_matrix(:,:,i_) = sqrt(r_eNodeBs)*a_n_original_map +
sqrt(1-r_eNodeBs)*a_n_random_matrix(:,:,i_);
                end
            else
                a_n_matrix = varargin{1};
            end

            an_ccorr = zeros(num_eNodeBs,num_eNodeBs);
            for i_=1:num_eNodeBs
                for j_=i_:num_eNodeBs
                    correlation =
corr2(a_n_matrix(:,:,i_),a_n_matrix(:,:,j_));
```

```
                    an_ccorr(i_,j_) = correlation;
                    an_ccorr(j_,i_) = correlation;
                end
            end

            %% R matrices for the map calculation
            switch n_neighbors
                case 4
                    R = [
                        1               r(d)            r(2*d)          r(d)
r(sqrt(2)*d)
                        r(d)            1               r(d)
r(sqrt(2)*d)   r(d)
                        r(2*d)          r(d)            1
r(sqrt(5)*d)   r(sqrt(2)*d)
                        r(d)            r(sqrt(2)*d)    r(sqrt(5)*d)    1
r(d)
                        r(sqrt(2)*d)    r(d)            r(sqrt(2)*d)    r(d)
1
                        ];
                case 8
                    R = [
                        1               r(d)            r(2*d)          r(d)
r(d)          r(sqrt(5)*d)    r(d)            r(3*d)          r(sqrt(2)*d)
                        r(d)            1               r(d)
r(sqrt(2)*d)   r(sqrt(2)*d)   r(sqrt(2)*d)    r(2*d)          r(2*d)
r(d)
                        r(2*d)          r(d)            1
r(sqrt(5)*d)   r(sqrt(5)*d)   r(d)            r(3*d)          r(d)
r(sqrt(2)*d)
                        r(d)            r(sqrt(2)*d)    r(sqrt(5)*d)    1
r(2*d)        r(sqrt(8)*d)    r(sqrt(2)*d)    r(sqrt(10)*d)   r(d)
                        r(d)            r(sqrt(2)*d)    r(sqrt(5)*d)    r(2*d)
1             r(2*d)          r(sqrt(2)*d)    r(sqrt(10)*d)   r(sqrt(5)*d)
                        r(sqrt(5)*d)    r(sqrt(2)*d)    r(d)
r(sqrt(8)*d)   r(2*d)         1               r(sqrt(10)*d)   r(sqrt(2)*d)
r(sqrt(5)*d)
                        r(d)            r(2*d)          r(3*d)
r(sqrt(2)*d)   r(sqrt(2)*d)   r(sqrt(10)*d)   1               r(4*d)
r(sqrt(5)*d)
                        r(3*d)          r(2*d)          r(d)
r(sqrt(10)*d)  r(sqrt(10)*d)  r(sqrt(2)*d)    r(4*d)          1
r(sqrt(5)*d)
                        r(sqrt(2)*d)    r(d)            r(sqrt(2)*d)    r(d)
r(sqrt(5)*d)  r(sqrt(5)*d)    r(sqrt(5)*d)    r(sqrt(5)*d)    1
                        ];
                otherwise
                    error('Only 4 and 8 values supported');
            end

            L            = chol(R,'lower');
            lambda_n_T   = L(end,:);
            R_tilde      = R(1:end-1,1:end-1);
            L_tilde      = chol(R_tilde,'lower');
            inv_L_tilde = inv(L_tilde);
```

```
            N_x = size(a_n_matrix,2);
            N_y = size(a_n_matrix,1);
            s = zeros(N_y,N_x,num_eNodeBs);

            %% Calculate space-correlated maps
            for y_=1:N_y
                for x_=1:N_x
                    % Substitutes the
LTE_aux_shadowFadingMapClaussen_get_neighbors function
                    %
LTE_aux_shadowFadingMapClaussen_get_neighbors(s,position,values)
                    s_tilde = zeros(n_neighbors,num_eNodeBs);
                    positions         = [x_+offsets(:,1) y_+offsets(:,2)];
                    positions_geq0    = positions>0;
                    positions_leqroi = [positions(:,1)<=N_x
positions(:,2)<=N_y];
                    positions_valid  =
(positions_geq0(:,1)&positions_geq0(:,2)) &
(positions_leqroi(:,1)&positions_leqroi(:,2));
                    for i_=1:n_neighbors
                        if positions_valid(i_)
                            neighbor_position = positions(i_,:);
                            s_tilde(i_,:) =
s(neighbor_position(2),neighbor_position(1),:);
                        end
                    end
                    % end of LTE_aux_shadowFadingMapClaussen_get_neighbors

                    inv_L_tilde_s_tilde = inv_L_tilde * s_tilde;
                    a_n_all = reshape(a_n_matrix(y_,x_,:),1,[]);
                    inv_L_tilde_s_tilde_a_n = [inv_L_tilde_s_tilde;a_n_all];
                    s(y_,x_,:) = lambda_n_T*inv_L_tilde_s_tilde_a_n;
                end
            end

            %% Calculate cross-correlation between maps
            sn_ccorr = zeros(num_eNodeBs,num_eNodeBs);
            for i_=1:num_eNodeBs
                for j_=i_:num_eNodeBs
                    correlation = corr2(s(:,:,i_),s(:,:,j_));
                    sn_ccorr(i_,j_) = correlation;
                    sn_ccorr(j_,i_) = correlation;
                end
            end
```

Code for small-scale fading generation

For each carrier:

```
    % Initial config (simulator-linked)
    config.system_bandwidth           = LTE_config.bandwidth;
```

```
    config.channel_type                   = LTE_config.channel_model.type;
    config.nTX                            = LTE_config.nTX;
    config.nRX                            = LTE_config.nRX;
    config.trace_length_s                 =
LTE_config.channel_model.trace_length;
    config.UE_speed                       = LTE_config.UE_speed; % converted to
m/s
    config.parallel_toolbox_installed =
LTE_config.parallel_toolbox_installed; % change it to false for testing
purposes, as if not you will not be able to debug properly
    config.feedback_channel_delay     = LTE_config.feedback_channel_delay;
    config.correlated_fading              =
LTE_config.channel_model.correlated_fading;
    config.f                              = LTE_config.frequency;
    config.trace_params                   = LTE_config.trace_params;
    config.TTI_length                     = LTE_config.TTI_length;
    config.tx_mode                        = LTE_config.tx_mode;
    config.non_parallel_channel_trace =
LTE_config.non_parallel_channel_trace;
end

% sigma_n2 = 10^((LTE_config.UE.receiver_noise_figure +
LTE_config.UE.thermal_noise_density)/10)/1000;    % Receiver noise variance
in Watt

% We now have all of the possible precoding combinations stored
precoding_configs = phy_modeling.miscUtils.get_all_precoding_combinations;

% Channel trace for the target and interfering channels
switch config.channel_type
    case 'winner+'
        channel_factory_H0 =
channel_gain_wrappers.winnerChannelFactory(config.system_bandwidth,config.tra
ce_params,LTE_config.winner_antenna_params);
        channel_factory_H1 =
channel_gain_wrappers.winnerChannelFactory(config.system_bandwidth,config.tra
ce_params,LTE_config.winner_antenna_params);
    otherwise
        channel_factory_H0 =
channel_gain_wrappers.pdpChannelFactory(config.system_bandwidth,config.trace_
params);
        channel_factory_H1 =
channel_gain_wrappers.pdpChannelFactory(config.system_bandwidth,config.trace_
params);
end
if LTE_config.debug_level>=1
    fprintf('Generating %dx%d channel trace of length
%3.2fs\n',config.nTX,config.nRX,ceil(config.trace_length_s));
end
H_trace0 =
channel_factory_H0.generate_FF_trace(config.trace_length_s/config.TTI_length)
;

% Interfering channel trace
if LTE_config.debug_level>=1
```

```
    fprintf('Generating %dx%d interfering channel trace of length
%3.2fs\n',config.nTX,config.nRX,ceil(config.trace_length_s));
end
H_trace1 =
channel_factory_H1.generate_FF_trace(config.trace_length_s/config.TTI_length)
;

% Commented from LL vs SL
%H_trace0 =
LTE_init_generate_FF_tracev2_LLvsSL(config.system_bandwidth,config.channel_ty
pe,config.nTX,config.nRX,config.trace_length_s,config.UE_speed,'UEchannel');
%H_trace1 =
LTE_init_generate_FF_tracev2_LLvsSL(config.system_bandwidth,config.channel_ty
pe,config.nTX,config.nRX,config.trace_length_s,config.UE_speed,'interferers')
;

%% Channel normalization

% Note: each MIMO channel is normalized to a mean power of one
H_trace_normalized        = H_trace0.H_RB_samples;
H_trace_interf_normalized = H_trace1.H_RB_samples;

% Free up memory
clear H_trace0;
clear H_trace1;

switch LTE_config.trace_version
    case 'v1'
        % v1 trace
        pregenerated_fast_fading =
phy_modeling.channelTraceFactory_v1.generate_channel_trace(config,precoding_c
onfigs,H_trace_normalized,H_trace_interf_normalized);
    otherwise
        % v2 trace
        pregenerated_fast_fading =
phy_modeling.channelTraceFactory_v2.generate_channel_trace(config,precoding_c
onfigs,H_trace_normalized,H_trace_interf_normalized);
end
```

Code for SINR Calculation

For each carrier:

```
%% Preallocate for the SINR matrices
num_eNodeBs = length(eNodeBs);

% Look for the eNodeB closer to the center (0,0) and store the eNodeBs'
% pixel position (for plotting purposes)
closest_distance = 10000;
center = [mean(networkPathlossMap.roi_x) mean(networkPathlossMap.roi_y)];
target_eNodeB = 1;
eNodeB_pixel_pos = zeros(num_eNodeBs,2);
```

```
RX_powers_W = zeros(size(networkPathlossMap.pathloss));
for b_ = 1:num_eNodeBs
    eNodeB_pixel_pos(b_,:) =
LTE_common_pos_to_pixel(eNodeBs(b_).pos,networkPathlossMap.coordinate_origin,
networkPathlossMap.data_res);
    distance = norm(center-eNodeBs(b_).pos);
    if distance<closest_distance
        closest_distance = distance;
        target_eNodeB = eNodeBs(b_).sectors(1).eNodeB_id;
    end

    % Matrix containing the received power
    if shadow_fading_used
        shadow_fading_new_map_size    = [size(networkPathlossMap.pathloss,1)
size(networkPathlossMap.pathloss,2)];
        if
strcmp(class(networkShadowFadingMap),'channel_gain_wrappers.shadowFadingDummy
Map')
            shadow_fading_current_eNodeB =
10.^(imresize(0,shadow_fading_new_map_size)/10);
        else
            shadow_fading_current_eNodeB =
10.^(imresize(networkShadowFadingMap.pathloss(:,:,b_),shadow_fading_new_map_s
ize)/10);
        end
    else
        shadow_fading_current_eNodeB = 1;
    end
    for s_ = 1:length(eNodeBs(b_).sectors)
        s_idx = eNodeBs(b_).sectors(s_).eNodeB_id;
        RX_powers_W(:,:,s_idx) =
eNodeBs(b_).sectors(s_).max_power./10.^(networkPathlossMap.pathloss(:,:,s_idx
)/10) ./ shadow_fading_current_eNodeB;
    end
end

%% Calculate SINR map for all sectors
SINR_linear_all = zeros(size(RX_powers_W));
SNR_linear_all  = zeros(size(RX_powers_W));
thermal_noise_W = 10^(LTE_config.UE.thermal_noise_density/10) / 1000 *
LTE_config.bandwidth * 10^(LTE_config.UE.receiver_noise_figure/10);

tot_eNodeBs = size(RX_powers_W,3);
for s_=1:tot_eNodeBs
    SNR_linear_all(:,:,s_)  = RX_powers_W(:,:,s_) ./ (thermal_noise_W);
    SINR_linear_all(:,:,s_) = RX_powers_W(:,:,s_) ./ (sum(RX_powers_W,3) +
thermal_noise_W - RX_powers_W(:,:,s_));
end
SNR_dB_all  = 10*log10(SNR_linear_all);
SINR_dB_all = 10*log10(SINR_linear_all);

% Calculate the matrix needed to show the SINR difference map
[SNR_dB_all_sorted   SNR_IX] = sort(SNR_dB_all,3);
[SINR_dB_all_sorted SINR_IX] = sort(SINR_dB_all,3);
```

```
max_SINR_dB_all  = SINR_dB_all_sorted(:,:,end);
SINR_assignment  = SINR_IX(:,:,end);
diff_SINR_dB_all = SINR_dB_all_sorted(:,:,end)-SINR_dB_all_sorted(:,:,end-1);
max_SNR_dB_all   = SNR_dB_all_sorted(:,:,end);

% Calculate sector sizes
cell_sizes = zeros(1,length(eNodeBs_sectors));
cell_centers_pixel = zeros(length(eNodeBs_sectors),2);
for s_idx = 1:length(eNodeBs_sectors)
    cell_sizes(s_idx) = sum(SINR_assignment(:)==s_idx);
    [row,col] = find(SINR_assignment==s_idx);
    cell_centers_pixel(s_idx,:) = [mean(col) mean(row)];
end

cell_centers =
LTE_common_pixel_to_pos(cell_centers_pixel,networkPathlossMap.coordinate_orig
in,networkPathlossMap.data_res);

target_eNodeB_area  = (SINR_assignment==target_eNodeB);

SINR_dB_ROI  = max_SINR_dB_all(:);
SINR_lin_ROI = 10.^(SINR_dB_ROI/10);
```

Code for Calculating Average Capacity

For each carrier

```
bandwidth        = LTE_config.N_RB*LTE_config.RB_bandwidth;
CP_length_s      = LTE_config.CP_length_samples/LTE_config.fs;
symbol_length_s = LTE_config.TTI_length/(LTE_config.N_sym*2);
CP_ratio         = 1-(CP_length_s/symbol_length_s);

nTXantennas         = 1;
subcarriers_per_RB = 12;
switch nTXantennas
    case 1
        nRef_sym = 4;
    case 2
        nRef_sym = 8;
    case 4
        nRef_sym = 12;
end
subframe_size_Sym = LTE_config.N_sym*subcarriers_per_RB*2*LTE_config.N_RB;
% 2 for 2 slots (2x0.5 ms)

RefSym_ratio  = 1-(nRef_sym /
(LTE_config.N_sym*subcarriers_per_RB*nTXantennas)); % Ratio of
reference_symbols/total_subframe_symbols
SyncSym_ratio = 1-(72 / (subframe_size_Sym*5)); % 72 symbols used for sync
every 5 subframes
```

```
% Integrate over all of the ROI (sum). Apply correction factors for used
bandwidth, Cyclic Prefix and reference/sync symbols.
sector_capacity_vec     =
bandwidth*CP_ratio*RefSym_ratio*SyncSym_ratio*log2(1+SINR_lin_ROI);

sector_avg_capacity_mbps = mean(sector_capacity_vec) / 1e6;
sector_min_capacity_mbps = min(sector_capacity_vec) / 1e6;
sector_max_capacity_mbps = max(sector_capacity_vec) / 1e6;

sector_capacity.avg_mbps = sector_avg_capacity_mbps;
sector_capacity.min_mbps = sector_min_capacity_mbps;
sector_capacity.max_mbps = sector_max_capacity_mbps;

% Plot throughtput mapping and related ECDSs
% if LTE_config.show_network > 0
% Load SNR-to-throughput mapping
throughput_mapper =
utils.throughputMapper(LTE_config.SNR_to_throughput_mapping);
% if ~shadow_fading_used
    figure_handle  = LTE_config.plots.sector_spectral_densities;
    figure_handle2 = LTE_config.plots.sector_spectral_densities2;
% else
%     figure_handle  = LTE_config.plots.sector_spectral_densities_shadow;
%     figure_handle2 = LTE_config.plots.sector_spectral_densities2_shadow;
% end
throughput_mapper.plot_with_cell_layout(max_SINR_dB_all,shadow_fading_used,ne
tworkPathlossMap,figure_handle,figure_handle2);
```

Code for Initialization

```
%% Other UE initialization, including adding a downlink and uplink channel
object to each user
% The downlink will contain pathloss maps, so depending on the user's
position, it will 'see' a certain pathloss.
% Add also the penetration loss and noise figure.
% The uplink is simply a delay between the UE and the eNodeB.
for u_=1:length(UEs)

    % Add penetration loss
    UEs(u_).penetration_loss = LTE_config.additional_penetration_loss;

    % Add receiver antenna gain
    UEs(u_).antenna_gain = LTE_config.UE.antenna_gain;

    % Add noise figure
    UEs(u_).receiver_noise_figure = LTE_config.UE.receiver_noise_figure;

    % Thermal noise (receiver) for the link quality model (in linear: watts)
    UEs(u_).thermal_noise_W_RB =
10^(0.1*LTE_config.UE.thermal_noise_density)/1000 * LTE_config.RB_bandwidth *
10^(UEs(u_).receiver_noise_figure/10);
```

```
    % Default tx mode for feedback (for the old trace format -v1- this
    % sets the only tx mode that can be used)
    UEs(u_).default_tx_mode = LTE_config.tx_mode;

    % LTE precoding codebook for all TX modes
    UEs(u_).codebook = phy_modeling.miscUtils.get_all_precoding_combinations;

    % Set signaling channel (eNodeB to UE)
    UEs(u_).eNodeB_signaling = network_elements.eNodebSignaling;

    % Number of RX antennas
    UEs(u_).nRX = LTE_config.nRX;

    % Set BLER curves for ACK/NACK calculation
    UEs(u_).BLER_curves = BLER_curves;

    % Clock
    UEs(u_).clock = networkClock;

    % CQI mapper
    UEs(u_).CQI_mapper = CQI_mapper;

    % Configure unquantized feedback
    UEs(u_).unquantized_CQI_feedback = LTE_config.unquantized_CQI_feedback;

    % Configure extra tracing
    UEs(u_).trace_SINR = LTE_config.trace_SINR;

    % Adaptive RI
    UEs(u_).adaptive_RI = LTE_config.adaptive_RI;
end
```

Code for Scheduling Algorithm

```
% Add RB grid representation and scheduler to each sector.
% Set also homogeneous power load
for b_ = 1:length(eNodeBs)
    for s_=1:length(eNodeBs(b_).sectors)

        % Set whether the eNodeBs will always transmit, even if no UEs are
attached.
        eNodeBs(b_).sectors(s_).always_on = LTE_config.always_on;
        max_data_power  = eNodeBs(b_).sectors(s_).max_power;
        signaling_power = eNodeBs(b_).sectors(s_).signaling_power;
        LTE_config.scheduler_params.max_power       = max_data_power; % For
backwards compatibility
        LTE_config.scheduler_params.CQI_params      = LTE_config.CQI_params;
        LTE_config.scheduler_params.default_tx_mode = LTE_config.tx_mode;

        % RB grid creation and initialization (in the constructor)
```

```
        eNodeBs(b_).sectors(s_).RB_grid =
network_elements.resourceBlockGrid(LTE_config.N_RB,LTE_config.sym_per_RB_nosy
nc,LTE_config.sym_per_RB_sync);

eNodeBs(b_).sectors(s_).RB_grid.set_homogeneous_power_allocation(eNodeBs(b_).
sectors(s_).max_power,eNodeBs(b_).sectors(s_).signaling_power);

        % Continue with Scheduler initialization
        eNodeBs(b_).sectors(s_).scheduler =
schedulers.schedulerFactory.create_scheduler(LTE_config.scheduler,LTE_config.
scheduler_params,eNodeBs(b_).sectors(s_));

        % Set scheduler SINR averaging algorithm

eNodeBs(b_).sectors(s_).scheduler.set_SINR_averager(the_SINR_averager);

        % Other data required to perform SINR averaging at the transmitter
side
        eNodeBs(b_).sectors(s_).scheduler.set_CQI_mapper(CQI_mapper);
        eNodeBs(b_).sectors(s_).scheduler.set_BLER_curves(BLER_curves);

        % Add genie information
        eNodeBs(b_).sectors(s_).scheduler.set_genie_UEs(UEs);
        eNodeBs(b_).sectors(s_).scheduler.set_genie_eNodeBs(eNodeBs);

        % Add TTI delay information

eNodeBs(b_).sectors(s_).scheduler.set_feedback_delay_TTIs(LTE_config.feedback
_channel_delay);
    end
end

classdef propFairSunScheduler < schedulers.lteScheduler
% A proportional fair LTE scheduler
% (c) Stefan Schwarz, INTHFT, 2010

   properties
       % See the lteScheduler class for a list of inherited attributes
       av_throughput % exponentially weighted throughputs
   end

   methods

       % Class constructor. Just specify where to attach the scheduler
       function obj =
propFairSunScheduler(scheduler_params,attached_eNodeB_sector)
           % Fill in basic parameters (handled by the superclass constructor)
           obj      =
obj@schedulers.lteScheduler(scheduler_params,attached_eNodeB_sector);
           obj.name = 'Proportional fair Sun scheduler';
       end

       % Dummy functions required by the lteScheduler Abstract class
implementation
```

```
        % Add UE (no memory, so empty)
        function add_UE(obj,UE_id)
        end
        % Delete UE (no memory, so empty)
        function remove_UE(obj,UE_id)
        end

        % Schedule the users in the given RB grid
        function schedule_users(obj,attached_UEs,last_received_feedbacks)
            % Power allocation
            % Nothing here. Leave the default one (homogeneous)

            RB_grid = obj.RB_grid;
            RB_grid.size_bits = 0;

            % For now use the static tx_mode assignment
            RB_grid.size_bits = 0;
            tx_mode      = obj.default_tx_mode;
            current_TTI = obj.clock.current_TTI;
            N_UE         = length(attached_UEs);
            N_RB         = RB_grid.n_RB;
            UE_id_list   = zeros(N_RB,1);

            if ~isempty(attached_UEs)
                 %% compute efficiency
                 [c,user_ind] =
obj.get_efficiency(N_UE,N_RB,last_received_feedbacks);
                 c = c';

                %% update average throughput
                TTI_to_read = max(current_TTI-obj.feedback_delay_TTIs-1,1); %
Realistically read the ACKed throughput
                for uu = 1:N_UE
                     obj.av_throughput(uu) =
obj.compute_av_throughput(uu,last_received_feedbacks,TTI_to_read);
                end

                %% PF scheduler
                RBs = obj.PF_scheduler(N_UE,N_RB,c,user_ind);

                for r_ = 1:N_RB
                    RB_tmp = RBs((r_-1)*N_UE+1:r_*N_UE);
                    ind = find(RB_tmp == 1);
                   if ~isempty(ind)
                     UE_id_list(r_) = attached_UEs(user_ind(ind)).id;
                   end
                end
                RB_grid.user_allocation(:) = UE_id_list;
                % CQI assignment. TODO: implement HARQ

obj.schedule_users_common(attached_UEs,last_received_feedbacks,current_TTI,tx
_mode);
            end
        end
```

```
        function RBs = PF_scheduler(obj,N_UE,N_RB,c,user_ind)
            % Core scheduling function (same in LL and SL)
            RB_set      = true(N_RB,1);
            RB_UEs      = false(N_RB,N_UE);
            alpha_temp = 1;
            % res         = find(RB_set);      % The RB set over which you will
schedule (right now the same as the RB_set. Specified in linear indices. Not
used in the newer implementation

            % Precalculated values taken out from the loop (speeds up
simulations)
            cleaned_c_log_matrix = log10(max(c,eps)*12*7);
            avgd_UE_throughputs  = (obj.av_const-
1)*obj.av_throughput(user_ind);

            % Calculate metric for each RB and attached user
            for rr = 1:N_RB
                res                        = find(RB_set);
                metric                     = -Inf(N_RB,N_UE);
                UE_avgd_pre_metric         = -
alpha_temp*log10(max(avgd_UE_throughputs+sum(RB_UEs.*c,1)*12*7,eps));
                UE_avgd_pre_metric_mat = UE_avgd_pre_metric(ones(1,N_RB),:);

                metric(res(1:sum(RB_set)),:) =
cleaned_c_log_matrix(res(1:sum(RB_set)),:)+UE_avgd_pre_metric_mat(res(1:sum(R
B_set)),:);
                % for u_ = 1:N_UE
                % for r_ = 1:N_RB
                % metric(res(r_),u_) = c(res(r_),u_)*12*7/((obj.av_const-
1)*obj.av_throughput(user_ind(u_))+RB_UEs(:,u_).'*c(:,u_)*12*7);      % 12*7
equals the number of elements in a RB
                % metric(res(r_),u_) = log10(max(c(res(r_),u_),eps)*12*7)-
alpha_temp*log10(max((obj.av_const-
1)*obj.av_throughput(user_ind(u_))+RB_UEs(:,u_).'*c(:,u_)*12*7,eps)); % Old
implementation
                % metric(res(r_),u_) = log10(max(c(res(r_),u_)*12*7,eps))-
alpha_temp*log10(max(obj.av_throughput(user_ind(u_)),eps));
                % end
                % end
                maxi             = max(metric(:));
                [RB_idx UE_idx] = find(metric == maxi);
                ind              = randi(length(RB_idx));

                RB_set(RB_idx(ind))               = false;
                RB_UEs(RB_idx(ind),UE_idx(ind)) = true;
            end
            RB_UEs = RB_UEs';
            RBs = RB_UEs(:);
        end
    end
end
```

Appendix B: Result for inter-band cases with additional guardband

Adjacent Channel Interference Ratio (ACIR) is the ratio of the total power transmitted from a source (base station or UE) to the total interference power affecting a victim receiver. It is represented by the following formula:

$$ACIR = \frac{1}{\left(\frac{1}{ACLR} + \frac{1}{ACS}\right)}$$

This formula shows that ACIR which the victim receiver experiences from an interferer transmitter is the sum of:

a. Adjacent Channel Leakage Ratio (ACLR): the power that interferer emits into victim's channel known as the "unwanted emission"

b. Adjacent Channel Selectivity (ACS): the power that victim picks up from interferer's channel

ACIR occurs because RF selectivity filters require a roll-off, and do not eliminate the signal completely. Therefore, the interferer emits some power in the adjacent channel which is picked up by the victim's receiver. In the downlink interference, $ACS_{UE} \ll ACLR_{eNB}$, so: $ACIR_{DL} \approx ACS_{UE}$. This makes the UE receiver is the major design factor. In the uplink interference, the UE transmitter is the major design factor because $ACIR_{UL} \approx ACLR_{UE}$.

Technical review for guardband setting including adjacent channel interference, adjacent channel leakage ration, adjacent channel selectivity, power mask and out of band emission are provided in 3GPP technical reports: [180] [71] [37] [101] [181] [91] [182] [75] & [72].

Based on discussion in Section 3.3.4 of Chapter II and assumptions in Table 7 about extra guard band that might be required for smaller block to minimize ACI, we show below a result for the second scenario that we introduced in that section.

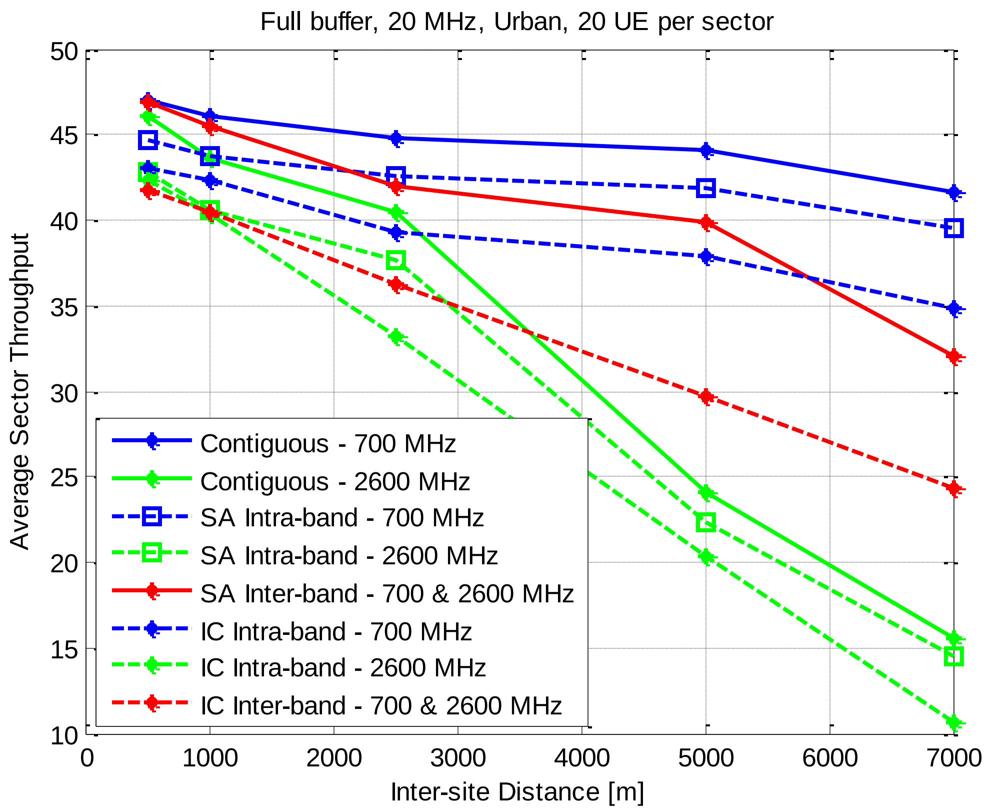

Figure 73: Changes when extra guard band applied

Compared to Figure 33 in Chapter II, applying extra guardband on systems that utilizes two 10 MHz blocks reduces the average sector throughput by 5-10%. This applies for both all SA and IC systems. This reduction due to allocating more bandwidth to guard band was discussed in Chapter V. We called it cost of fragmentation. It can be seen the intra-band SA systems are no longer provide the same capacity as the contiguous systems since they have slightly less spectrum to utilize.

Appendix C: Results for rural environment

In Chapter II, we only plotted figures with urban environment. Because in Chapter IV analysis other types of environments are assumed, we run simulation for rural environment. We didn't report them earlier to avoid plotting too many figures in the main body.

Figure 78 which show cell ranges in rural areas, has a similar trend to the one shown in Figure 22. The only difference is that in rural areas it has almost 4 times the distance in urban areas.

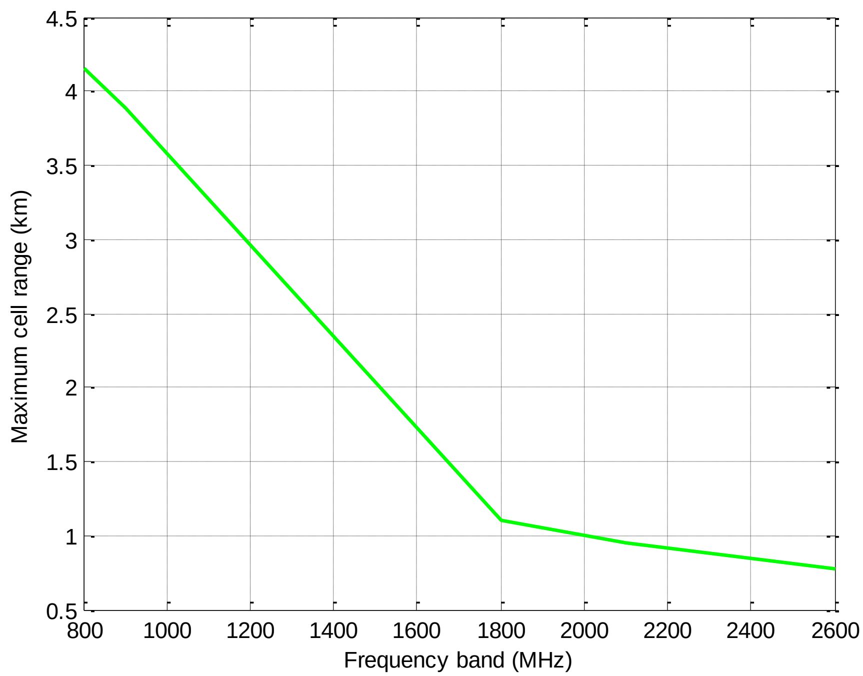

Figure 74: Cell ranges based on Okumura-Hata and COST 231-Hata propagation models in rural environment

Figure 79 is similar to Figure 23 which shows the coverage probability in urban regions. In this figure, high-frequency carriers have coverage probability at lower inter-site distances.

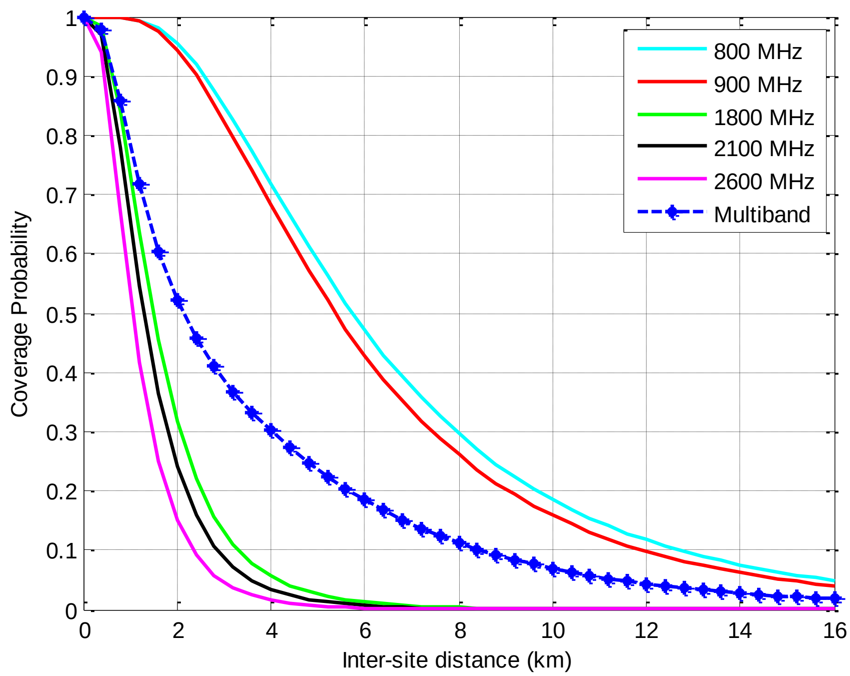

Figure 75: Coverage probability for a user at the cell-edge as frequency band and inter-site distance change in rural environment

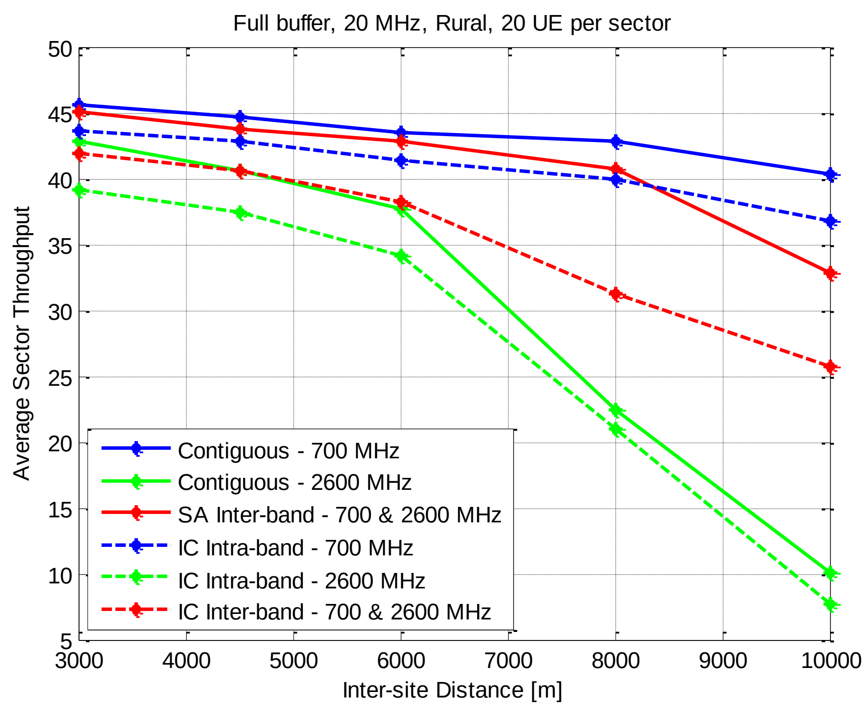

Figure 76: Average system throughput as inter-site distance changes

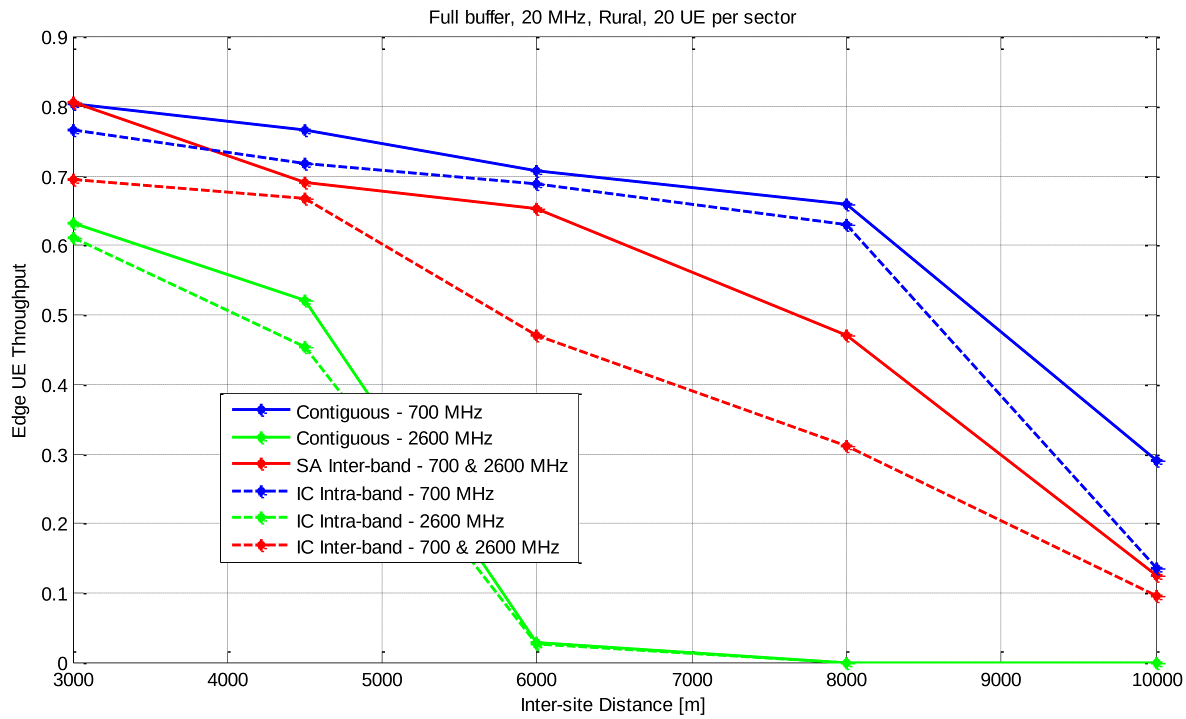

Figure 77: Throughput for UE at the cell edge

Figures 80 and 81, above, resemble Figures 31 and 33 we plotted in Chapter II. The throughput is larger in low-frequency bands as they have higher cell range in rural areas than in urban ones.

Appendix D: Plotted Curves from Simulation Runs

In Chapter IV, we run the LTE simulator many times at different inter-site distances until we find the maximum distance that maintain the performance requirement. Figure, below, is an example that shows three curves for three scenarios which maintain 2 Mbps of average UE throughput as inter-site distance and user density changes. in each curve, there are five points each represent type of region (i.e. from super dense to rural. Although in rural areas the cell range is larger, still the user density is lower than cells in super dense areas. Similar figure can be plotted for other scenarios with other requirements.

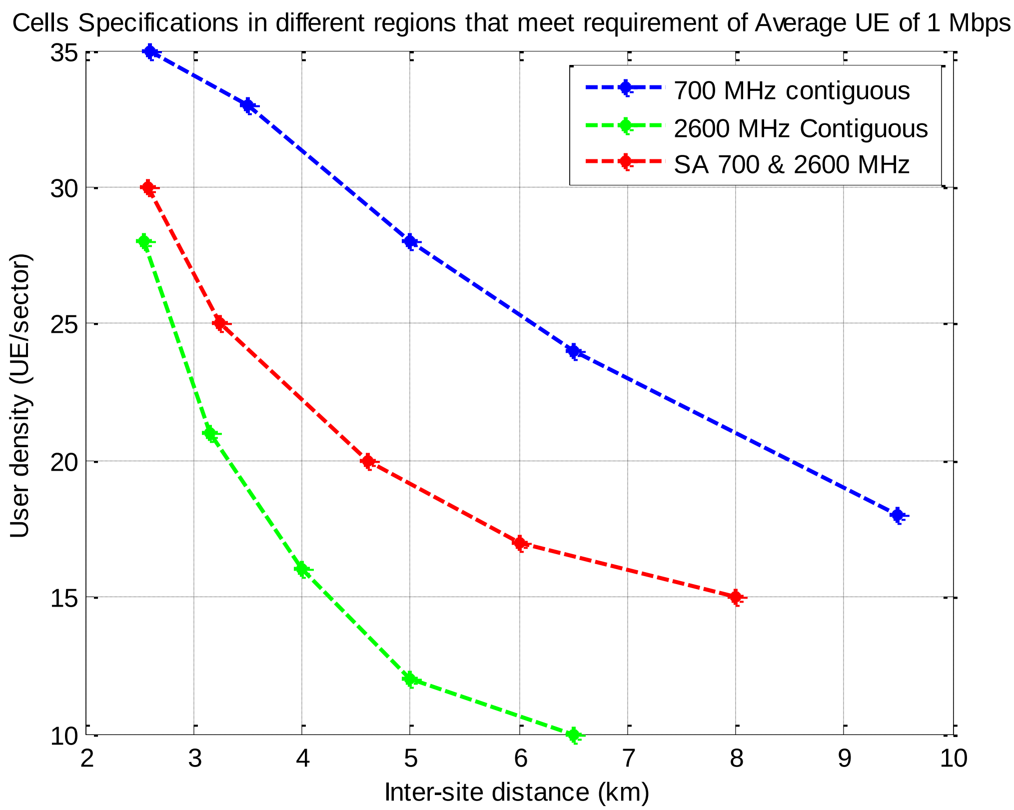

Figure 78: inter-site distances and users densities for five types of regions

Appendix E: Data for LTE Radio Equipment

As we mentioned in Chapter III, different websites do tear-down cost analysis for LTE devices. For example, teardown.com tears down all components of iPhone 6 as shown in the picture below.

Figure 79: Tear-down of all components (source: teardown.com)

Then, they look up their databases about all parts, to identify each component and its cost. Finally, they list all components costs and the total cost of the device as shown in the second picture below.

As we explained in Section 3 of Chapter III, we are interested in the baseband and RF parts. So, we collected the data shown in table blow based on these teardown methods done by those websites.

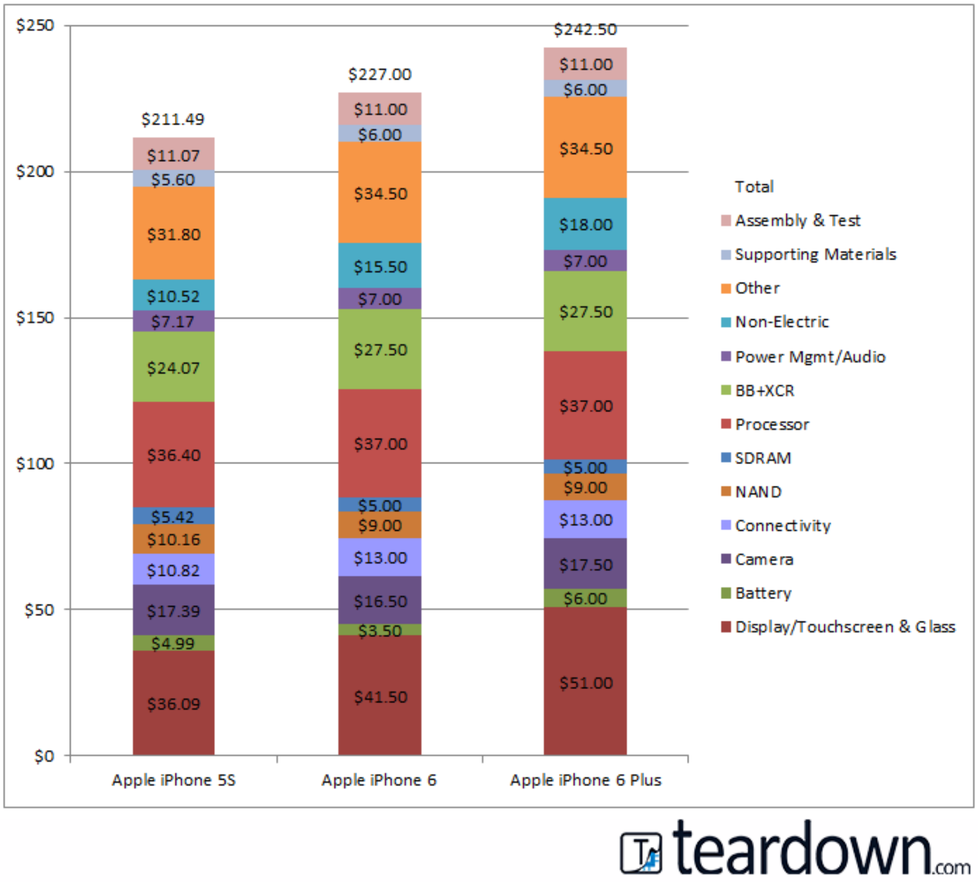

Figure 80: Cost of each component in the device (source: teardown.com)

Table 26:Collected costs data for LTE equipment

Device	Baseband	RF Front End	RF Transceiver	Device Total Cost
iPhone 4	$11.72	$8.25	$2.33	$187.5
iPhone 4S	$17.20	$2.00	$4.25	$188
HTC ThunderBolt	$29.00	$2.00	$4.00	$262
iPhone 5S	$16.75	$3.32	$4.00	$211.49
Samsung Galaxy S4	$34.00	$3.5	$4.00	$229.00
iPhone 6	$19.5	$4.5	$18.00	$227.00
Amazon Fire	$25.00	$5.00	$18.00	$209.00
Samsung S5 LTE-A	$40.51	$10.00	$13.19	$219.00

Appendix F: Data for Spectrum Auctions

In the tables below are auction data collected mainly by DotEcon. Some recent auction results were added from different websites.

Australia

Date	Number of available lots	License duration in years	Frequency Band	Headline price in local currency	MHz	Population of licensed area
22/03/2001	58	15	2GHz	8,750,000	5	12,400,000
22/03/2001	58	15	2GHz	9,450,000	5	12,400,000
22/03/2001	58	15	2GHz	2,652,000	5	4,297,000
22/03/2001	58	15	2GHz	2,122,000	5	3,246,700
22/03/2001	58	15	2GHz	1,273,000	5	1,921,100
22/03/2001	58	15	2GHz	636,000	5	1,094,900
22/03/2001	58	15	2GHz	742,700	5	1,189,100
22/03/2001	58	15	2GHz	212,200	5	224,300
22/03/2001	58	15	2GHz	106,100	5	90,000
22/03/2001	58	15	2GHz	212,200	5	320,600
22/03/2001	58	15	2GHz	2,775,000	5	4,297,000
22/03/2001	58	15	2GHz	2,220,000	5	3,246,700
22/03/2001	58	15	2GHz	1,332,000	5	1,921,100
22/03/2001	58	15	2GHz	666,000	5	1,094,900
22/03/2001	58	15	2GHz	777,000	5	1,189,100
22/03/2001	58	15	2GHz	53,000,000	20	4,297,000
22/03/2001	58	15	2GHz	42,400,000	20	3,246,700
22/03/2001	58	15	2GHz	25,400,000	20	1,921,100
22/03/2001	58	15	2GHz	12,700,000	20	1,094,900
22/03/2001	58	15	2GHz	14,800,000	20	1,189,100
22/03/2001	58	15	2GHz	26,500,000	10	4,297,000
22/03/2001	58	15	2GHz	21,200,000	10	3,246,700
22/03/2001	58	15	2GHz	79,500,000	10	12,400,000
22/03/2001	58	15	2GHz	159,000,000	20	12,400,000
22/03/2001	58	15	2GHz	241,000,000	20	16,200,000
22/03/2001	58	15	2GHz	79,500,000	10	12,400,000
22/03/2001	58	15	2GHz	79,500,000	10	12,400,000
22/03/2001	58	15	2GHz	245,000,000	20	16,200,000
22/03/2001	58	15	2GHz	2,220,000	10	368,200
22/03/2001	58	15	2GHz	2,220,000	10	305,100
22/03/2001	58	15	2GHz	3,330,000	10	583,500
22/03/2001	58	15	2GHz	2,220,000	10	39,500
22/03/2001	58	15	2GHz	2,220,000	10	281,100
22/03/2001	58	15	2GHz	4,440,000	10	641,200
22/03/2001	58	15	2GHz	5,550,000	10	773,200
22/03/2001	58	15	2GHz	2,220,000	10	258,200
22/03/2001	58	15	2GHz	2,220,000	10	308,600
22/03/2001	58	15	2GHz	1,110,000	10	241,800

22/03/2001	58	15	2GHz	2,120,000	10	368,200
22/03/2001	58	15	2GHz	2,120,000	10	305,100
22/03/2001	58	15	2GHz	3,180,000	10	583,500
22/03/2001	58	15	2GHz	2,324,000	10	39,500
22/03/2001	58	15	2GHz	2,324,000	10	281,100
22/03/2001	58	15	2GHz	4,644,000	10	641,200
22/03/2001	58	15	2GHz	5,804,000	10	773,200
22/03/2001	58	15	2GHz	2,120,000	10	258,200
22/03/2001	58	15	2GHz	2,120,000	10	308,600
22/03/2001	58	15	2GHz	1,060,000	10	241,800

Brazil

Date	Number of available lots	License duration in years	Frequency Band	Headline price in local currency	MHz	Population of licensed area
20/12/2007	36	15	2GHz	310,000,000	20	0
20/12/2007	36	15	2GHz	468,000,000	30	0
20/12/2007	36	15	2GHz	528,000,000	20	0
20/12/2007	36	15	2GHz	612,000,000	20	0
20/12/2007	36	15	2GHz	528,000,000	20	0
20/12/2007	36	15	2GHz	483,000,000	30	0
20/12/2007	36	15	2GHz	370,000,000	20	0
20/12/2007	36	15	2GHz	382,000,000	20	0
20/12/2007	36	15	2GHz	169,000,000	40	0
20/12/2007	36	15	2GHz	225,000,000	60	0
20/12/2007	36	15	2GHz	178,000,000	40	0
20/12/2007	36	15	2GHz	188,000,000	40	0
20/12/2007	36	15	2GHz	130,000,000	40	0
20/12/2007	36	15	2GHz	175,000,000	60	0
20/12/2007	36	15	2GHz	137,000,000	40	0
20/12/2007	36	15	2GHz	144,000,000	40	0
20/12/2007	36	15	2GHz	15,200,000	20	0
20/12/2007	36	15	2GHz	28,700,000	30	0
20/12/2007	36	15	2GHz	22,500,000	20	0
20/12/2007	36	15	2GHz	24,400,000	20	0
20/12/2007	36	15	2GHz	292,000	20	0
20/12/2007	36	15	2GHz	603,100	30	0
20/12/2007	36	15	2GHz	1,000,000	20	0
20/12/2007	36	15	2GHz	431,790	20	0
20/12/2007	36	15	2GHz	5,766,000	20	0
20/12/2007	36	15	2GHz	7,615,000	30	0
20/12/2007	36	15	2GHz	8,484,191	20	0
20/12/2007	36	15	2GHz	6,200,460	20	0
20/12/2007	36	15	2GHz	38,300,000	20	0
20/12/2007	36	15	2GHz	50,600,000	30	0
20/12/2007	36	15	2GHz	40,600,000	20	0
20/12/2007	36	15	2GHz	42,800,000	20	0

20/12/2007	36	15	2GHz	3,953,000	20	0
20/12/2007	36	15	2GHz	5,235,040	30	0
20/12/2007	36	15	2GHz	4,177,347	20	0
20/12/2007	36	15	2GHz	4,402,000	20	0

Canada

Date	Number of available lots	License duration in years	Frequency Band	Headline price in local currency	MHz	Population of licensed area
27/05/2008	292	10	2.1GHz	6,380,000	20	513,282
27/05/2008	292	10	2.1GHz	2,550,000	20	135,294
27/05/2008	292	10	2.1GHz	15,200,000	20	760,894
27/05/2008	292	10	2.1GHz	3,620,000	20	147,044
27/05/2008	292	10	2.1GHz	2,710,000	20	167,343
27/05/2008	292	10	2.1GHz	3,210,000	20	209,227
27/05/2008	292	10	2.1GHz	4,810,000	20	352,427
27/05/2008	292	10	2.1GHz	2,280,000	20	298,273
27/05/2008	292	10	2.1GHz	34,800,000	20	917,873
27/05/2008	292	10	2.1GHz	4,580,000	20	374,590
27/05/2008	292	10	2.1GHz	9,400,000	20	509,717
27/05/2008	292	10	2.1GHz	21,300,000	20	749,812
27/05/2008	292	10	2.1GHz	192,000,000	20	3,784,570
27/05/2008	292	10	2.1GHz	1,170,000	20	107,125
27/05/2008	292	10	2.1GHz	46,500,000	20	1,265,237
27/05/2008	292	10	2.1GHz	1,590,000	20	108,154
27/05/2008	292	10	2.1GHz	2,190,000	20	187,081
27/05/2008	292	10	2.1GHz	1,570,000	20	65,921
27/05/2008	292	10	2.1GHz	1,730,000	20	82,869
27/05/2008	292	10	2.1GHz	2,650,000	20	162,711
27/05/2008	292	10	2.1GHz	2,990,000	20	184,594
27/05/2008	292	10	2.1GHz	1,840,000	20	59,699
27/05/2008	292	10	2.1GHz	2,760,000	20	192,992
27/05/2008	292	10	2.1GHz	1,150,000	20	72,322
27/05/2008	292	10	2.1GHz	235,000,000	20	5,635,827
27/05/2008	292	10	2.1GHz	9,990,000	20	591,338
27/05/2008	292	10	2.1GHz	7,500,000	20	607,035
27/05/2008	292	10	2.1GHz	1,740,000	20	133,987
27/05/2008	292	10	2.1GHz	9,440,000	20	354,971
27/05/2008	292	10	2.1GHz	21,100,000	20	765,656
27/05/2008	292	10	2.1GHz	1,130,000	20	107,029
27/05/2008	292	10	2.1GHz	4,370,000	20	376,213
27/05/2008	292	10	2.1GHz	2,090,000	20	166,739
27/05/2008	292	10	2.1GHz	1,080,000	20	122,253
27/05/2008	292	10	2.1GHz	2,030,000	20	135,482
27/05/2008	292	10	2.1GHz	3,220,000	20	172,605
27/05/2008	292	10	2.1GHz	1,770,000	20	120,308
27/05/2008	292	10	2.1GHz	2,690,000	20	234,833

27/05/2008	292	10	2.1GHz	34,900,000	20	945,818
27/05/2008	292	10	2.1GHz	1,790,000	20	172,465
27/05/2008	292	10	2.1GHz	17,100,000	20	349,538
27/05/2008	292	10	2.1GHz	4,440,000	20	104,297
27/05/2008	292	10	2.1GHz	31,500,000	20	521,882
27/05/2008	292	10	2.1GHz	35,400,000	20	1,199,124
27/05/2008	292	10	2.1GHz	1,470,000	20	175,718
27/05/2008	292	10	2.1GHz	1,920,000	20	156,171
27/05/2008	292	10	2.1GHz	54,100,000	20	1,091,673
27/05/2008	292	10	2.1GHz	2,220,000	20	198,479
27/05/2008	292	10	2.1GHz	3,620,000	20	158,271
27/05/2008	292	10	2.1GHz	1,340,000	20	132,914
27/05/2008	292	10	2.1GHz	5,160,000	20	368,647
27/05/2008	292	10	2.1GHz	117,000,000	20	2,310,047
27/05/2008	292	10	2.1GHz	5,670,000	20	389,247
27/05/2008	292	10	2.1GHz	2,010,000	20	165,741
27/05/2008	292	10	2.1GHz	1,080,000	20	106,015
27/05/2008	292	10	2.1GHz	2,160,000	20	174,289
27/05/2008	292	10	2.1GHz	2,140,000	20	200,007
27/05/2008	292	10	2.1GHz	1,350,000	20	60,717
27/05/2008	292	10	2.1GHz	767,000	20	92,707
27/05/2008	292	10	2.1GHz	760,000	20	513,282
27/05/2008	292	10	2.1GHz	3,040,000	20	1,043,232
27/05/2008	292	10	2.1GHz	1,480,000	20	728,997
27/05/2008	292	10	2.1GHz	7,100,000	20	1,590,736
27/05/2008	292	10	2.1GHz	168,000,000	20	5,151,224
27/05/2008	292	10	2.1GHz	51,900,000	20	2,122,177
27/05/2008	292	10	2.1GHz	176,000	20	187,081
27/05/2008	292	10	2.1GHz	279,000,000	20	8,811,117
27/05/2008	292	10	2.1GHz	2,730,000	20	785,481
27/05/2008	292	10	2.1GHz	39,000,000	20	1,118,283
27/05/2008	292	10	2.1GHz	40,400,000	20	975,717
27/05/2008	292	10	2.1GHz	32,700,000	20	2,979,436
27/05/2008	292	10	2.1GHz	101,000,000	20	3,907,624
27/05/2008	292	10	2.1GHz	184,000	20	92,707
27/05/2008	292	10	2.1GHz	440,000	10	513,282
27/05/2008	292	10	2.1GHz	1,670,000	10	1,043,232
27/05/2008	292	10	2.1GHz	1,720,000	10	728,997
27/05/2008	292	10	2.1GHz	3,100,000	10	1,590,736
27/05/2008	292	10	2.1GHz	112,000,000	10	5,151,224
27/05/2008	292	10	2.1GHz	30,400,000	10	2,122,177
27/05/2008	292	10	2.1GHz	356,000	10	187,081
27/05/2008	292	10	2.1GHz	131,000,000	10	8,811,117
27/05/2008	292	10	2.1GHz	1,500,000	10	785,481
27/05/2008	292	10	2.1GHz	13,800,000	10	1,118,283
27/05/2008	292	10	2.1GHz	24,200,000	10	975,717
27/05/2008	292	10	2.1GHz	18,100,000	10	2,979,436
27/05/2008	292	10	2.1GHz	67,400,000	10	3,907,624
27/05/2008	292	10	2.1GHz	104,000	10	92,707
27/05/2008	292	10	2.1GHz	380,000	10	513,282

27/05/2008	292	10	2.1GHz	291,000	10	135,294
27/05/2008	292	10	2.1GHz	947,000	10	760,894
27/05/2008	292	10	2.1GHz	289,000	10	147,044
27/05/2008	292	10	2.1GHz	599,000	10	167,343
27/05/2008	292	10	2.1GHz	609,000	10	209,227
27/05/2008	292	10	2.1GHz	976,000	10	352,427
27/05/2008	292	10	2.1GHz	987,000	10	298,273
27/05/2008	292	10	2.1GHz	2,480,000	10	917,873
27/05/2008	292	10	2.1GHz	552,000	10	374,590
27/05/2008	292	10	2.1GHz	3,590,000	10	509,717
27/05/2008	292	10	2.1GHz	5,250,000	10	749,812
27/05/2008	292	10	2.1GHz	96,600,000	10	3,784,570
27/05/2008	292	10	2.1GHz	512,000	10	107,125
27/05/2008	292	10	2.1GHz	27,100,000	10	1,265,237
27/05/2008	292	10	2.1GHz	1,330,000	10	108,154
27/05/2008	292	10	2.1GHz	356,000	10	187,081
27/05/2008	292	10	2.1GHz	1,470,000	10	65,921
27/05/2008	292	10	2.1GHz	1,560,000	10	82,869
27/05/2008	292	10	2.1GHz	1,090,000	10	162,711
27/05/2008	292	10	2.1GHz	1,020,000	10	184,594
27/05/2008	292	10	2.1GHz	1,410,000	10	59,699
27/05/2008	292	10	2.1GHz	905,000	10	192,992
27/05/2008	292	10	2.1GHz	503,000	10	72,322
27/05/2008	292	10	2.1GHz	96,400,000	10	5,635,827
27/05/2008	292	10	2.1GHz	2,640,000	10	591,338
27/05/2008	292	10	2.1GHz	2,600,000	10	607,035
27/05/2008	292	10	2.1GHz	882,000	10	133,987
27/05/2008	292	10	2.1GHz	1,380,000	10	354,971
27/05/2008	292	10	2.1GHz	4,360,000	10	765,656
27/05/2008	292	10	2.1GHz	932,000	10	107,029
27/05/2008	292	10	2.1GHz	1,580,000	10	376,213
27/05/2008	292	10	2.1GHz	739,000	10	166,739
27/05/2008	292	10	2.1GHz	544,000	10	122,253
27/05/2008	292	10	2.1GHz	436,000	10	135,482
27/05/2008	292	10	2.1GHz	805,000	10	172,605
27/05/2008	292	10	2.1GHz	514,000	10	120,308
27/05/2008	292	10	2.1GHz	802,000	10	234,833
27/05/2008	292	10	2.1GHz	13,500,000	10	945,818
27/05/2008	292	10	2.1GHz	773,000	10	172,465
27/05/2008	292	10	2.1GHz	4,970,000	10	349,538
27/05/2008	292	10	2.1GHz	2,430,000	10	104,297
27/05/2008	292	10	2.1GHz	12,700,000	10	521,882
27/05/2008	292	10	2.1GHz	8,990,000	10	1,199,124
27/05/2008	292	10	2.1GHz	571,000	10	175,718
27/05/2008	292	10	2.1GHz	473,000	10	156,171
27/05/2008	292	10	2.1GHz	8,390,000	10	1,091,673
27/05/2008	292	10	2.1GHz	669,000	10	198,479
27/05/2008	292	10	2.1GHz	239,000	10	158,271
27/05/2008	292	10	2.1GHz	262,000	10	132,914
27/05/2008	292	10	2.1GHz	756,000	10	368,647

27/05/2008	292	10	2.1GHz	56,400,000	10	2,310,047
27/05/2008	292	10	2.1GHz	1,750,000	10	389,247
27/05/2008	292	10	2.1GHz	559,000	10	165,741
27/05/2008	292	10	2.1GHz	209,000	10	106,015
27/05/2008	292	10	2.1GHz	589,000	10	174,289
27/05/2008	292	10	2.1GHz	562,000	10	200,007
27/05/2008	292	10	2.1GHz	236,000	10	60,717
27/05/2008	292	10	2.1GHz	101,000	10	92,707
27/05/2008	292	10	2.1GHz	3,340,000	10	513,282
27/05/2008	292	10	2.1GHz	1,870,000	10	135,294
27/05/2008	292	10	2.1GHz	7,240,000	10	760,894
27/05/2008	292	10	2.1GHz	1,970,000	10	147,044
27/05/2008	292	10	2.1GHz	2,300,000	10	167,343
27/05/2008	292	10	2.1GHz	2,730,000	10	209,227
27/05/2008	292	10	2.1GHz	4,090,000	10	352,427
27/05/2008	292	10	2.1GHz	1,560,000	10	298,273
27/05/2008	292	10	2.1GHz	14,500,000	10	917,873
27/05/2008	292	10	2.1GHz	1,960,000	10	374,590
27/05/2008	292	10	2.1GHz	5,190,000	10	509,717
27/05/2008	292	10	2.1GHz	9,570,000	10	749,812
27/05/2008	292	10	2.1GHz	128,000,000	10	3,784,570
27/05/2008	292	10	2.1GHz	679,000	10	107,125
27/05/2008	292	10	2.1GHz	33,200,000	10	1,265,237
27/05/2008	292	10	2.1GHz	1,670,000	10	108,154
27/05/2008	292	10	2.1GHz	1,270,000	10	187,081
27/05/2008	292	10	2.1GHz	1,780,000	10	65,921
27/05/2008	292	10	2.1GHz	1,660,000	10	82,869
27/05/2008	292	10	2.1GHz	1,710,000	10	162,711
27/05/2008	292	10	2.1GHz	1,790,000	10	184,594
27/05/2008	292	10	2.1GHz	1,500,000	10	59,699
27/05/2008	292	10	2.1GHz	1,120,000	10	192,992
27/05/2008	292	10	2.1GHz	692,000	10	72,322
27/05/2008	292	10	2.1GHz	103,000,000	10	5,635,827
27/05/2008	292	10	2.1GHz	4,970,000	10	591,338
27/05/2008	292	10	2.1GHz	5,110,000	10	607,035
27/05/2008	292	10	2.1GHz	1,230,000	10	133,987
27/05/2008	292	10	2.1GHz	2,840,000	10	354,971
27/05/2008	292	10	2.1GHz	4,920,000	10	765,656
27/05/2008	292	10	2.1GHz	848,000	10	107,029
27/05/2008	292	10	2.1GHz	3,250,000	10	376,213
27/05/2008	292	10	2.1GHz	1,720,000	10	166,739
27/05/2008	292	10	2.1GHz	688,000	10	122,253
27/05/2008	292	10	2.1GHz	1,390,000	10	135,482
27/05/2008	292	10	2.1GHz	2,050,000	10	172,605
27/05/2008	292	10	2.1GHz	988,000	10	120,308
27/05/2008	292	10	2.1GHz	2,420,000	10	234,833
27/05/2008	292	10	2.1GHz	15,100,000	10	945,818
27/05/2008	292	10	2.1GHz	1,600,000	10	172,465
27/05/2008	292	10	2.1GHz	5,760,000	10	349,538
27/05/2008	292	10	2.1GHz	2,690,000	10	104,297

27/05/2008	292	10	2.1GHz	12,000,000	10	521,882
27/05/2008	292	10	2.1GHz	19,200,000	10	1,199,124
27/05/2008	292	10	2.1GHz	866,000	10	175,718
27/05/2008	292	10	2.1GHz	869,000	10	156,171
27/05/2008	292	10	2.1GHz	16,700,000	10	1,091,673
27/05/2008	292	10	2.1GHz	1,020,000	10	198,479
27/05/2008	292	10	2.1GHz	2,120,000	10	158,271
27/05/2008	292	10	2.1GHz	798,000	10	132,914
27/05/2008	292	10	2.1GHz	2,010,000	10	368,647
27/05/2008	292	10	2.1GHz	62,100,000	10	2,310,047
27/05/2008	292	10	2.1GHz	2,800,000	10	389,247
27/05/2008	292	10	2.1GHz	998,000	10	165,741
27/05/2008	292	10	2.1GHz	662,000	10	106,015
27/05/2008	292	10	2.1GHz	992,000	10	174,289
27/05/2008	292	10	2.1GHz	1,020,000	10	200,007
27/05/2008	292	10	2.1GHz	652,000	10	60,717
27/05/2008	292	10	2.1GHz	291,000	10	92,707
27/05/2008	292	10	2.1GHz	6,380,000	20	513,282
27/05/2008	292	10	2.1GHz	2,630,000	20	135,294
27/05/2008	292	10	2.1GHz	15,300,000	20	760,894
27/05/2008	292	10	2.1GHz	3,880,000	20	147,044
27/05/2008	292	10	2.1GHz	3,060,000	20	167,343
27/05/2008	292	10	2.1GHz	3,580,000	20	209,227
27/05/2008	292	10	2.1GHz	5,120,000	20	352,427
27/05/2008	292	10	2.1GHz	2,480,000	20	298,273
27/05/2008	292	10	2.1GHz	34,900,000	20	917,873
27/05/2008	292	10	2.1GHz	4,450,000	20	374,590
27/05/2008	292	10	2.1GHz	10,500,000	20	509,717
27/05/2008	292	10	2.1GHz	21,900,000	20	749,812
27/05/2008	292	10	2.1GHz	234,000,000	20	3,784,570
27/05/2008	292	10	2.1GHz	1,200,000	20	107,125
27/05/2008	292	10	2.1GHz	44,600,000	20	1,265,237
27/05/2008	292	10	2.1GHz	1,720,000	20	108,154
27/05/2008	292	10	2.1GHz	2,100,000	20	187,081
27/05/2008	292	10	2.1GHz	1,530,000	20	65,921
27/05/2008	292	10	2.1GHz	1,760,000	20	82,869
27/05/2008	292	10	2.1GHz	2,530,000	20	162,711
27/05/2008	292	10	2.1GHz	2,840,000	20	184,594
27/05/2008	292	10	2.1GHz	1,720,000	20	59,699
27/05/2008	292	10	2.1GHz	2,690,000	20	192,992
27/05/2008	292	10	2.1GHz	1,490,000	20	72,322
27/05/2008	292	10	2.1GHz	314,000,000	20	5,635,827
27/05/2008	292	10	2.1GHz	14,800,000	20	591,338
27/05/2008	292	10	2.1GHz	15,200,000	20	607,035
27/05/2008	292	10	2.1GHz	3,360,000	20	133,987
27/05/2008	292	10	2.1GHz	9,560,000	20	354,971
27/05/2008	292	10	2.1GHz	21,200,000	20	765,656
27/05/2008	292	10	2.1GHz	2,240,000	20	107,029
27/05/2008	292	10	2.1GHz	5,770,000	20	376,213
27/05/2008	292	10	2.1GHz	3,470,000	20	166,739

27/05/2008	292	10	2.1GHz	1,020,000	20	122,253
27/05/2008	292	10	2.1GHz	2,140,000	20	135,482
27/05/2008	292	10	2.1GHz	3,350,000	20	172,605
27/05/2008	292	10	2.1GHz	1,770,000	20	120,308
27/05/2008	292	10	2.1GHz	3,090,000	20	234,833
27/05/2008	292	10	2.1GHz	34,900,000	20	945,818
27/05/2008	292	10	2.1GHz	1,930,000	20	172,465
27/05/2008	292	10	2.1GHz	18,200,000	20	349,538
27/05/2008	292	10	2.1GHz	4,430,000	20	104,297
27/05/2008	292	10	2.1GHz	31,500,000	20	521,882
27/05/2008	292	10	2.1GHz	36,700,000	20	1,199,124
27/05/2008	292	10	2.1GHz	1,670,000	20	175,718
27/05/2008	292	10	2.1GHz	1,920,000	20	156,171
27/05/2008	292	10	2.1GHz	57,400,000	20	1,091,673
27/05/2008	292	10	2.1GHz	2,480,000	20	198,479
27/05/2008	292	10	2.1GHz	3,580,000	20	158,271
27/05/2008	292	10	2.1GHz	1,350,000	20	132,914
27/05/2008	292	10	2.1GHz	5,160,000	20	368,647
27/05/2008	292	10	2.1GHz	117,000,000	20	2,310,047
27/05/2008	292	10	2.1GHz	6,060,000	20	389,247
27/05/2008	292	10	2.1GHz	2,200,000	20	165,741
27/05/2008	292	10	2.1GHz	1,160,000	20	106,015
27/05/2008	292	10	2.1GHz	2,250,000	20	174,289
27/05/2008	292	10	2.1GHz	2,010,000	20	200,007
27/05/2008	292	10	2.1GHz	1,270,000	20	60,717
27/05/2008	292	10	2.1GHz	864,000	20	92,707

United States

Date	Number of available lots	License duration in years	Frequency Band	Headline price in local currency	MHz	Population of licensed area
18/09/2006	1122	15	2.1GHz	437,000	20	526,106
18/09/2006	1122	15	2.1GHz	316,000	10	526,106
18/09/2006	1122	15	2.1GHz	3,513,000	20	748,817
18/09/2006	1122	15	2.1GHz	2,229,000	10	748,817
18/09/2006	1122	15	2.1GHz	76,800,000	20	7,954,554
18/09/2006	1122	15	2.1GHz	30,500,000	10	7,954,554
18/09/2006	1122	15	2.1GHz	1,533,000	20	605,393
18/09/2006	1122	15	2.1GHz	1,070,000	10	605,393
18/09/2006	1122	15	2.1GHz	2,915,000	20	1,171,669
18/09/2006	1122	15	2.1GHz	2,962,000	10	1,171,669
18/09/2006	1122	15	2.1GHz	5,812,000	20	1,902,640
18/09/2006	1122	15	2.1GHz	5,618,000	10	1,902,640
18/09/2006	1122	15	2.1GHz	5,803,000	20	1,493,518
18/09/2006	1122	15	2.1GHz	3,706,000	10	1,493,518
18/09/2006	1122	15	2.1GHz	1,693,000	20	1,507,759
18/09/2006	1122	15	2.1GHz	1,206,000	10	1,507,759

18/09/2006	1122	15	2.1GHz	4,997,000	20	809,979
18/09/2006	1122	15	2.1GHz	1,282,000	10	809,979
18/09/2006	1122	15	2.1GHz	468,000,000	20	25,700,000
18/09/2006	1122	15	2.1GHz	364,000,000	10	25,700,000
18/09/2006	1122	15	2.1GHz	2,373,000	20	1,125,265
18/09/2006	1122	15	2.1GHz	1,935,000	10	1,125,265
18/09/2006	1122	15	2.1GHz	77,800,000	20	7,309,792
18/09/2006	1122	15	2.1GHz	56,100,000	10	7,309,792
18/09/2006	1122	15	2.1GHz	149,000,000	20	8,403,130
18/09/2006	1122	15	2.1GHz	76,100,000	10	8,403,130
18/09/2006	1122	15	2.1GHz	246,000	20	363,970
18/09/2006	1122	15	2.1GHz	109,000	10	363,970
18/09/2006	1122	15	2.1GHz	8,842,000	20	1,446,123
18/09/2006	1122	15	2.1GHz	4,213,000	10	1,446,123
18/09/2006	1122	15	2.1GHz	200,000	20	334,087
18/09/2006	1122	15	2.1GHz	113,000	10	334,087
18/09/2006	1122	15	2.1GHz	1,221,000	20	826,284
18/09/2006	1122	15	2.1GHz	951,000	10	826,284
18/09/2006	1122	15	2.1GHz	14,000,000	20	1,854,853
18/09/2006	1122	15	2.1GHz	9,638,000	10	1,854,853
18/09/2006	1122	15	2.1GHz	10,500,000	20	1,831,510
18/09/2006	1122	15	2.1GHz	7,463,000	10	1,831,510
18/09/2006	1122	15	2.1GHz	28,600,000	20	1,722,764
18/09/2006	1122	15	2.1GHz	7,025,000	10	1,722,764
18/09/2006	1122	15	2.1GHz	706,000	20	823,517
18/09/2006	1122	15	2.1GHz	422,000	10	823,517
18/09/2006	1122	15	2.1GHz	438,000	20	528,224
18/09/2006	1122	15	2.1GHz	293,000	10	528,224
18/09/2006	1122	15	2.1GHz	13,700,000	20	2,031,519
18/09/2006	1122	15	2.1GHz	8,318,000	10	2,031,519
18/09/2006	1122	15	2.1GHz	5,034,000	20	932,115
18/09/2006	1122	15	2.1GHz	2,402,000	10	932,115
18/09/2006	1122	15	2.1GHz	7,658,000	20	878,267
18/09/2006	1122	15	2.1GHz	1,362,000	10	878,267
18/09/2006	1122	15	2.1GHz	3,067,000	20	587,297
18/09/2006	1122	15	2.1GHz	1,796,000	10	587,297
18/09/2006	1122	15	2.1GHz	656,000	20	604,799
18/09/2006	1122	15	2.1GHz	475,000	10	604,799
18/09/2006	1122	15	2.1GHz	1,502,000	20	668,214
18/09/2006	1122	15	2.1GHz	1,500,000	10	668,214
18/09/2006	1122	15	2.1GHz	13,600,000	20	1,885,190
18/09/2006	1122	15	2.1GHz	5,565,000	10	1,885,190
18/09/2006	1122	15	2.1GHz	27,200,000	20	3,642,540
18/09/2006	1122	15	2.1GHz	16,100,000	10	3,642,540
18/09/2006	1122	15	2.1GHz	61,100,000	20	5,602,222
18/09/2006	1122	15	2.1GHz	21,300,000	10	5,602,222
18/09/2006	1122	15	2.1GHz	1,765,000	20	692,265
18/09/2006	1122	15	2.1GHz	1,109,000	10	692,265
18/09/2006	1122	15	2.1GHz	2,194,000	20	763,795
18/09/2006	1122	15	2.1GHz	1,807,000	10	763,795

18/09/2006	1122	15	2.1GHz	28,500,000	20	2,395,997
18/09/2006	1122	15	2.1GHz	25,900,000	10	2,395,997
18/09/2006	1122	15	2.1GHz	1,781,000	20	720,434
18/09/2006	1122	15	2.1GHz	1,435,000	10	720,434
18/09/2006	1122	15	2.1GHz	605,000	20	332,409
18/09/2006	1122	15	2.1GHz	316,000	10	332,409
18/09/2006	1122	15	2.1GHz	855,000	20	468,178
18/09/2006	1122	15	2.1GHz	581,000	10	468,178
18/09/2006	1122	15	2.1GHz	1,752,000	20	768,701
18/09/2006	1122	15	2.1GHz	1,008,000	10	768,701
18/09/2006	1122	15	2.1GHz	1,140,000	20	496,538
18/09/2006	1122	15	2.1GHz	1,175,000	10	496,538
18/09/2006	1122	15	2.1GHz	35,300,000	20	5,471,412
18/09/2006	1122	15	2.1GHz	22,700,000	10	5,471,412
18/09/2006	1122	15	2.1GHz	5,247,000	20	1,248,824
18/09/2006	1122	15	2.1GHz	2,285,000	10	1,248,824
18/09/2006	1122	15	2.1GHz	3,366,000	20	444,594
18/09/2006	1122	15	2.1GHz	942,000	10	444,594
18/09/2006	1122	15	2.1GHz	1,289,000	20	720,375
18/09/2006	1122	15	2.1GHz	1,191,000	10	720,375
18/09/2006	1122	15	2.1GHz	4,595,000	20	983,329
18/09/2006	1122	15	2.1GHz	2,606,000	10	983,329
18/09/2006	1122	15	2.1GHz	4,361,000	20	576,081
18/09/2006	1122	15	2.1GHz	1,363,000	10	576,081
18/09/2006	1122	15	2.1GHz	1,085,000	20	519,208
18/09/2006	1122	15	2.1GHz	601,000	10	519,208
18/09/2006	1122	15	2.1GHz	9,214,000	20	1,851,367
18/09/2006	1122	15	2.1GHz	5,075,000	10	1,851,367
18/09/2006	1122	15	2.1GHz	3,370,000	20	1,199,373
18/09/2006	1122	15	2.1GHz	1,723,000	10	1,199,373
18/09/2006	1122	15	2.1GHz	21,900,000	20	2,184,860
18/09/2006	1122	15	2.1GHz	6,833,000	10	2,184,860
18/09/2006	1122	15	2.1GHz	6,644,000	20	1,133,004
18/09/2006	1122	15	2.1GHz	5,430,000	10	1,133,004
18/09/2006	1122	15	2.1GHz	12,400,000	20	2,349,060
18/09/2006	1122	15	2.1GHz	7,945,000	10	2,349,060
18/09/2006	1122	15	2.1GHz	311,000	20	327,645
18/09/2006	1122	15	2.1GHz	208,000	10	327,645
18/09/2006	1122	15	2.1GHz	14,800,000	20	2,971,829
18/09/2006	1122	15	2.1GHz	8,173,000	10	2,971,829
18/09/2006	1122	15	2.1GHz	520,000	20	519,348
18/09/2006	1122	15	2.1GHz	212,000	10	519,348
18/09/2006	1122	15	2.1GHz	16,000,000	20	4,692,460
18/09/2006	1122	15	2.1GHz	10,200,000	10	4,692,460
18/09/2006	1122	15	2.1GHz	1,663,000	20	1,294,395
18/09/2006	1122	15	2.1GHz	1,929,000	10	1,294,395
18/09/2006	1122	15	2.1GHz	79,000,000	20	6,963,637
18/09/2006	1122	15	2.1GHz	50,300,000	10	6,963,637
18/09/2006	1122	15	2.1GHz	162,000	20	269,986
18/09/2006	1122	15	2.1GHz	85,000	10	269,986

18/09/2006	1122	15	2.1GHz	1,217,000	20	671,225
18/09/2006	1122	15	2.1GHz	984,000	10	671,225
18/09/2006	1122	15	2.1GHz	929,000	20	433,250
18/09/2006	1122	15	2.1GHz	683,000	10	433,250
18/09/2006	1122	15	2.1GHz	195,000	20	286,745
18/09/2006	1122	15	2.1GHz	86,000	10	286,745
18/09/2006	1122	15	2.1GHz	9,348,000	20	1,881,991
18/09/2006	1122	15	2.1GHz	7,920,000	10	1,881,991
18/09/2006	1122	15	2.1GHz	22,400,000	20	2,255,183
18/09/2006	1122	15	2.1GHz	15,800,000	10	2,255,183
18/09/2006	1122	15	2.1GHz	228,000,000	20	10,300,000
18/09/2006	1122	15	2.1GHz	162,000,000	10	10,300,000
18/09/2006	1122	15	2.1GHz	930,000	20	936,245
18/09/2006	1122	15	2.1GHz	455,000	10	936,245
18/09/2006	1122	15	2.1GHz	1,308,000	20	725,847
18/09/2006	1122	15	2.1GHz	327,000	10	725,847
18/09/2006	1122	15	2.1GHz	12,700,000	20	3,066,469
18/09/2006	1122	15	2.1GHz	10,400,000	10	3,066,469
18/09/2006	1122	15	2.1GHz	650,000	20	630,898
18/09/2006	1122	15	2.1GHz	289,000	10	630,898
18/09/2006	1122	15	2.1GHz	1,048,000	20	854,714
18/09/2006	1122	15	2.1GHz	659,000	10	854,714
18/09/2006	1122	15	2.1GHz	12,300,000	20	1,416,914
18/09/2006	1122	15	2.1GHz	5,112,000	10	1,416,914
18/09/2006	1122	15	2.1GHz	11,900,000	20	2,444,643
18/09/2006	1122	15	2.1GHz	8,952,000	10	2,444,643
18/09/2006	1122	15	2.1GHz	206,000	20	226,586
18/09/2006	1122	15	2.1GHz	76,000	10	226,586
18/09/2006	1122	15	2.1GHz	18,900,000	20	1,882,332
18/09/2006	1122	15	2.1GHz	16,500,000	10	1,882,332
18/09/2006	1122	15	2.1GHz	3,320,000	20	997,824
18/09/2006	1122	15	2.1GHz	2,554,000	10	997,824
18/09/2006	1122	15	2.1GHz	610,000	20	625,002
18/09/2006	1122	15	2.1GHz	321,000	10	625,002
18/09/2006	1122	15	2.1GHz	297,000	20	252,280
18/09/2006	1122	15	2.1GHz	113,000	10	252,280
18/09/2006	1122	15	2.1GHz	4,212,000	20	1,432,518
18/09/2006	1122	15	2.1GHz	3,258,000	10	1,432,518
18/09/2006	1122	15	2.1GHz	10,800,000	20	1,578,903
18/09/2006	1122	15	2.1GHz	7,207,000	10	1,578,903
18/09/2006	1122	15	2.1GHz	1,029,000	20	481,137
18/09/2006	1122	15	2.1GHz	782,000	10	481,137
18/09/2006	1122	15	2.1GHz	8,646,000	20	676,258
18/09/2006	1122	15	2.1GHz	5,531,000	10	676,258
18/09/2006	1122	15	2.1GHz	3,561,000	20	623,252
18/09/2006	1122	15	2.1GHz	1,460,000	10	623,252
18/09/2006	1122	15	2.1GHz	3,264,000	20	396,754
18/09/2006	1122	15	2.1GHz	443,000	10	396,754
18/09/2006	1122	15	2.1GHz	6,854,000	20	1,725,338
18/09/2006	1122	15	2.1GHz	3,210,000	10	1,725,338

18/09/2006	1122	15	2.1GHz	2,554,000	20	739,673
18/09/2006	1122	15	2.1GHz	2,032,000	10	739,673
18/09/2006	1122	15	2.1GHz	1,710,000	20	601,654
18/09/2006	1122	15	2.1GHz	647,000	10	601,654
18/09/2006	1122	15	2.1GHz	3,594,000	20	536,758
18/09/2006	1122	15	2.1GHz	1,320,000	10	536,758
18/09/2006	1122	15	2.1GHz	496,000	20	456,637
18/09/2006	1122	15	2.1GHz	595,000	10	456,637
18/09/2006	1122	15	2.1GHz	2,875,000	20	573,616
18/09/2006	1122	15	2.1GHz	622,000	10	573,616
18/09/2006	1122	15	2.1GHz	1,293,000	20	333,519
18/09/2006	1122	15	2.1GHz	147,000	10	333,519
18/09/2006	1122	15	2.1GHz	4,066,000	20	1,614,850
18/09/2006	1122	15	2.1GHz	3,069,000	10	1,614,850
18/09/2006	1122	15	2.1GHz	369,000	20	329,136
18/09/2006	1122	15	2.1GHz	356,000	10	329,136
18/09/2006	1122	15	2.1GHz	1,361,000	20	405,160
18/09/2006	1122	15	2.1GHz	580,000	10	405,160
18/09/2006	1122	15	2.1GHz	315,000	20	263,904
18/09/2006	1122	15	2.1GHz	147,000	10	263,904
18/09/2006	1122	15	2.1GHz	1,129,000	20	859,559
18/09/2006	1122	15	2.1GHz	604,000	10	859,559
18/09/2006	1122	15	2.1GHz	191,000	20	303,852
18/09/2006	1122	15	2.1GHz	197,000	10	303,852
18/09/2006	1122	15	2.1GHz	31,300,000	20	3,558,651
18/09/2006	1122	15	2.1GHz	11,200,000	10	3,558,651
18/09/2006	1122	15	2.1GHz	705,000	20	517,462
18/09/2006	1122	15	2.1GHz	300,000	10	517,462
18/09/2006	1122	15	2.1GHz	432,000	20	369,014
18/09/2006	1122	15	2.1GHz	184,000	10	369,014
18/09/2006	1122	15	2.1GHz	23,800,000	20	2,469,340
18/09/2006	1122	15	2.1GHz	10,900,000	10	2,469,340
18/09/2006	1122	15	2.1GHz	9,657,000	20	1,683,257
18/09/2006	1122	15	2.1GHz	5,754,000	10	1,683,257
18/09/2006	1122	15	2.1GHz	515,000	20	528,671
18/09/2006	1122	15	2.1GHz	228,000	10	528,671
18/09/2006	1122	15	2.1GHz	1,394,000	20	558,913
18/09/2006	1122	15	2.1GHz	1,193,000	10	558,913
18/09/2006	1122	15	2.1GHz	1,495,000	20	384,577
18/09/2006	1122	15	2.1GHz	1,359,000	10	384,577
18/09/2006	1122	15	2.1GHz	1,388,000	20	933,823
18/09/2006	1122	15	2.1GHz	486,000	10	933,823
18/09/2006	1122	15	2.1GHz	1,114,000	20	241,903
18/09/2006	1122	15	2.1GHz	207,000	10	241,903
18/09/2006	1122	15	2.1GHz	308,000	20	318,374
18/09/2006	1122	15	2.1GHz	414,000	10	318,374
18/09/2006	1122	15	2.1GHz	41,800,000	20	4,498,286
18/09/2006	1122	15	2.1GHz	30,000,000	10	4,498,286
18/09/2006	1122	15	2.1GHz	2,289,000	10	487,723
18/09/2006	1122	15	2.1GHz	1,293,000	20	350,059

18/09/2006	1122	15	2.1GHz	566,000	10	350,059
18/09/2006	1122	15	2.1GHz	369,000	20	230,253
18/09/2006	1122	15	2.1GHz	89,000	10	230,253
18/09/2006	1122	15	2.1GHz	173,000	20	111,195
18/09/2006	1122	15	2.1GHz	36,000	10	111,195
18/09/2006	1122	15	2.1GHz	535,000	20	175,427
18/09/2006	1122	15	2.1GHz	128,000	10	175,427
18/09/2006	1122	15	2.1GHz	522,000	20	371,691
18/09/2006	1122	15	2.1GHz	146,000	10	371,691
18/09/2006	1122	15	2.1GHz	373,000	20	82,608
18/09/2006	1122	15	2.1GHz	447,000	20	213,696
18/09/2006	1122	15	2.1GHz	137,000	10	213,696
18/09/2006	1122	15	2.1GHz	940,000	20	519,143
18/09/2006	1122	15	2.1GHz	404,000	10	519,143
18/09/2006	1122	15	2.1GHz	703,000	20	252,656
18/09/2006	1122	15	2.1GHz	652,000	10	252,656
18/09/2006	1122	15	2.1GHz	6,735,000	20	1,044,156
18/09/2006	1122	15	2.1GHz	1,737,000	10	1,044,156
18/09/2006	1122	15	2.1GHz	411,000	20	379,321
18/09/2006	1122	15	2.1GHz	185,000	10	379,321
18/09/2006	1122	15	2.1GHz	1,040,000	20	288,047
18/09/2006	1122	15	2.1GHz	86,000	10	288,047
18/09/2006	1122	15	2.1GHz	68,000	20	61,758
18/09/2006	1122	15	2.1GHz	19,000	10	61,758
18/09/2006	1122	15	2.1GHz	4,295,000	20	1,175,577
18/09/2006	1122	15	2.1GHz	2,368,000	10	1,175,577
18/09/2006	1122	15	2.1GHz	1,204,000	20	454,539
18/09/2006	1122	15	2.1GHz	485,000	10	454,539
18/09/2006	1122	15	2.1GHz	7,727,000	20	1,384,426
18/09/2006	1122	15	2.1GHz	2,248,000	10	1,384,426
18/09/2006	1122	15	2.1GHz	20,200,000	20	1,698,197
18/09/2006	1122	15	2.1GHz	10,100,000	10	1,698,197
18/09/2006	1122	15	2.1GHz	954,000	20	139,761
18/09/2006	1122	15	2.1GHz	50,000	10	139,761
18/09/2006	1122	15	2.1GHz	76,800,000	20	7,645,530
18/09/2006	1122	15	2.1GHz	49,800,000	10	7,645,530
18/09/2006	1122	15	2.1GHz	343,000	20	222,147
18/09/2006	1122	15	2.1GHz	200,000	10	222,147
18/09/2006	1122	15	2.1GHz	757,000	20	202,679
18/09/2006	1122	15	2.1GHz	431,000	10	202,679
18/09/2006	1122	15	2.1GHz	11,200,000	20	1,349,267
18/09/2006	1122	15	2.1GHz	4,789,000	10	1,349,267
18/09/2006	1122	15	2.1GHz	41,100,000	20	5,632,853
18/09/2006	1122	15	2.1GHz	18,500,000	10	5,632,853
18/09/2006	1122	15	2.1GHz	921,000	20	549,012
18/09/2006	1122	15	2.1GHz	701,000	10	549,012
18/09/2006	1122	15	2.1GHz	1,542,000	20	978,369
18/09/2006	1122	15	2.1GHz	1,174,000	10	978,369
18/09/2006	1122	15	2.1GHz	7,911,000	20	2,141,060
18/09/2006	1122	15	2.1GHz	5,654,000	10	2,141,060

18/09/2006	1122	15	2.1GHz	995,000	20	388,007
18/09/2006	1122	15	2.1GHz	781,000	10	388,007
18/09/2006	1122	15	2.1GHz	296,000	20	190,340
18/09/2006	1122	15	2.1GHz	148,000	10	190,340
18/09/2006	1122	15	2.1GHz	605,000	20	374,626
18/09/2006	1122	15	2.1GHz	441,000	10	374,626
18/09/2006	1122	15	2.1GHz	870,000	20	481,633
18/09/2006	1122	15	2.1GHz	674,000	10	481,633
18/09/2006	1122	15	2.1GHz	1,180,000	20	258,790
18/09/2006	1122	15	2.1GHz	654,000	10	258,790
18/09/2006	1122	15	2.1GHz	503,000	20	279,600
18/09/2006	1122	15	2.1GHz	184,000	10	279,600
18/09/2006	1122	15	2.1GHz	24,200,000	20	3,984,105
18/09/2006	1122	15	2.1GHz	9,878,000	10	3,984,105
18/09/2006	1122	15	2.1GHz	124,000	20	92,360
18/09/2006	1122	15	2.1GHz	28,000	10	92,360
18/09/2006	1122	15	2.1GHz	1,193,000	20	408,708
18/09/2006	1122	15	2.1GHz	355,000	10	408,708
18/09/2006	1122	15	2.1GHz	528,000	20	404,902
18/09/2006	1122	15	2.1GHz	639,000	10	404,902
18/09/2006	1122	15	2.1GHz	436,000	20	166,564
18/09/2006	1122	15	2.1GHz	349,000	10	166,564
18/09/2006	1122	15	2.1GHz	406,000	20	399,183
18/09/2006	1122	15	2.1GHz	341,000	10	399,183
18/09/2006	1122	15	2.1GHz	2,753,000	20	829,735
18/09/2006	1122	15	2.1GHz	1,863,000	10	829,735
18/09/2006	1122	15	2.1GHz	809,000	20	306,120
18/09/2006	1122	15	2.1GHz	761,000	10	306,120
18/09/2006	1122	15	2.1GHz	190,000	20	162,397
18/09/2006	1122	15	2.1GHz	95,000	10	162,397
18/09/2006	1122	15	2.1GHz	2,280,000	20	574,876
18/09/2006	1122	15	2.1GHz	626,000	10	574,876
18/09/2006	1122	15	2.1GHz	3,261,000	20	670,013
18/09/2006	1122	15	2.1GHz	993,000	10	670,013
18/09/2006	1122	15	2.1GHz	16,200,000	20	2,088,974
18/09/2006	1122	15	2.1GHz	7,312,000	10	2,088,974
18/09/2006	1122	15	2.1GHz	17,200,000	20	1,709,797
18/09/2006	1122	15	2.1GHz	10,400,000	10	1,709,797
18/09/2006	1122	15	2.1GHz	534,000	20	401,766
18/09/2006	1122	15	2.1GHz	257,000	10	401,766
18/09/2006	1122	15	2.1GHz	234,000	20	193,872
18/09/2006	1122	15	2.1GHz	88,000	10	193,872
18/09/2006	1122	15	2.1GHz	2,894,000	20	921,086
18/09/2006	1122	15	2.1GHz	1,633,000	10	921,086
18/09/2006	1122	15	2.1GHz	2,548,000	20	955,602
18/09/2006	1122	15	2.1GHz	1,721,000	10	955,602
18/09/2006	1122	15	2.1GHz	27,100,000	20	3,407,197
18/09/2006	1122	15	2.1GHz	14,000,000	10	3,407,197
18/09/2006	1122	15	2.1GHz	4,735,000	20	999,882
18/09/2006	1122	15	2.1GHz	2,082,000	10	999,882

18/09/2006	1122	15	2.1GHz	216,000,000	20	18,000,000
18/09/2006	1122	15	2.1GHz	115,000,000	10	18,000,000
18/09/2006	1122	15	2.1GHz	21,900,000	20	2,813,833
18/09/2006	1122	15	2.1GHz	15,600,000	10	2,813,833
18/09/2006	1122	15	2.1GHz	4,658,000	20	1,419,998
18/09/2006	1122	15	2.1GHz	3,194,000	10	1,419,998
18/09/2006	1122	15	2.1GHz	80,800,000	20	9,111,806
18/09/2006	1122	15	2.1GHz	30,700,000	10	9,111,806
18/09/2006	1122	15	2.1GHz	8,878,000	20	2,311,567
18/09/2006	1122	15	2.1GHz	6,614,000	10	2,311,567
18/09/2006	1122	15	2.1GHz	358,000	20	336,820
18/09/2006	1122	15	2.1GHz	255,000	10	336,820
18/09/2006	1122	15	2.1GHz	764,000	20	791,776
18/09/2006	1122	15	2.1GHz	377,000	10	791,776
18/09/2006	1122	15	2.1GHz	15,900,000	20	2,883,737
18/09/2006	1122	15	2.1GHz	11,100,000	10	2,883,737
18/09/2006	1122	15	2.1GHz	226,000	20	200,681
18/09/2006	1122	15	2.1GHz	180,000	10	200,681
18/09/2006	1122	15	2.1GHz	1,067,000	20	677,674
18/09/2006	1122	15	2.1GHz	411,000	10	677,674
18/09/2006	1122	15	2.1GHz	33,300,000	20	4,135,291
18/09/2006	1122	15	2.1GHz	15,800,000	10	4,135,291
18/09/2006	1122	15	2.1GHz	1,809,000	20	626,932
18/09/2006	1122	15	2.1GHz	1,111,000	10	626,932
18/09/2006	1122	15	2.1GHz	4,254,000	20	1,211,537
18/09/2006	1122	15	2.1GHz	2,440,000	10	1,211,537
18/09/2006	1122	15	2.1GHz	2,521,000	10	3,917,222
18/09/2006	1122	15	2.1GHz	40,000	20	0
18/09/2006	1122	15	2.1GHz	30,000	10	0
18/09/2006	1122	15	2.1GHz	396,000,000	20	16,100,000
18/09/2006	1122	15	2.1GHz	179,000,000	20	15,600,000
18/09/2006	1122	15	2.1GHz	255,000,000	20	8,091,720
18/09/2006	1122	15	2.1GHz	82,600,000	20	5,036,646
18/09/2006	1122	15	2.1GHz	65,200,000	20	4,775,452
18/09/2006	1122	15	2.1GHz	36,800,000	20	4,279,111
18/09/2006	1122	15	2.1GHz	27,000,000	20	4,123,740
18/09/2006	1122	15	2.1GHz	133,000,000	20	4,182,658
18/09/2006	1122	15	2.1GHz	50,700,000	20	5,120,721
18/09/2006	1122	15	2.1GHz	25,900,000	20	4,393,382
18/09/2006	1122	15	2.1GHz	25,100,000	20	2,518,470
18/09/2006	1122	15	2.1GHz	35,600,000	20	3,876,380
18/09/2006	1122	15	2.1GHz	10,700,000	20	2,035,968
18/09/2006	1122	15	2.1GHz	43,700,000	20	2,512,431
18/09/2006	1122	15	2.1GHz	29,100,000	20	2,836,298
18/09/2006	1122	15	2.1GHz	7,206,000	20	1,863,479
18/09/2006	1122	15	2.1GHz	30,000,000	20	3,751,674
18/09/2006	1122	15	2.1GHz	19,000,000	20	2,813,833
18/09/2006	1122	15	2.1GHz	13,000,000	20	2,405,327
18/09/2006	1122	15	2.1GHz	27,900,000	20	2,343,058
18/09/2006	1122	15	2.1GHz	17,800,000	20	1,500,741

18/09/2006	1122	15	2.1GHz	25,900,000	20	2,265,195
18/09/2006	1122	15	2.1GHz	19,500,000	20	1,553,843
18/09/2006	1122	15	2.1GHz	14,700,000	20	1,627,081
18/09/2006	1122	15	2.1GHz	1,707,000	20	1,170,111
18/09/2006	1122	15	2.1GHz	18,400,000	20	3,072,149
18/09/2006	1122	15	2.1GHz	12,000,000	20	1,682,585
18/09/2006	1122	15	2.1GHz	7,018,000	20	1,474,128
18/09/2006	1122	15	2.1GHz	6,016,000	20	1,198,637
18/09/2006	1122	15	2.1GHz	13,300,000	20	1,789,457
18/09/2006	1122	15	2.1GHz	7,369,000	20	1,394,666
18/09/2006	1122	15	2.1GHz	8,505,000	20	1,148,618
18/09/2006	1122	15	2.1GHz	6,819,000	20	1,559,975
18/09/2006	1122	15	2.1GHz	5,230,000	20	1,037,831
18/09/2006	1122	15	2.1GHz	7,722,000	20	1,640,558
18/09/2006	1122	15	2.1GHz	21,700,000	20	1,106,808
18/09/2006	1122	15	2.1GHz	4,763,000	20	968,313
18/09/2006	1122	15	2.1GHz	6,544,000	20	962,886
18/09/2006	1122	15	2.1GHz	7,659,000	20	1,374,649
18/09/2006	1122	15	2.1GHz	4,431,000	20	848,153
18/09/2006	1122	15	2.1GHz	7,523,000	20	940,795
18/09/2006	1122	15	2.1GHz	6,972,000	20	882,567
18/09/2006	1122	15	2.1GHz	26,600,000	20	1,041,276
18/09/2006	1122	15	2.1GHz	3,596,000	20	844,001
18/09/2006	1122	15	2.1GHz	14,400,000	20	1,049,422
18/09/2006	1122	15	2.1GHz	8,546,000	20	1,231,311
18/09/2006	1122	15	2.1GHz	9,112,000	20	1,085,874
18/09/2006	1122	15	2.1GHz	1,337,000	20	805,133
18/09/2006	1122	15	2.1GHz	4,133,000	20	824,008
18/09/2006	1122	15	2.1GHz	3,583,000	20	876,156
18/09/2006	1122	15	2.1GHz	9,050,000	20	1,122,750
18/09/2006	1122	15	2.1GHz	1,125,000	20	694,960
18/09/2006	1122	15	2.1GHz	2,666,000	20	650,154
18/09/2006	1122	15	2.1GHz	631,000	20	631,362
18/09/2006	1122	15	2.1GHz	1,705,000	20	750,963
18/09/2006	1122	15	2.1GHz	1,746,000	20	671,232
18/09/2006	1122	15	2.1GHz	3,103,000	20	841,604
18/09/2006	1122	15	2.1GHz	7,638,000	20	740,395
18/09/2006	1122	15	2.1GHz	5,838,000	20	865,941
18/09/2006	1122	15	2.1GHz	14,000,000	20	1,434,033
18/09/2006	1122	15	2.1GHz	9,191,000	20	1,009,496
18/09/2006	1122	15	2.1GHz	7,292,000	20	750,162
18/09/2006	1122	15	2.1GHz	1,900,000	20	608,479
18/09/2006	1122	15	2.1GHz	7,337,000	20	812,649
18/09/2006	1122	15	2.1GHz	2,058,000	20	673,884
18/09/2006	1122	15	2.1GHz	545,000	20	482,671
18/09/2006	1122	15	2.1GHz	2,954,000	20	744,164
18/09/2006	1122	15	2.1GHz	903,000	20	507,828
18/09/2006	1122	15	2.1GHz	3,783,000	20	650,501
18/09/2006	1122	15	2.1GHz	5,460,000	20	615,301
18/09/2006	1122	15	2.1GHz	7,434,000	20	969,387

18/09/2006	1122	15	2.1GHz	6,044,000	20	1,131,184
18/09/2006	1122	15	2.1GHz	3,936,000	20	753,197
18/09/2006	1122	15	2.1GHz	4,142,000	20	799,407
18/09/2006	1122	15	2.1GHz	7,337,000	20	1,159,836
18/09/2006	1122	15	2.1GHz	735,000	20	534,678
18/09/2006	1122	15	2.1GHz	2,215,000	20	843,746
18/09/2006	1122	15	2.1GHz	1,797,000	20	509,246
18/09/2006	1122	15	2.1GHz	2,449,000	20	576,993
18/09/2006	1122	15	2.1GHz	2,439,000	20	602,894
18/09/2006	1122	15	2.1GHz	1,159,000	20	679,622
18/09/2006	1122	15	2.1GHz	1,097,000	20	700,820
18/09/2006	1122	15	2.1GHz	6,816,000	20	540,258
18/09/2006	1122	15	2.1GHz	1,203,000	20	509,074
18/09/2006	1122	15	2.1GHz	1,630,000	20	480,091
18/09/2006	1122	15	2.1GHz	1,228,000	20	646,586
18/09/2006	1122	15	2.1GHz	459,000	20	406,934
18/09/2006	1122	15	2.1GHz	1,205,000	20	476,531
18/09/2006	1122	15	2.1GHz	2,984,000	20	512,351
18/09/2006	1122	15	2.1GHz	3,006,000	20	549,033
18/09/2006	1122	15	2.1GHz	2,671,000	20	2,176,135
18/09/2006	1122	15	2.1GHz	2,318,000	20	583,845
18/09/2006	1122	15	2.1GHz	8,486,000	20	1,375,765
18/09/2006	1122	15	2.1GHz	1,475,000	20	403,070
18/09/2006	1122	15	2.1GHz	4,146,000	20	536,691
18/09/2006	1122	15	2.1GHz	770,000	20	464,066
18/09/2006	1122	15	2.1GHz	1,763,000	20	661,645
18/09/2006	1122	15	2.1GHz	405,000	20	359,062
18/09/2006	1122	15	2.1GHz	473,000	20	473,043
18/09/2006	1122	15	2.1GHz	1,299,000	20	392,302
18/09/2006	1122	15	2.1GHz	541,000	20	385,090
18/09/2006	1122	15	2.1GHz	3,012,000	20	456,022
18/09/2006	1122	15	2.1GHz	347,000	20	347,387
18/09/2006	1122	15	2.1GHz	5,886,000	20	489,330
18/09/2006	1122	15	2.1GHz	2,511,000	20	470,658
18/09/2006	1122	15	2.1GHz	3,027,000	20	440,801
18/09/2006	1122	15	2.1GHz	2,185,000	20	563,598
18/09/2006	1122	15	2.1GHz	453,000	20	452,846
18/09/2006	1122	15	2.1GHz	1,464,000	20	417,939
18/09/2006	1122	15	2.1GHz	1,331,000	20	315,538
18/09/2006	1122	15	2.1GHz	3,315,000	20	518,821
18/09/2006	1122	15	2.1GHz	536,000	20	380,783
18/09/2006	1122	15	2.1GHz	846,000	20	426,526
18/09/2006	1122	15	2.1GHz	2,482,000	20	483,924
18/09/2006	1122	15	2.1GHz	847,000	20	299,896
18/09/2006	1122	15	2.1GHz	4,054,000	20	408,326
18/09/2006	1122	15	2.1GHz	564,000	20	537,484
18/09/2006	1122	15	2.1GHz	2,191,000	20	373,638
18/09/2006	1122	15	2.1GHz	345,000	20	328,695
18/09/2006	1122	15	2.1GHz	2,553,000	20	424,607
18/09/2006	1122	15	2.1GHz	6,730,000	20	350,761

18/09/2006	1122	15	2.1GHz	649,000	20	294,558
18/09/2006	1122	15	2.1GHz	1,113,000	20	458,614
18/09/2006	1122	15	2.1GHz	2,024,000	20	399,347
18/09/2006	1122	15	2.1GHz	853,000	20	358,365
18/09/2006	1122	15	2.1GHz	974,000	20	401,762
18/09/2006	1122	15	2.1GHz	2,474,000	20	412,153
18/09/2006	1122	15	2.1GHz	725,000	20	569,463
18/09/2006	1122	15	2.1GHz	310,000	20	280,843
18/09/2006	1122	15	2.1GHz	320,000	20	320,204
18/09/2006	1122	15	2.1GHz	458,000	20	314,866
18/09/2006	1122	15	2.1GHz	1,681,000	20	380,841
18/09/2006	1122	15	2.1GHz	1,559,000	20	354,878
18/09/2006	1122	15	2.1GHz	412,000	20	322,959
18/09/2006	1122	15	2.1GHz	349,000	20	284,664
18/09/2006	1122	15	2.1GHz	2,657,000	20	476,230
18/09/2006	1122	15	2.1GHz	364,000	20	322,549
18/09/2006	1122	15	2.1GHz	1,055,000	20	333,055
18/09/2006	1122	15	2.1GHz	725,000	20	251,662
18/09/2006	1122	15	2.1GHz	1,173,000	20	243,815
18/09/2006	1122	15	2.1GHz	2,620,000	20	446,997
18/09/2006	1122	15	2.1GHz	433,000	20	232,621
18/09/2006	1122	15	2.1GHz	1,389,000	20	341,367
18/09/2006	1122	15	2.1GHz	1,510,000	20	332,807
18/09/2006	1122	15	2.1GHz	2,319,000	20	443,343
18/09/2006	1122	15	2.1GHz	265,000	20	264,919
18/09/2006	1122	15	2.1GHz	391,000	20	347,214
18/09/2006	1122	15	2.1GHz	303,000	20	302,963
18/09/2006	1122	15	2.1GHz	1,197,000	20	368,021
18/09/2006	1122	15	2.1GHz	1,702,000	20	280,150
18/09/2006	1122	15	2.1GHz	2,339,000	20	300,826
18/09/2006	1122	15	2.1GHz	665,000	20	250,929
18/09/2006	1122	15	2.1GHz	559,000	20	259,088
18/09/2006	1122	15	2.1GHz	1,008,000	20	293,000
18/09/2006	1122	15	2.1GHz	683,000	20	298,975
18/09/2006	1122	15	2.1GHz	592,000	20	241,023
18/09/2006	1122	15	2.1GHz	247,000	20	219,469
18/09/2006	1122	15	2.1GHz	592,000	20	368,536
18/09/2006	1122	15	2.1GHz	472,000	20	312,952
18/09/2006	1122	15	2.1GHz	359,000	20	242,628
18/09/2006	1122	15	2.1GHz	427,000	20	335,227
18/09/2006	1122	15	2.1GHz	477,000	20	294,676
18/09/2006	1122	15	2.1GHz	1,767,000	20	440,888
18/09/2006	1122	15	2.1GHz	313,000	20	255,399
18/09/2006	1122	15	2.1GHz	631,000	20	264,436
18/09/2006	1122	15	2.1GHz	1,500,000	20	325,957
18/09/2006	1122	15	2.1GHz	954,000	20	307,402
18/09/2006	1122	15	2.1GHz	227,000	20	227,412
18/09/2006	1122	15	2.1GHz	330,000	20	250,158
18/09/2006	1122	15	2.1GHz	734,000	20	339,486
18/09/2006	1122	15	2.1GHz	263,000	20	250,291

18/09/2006	1122	15	2.1GHz	2,920,000	20	246,190
18/09/2006	1122	15	2.1GHz	284,000	20	239,086
18/09/2006	1122	15	2.1GHz	609,000	20	255,602
18/09/2006	1122	15	2.1GHz	227,000	20	201,437
18/09/2006	1122	15	2.1GHz	301,000	20	194,740
18/09/2006	1122	15	2.1GHz	153,000	20	153,172
18/09/2006	1122	15	2.1GHz	464,000	20	205,009
18/09/2006	1122	15	2.1GHz	385,000	20	183,632
18/09/2006	1122	15	2.1GHz	858,000	20	197,073
18/09/2006	1122	15	2.1GHz	555,000	20	311,121
18/09/2006	1122	15	2.1GHz	794,000	20	225,965
18/09/2006	1122	15	2.1GHz	194,000	20	194,477
18/09/2006	1122	15	2.1GHz	180,000	20	170,943
18/09/2006	1122	15	2.1GHz	685,000	20	226,778
18/09/2006	1122	15	2.1GHz	539,000	20	260,283
18/09/2006	1122	15	2.1GHz	327,000	20	217,858
18/09/2006	1122	15	2.1GHz	189,000	20	188,831
18/09/2006	1122	15	2.1GHz	1,126,000	20	300,904
18/09/2006	1122	15	2.1GHz	306,000	20	222,581
18/09/2006	1122	15	2.1GHz	970,000	20	244,043
18/09/2006	1122	15	2.1GHz	162,000	20	162,453
18/09/2006	1122	15	2.1GHz	765,000	20	213,517
18/09/2006	1122	15	2.1GHz	1,834,000	20	191,701
18/09/2006	1122	15	2.1GHz	203,000	20	179,669
18/09/2006	1122	15	2.1GHz	1,917,000	20	183,577
18/09/2006	1122	15	2.1GHz	395,000	20	231,809
18/09/2006	1122	15	2.1GHz	132,000	20	132,008
18/09/2006	1122	15	2.1GHz	157,000	20	157,110
18/09/2006	1122	15	2.1GHz	303,000	20	151,337
18/09/2006	1122	15	2.1GHz	200,000	20	199,750
18/09/2006	1122	15	2.1GHz	162,000	20	161,946
18/09/2006	1122	15	2.1GHz	191,000	20	190,868
18/09/2006	1122	15	2.1GHz	145,000	20	145,035
18/09/2006	1122	15	2.1GHz	757,000	20	173,489
18/09/2006	1122	15	2.1GHz	1,876,000	20	319,426
18/09/2006	1122	15	2.1GHz	207,000	20	207,033
18/09/2006	1122	15	2.1GHz	251,000	20	251,494
18/09/2006	1122	15	2.1GHz	1,120,000	20	264,002
18/09/2006	1122	15	2.1GHz	244,000	20	231,969
18/09/2006	1122	15	2.1GHz	135,000	20	134,953
18/09/2006	1122	15	2.1GHz	192,000	20	191,822
18/09/2006	1122	15	2.1GHz	203,000	20	203,171
18/09/2006	1122	15	2.1GHz	152,000	20	152,307
18/09/2006	1122	15	2.1GHz	629,000	20	133,358
18/09/2006	1122	15	2.1GHz	1,477,000	20	233,450
18/09/2006	1122	15	2.1GHz	241,000	20	147,250
18/09/2006	1122	15	2.1GHz	273,000	20	160,245
18/09/2006	1122	15	2.1GHz	533,000	20	174,367
18/09/2006	1122	15	2.1GHz	902,000	20	164,875
18/09/2006	1122	15	2.1GHz	206,000	20	182,791

18/09/2006	1122	15	2.1GHz	152,000	20	144,919
18/09/2006	1122	15	2.1GHz	264,000	20	129,144
18/09/2006	1122	15	2.1GHz	380,000	20	142,950
18/09/2006	1122	15	2.1GHz	408,000	20	165,740
18/09/2006	1122	15	2.1GHz	146,000	20	146,438
18/09/2006	1122	15	2.1GHz	181,000	20	181,269
18/09/2006	1122	15	2.1GHz	115,000	20	114,706
18/09/2006	1122	15	2.1GHz	196,000	20	128,852
18/09/2006	1122	15	2.1GHz	1,193,000	20	148,337
18/09/2006	1122	15	2.1GHz	167,000	20	142,670
18/09/2006	1122	15	2.1GHz	1,113,000	20	195,033
18/09/2006	1122	15	2.1GHz	445,000	20	130,571
18/09/2006	1122	15	2.1GHz	364,000	20	118,769
18/09/2006	1122	15	2.1GHz	729,000	20	174,706
18/09/2006	1122	15	2.1GHz	589,000	20	120,293
18/09/2006	1122	15	2.1GHz	693,000	20	157,322
18/09/2006	1122	15	2.1GHz	722,000	20	143,377
18/09/2006	1122	15	2.1GHz	225,000	20	141,472
18/09/2006	1122	15	2.1GHz	329,000	20	207,355
18/09/2006	1122	15	2.1GHz	181,000	20	180,936
18/09/2006	1122	15	2.1GHz	150,000	20	149,577
18/09/2006	1122	15	2.1GHz	517,000	20	258,916
18/09/2006	1122	15	2.1GHz	631,000	20	137,916
18/09/2006	1122	15	2.1GHz	156,000	20	148,955
18/09/2006	1122	15	2.1GHz	922,000	20	153,472
18/09/2006	1122	15	2.1GHz	477,000	20	112,249
18/09/2006	1122	15	2.1GHz	150,000	20	150,433
18/09/2006	1122	15	2.1GHz	433,000	20	120,044
18/09/2006	1122	15	2.1GHz	599,000	20	131,420
18/09/2006	1122	15	2.1GHz	1,322,000	20	124,130
18/09/2006	1122	15	2.1GHz	163,000	20	163,256
18/09/2006	1122	15	2.1GHz	523,000	20	121,123
18/09/2006	1122	15	2.1GHz	873,000	20	159,576
18/09/2006	1122	15	2.1GHz	460,000	20	131,923
18/09/2006	1122	15	2.1GHz	712,000	20	135,758
18/09/2006	1122	15	2.1GHz	188,000	20	114,996
18/09/2006	1122	15	2.1GHz	137,000	20	120,822
18/09/2006	1122	15	2.1GHz	110,000	20	110,156
18/09/2006	1122	15	2.1GHz	786,000	20	125,834
18/09/2006	1122	15	2.1GHz	714,000	20	125,761